CLIMATE ANALYSIS IN THE CENTRAL PYRENEES FROM INSTRUMENTAL AND PALEOCLIMATE PROXY DATA

Nuria Pérez Zanón

Centre for Climate Change

UNIVERSITAT ROVIRA i VIRGILI

Laboratoire d'Océanographie et du Climat
Expérimentations et Approches Numériques

MUSÉUM NATIONAL D'HISTOIRE NATURELLE

UNIVERSITAT DE BARCELONA

Climate Analysis in the Central Pyrenees from Instrumental and Paleoclimate Proxy Data | Doctoral Thesis | Nuria Pérez Zanón

2017

Climate Analysis in the Central Pyrenees from Instrumental and Paleoclimate Proxy Data

Nuria Pérez Zanón
Doctoral Thesis
2017

UNIVERSITAT ROVIRA i VIRGILI

MUSÉUM NATIONAL D'HISTOIRE NATURELLE

UNIVERSITAT ROVIRA I VIRGILI
CLIMATE ANALYSIS IN THE CENTRAL PYRENEES FROM INSTRUMENTAL AND PALEOCLIMATE PROXY DATA
Nuria Pérez Zanón

UNIVERSITAT ROVIRA I VIRGILI
CLIMATE ANALYSIS IN THE CENTRAL PYRENEES FROM INSTRUMENTAL AND PALEOCLIMATE PROXY DATA
Nuria Pérez Zanón

Nuria Pérez Zanón

CLIMATE ANALYSIS IN THE CENTRAL PYRENEES FROM INSTRUMENTAL AND PALEOCLIMATE PROXY DATA.

PhD Thesis

Supervised by

Dr. Fco. Javier Sigró Rodríguez
Profr. Geography
URV-C3

Dr. Myriam Khodri
Research Scientist IRD-IPSL

Dr. Teresa Vegas Vilarrúbia
Profr.Ecology UB

Geography Department
Centre for Climate Change
Vila-seca
2017

UNIVERSITAT ROVIRA I VIRGILI
CLIMATE ANALYSIS IN THE CENTRAL PYRENEES FROM INSTRUMENTAL AND PALEOCLIMATE PROXY DATA
Nuria Pérez Zanón

WE STATE that the present study, entitled "CLIMATE ANALYSIS IN THE CENTRAL PYRENEES FROM INSTRUMENTAL AND PALEOCLIMATE PROXY DATA", presented by Nuria Pérez Zanón for the award of the degree of Doctor with International mention, has been carried out under our supervision at the Centre for Climate Change (Department of Geography, URV), the Laboratoire d'Océanographie et du Climat: Expérimentation et aproches numériques (LOCEAN) unit of research of the Muséum National d'Histoire Naturelle and the deparment of Evolutive Biology, Ecology and Environmental Science of the University of Barcelona.

Vila-seca, 29 de juny de 2017

Doctoral thesis supervisors

Dr. Fco. Javier Sigró Rodríguez

Dr. Myriam Khodri

Dr. Teresa Vegas-Vilarrúbia

UNIVERSITAT ROVIRA I VIRGILI
CLIMATE ANALYSIS IN THE CENTRAL PYRENEES FROM INSTRUMENTAL AND PALEOCLIMATE PROXY DATA
Nuria Pérez Zanón

A mis padres.

UNIVERSITAT ROVIRA I VIRGILI
CLIMATE ANALYSIS IN THE CENTRAL PYRENEES FROM INSTRUMENTAL AND PALEOCLIMATE PROXY DATA
Nuria Pérez Zanón

Acknowledgements

Until a few days ago I had not thought about the acknowledgments of the thesis. However, I cannot miss the opportunity to humanize this work by showing my gratitude to all the people who, in one way or another, have contributed to the development of this doctoral thesis.

First, I want to thank my supervisors Dr. Javier Sigró, Dr. Teresa Vegas and Dr. Myriam Khodri for their help and confidence. Thanks to Javier for the support and patience he has given me during these three years. To Teresa, I thank her for trusting in my work for her project and for showing me the importance, beauty and complexity that limnology hides. But especially I want to thank Myriam, who welcomed me on my arrival in Paris, with whom I have worked for more than a year and reminded me how important is not to settle without understanding. Thanks also to Robert Sala, director of the doctoral program, for his help and patience with my thesis and stay managment.

In these three years there have been several moves and collaborations. I would like to thank all the colleagues of C3, especially the Tortosa Staff for their welcome at my arrival: lunches, the greenway, the Journal Club, organize the CLIMATE-ES ... To the colleagues of LOCEAN: especially Dr Yassine Ait Brahim, Dr. Emilie Dassie and Dr. Abdel Sifeddine; And the National Museum of Natural History: Chafika Falgueres and Dr. Christophe Falgueres; Thank you all for your kindness! I would also like to thank all the collaborators of the Montcortès project for this thesis, I would have liked to have more talks with you, especially Emilia Gutiérrez, Isabel Dorado, Mari Carmen Trapote and Carla Vazquez. And back to Vila-seca, a new welcome, with JR waiting on Wednesdays of Alba and Olga; Thank you all!

During these three years I have also had time to make new friends. Thanks to Linden and Tim for their energy. Thank you all the people with whom I have shared experiences and knowledge in Paris: Rufianes, Felipe Zapata, Laura Miñones, "Nurice", Diego Santodo, Juan Pimentel, Rita Casas, Soraya Moradi and Charlie. A memory for the people I shared with the night of November 13, 2015 in Paris, especially Marta Garcia, Ruth Marañón, Alba Peinado and Gabo "Percu".

Not everything has been new at this time and I am glad. I am glad to have friends who have supported me since before starting the thesis like Noa Barja. Friends who welcome you to the return of Paris with a banner like Edo and Laura. I am glad to have friends who were first mentors like Juan Carlos Peña. Thank you! This reminds me of where it all began ... a memory of gratitude for the colleagues of the Department of Climatology of the Servei Meteorològic de Catalunya, including Antonio Gazquez and Montse Arán, for sharing the fascination with climatology.

I must also acknowledge and thank the affection of people very close as Mercedes Lopez, always to the rescue, and family. The same recognition to the Ruiz Cubero and the memory of who is missing.

Finally, I am very grateful to my parents and siblings, for being always there, to the going and the return of everything. I love you. And also grateful to Ernesto Ruiz for his love, support and, of course, for the beautiful drawing on this thesis cover.

This thesis has been funded by the Martí Franquès predoctoral program.

Abstract

This thesis deals with the thermopluviometric series that characterize the climate of the central Pyrenees during the instrumental period, which also allow to carry out analyzes with natural records capable of capturing the climatic signal during the last 500 years. These thermopluviometric series have been obtained from data observed in-situ, both in manual and automatic observatories, during the instrumental period 1910-2013 for the longer series of maximum and minimum temperature and precipitation available in the study area. After quality controlling the observed data and applying the most appropriate homogenization method, the series of regional anomalies show the variability and climate change at annual and seasonal scales. The sediments of Lake Montcortès have been analyzed to know the influence of the climate on the mixing regime of the water column of the lake that was considered meromictic, showing that the current climate change is taking control in its capacity of oxygenation. On the other hand, tree ring thickness chronologies have been used to evaluate their ability to capture the regional climatic signal as well as the weather regimes of the North Atlantic in summer. To this end, the regional climate of the central Pyrenees has been characterized by synoptic compositions (composites) of sea level pressure in normal and extreme summers (through regional series of anomalies).

Resumen

Se presentan las series termopluviométricas que caracterizan el clima del Pirineo central durante el período instrumental, que permiten, además, realizar los análisis obtenidos con registros naturales capaces de capturar la señal climática durante los últimos 500 años. Estas series termopluviométricas han sido obtenidas a partir de datos observados in-situ, tanto en observatorios manuales como automáticos, durante el período instrumental 1910–2013, tratándose de las series de temperatura y precipitación de alta calidad más largas disponibles en la zona de estudio. Tras controlar los datos observados de calidad y aplicar el método de homogenización más adecuado, las series de anomalías regionales muestran la variabilidad y cambio del clima en escalas anuales y estacionales. Los sedimentos del lago Montcortès han sido analizados para conocer la influencia del clima en la alteración del régimen de la mezcla de la columna del agua del lago que se consideraba meromíctico, mostrando que el actual cambio climático está tomando el control sobre su capacidad de oxigenación. Por su parte, cronologías del grosor de anillos de los árboles han sido utilizadas para evaluar su capacidad de capturar la señal climática regional, así como los regímenes de tiempo de escala sinóptica del Atlántico Norte en verano. Para ello, el clima regional del Pirineo central ha sido caracterizado mediante composiciones sinópticas (composites) de presión a nivel del mar en los veranos normales y extremos (mediante las series de anomalías regionales).

Contents

Scientific activities during the PhD

Associated publications

1. Peer reviewed papers:

Pérez-Zanón, N., Sigró, J., Domonkos, P., Ashcroft, L., 2015. Comparison of HOMER and ACMANT homogenization methods using a central Pyrenees temperature dataset. Adv. Sci. Res. 12, 111–119. doi:10.5194/asr-12-111-2015

Pérez-Zanón, N., Sigró, J., Ashcroft, L., 2016. Temperature and precipitation regional climate series over the central Pyrenees during 1910-2013. Int. J. Climatol. 1–16. doi:10.1002/joc.4823

2. Submitted Papers:

Vegas-Vilarúbia, T., Corella, P., **Pérez-Zanón, N.**, Buchaca, T., Trapote, M.C., López, P., Sigró, J., Rull, V. Historical shifts in oxygenation regime as recorded in the

laminated sediments of lake Montcortès (central Pyrenees): A continental-scale phenomenon? STOTEN [submitted].

3. Papers in preparation:

Pérez-Zanón, N., Khodri, M., Sigró, J., Gutiérrez, E., 2017: Role of North Atlantic weather regimes in the central Pyrenees climate from instrumental and tree-ring data. [in preparation]

Other relevant scientific activities during the PhD:

1. Stays abroad

LOCEAN — Laboratoire d'Oceanographie et du Climat, unit of research of Muséum National d'Histoire Naturelle, September 2015 – December 2016, at Université Piere et Marie Curie (UPMC), Paris, France.

2. Peer Reviwed Papers

Pérez-Zanón, N., Casas-Castillo, M.C., Rodríguez-Solà, R., Peña, J.C., Rius, A., Solé, J.G., Redaño, Á., 2015. Analysis of extreme rainfall in the Ebre Observatory (Spain). Theor. Appl. Climatol. doi:10.1007/s00704-015-1476-0

Rull, V., Trapote, M.C., Safont, E., Cañellas-Boltà, N., **Pérez-Zanón, N.**, Sigró, J., Buchaca, T., Vegas-Vilarrúbia, T., 2017. Seasonal patterns of pollen sedimentation in Lake Montcortès (Central Pyrenees) and potential applications to high-resolution paleoecology: a 2-year pilot study. J. Paleolimnol. 57, 95–108. doi:10.1007/s10933-016-9933-z

3. Submitted Papers

Ait Brahim, Y., Cheng, H., Sifeddine, A., Cruz, F.W., Sha, L., Khodri, M., **Pérez-Zanón, N.**, Bouchaou, L., Apaéstegui, J., Beraaouz, E.H., Wassenburg, J.A., Guyot, J.L. Oxygen isotope speleothem record of decadal to multidecadal hydroclimate variations in Southwestern Morocco during the last millennium. Earth Planet. Sci. Lett.

4. Conference contributions:

2017:

Vegas-Vilarúbia, T., Corella, P., **Pérez-Zanón, N.**, Buchaca, T., Trapote, M.C., López, P., Sigró, J., Rull, V. Historical shifts in oxygenation regime as recorded in the laminated sediments of lake Montcortès (Central Pyrenees). Past Globl Chabges (PAGES), Zaragoza, Spain, 9–13 May, 2017 (Poster).

Rull, V., Trapote, M.C., Safont, E., Cañellas-Boltà, N., **Pérez-Zanón, N.**, Sigró, J., Buchaca, T., Vegas-Vilarrúbia, T. Seasonal patterns of pollen sedimentation in a Pyrenees varved lake (Montcortès): applications to high resolution paleoecology. Past Globl Chabges (PAGES), Zaragoza, Spain, 9–13 May, 2017 (Poster).

Ait Brahim, Y., Sifeddine, A., Khodri, M., Cheng, H., Cruz, F.W., Sha, L., **Perez-Zanon, N**., Wassenbur, J.A., Bouchaou, L. Speleothem δ18O record of multidecadal Atlantic oscillations during the last millennium in Morocco. Past Globl Chabges (PAGES), Zaragoza, Spain, 9–13 May, 2017 (Poster).

Ait Brahim, Y., Sifeddine, A., Khodri, M., Bouchaou, L., Cruz, F.W., **Pérez-Zanón, N.**, Wassenburg, J.A. and Cheng, H. Regional influence of decadal to multidecadal Atlantic Oscillations during the last two millennia in Morocco, inferred from two high resolution δ18O speleothem records. EGU General Assembly, Viena, Austria, 23–28 April, 2017 (Poster).

2016:

Pérez-Zanón, N., Khodry, M., Sigró, J., Gutiérrez, E. Climate change in the central Pyrenees: Weather regime analysis from instrumental and tree-rings. 4ème journées Climat et Impacts, Orsay, France, 15–16 November, 2016. (Poster)

Ait Brahim, Y., Sifeddine, A., Khodri, M., Cruz, F.W., **Pérez-Zanón, N.**, Sha, L., Wassenburg, J.A., Bouchaou, L. Regional influence of decadal to multidecadal Atlantic Oscillations in Morocco during the last 1200 years. American Geophisical Union Fall Meeting, San Francisco, California, U.S.A., 12–16 December 2016 (Poster)

2015:

Trapote, M.C., López, P., Gomà, J., Safont, E., Cañellas-Boltà, N., Buchaca, T., **Pérez-Zanón, N.**, Sigró, J., Rull, V., Vegas-Vilarrúbia, T. Limnological cycle of a meromictic lake (Montcortès, Pyrenees) and its relationship to sediment varve formation. Aquatic Sciences Meeting, Granada, Spain, 22–27 February 2015. (Poster)

Peña, J.C., **Pérez-Zanón, N.**, Aran, M., Rius, A., Casas-Castillo, M.C., Rodríguez-Solà, R., Redaño, A. Analysis of meteorological temporal scales and synoptic types related to episodes of severe rainfall in the southern part of Catalonia (Spain). International Symposium CLIMATE-ES 2015, 11–13 March 2015, Tortosa, Spain. (Poster)

Pérez-Zanón, N., Sigró, J. Homogenizated dataset for central Pyrenees during the period 1910–2013. International Symposium CLIMATE-ES 2015, 11–13 March 2015, Tortosa, Spain. (Oral Presentation)

Vegas Vilarrúbia, T., Trapote, M., López, P., Safont, E., CañellasBoltà, N., Gomà, J., Buchaca, T., Rull, V., **Pérez, N.**, Sigró, X., Corella, P., Giralt., S. Revisiting meromictic Montcortès lake: Has the mixing regime changed? 9th Symposium for European Freshwater Science, Geneva, Switzerland, 5–10 July 2015. (Oral presentation)

Peña, J.C., Aran, M., **Pérez-Zanón, N.**, Casas-Castillo, M.C., Rodríguez-Solà, R., Llabrés, A., Redaño, A. Análisis de las situaciones sinópticas correspondientes a episodios de lluvia severa en Barcelona. XXXV Reunión Bienal de la Real Sociedad Española de Física. Gijón, Spain, 13–17 july 2015. (Poster)

Aran, M., Peña, J.C., Pineda, N., Soler, X., **Pérez-Zanón, N**. Ten-year lightning patterns in Catalonia using Principal Component Analysis. 8th European Conference on Severe Storms. Wiener Neustadt, Austria, 14–18 September 2015. (Poster)

Trapote, M.C., López, P., Puche, E., Safont, E., Cañellas-Boltà, N., Gomà, J., Buchaca, T., **Pérez-Zanón. N.**, Sigró, J., Rull, V. Modern Limnology and Varve Formation Processes in Lake Montcortès (Southern Pyrenees, Spain). American Geophisical Union Fall Meeting, San Francisco, California, U.S.A., 14–18 December 2015. (Poster)

2014:

Perez-Zanón, N., Sigro, J., Domonkos, P. HOMER and ACMANT comparison methods for central Pyrenees temperatura. 14th EMS Annual Meeting & 10th European Conference on Applied Climatology (ECAC), 6–10 October 2014, Prague, Czech Republic. (Poster)

5. Awards:

Eduard Fontserè Prize 2015 International category to the publication: Principal sequence pattern analysis of episodes of excess mortality due to heat in the Barcelona metropolitan area. Peña, J.C., Aran, M., Raso, J.M., **Pérez-Zanón, N**., 2015. International Journal of Biometeorology 59(4): 435–446. DOI: 10.1007/s00484-014-0857-x.

6. Scientific dissemination:

Pérez-Zanón, N. Clima y Cambio Climático. Les colloques des résidentes du College d'Espagne, Cité Internationale Universitaire de Paris, Paris, France, 2nd December 2015.

Pérez-Zanón, N. Series de temperatura y precipitación en el Pirineo central para el periodo 1910–2013. Exposition ConSciences Climatique au College d'Espagne, Cité Internationale Universitaire de Paris, Paris, France, 20–31 Janvier 2016.

Pérez-Zanón, N. Climatología: del Cambio Climático actual a la reconstrucción climática. Les colloques des résidentes du College d'Espagne, Cité Internationale Universitaire de Paris, Paris, France, 28th November 2016.

7. Datasets:

Centre for Climate Change / URV. (2016). Regional anomaly series for central Pyrenees. http://www.c3.urv.cat/data1.html

8. Conference Organization:

Member of Local Organizing Committee of International Symposium CLIMATE-ES 2015, held in Tortosa, Spain, 11–13 March 2015.

9. Collaboration in projects during the PhD program:

High resolution Paleoclimatology (annual) in the varved sediments of lake Montcortès during the last 500 years: from Little Ice Age to Global Warming (MONTCORTÈS-500). Call for Non-oriented Projects of Fundamental research, 2012. Grant Number: CGL2012-33665. Ministry of Economy, Industry and Competitivity, Spain.

Chapter 1 — Introduction

The study of climate is essential due to its impact on the environment and human activities (Smithers and Smit, 1997). It's necessary to expand knowledge on climate variability, as understood as variations in the mean state of climate on all scales, and on climate change, as refering to a prolonged variation of the mean climate state or its variability, in order to understand its causes, whether natural or anthropogenic. In this way, the ability to predict future variations will improve, enabling the anticipation of possible negative impacts of climate and giving the opportunity to develop effective adaptation and mitigation tools for the maintenance of capital (both natural and human; Intergovernmental Panel on Climate Change, IPCC, 2001).

Nowadays, the efforts of the scientific community to this aim are becoming patent, in part because of political participation. One of the organisms which provides most visibility is the IPPC. It was founded in 1988 to provide comprehensive assessments of the states of scientific, technical and socio-economic knowledge on climate change. Nevertheless, these efforts must be maintained, principally because there are large

uncertainties in model based future climate projections, since many climate models do not agree on the sign or amplitude of future climate changes (Shiogama *et al.*, 2016).

This detailed knowledge can be achieved by studying climate at different spatial scales: global climate, which is principally driven by solar energy input, but includes other factors such as Earth orbital variations, air composition modifications and feedbacks between climate system components (e.g. ocean-atmosphere coupling); and regional climate, for which, in addition global sources of climate variability, latitudinal position, land cover, water bodies and mountain range location are determinant factors (Ackerman and Knox, 2006). Furthermore, different time scales can be studied in order to improve our capabilities in climate variability prediction (Buchdahl, 1999). Several forcings, understanding imposed perturbations of Earth's energy balance (National Research Council; NRC, 2001), act over the climatic system and their components causing fluctuations of observed climate on different time scales, such as solar radiation which varies 0.1 % of its luminosity over the course of 11 years (NRC, 2012) or ocean-atmosphere coupling which introduce climate fluctuations due to their difference in heat capacity (Vuille and Garreaud, 2012).

In any case, three types of data are used by scientist to study climate: observed, modelled and reanalysis. Observed data come from the measurement by direct contact of instruments (e.g. thermometers, barometers, ….), such as those installed on weather stations or radiosonde, or by remote sensing, like radar or satellite information, coming from measurements of radiations which can be later converted to a climate variable observation (Henderson-Sellers and Robinson, 1986). However, observations provided by remote sensing are not capable of providing yet, the required accuracy and homogeneity, as measurements of many of the elements that are reported from land-based surface stations (World Meteorological Organization; WMO, 2011). Due to their short period of records remotely sensed data generally cannot be used to infer long-term climate variability and change. From all those data, complete datasets in gridded format of different climate variables are available for and by the climate scientific community. Another kind of data which can be considered as observed data is proxy data: measurements of conditions that are indirectly related to climate such as ice core samples, varves sediments, coral reefs and tree-ring growth (WMO, 2011). These data allow scientists to reconstruct past climate in order to extend our understandings of climate variability far beyond the instrumental period (Goosse, 2015).

The output of climate models are modelled data. These models are a mathematical representation of the climate system based on physical, biological and chemical principles and also require some inputs derived from observations or other model studies (Goosse, 2015). Depending on the field of expertise, scientists work to improve one part or the full model, or use the model output to climatic applications (Plummer *et al.*, 2003). Finally, it should be noted that reanalyses are an hybrid of both observed and modelled data, created via an unchanging ("frozen") data assimilation scheme and model(s) (Dee *et al.*, 2016). However, reanalysis are typically considered as observed data even though they present differences with observational datasets (Parker, 2016).

Two crucial concepts have been mentioned during this little data description: data accuracy and homogeneity. Both are related to the quality of the data used in climate analysis and are fundamental for the confidence in our scientific results. The quality of the observed data is particularly important as it is these data on which all research relies. When long-term data are required, in-situ observed data are generally used, as it is the oldest method to measure atmospheric variables. So, quality control (QC) procedures should be applied in order to detect, and correct if it is possible, the errors made in the process of recording, manipulating, formatting, transmitting and archiving data, while homogeneity testing should be performed to ensure that time fluctuations in the data are only due to the vagaries of weather and climate (Aguilar *et al.*, 2003).

This thesis addresses the study of the climate of central Pyrenees in the context of the project “High resolution Paleoclimatology (annual) in the varved sediments of lake Montcortès during the last 500 years: from Little Ice Age to Global Warming (MONTCORTÈS-500)” (Pérez-Zanón *et al.*, 2015, 2016; Rull *et al.*, 2017; Rull and Vegas-Vilarrúbia, 2014) supported by the Spanish Ministry of Economy and Competitiveness. For this purpose, high-quality data observed in the study area characterize the regional climate during the instrumental period while proxy data from Pyrenees extend the time scale back in time giving the chance to improve our knowledge of climate variability on this area. The incidence of a larger spatial scale in the climate of the regional Pyrenees, in particular the North Atlantic – European sector in summer, is also studied thanks to the use of gridded data from observations and reanalysis.

This chapter is divided into four parts. In the first section, some crucial characteristics of mountain regions crucial and a review of climate studies in this area are presented; in the second section the Pyrenees features and latest research advances are introduced; The third section describes the objectives and finally, structure of this manuscript is presented.

1.1. Mountain regions

The climatic conditions in mountain areas, as barriers on the planetary-scale atmospheric circulation (Barry, 2008), give rise to high rates of precipitation compared to bordering areas, particularly when oceans are close (Beniston, 2006). So, mountains act as gatherers for water for consumption, for hydroelectric power generation and agriculture production. Major forest reserves are often found in mountainous regions (Barry, 2008). The key role of forest in climate change mitigation has been recognized by the United Nations in agreement with the twenty-first session of the Conference of the Parties (COP21; United Nations framework Convention on Climate Change, 2015) because of their capability of absorbing immense amounts of carbon dioxide and negative effects of deforestation on climate change. Furthermore, ecologist also defend mountainous regions because of their high biodiversity, mainly due to topographic diversity, creating great diversity of habitats as a result of great variety of micro-climates, substrate types, water and nutrient regimes (Stephen *et al.*, 2010).

Scientific research on mountains did not start until the late eighteenth century and, primarily, was accomplished by biologists, geologists and ecologists (Barry, 2008). Thanks to these disciplines, which take into consideration environmental features, observations of weather and climate were recorded, although this information is consequently scattered throughout the scientific literature (Barry, 2008). Some variables such as wind, temperature and humidity are relatively simply related comparing measurements done in the free air and on the top of isolated high mountains (Coulter, 1967). A negative effect was that instead of maintaining observatories in mountainous regions to study upper air atmosphere, radiosonde measurements were considered enough in many places (Coulter, 1967), and their necessity are still claimed (Pepin *et al.*, 2015).

Particular climatic process occurring in mountains are a function of landmass at a particular elevation (Ekhart, 1948). Topographic features (slope, aspect and exposure) determine different local climates on the same mountain range (Beniston, 2006). Variables such as solar radiation, precipitation, temperature and cloudiness can vary strongly in short distances (Barry, 2008; Beniston, 2006). Ekhart (1948) differentiated the atmosphere over mountains into three parts: slope atmosphere, valley atmosphere and enveloping mountain atmosphere. 'Free air' is above the last one (as cited in Barry, 2008). Most of the weather processes involved are widely studied including temperature inversion, the Foehn effect and atmospheric pollution (Beniston, 2006).

The latest research on mountainous climate has been focused on vertical precipitation gradients and snow line, airflow, data acquisition systems and recent climate change (Barry, 2012). These topics are still being studied, such as the response of orographic precipitation which, in an idealized mid-latitude mountain, shows a dependency of synoptic scale storminess affecting the number of hours of precipitation events (Shi *et al.*, 2014) or the altitudinal dependency of climate change signals of precipitation until the end of 21st century over many parts of Europe evaluating experiments computed by using different Regional Climate Models (RCM) and driven by different Global Climate Models (GCM; Kotlarski *et al.*, 2015). High-resolution RCM are also used to simulate the diurnal winds in the Rocky Mountains, showing an opposite sign in the strength of daytime and night-time flows under the observed climate warming (Letcher *et al.*, 2017). Physical mechanisms (albedo, cloudiness, water vapour and radiative fluxes, aerosols and combined mechanisms) that may contribute to elevation-dependent warming are reviewed in Pepin et al., 2015, highlighting the importance of in-situ data on mountainous regions and the impact of climate change over these areas on population.

Mountain regions give the opportunity to find natural registers which have been not perturbed by human activities and that can be used as proxy data such as glaciers, which extend climate knowledge since the beginning of the Holocene (Nesje *et al.*, 2008; Owen *et al.*, 2009), or mountain lakes sediments, which allow scientists to reconstruct past floods (Schiefer *et al.*, 2011), precipitation occurrence (Ackerman and Knox, 2006) or temperature evolution (HEIRI and LOTTER, 2005; Tyler *et al.*, 2010) separate from ecosystem features (Schmidt *et al.*, 2002; Street-Perrott *et al.*, 2007). Sediments from

high-resolution floodplains in the Alps are also used to reconstruct paleofloods (Schulte *et al.*, 2015); while different procedures have been applied on tree-ring data to achieve large-scale temperature reconstructions (Briffa *et al.*, 2004; Schneider *et al.*, 2015; Stoffel *et al.*, 2015) and the Atlantic multidecadal Oscillation (AMO) (Gray *et al.*, 2004), a mode of variability of the North Atlantic Ocean characterized by the Sea Surface Temperature (SST), however, in these cases, not only mountainous regions are considered but also northern data sites.

Their vulnerability, in the context of the present climate change, has been interpreted from the observed and expected above-average warming (Beniston, 2003). This increasing temperature impacts on the snow-melt period, reducing glacier extension, increasing ecosystem degradation and extinction of endemic species while capacities of adaptation are limited. Droughts are expected to increase in mountain areas where warmer and drier conditions are projected (IPCC, 2007). The variation in snow cover, precipitation events (both amount and intensity) and temperature increase may modify the occurrence of floods and landslides which can be disastrous, resulting in substantial material losses and/or large numbers of fatalities (Stoffel *et al.*, 2015) The occurrence of floods in mountain basins is more expected than in other areas due to their often rapid response to intense rainfall rates, high slopes and a quasi-circular morphology (Stoffel *et al.*, 2015). On the other hand, due to the projected increase of temperature, fuel dryness and a reduction in relative humidity are expected, being severe in those regions where rainfall decreases. So, fire risk may have a very strong impact in areas where forest land cover is high, such as the Spanish Pyrenees (Moriondo et al., 2006). Moreover, the impact of future climate change on energy production is also the subject of attention, for example, shortfalls in hydropower generation due to a seasonal shift in lake water inflow might be expected in New Zealand mountain basins (Caruso *et al.*, 2017).

Finally, more than half of the world's population is supported by the resources provided by the mountains (Beniston, 2006), which makes essentially the study of these essential areas given the development and management capacity of the current advanced societies.

1.2. Study site

The Pyrenees is a mountainous range in southwestern Europe, which acts as a natural border between France and Spain (Ariño *et al.*, 2012) and contains all the territories of the Principality of Andorra (Pyrenees Climate Change Observatory; OPCC, 2013). Its physical definition is not simple due to its contact and transitions with the Cantabrian mountain range and the Catalan pre-coastal range (Laborie and Pala, 1989). However, the Work Community of the Pyrenees, founded in 1983 supported by the European Council, defines the region in the French side by the altitude following a law of 1985, while the southern side corresponds to a "conventional definition" (Figure 1.1; atlas.ctp.org).

Figure 1.1: Pyrenees boundary (red line) and hydrographical net (blue lines) (source: OPCC, 2013). Area watered by resources from the massif is shown in dark yellow shadow.

The Pyrenees constitute a wide area of 49,850 km^2 that extends from west to east over a length of 520 km, and from north to south over 150 km. Two-thirds of its surface is located on the southern slope with a less strong slope (Comunidad de trabajo de los Pirineos, 2006). The highest summit is 3404 m above sea level and its toponym is Aneto

(OPCC, 2013). The first time of climbing one of the highest summits of the Pyrenees was in 1802, when Ramond de Carbonnières reached Monte Perdido (3355 m) gathering naturalistic observations (Laborie and Pala, 1989).

Any decision of management on the Pyrenees may affect to 1,155,000 people living in the area (2006 census in OPCC, 2013), unevenly distributed with two centres of greater concentration: Andorra and Pamplona; even more considering the hydric resources of four major hydrological basins: Ebro, Garona, Adour and internal basins of Catalonia (Figure 1.1); and even more, if we considered the global effect of forest (43 % of Pyrenees surfaces; OPCC, 2013) as a CO_2 drain (Figure 1.2).

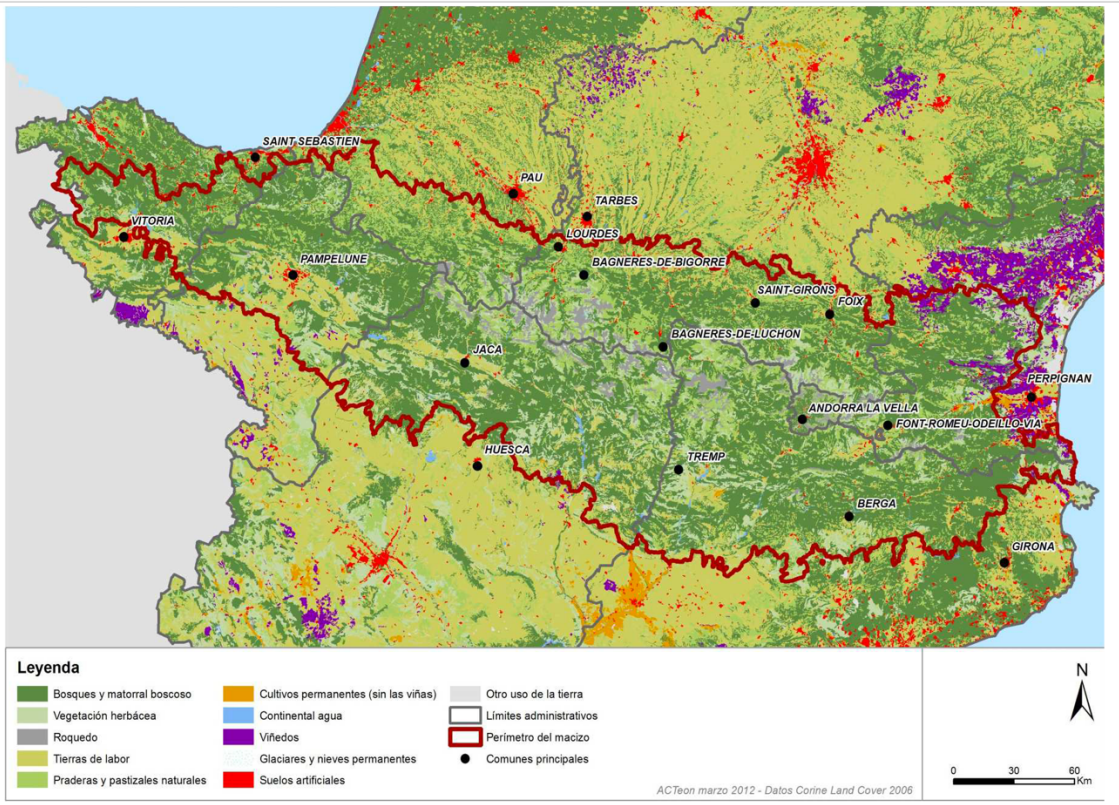

Figure 1.2:Land use in the Pyrenees (source: OPCC, 2013).

To confine the negative effects of climate change and to adapt the area to its possible consequences, the OPCC was founded as an initiative of the Work Community of the Pyrenees. It has been renewed until 2019, and different reports are already published which are a good source of information on: climate, biodiversity, forest, natural hazards, water, adaptation, teledetection and cartography. The OPCC is an important initiative to

provide policymakers with assessments which allow them to take sound evidence-based decisions.

The Pyrenees climate is not homogeneous due to being influenced by the Atlantic Ocean on the west and the Mediterranean Sea on the east as well as its relief (Beguería *et al.*, 2003; OPCC, 2013). However, five climatic regions are detected by Duquense (2008) and accepted by OPCC (2013) considering the temperature and precipitation distribution (Figures 1.3 and 1.4). These are, from west to east: oceanic, sub-oceanic, sub-continental with Mediterranean influence, cold sub-oceanic and Mediterranean with sub-continental tendency. This division also relies on the storm track influence on the two slopes of the mountain (see Duquense, 2008).

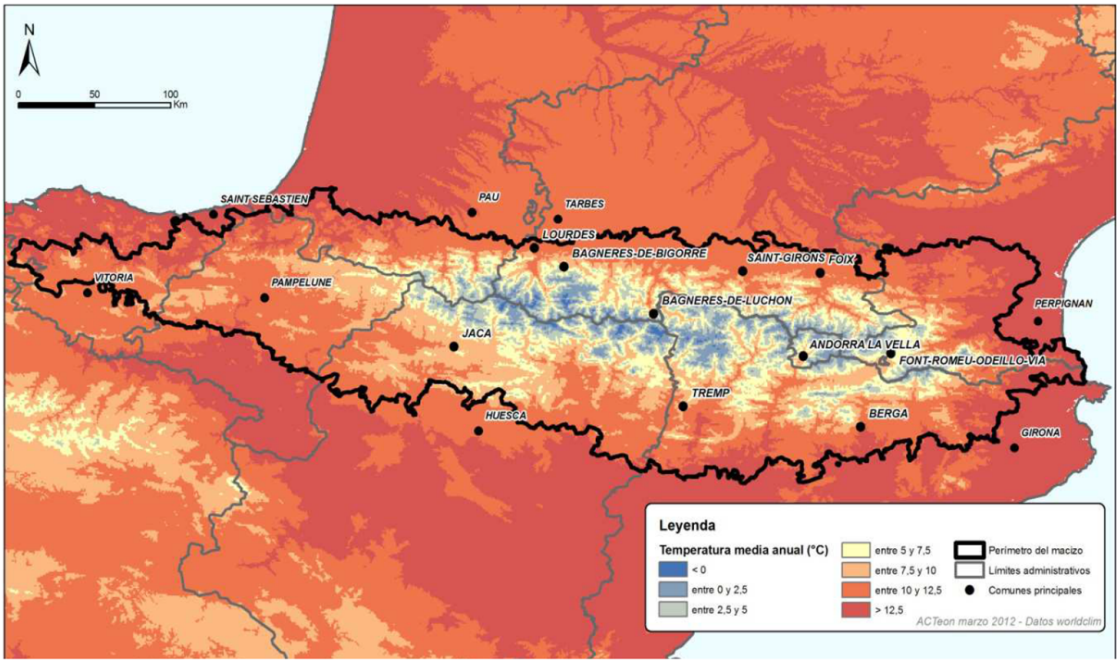

Figure 1.3: Mean annual temperature on Pyrenees during the period 1960–1990 (source: OPCC, 2013).

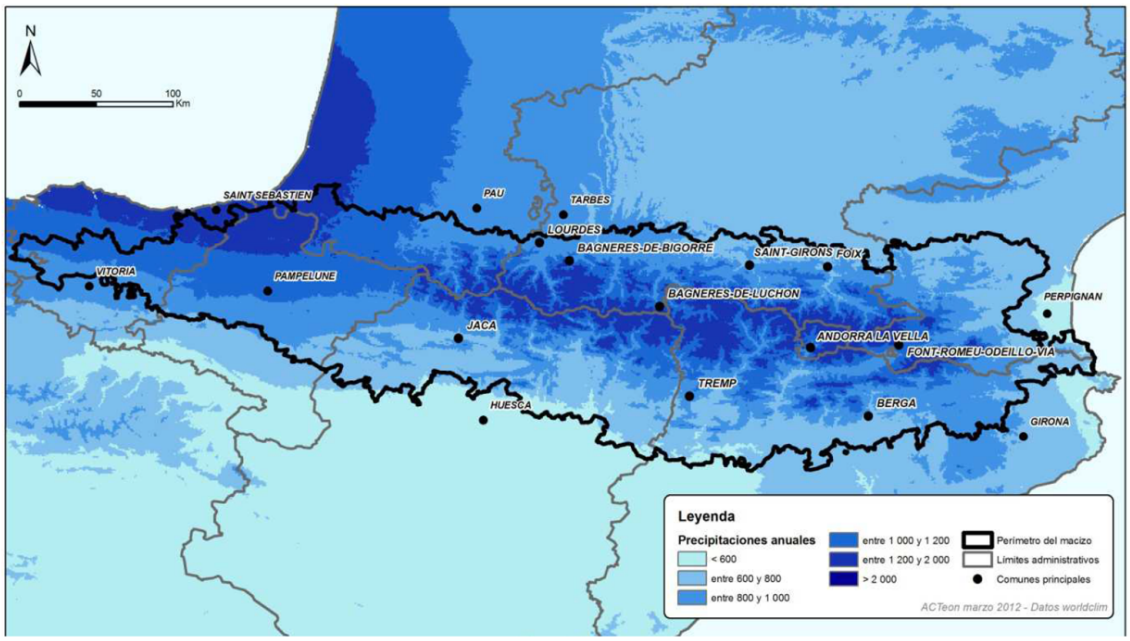

Figure 1.4: Mean annual precipitation on Pyrenees during the period 1960–1990 (source: OPCC, 2013).

The studies of climate in the Pyrenees are few (Duquense, 2008) compared with other mountainous regions, although hydrological models predict greater climatic anomalies in the Pyrenees than in the Alps. In recent years, one of the most deeply studied specialties is the hydrological response of the Pyrenees catchments to precipitation, temperature and snow cover variations and considering land-use change, such as agriculture abandonment and reforestation. These studies were mainly carried on by the Pyrenees Institute of Ecology. During the second half of 20th century, a decrease on discharge basins are related not only to precipitation and temperature variations but to land-use and plant cover changes (Beguería *et al.*, 2003). Negative trends in flood intensity but an increase of low flows occurrences also were detected due to precipitation events during the same period (López-Moreno *et al.*, 2006). Other works considered the Ebro basin, observing an increasing in the number of winter warm days and nights, and projecting a continued increase for the 21th century even doubling their occurrences especially in mountain areas (López-Moreno *et al.*, 2014).

The standardised precipitation-evapotranspiration index (SPEI), a multiscale drought index based on climatic data, was also studied in the same area, showing the influence on the hydrological characteristics in different time scales and fast response on mountain regions (López-Moreno *et al.*, 2013). The snow cover in the Pyrenees is

above 1650 m a.s.l. between December and April, which has shown a negative trend in snow pack during the second half of 20th century caused by the atmospheric circulation characterized by an increase of the North Atlantic Oscillation (NAO) (López-Moreno, 2005; López-Moreno and Vicente-Serrano, 2007). The interanual variability of the number of snow and precipitation days are related to the weather types over the Iberian Peninsula and influenced by the distance to the sea and the elevation (Buisan *et al.*, 2015). So, circulation patterns in winter lead the precipitation, temperature and snow cover variation (Buisan *et al.*, 2016). The future reduction of snow cover may reach 78% and the length of the season 70% (López-Moreno *et al.*, 2009), while, in terms of precipitation, extreme events and drought periods tends to increase as shown in RCM for the 21th century (López-Moreno and Beniston, 2008). However, the bias of RCM on precipitation and temperature are 20 % and 1℃, respectively (López-Moreno *et al.*, 2008), meaning there is still uncertainty around these projections.

Reconstructions have also been developed over the Pyrenees. Past temperature have been obtained for different periods using tree-ring chronologies (Büntgen *et al.*, 2008, 2017; Dorado Liñán *et al.*, 2012; Esper *et al.*, 2015a; Tardif *et al.*, 2003). The good quality of the dendrological methodology applied in these publications are not questionable, however, from a climatological point of view some limitations can be highlighted: typically the reconstruction is performed on May to September temperatures since it shows better correlations in this period, instead of summer or winter, when climate indexes, like winter NAO (Portis *et al.*, 2001), are clearly defined; the climate data used to the calibration are not ideal, since neither quality control nor homogenization is performed or only observations in particular places are considered, which can be subjected to the topographic features perturbations since data are collected from remote areas; finally, there is a lack of information about atmospheric circulation related to observed climate in the area.

Lake sediments, for their part, allow climate variability knowledge to be extend back in time due to the information contained in their sediments, specially thus showing laminated formations (varved; Gold, 2009). However, this and other climate proxies contained in lacustrine sediments can also depend on past environmental conditions and human activities (Aranbarri *et al.*, 2017). Atmospheric pollution (Corella *et al.*, 2017), erosion fluxes (Mazier and Bard, 2016), vegetation and limnological response (Vegas-

Vilarrúbia *et al.*, 2013) and hydrological dependency (Morellón *et al.*, 2009) of sediments formation conducted by climate have been widely studied in different lakes in the Pyrenees. Cold and arid periods have been identified in the central-western Spanish Pyrenees over the last 30.000 years (González-Sampériz *et al.*, 2006) as well as three millennia heavy rainfall events, in sub-decadal scale and their relation with the Mediterranean Oscillation (MO) in western Mediterranean (Corella *et al.*, 2016).

Glacier studies (Cía *et al.*, 2005; García-Ruiz *et al.*, 2003; Pallas *et al.*, 2010) and multi-proxy reconstructions (Morellón *et al.*, 2012; Moreno *et al.*, 2012) have also been carried out in the Pyrenees. This last method is considered of high value by combining proxies errors and loss of information can be avoided (Li *et al.*, 2010; Moberg *et al.*, 2005).

As it has been highlighted previously, high-quality observed data covering the instrumental period (Hulme and Jones, 1994) are necessary to perform climatological studies in order to remove non-climatic factors (Aguilar *et al.*, 2003). For this purpose, recent publications of quality-controlled and homogenized data have been done in the Pyrenees (Cuadrat *et al.*, 2013; Esteban *et al.*, 2007, 2012; Notivoli *et al.*, 2013). However, these datasets are obtained in a concrete area of the Pyrenees or are covering the last 60 years only, which can be considered not long ehough to assess low-frequency variability or paleoclimatology studies, among others purpose of long-term and high-quality series (Brunet *et al.*, 2002).

This area is vulnerable to risk of fires and floods as any mountainous region. For example, the flash flood that occurred in the Arás basin in 1996 resulting in 87 fatalities (Gutiérrez *et al.*, 1998) or in the Aude river in 1999 (Gaume *et al.*, 2004; Vinet, 2008). Snow avalanches are also a hazard in Pyrenees (Muntán *et al.*, 2009), for population and economical activities as tourism and cattle industry which are developed on there (Marín-Yaseli and Martínez, 2003).

1.3. Research aims and objectives

The effort of an interdisciplinary research team to obtain paleoclimatic reconstructions of the past 500 years is gathered in the MONCORTÈS-500 project. Taking advantage of the varved sediments of Montcortès lake in the central Pyrenees (see Chapter 4), these

reconstructions are expected to be of high-resolution (sub-decadal – annual – seasonal). The robustness of its chronology was previously proved and laid the groundwork to improve the resolution of the reconstructions. Thus, the sedimentological process over the last 6000 years showed its capability to preserve laminated deposition suggesting to be dependent on climate (Corella, 2009; Corella *et al.*, 2011), while warm and higher rainfall frequency periods were detected during the last 1.500 years by analysing the composition and the thickness of the varves (Corella *et al.*, 2012).

The novelty of this project relies on the study of the most recent period with high resolution as the upper part of the core was recovered almost unaltered. Furthermore, the last 500 years are interesting as they include the transition between the Little Ice Age (LIA; Mann *et al.*, 2009) and the present Global Warming. Finally, multi-proxy analysis was proposed using Montcortès proxies (diatoms, varve thickness, pollen, pigments, geochemical) and dendrological data.

Since the beginning of this project, some studies (belonging to the project or external) of Montcortès lake have been published. Thus, the seasonal pattern of pollen sedimentation has been characterized by two years of monitoring and show a relationship with meteorological variables (Rull *et al.*, 2017); the evolution of the agriculture and the landscape modifications have been identified by combining Montcortès sediments and historical documentation (Rull and Vegas-Vilarrúbia, 2015); even multi-proxy studies have been carried on considering different lakes in the Pyrenees to synthetize the environmental variations since the Last Glacial Maximum (Aranbarri *et al.*, 2017); and the sedimentation composition and atmospheric pollution link has been showed for the last 700 years (Corella *et al.*, 2017).

For its part, recent dendrological studies in the Pyrenees contribute with new techniques, as the 20th century analysis of $\delta^{13}C$ and $\delta^{18}O$ isotope ratios of *Pinus uncinata* against precipitation and temperature indexes (Konter *et al.*, 2014) and the latest tree-ring analysis, highlighting the relevance of combining maximum latewood density with GCM to understanding regional climate (Büntgen *et al.*, 2017).

Nevertheless, while the bulk of the Montcortès-500 project's objectives lie in biological information, climate data and analyses are essential for its development, such as how weather and climate affect limnological observations in the Montcortès annual cycle

(Rull *et al.*, 2017). Therefore, the main objective of this thesis is to characterize the observed climate in the central Pyrenees during the instrumental period and to evaluate the potential of proxy data to capture and reconstruct past regional or large-scale climate. To achieve these goals the scientific and technical specific objectives can be divided in four blocks:

1. To obtain a high-quality regional climate series for central Pyrenees:

2. Detect the role played by the synoptic scale on the regional central Pyrenees climate.

3. Evaluate the potential of limnological sediments and tree-ring chronologies to capture observed climatological variability and change whether regional or large-scale.

4. Evaluate the capability to reconstruct past climate by using paleoclimate proxies from the central Pyrenees.

1.4. Thesis outline

This PhD thesis is structured in 6 chapters, being the present chapter 1 the introduction, in which the general concepts and aims have been contextualized.

Chapter 2 is the "Comparison of HOMER and ACMANT homogenization methods using a central Pyrenees temperature dataset" article published in Advances in Sciences and Research, the peer-reviewed international proceedings journal of the European Meteorological Society (EMS). Dr. Javier Sigró, Dr. Peter Domonkos and Dr. Linden Ashcroft lent support, with their proven expertise, to develop high level research, while three unknown referees evaluated it improving the form and content of this research.

Chapter 3 is the "Temperature and precipitation regional climate series over the central Pyrenees during 1910-2013" article published in the International Journal of Climatology, one of the most prestigious journal in this expertise area (journal impact factor 3.760 in 2016 from the Q1 in Meterology and Atmospheric science). It is also a peer-reviewed journal, and, in addition, it is indexed on Journal Citation Reports and belongs to the publications of the Royal Meteorological Society. The support of Dr.

Javier Sigro and Dr. Linden Ashcroft was fundamental to achieve this item and, thanks to two unknown referees, it was published reaching the standards of this high level research journal.

The article "Historical shifts in oxygenation regime as recorded in the laminated sediments of lake Montcortès (central Pyrenees): a continental-scale phenomenon?" constitutes chapter 4 and has been submited to Science of the Total Enviorment journal (STOTEN). STOTEN is an international journal speciallized on studies which focus on the interaction of the atmosphere, hydrosphere, biosphere, lithosphere, and anthroposphere (journal impact factor 4.900 in 2016 from the Q1 in Environmental Sciences). This article is leaded by Dr. Teresa Vegas-Vilarrúbia, the IP of Montcortès-500 project, followed by Dr. Pablo Corella. Their expertise contributes with the most reliability in the limnological results and allows to me to cooperate with analyses on the potential relationships between sediment proxies of the lake's oxygen shifts over time and climate.

Chapter 5 presents the preliminary results of the draft of the article "Role of North Atlantic weather regimes in central Pyrenees climate from instrumental and tree-ring data". This work is being developed with the support of Dr. Myriam Khodri and Dr. Javier Sigró, the data provided by Dr. Emilia Gutiérrez.

Finally, chapter 6 present the conclusions and most important remarks of the articles presented, as well as future work proposals.

1.5. References

Ackerman SA, Knox J. 2006. *Meteorology: understanding the atmosphere*. Brooks/Cole, 575 pp.

Aguilar E, Auer I, Brunet M, Peterson TC, Wieringa J. 2003. *Guidelines on climate metadata and homogenization*. World Meteorological Organization: World Climate Programme Data and Monitoring WCDMP-No. 53, WMO-TD No. 1186. WMO: Geneva (Switzerland), 55 pp.

Aranbarri J, Pérez-Sanz A, Gil-Romera G, Moreno A, Leunda M, Sevilla-Callejo M, Corella JP, Morellón M, Oliva B, Valero-Garcés B. 2017. Environmental and climate change in the southern Central Pyrenees since the Last Glacial Maximum: A view from the lake records. *Catena* **149**(3): 668–688. DOI: 10.1016/j.catena.2016.07.041.

Ariño AH, Otegui J, Villarroya A, Zabalza AP De. 2012. Primary Biodiversity Data Records in the Pyrenees. *Environmental Engineering and Management Journal* **11**(6): 1059–1075.

Barry RG. 2008. *Mountain weather and climate*. Routledge: London (UK), 402 pp.

Barry RG. 2012. Recent advances in mountain climate research. *Theoretical and Applied Climatology*. Springer Vienna **110**(4): 549–553. DOI: 10.1007/s00704-012-0695-x.

Beguería S, López-Moreno JI, Lorente A, Seeger M, García-Ruiz JM. 2003. Assessing the Effect of Climate Oscillations and Land-use Changes on Streamflow in the Central Spanish Pyrenees. *AMBIO: A Journal of the Human Environment* **32**(4): 283–286. DOI: 10.1579/0044-7447-32.4.283.

Beniston M. 2006. Mountain Climates and Climatic Change: An Overview of Processes Focusing on the European Alps. *Pure and Applied Geophysics* **162**(8): 1587–1606. DOI: 10.1007/s00024-005-2684-9.

Beniston M. 2003. Climatic change in mountain regions: A review of possible impacts. *Climatic Change* **59**(1): 5–31. DOI: 10.1023/A:1024458411589.

Briffa KR, Osborn TJ, Schweingruber FH. 2004. Large-scale temperature inferences from tree rings: a review. *Global and Planetary Change* **40**(1): 11–26. DOI: 10.1016/S0921-8181(03)00095-X.

Brunet M, Saladié O, Jones P, Sigró J, Aguilar E, Moberg A, Lister D, Walther A, Almarza C. 2002. *A case-study/guidance on the development of long-term daily adjusted temperature datasets*. World Meteorological lOrganization: WCDMP-66/WMO-TD-1425, Geneva (Switzerland), 43 pp.

Buchdahl J. 1999. *Global climate change student guid : a review of contemporary and prehistoric global climate change*. Manchester Metropolitan University: Manchester, 99 pp.

Buisan ST, Saz MA, López-Moreno JI. 2015. Spatial and temporal variability of winter snow and precipitation days in the western and central Spanish Pyrenees. *International Journal of Climatology* **35**(2): 259–274. DOI: 10.1002/joc.3978.

Buisan S, López-Moreno J, Saz M, Kochendorfer J. 2016. Impact of weather type variability on winter precipitation, temperature and annual snowpack in the Spanish Pyrenees. *Climate Research* **69**(1): 79–92. DOI: 10.3354/cr01391.

Büntgen U, Frank D, Grudd H, Esper J. 2008. Long-term summer temperature variations in the Pyrenees. *Climate Dynamics* **31**(6): 615–631. DOI: 10.1007/s00382-008-0390-x.

Büntgen U, Krusic PJ, Verstege A, Barreda GS, Wagner S, Camarero JJ, Ljungqvist FC, Zorita E, Oppenheimer C, Konter O, Tegel W, Gärtner H, Cherubini P, Reinig F, Esper J. 2017. New tree-ring evidence from the Pyrenees reveals Western Mediterranean climate variability since medieval times. *Journal of Climate* [in press]. DOI: 10.1175/JCLI-D-16-0526.1.

Caruso BS, King R, Newton S, Zammit AC. 2017. Simulation of climate change effects on hydropower operations in mountain headwater lakes, New Zealand. *River Research and Applications* **33**(1): 147–161. DOI: 10.1002/rra.3056.

Cía JC, Andrés AJ, Sánchez MAS, Novau JC, Moreno JIL. 2005. Responses to climatic changes since the Little Ice Age on Maladeta Glacier (Central Pyrenees). *Geomorphology* **68**(3): 167–182. DOI: 10.1016/j.geomorph.2004.11.012.

Comunidad de trabajo de los Pirineos. 2006. *Atlas estadístico del Pirineo*. *http://atlas.ctp.org/site_es/p1_present_es.php [accessed 4 April 2017]*.

Corella JP, Valero-Garcés BL, Vicente- Serrano SM, Brauer A, Benito G. 2016. Three millennia of heavy rainfalls in Western Mediterranean: frequency, seasonality and atmospheric drivers. *Scientific Reports*. Nature Publishing Group **6**(38206): 1–11. DOI: 10.1038/srep38206.

Corella JP, Valero-Garcés BL, Wang F, Martínez-Cortizas A, Cuevas CA, Saiz-Lopez A. 2017. 700 years reconstruction of mercury and lead atmospheric deposition in the Pyrenees (NE Spain). *Atmospheric Environment* **155**: 97–107. DOI: 10.1016/j.atmosenv.2017.02.018.

Corella JP. 2009. Facies laminadas en la secuencia sedimentaria del lago de Montcortés (Lleida) durante los últimos 6.000 años. *Geogaceeta* **46**: 103–106.

Corella JP, Amrani A El, Sigró J, Morellón M, Rico E, Valero-Garcés BL. 2011. Recent evolution of Lake Arreo, northern Spain: influences of land use change and climate. *Journal of Paleolimnology*. Springer Netherlands **46**(3): 469–485. DOI: 10.1007/s10933-010-9492-7.

Corella JP, Brauer A, Mangili C, Rull V, Vegas-Vilarrúbia T, Morellón M, Valero-Garcés BL. 2012. The 1.5-ka varved record of Lake Montcortès (southern Pyrenees, NE Spain). *Quaternary Research* **78**(2): 323–332. DOI: 10.1016/j.yqres.2012.06.002.

Coulter JD. 1967. Mountain climate. *New Zealand Ecological Society* **14**(14): 40–57.Cuadrat JM, Serrano R, Saz MA, Tejedor E, Prohom M, Cunillera J, Esteban P. 2013. Creación de una base de datos homogenizada de temperaturas para los Pirineos (1950-2010). *Geographicalia* **63**–**64**: 63–74.

Dee D, Fasullo J, Shea D, Walsh J, National Center for Atmospheric Research Staff. 2016. *The Climate Data Guide: Atmospheric Reanalysis: Overview & Comparison*

Tables. https://climatedataguide.ucar.edu/climate-data/atmospheric-reanalysis-overview-comparison-tables [accessed 10 April 2017].

Dorado Liñán I, Büntgen U, González-Rouco F, Zorita E, Montávez JP, Gómez-Navarro JJ, Brunet M, Heinrich I, Helle G, Gutiérrez E. 2012. Estimating 750 years of temperature variations and uncertainties in the Pyrenees by tree-ring reconstructions and climate simulations. *Climate of the Past* **8**(3): 919–933. DOI: 10.5194/cp-8-919-2012.

Duquense C. 2008. Faire du l'observatoire du changement climatique dans le Pyrénées un outil d'aide à la decision. Univeristé Joseph Fourier.

Ekhart E. 1948. De la structure de l'atmosphère dans la montagne. *La Météorologie* **3**(3): 3–26.

Esper J, Konter O, Krusic PJ, Saurer M, Holzkämper S, Büntgen U. 2015. Long-term summer temperature variations in the Pyrenees from detrended stable carbon isotopes. *Geochronometria* **42**(1): 53–59. DOI: 10.1515/geochr-2015-0006.

Esteban P, Prohom M, Aguilar E. 2012. Tendencias recientes e índices de cambio climático de la temperatura y la precipitación en Andorra, Pirineos (1935-2008). *Pirineos* **167**: 87–106. DOI: 10.3989/Pirineos.2012.167005.

Esteban P, Prohom M, Aguilar E, Mestre O. 2007. Temporal and spatial temperature variability and change over Spain during 1850–2005. *Journal of Geophysical Research* **112**(D12): D12117. DOI: 10.1029/2006JD008249.

García-Ruiz JM, Valero-Garcés BL, Martí-Bono C, González-Sampériz P. 2003. Asynchroneity of maximum glacier advances in the central Spanish Pyrenees. *Journal of Quaternary Science*. John Wiley & Sons, Ltd. **18**(1): 61–72. DOI: 10.1002/jqs.715.

Gaume E, Livet M, Desbordes M, Villeneuve J-P. 2004. Hydrological analysis of the river Aude, France, flash flood on 12 and 13 November 1999. *Journal of Hydrology* **286**(1): 135–154. DOI: 10.1016/j.jhydrol.2003.09.015.

Gold C. 2009. *Varves in lacustrine sediments – an overview*. www.geo.tu-freiberg.de *[accessed 10 May 2017]*,11 pp.

González-Sampériz P, Valero-Garcés BL, Moreno A, Jalut G, García-Ruiz JM, Martí-Bono C, Delgado-Huertas A, Navas A, Otto T, Dedoubat JJ. 2006. Climate variability in the Spanish Pyrenees during the last 30,000 yr revealed by the El Portalet sequence. *Quaternary Research* **66**(1): 38–52. DOI: 10.1016/j.yqres.2006.02.004.

Goosse H. 2015. *Climate system dynamics and modelling*. Cambridge University Press: Louvain, 358 pp.

Gray ST, Graumlich LJ, Betancourt JL, Pederson GT. 2004. A tree-ring based reconstruction of the Atlantic Multidecadal Oscillation since 1567 A.D. *Geophysical Research Letters* **31**(12): 1-4. DOI: 10.1029/2004GL019932.

Gutiérrez F, Gutiérrez M, Sancho C. 1998. Geomorphological and sedimentological analysis of a catastrophic flash flood in the Arás drainage basin (Central Pyrenees, Spain). *Geomorphology* **22**(3–4): 265–283. DOI: 10.1016/S0169-555X(97)00087-1.

Henderson-Sellers A, Robinson PJ. 1986. *Contemporary climatology*. Longman Scientific & Technical.Hulme M, Jones PD. 1994. Global climate change in the instrumental period. *Environmental Pollution* **83**(1–2): 23–36. DOI: 10.1016/0269-7491(94)90019-1.

IPCC. 2001. *Climate Change 2001: The Scientific Basis. Contribution of Working Group I to the Third Assessment Report of the Intergovernmental Panel on Climate Change. Climate Change 2001: The Scientific Basis. Contribution of Working Group I to the Third Assessment Report of the Intergovernmental Panel on Climate Change.* Cambridge University Press: Cambrige, United Kingdom and New York, USA. DOI: 10.1256/004316502320517344, 881 pp.

IPCC. 2007. Climate Change 2007: impacts, adaptation and vulnerability. In: Parry ML, Canziani OF, Palutikof JP, van der Linden PJ and Hanson CE (eds) *Climate Change 2007: Impacts, Adaptation and Vulnerability. Contribution of Working Group II to the Fourth Assessment Report of the Intergovernmental Panel on Climate Change*. Cambridge University Press: Cambridge, UK, 976 pp.

Konter O, Holzkämper S, Helle G, Büntgen U, Saurer M, Esper J. 2014. Climate sensitivity and parameter coherency in annually resolved δ13C and δ18O from Pinus

uncinata tree-ring data in the Spanish Pyrenees. *Chemical Geology* **377**: 12–19. DOI: 10.1016/j.chemgeo.2014.03.021.

Kotlarski S, Lüthi D, Schär C. 2015. The elevation dependency of 21st century European climate change: an RCM ensemble perspective. *International Journal of Climatology*. Wiley Subscription Services, Inc., A Wiley Company **35**(13): 3902–3920. DOI: 10.1002/joc.4254.

Laborie JP, Pala JM. 1989. *El Pirineo, presentación de una montaña fronteriza*. Madrid, 121 pp.

Letcher TW, Minder JR, Letcher TW, Minder JR. 2017. The Simulated Response of Diurnal Mountain Winds to Regionally Enhanced Warming Caused by the Snow Albedo Feedback. *Journal of the Atmospheric Sciences* **74**(1): 49–67. DOI: 10.1175/JAS-D-16-0158.1.

Li B, Nychka DW, Ammann CM. 2010. The Value of Multiproxy Reconstruction of Past Climate. *Journal of the American Statistical Association*. Taylor & Francis **105**(491): 883–895. DOI: 10.1198/jasa.2010.ap09379.

López-Moreno JI. 2005. Recent Variations of Snowpack Depth in the Central Spanish Pyrenees. *Arctic, Antarctic, and Alpine Research* **37**(2): 253–260. DOI: 10.1657/1523-0430(2005)037[0253:RVOSDI]2.0.CO;2.

López-Moreno JI, Beguería S, García-Ruiz JM. 2006. Trends in high flows in the central Spanish Pyrenees: response to climatic factors or to land-use change? *Hydrological Sciences Journal* **51**(6): 1039–1050. DOI: 10.1623/hysj.51.6.1039.

López-Moreno JI, Beniston M. 2008. Daily precipitation intensity projected for the 21st century: seasonal changes over the Pyrenees. *Theoretical and Applied Climatology* **95**(3): 375–384. DOI: 10.1007/s00704-008-0015-7.

López-Moreno JI, El-Kenawy A, Revuelto J, Azorín-Molina C, Morán-Tejeda E, Lorenzo-Lacruz J, Zabalza J, Vicente-Serrano SM. 2014. Observed trends and future projections for winter warm events in the Ebro basin, northeast Iberian Peninsula. *International Journal of Climatology* **34**(1): 49–60. DOI: 10.1002/joc.3665.

López-Moreno JI, Goyette S, Beniston M. 2009. Impact of climate change on snowpack in the Pyrenees: Horizontal spatial variability and vertical gradients. *Journal of Hydrology* **374**(3–4): 384–396. DOI: 10.1016/j.jhydrol.2009.06.049.

López-Moreno JI, Goyette S, Beniston M. 2008. Climate change prediction over complex areas: spatial variability of uncertainties and prediction over the Pyrenees from a set of regional climate models. *International Journal of Climatology* **28**(11): 1535–1550. DOI: 10.1002/joc1645.

López-Moreno JI, Vicente-Serrano SM, Zabalza J, Beguería S, Lorenzo-Lacruz J, Azorin-Molina C, Morán-Tejeda E. 2013. Hydrological response to climate variability at different time scales: A study in the Ebro basin. *Journal of Hydrology* **477**: 175–188. DOI: 10.1016/j.jhydrol.2012.11.028.

López-Moreno JI, Vicente-Serrano SM. 2007. Atmospheric circulation influence on the interannual variability of snow pack in the Spanish Pyrenees during the second half of the 20th century. *Nordic Hidrology* **38**(1): 33–44. DOI: 10.2166/nh.2007.030.

Mann ME, Zhang Z, Rutherford S, Bradley RS, Hughes MK, Shindell D, Ammann C, Faluvegi G, Ni F. 2009. Global signatures and dynamical origins of the Little Ice Age and Medieval Climate Anomaly. *Science (New York, N.Y.)*. American Association for the Advancement of Science **326**(5957): 1256–1260. DOI: 10.1126/science.1177303.

Marín-Yaseli ML, Martínez TL. 2003. Competing for Meadows. *Mountain Research and Development* **23**(2): 169–176. DOI: 10.1659/0276-4741(2003)023[0169:CFM]2.0.CO;2.

Mazier F, Bard E. 2016. Pyrenean Erosion fluxes over the Neoglacial period: From local meteorological climate dynamics to global ones. *Geophysical Research Abstracts EGU General Assembly Anaëlle Simonneau Emmanuel Chapron Hervé Guyard* **18**(12234): 2016–17689.

Moberg A, Sonechkin DM, Holmgren K, Datsenko NM, Karlén W. 2005. Highly variable Northern Hemisphere temperatures reconstructed from low- and high-resolution proxy data. *Nature*. Nature Publishing Group **433**(7026): 613–617. DOI: 10.1038/nature03265.

Morellón M, Pérez-Sanz A, Corella JP, Büntgen U, Catalán J, González-Sampériz P, González-Trueba JJ, López-Sáez JA, Moreno A, Pla-Rabes S, Saz-Sánchez MÁ, Scussolini P, Serrano E, Steinhilber F, Stefanova V, Vegas-Vilarrúbia T, Valero-Garcés B. 2012. A multi-proxy perspective on millennium-long climate variability in the southern Pyrenees. *Climate of the Past*. Copernicus GmbH **8**(2): 683–700. DOI: 10.5194/cp-8-683-2012.

Morellón M, Valero-Garcés B, Anselmetti F, Ariztegui D, Schnellmann M, Moreno A, Mata P, Rico MT, Corella JP. 2009. Late Quaternary deposition and facies model for karstic Lake Estanya (North-eastern Spain). *Sedimentology*. Blackwell Publishing Ltd **56**(5): 1505–1534. DOI: 10.1111/j.1365-3091.2008.01044.x.

Moreno A, Pérez A, Frigola J, Nieto-Moreno V, Rodrigo-Gámiz M, Martrat B, González-Sampériz P, Morellón M, Martín-Puertas C, Corella JP, Belmonte Á, Sancho C, Cacho I, Herrera G, Canals M, Grimalt JO, Jiménez-Espejo F, Martínez-Ruiz F, Vegas-Vilarrúbia T, Valero-Garcés BL. 2012. The Medieval Climate Anomaly in the Iberian Peninsula reconstructed from marine and lake records. *Quaternary Science Reviews* **43**: 16–32.

Muntán E, García C, Oller P, Martí G, García A, Gutiérrez E. 2009. Reconstructing snow avalanches in the Southeastern Pyrenees. *Nat. Hazards Earth Syst. Sci* **9**(5): 1599–1612.

National Research Council. 2001. *Climate Change Science: An analysis of some key questions*. National Academies Press: Washington, D.C. DOI: 10.17226/10139, 42 pp.

National Research Council. 2012. *The Effects of Solar Variability on Earth's Climate*. National Academies Press: Washington, D.C. DOI: 10.17226/13519, 70 pp.

Nesje A, Bakke J, Dahl SO, Lie Ø, Matthews JA. 2008. Norwegian mountain glaciers in the past, present and future. *Global and Planetary Change* **60**(1): 10–27. DOI: 10.1016/j.gloplacha.2006.08.004.

Notivoli RS, Prohom M, Cuadrat JM, Cunillera J, Sánchez MASAZ, Vargas ET, Esteban P, Soubeyroux J, Deaux N. 2013. Creation of a homogenized climate data base

for the Pyrenees mountain range. *9th EUMETNET Data Management Workshop*. Madrid.

OPCC. 2013. *Estudio sobre la adaptación al cambio climático en los Pirineos*. *http://www.opcc-ctp.org/etudes/synthese_biblio_climat.pdf [accessed 11 November 2016]*, 137p.

Owen LA, Thackray G, Anderson RS, Briner J, Kaufman D, Roe G, Pfeffer W, Yi C. 2009. Integrated research on mountain glaciers: Current status, priorities and future prospects. *Geomorphology* **103**(2): 158–171. DOI: 10.1016/j.geomorph.2008.04.019.

Pallas R, Rodes A, Braucher R, Bourles D, Delmas M, Calvet M, Gunnell Y. 2010. Small, isolated glacial catchments as priority targets for cosmogenic surface exposure dating of Pleistocene climate fluctuations, southeastern Pyrenees. *Geology*. Geological Society of America **38**(10): 891–894. DOI: 10.1130/G31164.1.

Parker WS. 2016. Reanalyses and Observations: What's the Difference? *Bulletin of the American Meteorological Society* **97**(9): 1565–1572. DOI: 10.1175/BAMS-D-14-00226.1.

Pepin N, Bradley RS, Diaz HF, Baraer M, Caceres EB, Forsythe N, Fowler H, Greenwood G, Hashmi MZ, Liu XD, Miller JR, Ning L, Ohmura A, Palazzi E, Rangwala I, Schöner W, Severskiy I, Shahgedanova M, Wang MB, Williamson SN, Yang DQ. 2015. Elevation-dependent warming in mountain regions of the world. *Nature Climate Change* **5**(5): 424–430. DOI: 10.1038/nclimate2563.

Pérez-Zanón N, Sigró J, Ashcroft L. 2017. Temperature and precipitation regional climate series over the central Pyrenees during 1910–2013. *International Journal of Climatology* **37**(4):1922–1937. DOI: 10.1002/joc.4823.

Pérez-Zanón N, Sigró J, Domonkos P, Ashcroft L. 2015. Comparison of HOMER and ACMANT homogenization methods using a central Pyrenees temperature dataset. *Advances in Science and Research*. Copernicus GmbH **12**(1): 111–119. DOI: 10.5194/asr-12-111-2015.

Plummer N, Allsopp T, Lopez JA. 2003. *Guidelines on Climate Observation Networks and Systems*. WMO/TD No. 1185.

Portis DH, Walsh JE, Lamb PJ. 2001. Seasonality of the North Atlantic Oscillation. American Meteorological Society 14: 2069-2078. DOI: 10.1175/1520-0442(2001)014<2069:SOTNAO>2.0.CO;2.

Rull V, Trapote MC, Safont E, Cañellas-Boltà N, Pérez-Zanón N, Sigró J, Buchaca T, Vegas-Vilarrúbia T. 2017. Seasonal patterns of pollen sedimentation in Lake Montcortès (Central Pyrenees) and potential applications to high-resolution paleoecology: a 2-year pilot study. *Journal of Paleolimnology* **57**(1): 95–108. DOI: 10.1007/s10933-016-9933-z.

Rull V, Vegas-Vilarrúbia T. 2015. Crops and weeds from the Estany de Montcortés catchment, central Pyrenees, during the last millennium: A comparison of palynological and historical records. *Vegetation History and Archaeobotany*. Springer New York LLC **24**(6): 699–710. DOI: 10.1007/s00334-015-0525-z.

Rull V, Vegas-Vilarrubia T. 2014. Preliminary report on a mid-19th century Cannabis pollen peak in NE Spain: Historical context and potential chronological significance. *The Holocene*. SAGE PublicationsSage UK: London, England **24**(10): 1378–1383. DOI: 10.1177/0959683614540964.

Schiefer E, Gilbert R, Hassan MA. 2011. A lake sediment-based proxy of floods in the Rocky Mountain Front Ranges, Canada. *Journal of Paleolimnology*. Springer Netherlands **45**(2): 137–149. DOI: 10.1007/s10933-010-9485-6.

Schmidt R, Koinig KA, Thompson R, Kamenik C. 2002. A multi proxy core study of the last 7000 years of climate and alpine land-use impacts on an Austrian mountain lake (Unterer Landschitzsee, Niedere Tauern). *Palaeogeography, Palaeoclimatology, Palaeoecology* **187**(1): 101–120. DOI: 10.1016/S0031-0182(02)00511-4.

Schneider L, Smerdon JE, Büntgen U, Wilson RJS, Myglan VS, Kirdyanov A V., Esper J. 2015. Revising midlatitude summer temperatures back to A.D. 600 based on a wood density network. *Geophysical Research Letters* **42**(11): 4556–4562. DOI: 10.1002/2015GL063956.

Schulte L, Peña JC, Carvalho F, Schmidt T, Julià R, Llorca J, Veit H. 2015. A 2600-year history of floods in the Bernese Alps, Switzerland: frequencies, mechanisms and

climate forcing. *Hydrol. Earth Syst. Sci* **19**(7): 3047–3072. DOI: 10.5194/hess-19-3047-2015.

Shi X, Durran DR, Shi X, Durran DR. 2014. The Response of Orographic Precipitation over Idealized Midlatitude Mountains Due to Global Increases in CO_2. *Journal of Climate* **27**(11): 3938–3956. DOI: 10.1175/JCLI-D-13-00460.1.

Shiogama H, Stone D, Emori S, Takahashi K, Mori S, Maeda A, Ishizaki Y, Allen MR, Brunner S, Eickemeier P, Kriemann B, Savolainen J, Schlömer S, Stechow C von, Zwickel T, Minx JC. 2016. Predicting future uncertainty constraints on global warming projections. *Scientific Reports*. Nature Publishing Group **6**(1): 18903. DOI: 10.1038/srep18903.

Smithers J, Smit B. 1997. Human adaptation to climatic variability and change. *Global Environmental Change* **7**(2): 129–146. DOI: 10.1016/S0959-3780(97)00003-4.

Stephen EM, Rudmann-Maurer K, Körner C. 2010. *Mountain Biodiversity and Global Change*. Global Mountain Biodiversity Assessment (GMBA) of DIVERSITAS: Basel, 64 pp.

Stoffel M, Khodri M, Corona C, Guillet S, Poulain V, Bekki S, Guiot J, Luckman BH, Oppenheimer C, Lebas N, Beniston M, Masson-Delmotte V. 2015. Estimates of volcanic-induced cooling in the Northern Hemisphere over the past 1,500 years. *Nature Geoscience* **8**(10): 784–788. DOI: 10.1038/ngeo2526.

Street-Perrott FA, Barker PA, Swain DL, Ficken KJ, Wooller MJ, Olago DO, Huang Y. 2007. Late Quaternary changes in ecosystems and carbon cycling on Mt. Kenya, East Africa: a landscape-ecological perspective based on multi-proxy lake-sediment influxes. *Quaternary Science Reviews* **26**(13): 1838–1860. DOI: 10.1016/j.quascirev.2007.02.014.

Tardif J, Camarero JJ, Ribas M, Gutiérrez E. 2003. Spatiotemporal variability in tree growth in the Central Pyrenees: Climatic and site influences. *Ecological Monographs* **73**(2): 241–257.

United Nations framework Convention on Climate Change. 2015. *Adoption of the Paris agreement*.

ttp://unfccc.int/files/essential_background/convention/application/pdf/english_paris_agreement.pdf [accessed 24 April 2017]. Paris, 27 pp.

Vegas-Vilarrúbia T, González-Sampériz P, Morellón M, Gil-Romera G, Pérez-Sanz A, Valero-Garcés B. 2013. Diatom and vegetation responses to Late Glacial and Early Holocene climate changes at Lake Estanya (Southern Pyrenees, NE Spain). *Palaeogeography, Palaeoclimatology, Palaeoecology* **392**: 335–349. DOI: 10.1016/j.palaeo.2013.09.011.

Vinet F. 2008. Geographical analysis of damage due to flash floods in southern France: The cases of 12–13 November 1999 and 8–9 September 2002. *Applied Geography* **28**(4): 323–336. DOI: 10.1016/j.apgeog.2008.02.007.

Vuille M, Garreaud RD. 2012. Ocean–Atmosphere Interactions on Interannual to Decadal Time Scales. *The SAGE Handbook of Environmental Change: Volume 1*. SAGE Publications Ltd: 1 Oliver's Yard, 55 City Road, London EC1Y 1SP United Kingdom, 471–496. DOI: 10.4135/9781446253045.n22.

World Meteorological Organization. 2011. *Guide to Climatological Practices*. Geneva, 113 pp.

Chapter 2 — Comparison of homogenization methods

Pérez-Zanón, N., Sigró, J., Domonkos, P., Ashcroft, L., 2015. Comparison of HOMER and ACMANT homogenization methods using a central Pyrenees temperature dataset. Adv. Sci. Res. 12, 111–119. doi:10.5194/asr-12-111-2015

Adv. Sci. Res., 12, 111–119, 2015
www.adv-sci-res.net/12/111/2015/
doi:10.5194/asr-12-111-2015

Advances in Science & Research
Open Access Proceedings

14th EMS Annual Meeting & 10th European Conference on Applied Climatology (ECAC)

Comparison of HOMER and ACMANT homogenization methods using a central Pyrenees temperature dataset

N. Pérez-Zanón, J. Sigró, P. Domonkos, and L. Ashcroft

Center for Climate Change (C3), Campus Terres de l'Ebre, Universitat Rovira i Virgili, Tortosa, Spain

Correspondence to: N. Pérez-Zanón (nuria.perez@urv.cat)

Received: 13 January 2015 – Revised: 19 May 2015 – Accepted: 27 May 2015 – Published: 9 June 2015

Abstract. The aim of this research is to compare the results of two modern multiple break point homogenization methods, namely ACMANT and HOMER, over a Pyrenees temperature dataset in order to detect differences between their outputs which can affect future studies. Both methods are applied to a dataset of 44 monthly maximum and minimum temperature series placed around central Pyrenees and covering the 1910–2013 period. The results indicate that the automatic method ACMANT produces credible results. While HOMER detects more breaks supported by metadata, this method is also more dependent on the user skill and thus sensitive to subjective errors.

1 Introduction

The latest report of the Intergovernmental Panel on Climate Change indicates that the Mediterranean region is one of the most vulnerable areas of the Earth to global warming (Barros et al., 2014).

The Pyrenees in southwestern Europe is a particularly valuable mountain range because of its biodiversity and water resources which allow population development through agriculture, hydropower energy and tourism (López-Moreno et al., 2008). Future climate scenarios indicate that a decrease in snow cover in this region is likely during the next century (López-Moreno et al., 2009). Therefore it is essentially important to learn and understand more precisely the climate and climate change of this important area.

For any type of climate analysis, including paleoclimatology studies, which use climate series for calibration of the proxies (Bradley, 1999), the use of a high-quality observed dataset is essential. There are several reasons why inhomogeneities (changes in the meteorological records due to non-climatic factors) occur in observational series, such as stations relocation, changes in the environment around the station, changes in the observing time (Aguilar et al., 2003; Brunet et al., 2008).

To detect and correct inhomogeneities, a large number of methods have been developed (Venema et al., 2012). In the present study, two modern multiple break point homogenization methods developed during the Action COST-ES0601 (HOME), namely HOMER (HOMogenization software in R, Mestre et al., 2013) and ACMANT (Adapted Caussinus-Mestre Algorithm for Networks of Temperature series, Domonkos, 2011b), are used. We considered it important to select methods that treat multiple occurences of inhomogeneities with adequate statistical tools, as observed temperature series usually contain 5 or more inhomogeneities per 100 years on average (Domonkos, 2011a; Venema et al., 2012; Willett et al., 2014). While ACMANT is fully automatic, and thus convenient to use for large datasets, the use of HOMER can include the consideration of metadata (document information about the geographical and technical evolution of the observations) because HOMER is an interactive method.

Previous studies in the Pyrenees have developed homogenized series for different spatial and temporal coverage: Bücher and Dessens (1991) examined one station using a bivariate test to detect systematic changes in the mean, while Esteban et al. (2012) used HOMER to homogenize three stations in Andorra. Cuadrat et al. (2013) have recently produced a homogenized dataset for the whole Pyrenees but only for the 1950–2010 period.

For this study, 123 series of either automatic or manual observations were gathered around the Pyrenees covering 1910–2013. Section 2 describes the data in more detail, while

Published by Copernicus Publications.

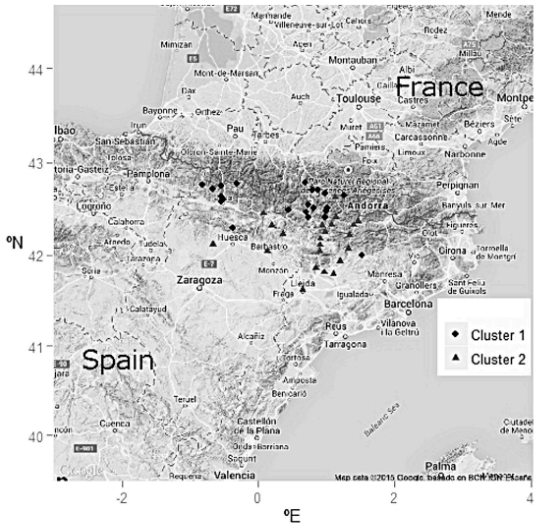

Figure 1. Location of the study area and stations in cluster 1 (black circles) and cluster 2 (grey triangles) using RGoogleMaps package (Kilibarda and Bajat, 2012).

Sect. 3 presents the homogenization methods employed. In Sect. 4, we show the comparison between the two homogenization techniques before drawing conclusions in Sect. 5.

2 Data

The Pyrenees is a mountainous region located in the southwest of Europe and influenced by Atlantic and Mediterranean climate features (e.g. López-Moreno et al., 2008). For this region, 123 series were obtained from the Spanish National Meteorology Agency (AEMET) and the Catalonia Meteorological Service (SMC). The series are of various lengths and cover the period 1910–2013. To develop long-term series, short periods of neighbouring observations were merged and the date of the combination was stored as metadata. The maximum distance accepted in combinations was 7.7 km (in Boí), while the mean difference of altitude was 147 m due to the complexity of the terrain.

Internal consistencies and temporal coherency quality control tests were run on the daily data, following Brunet et al. (2008). More than 834 000 values for each variable (maximum and minimum daily temperature) were examined, with 61 values corrected and 573 set to missing.

Monthly averages of maximum (T_{max}), minimum (T_{min}) and mean temperature (T_{mean}), calculated as the average of T_{max} and T_{min}, were calculated with the missing data tolerance that no more than 7 non-consecutive or 5 consecutive missing daily values for a month were allowed.

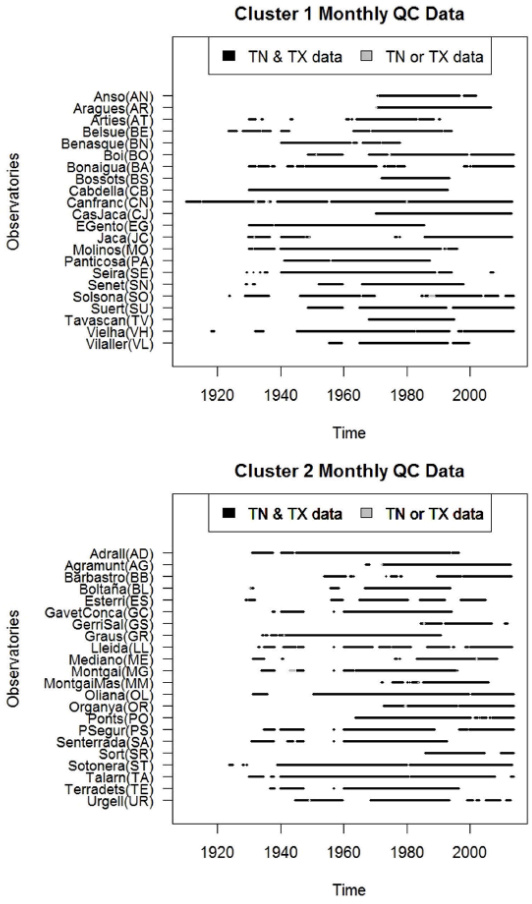

Figure 2. The temporal coverage of monthly maximum (T_X) and minimum (T_N) temperature data for each climatological cluster.

Monthly data must satisfy minimum requirements in terms of the length and completeness to run both HOMER and ACMANT. Finally, 44 T_{min} and 44 T_{max} series are included in the dataset prepared for the homogenization.

Next, the time series were sorted into two climatological clusters, applying a cluster analysis on monthly T_{mean} (see Sect. 3.1). Each cluster contained 22 series. For each cluster, monthly quality control was applied to detect additional outliers using the Fast QC routine included in HOMER. A total of 13 monthly values were removed from Cluster 1 and 34 from Cluster 2. The obtained series will be referred as QC data and the place and period of data coverage for each station is shown in Figs. 1 and 2.

To perform the comparison between the homogenization methods, only the periods homogenized by ACMANT (varies according to series) are taken into account (see

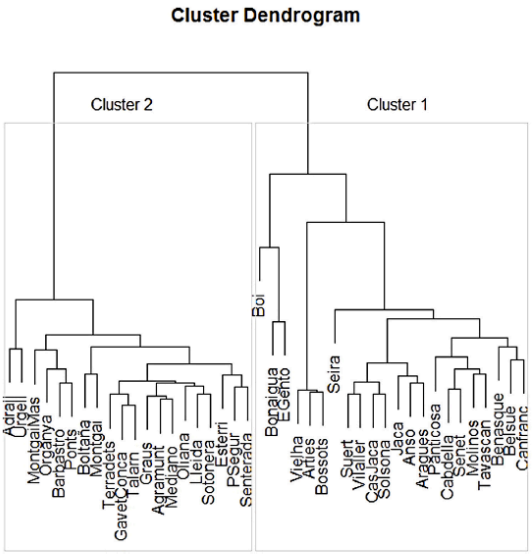

Figure 3. Result of the hierarchical cluster analysis on the first step of computation (see Sect. 3.1).

Sect. 3.3). For these periods, the percentages of monthly missing values ranges between 0.5 and 44 % and 31 series have less than 20 % of missing values.

3 Methodology

3.1 Cluster analysis

As HOMER is interactive software, in order to make the homogenization process more easily manageable, the series were split into two groups. Cluster analysis was applied on T_{mean} data, and not T_{max} or T_{min}, to reduce the likelihood of simultaneous breaks being clustered together. Euclidean distance was calculated between T_{mean} series after normalization (mean $= 0$; standard deviation $= 1$). A hierarchical cluster analysis was applied using Ward agglomeration method, where the analysis starts with as many clusters as the number of time series and the clusters are built by adding T_{mean} series of the least distance in each step (Wilks, 2011).

The Pyrenees series cover different sections of the period 1910–2013, and two pairs of series (EGento and Benasque, with Sort and GerriSal) do not have overlapping sections (see Fig. 2) making cluster analysis impossible. For this reason, the cluster analysis had to be performed twice: first, without the two non-overlapping series to define the two clusters, and second, changing the pairs of series, to include the series that were excluded in the first step to determine to which cluster they belong. The result of cluster analysis for the first step is shown in Fig. 3, and the excluded series were assigned to cluster 2.

3.2 Homogenization methods

Two modern homogenization methods, HOMER (Mestre et al., 2013) and ACMANT (Domonkos, 2011b, 2014) were applied. Both methods were developed during the HOME Cost Action (Venema et al., 2012). HOMER was designed to include the best segments and features of some other state-of-the-art methods: PRODIGE (Caussinus and Mestre, 2004), ACMANT and Joint Detection (Picard et al., 2011).

ACMANT can be applied on both daily and monthly data, but as HOMER works only with monthly data, we ran both methods on monthly data. The two methods have several similarities: both methods are based on the optimal step function fitting (Hawkins, 1972) with the Caussinus Lyazrhi criterion (Caussinus and Lyazrhi, 1997) for optimizing the number of steps (also referred to as "breaks"). Both methods also include the bivariate detection for shifts in the annual means and the summer–winter differences (Domonkos, 2011b), and the minimization of the residual variance (ANOVA, Caussinus and Mestre, 2004) in finding the optimal adjustment terms.

On the other hand, the two methods differ in several other aspects: while HOMER implements a pairwise comparison and a network-wide harmonization in the break detection, ACMANT uses weighted reference time series. A new feature of the most recent ACMANT version (Domonkos, 2014) is that it can also detect relatively short-term inhomogeneities, which are known to be important for long-term data quality (Domonkos, 2011a).

As ACMANT is fully automatic, it can easily be applied to large datasets, while the interactive HOMER allows human intervention to the homogenization procedure and it is possible to decide about the significance of indicated breaks, based on metadata or research experience (Mestre et al., 2013).

HOMER was run comparing all the stations from each cluster separately with annual and seasonal detection, while using ACMANT, again all the time series within clusters were used together and the outlier filtering "off" option was selected, as the input dataset had been quality controlled earlier. HOMER is a user dependent method, and the main way of running the program can be summarised in three steps. First, big break points are identified and corrected. The second step is to repeat the detection in order to evaluate which break points are identified by metadata, and detect those breaks which have smaller amplitude than previously corrected. Finally, annual series are compared by plotting QC data with the homogenized series output. These plots (not shown) allow the user to understand and review the corrections applied. For detection, the three available methods (pairwise detection, joint-segmentation method and ACMANT detection) were considered.

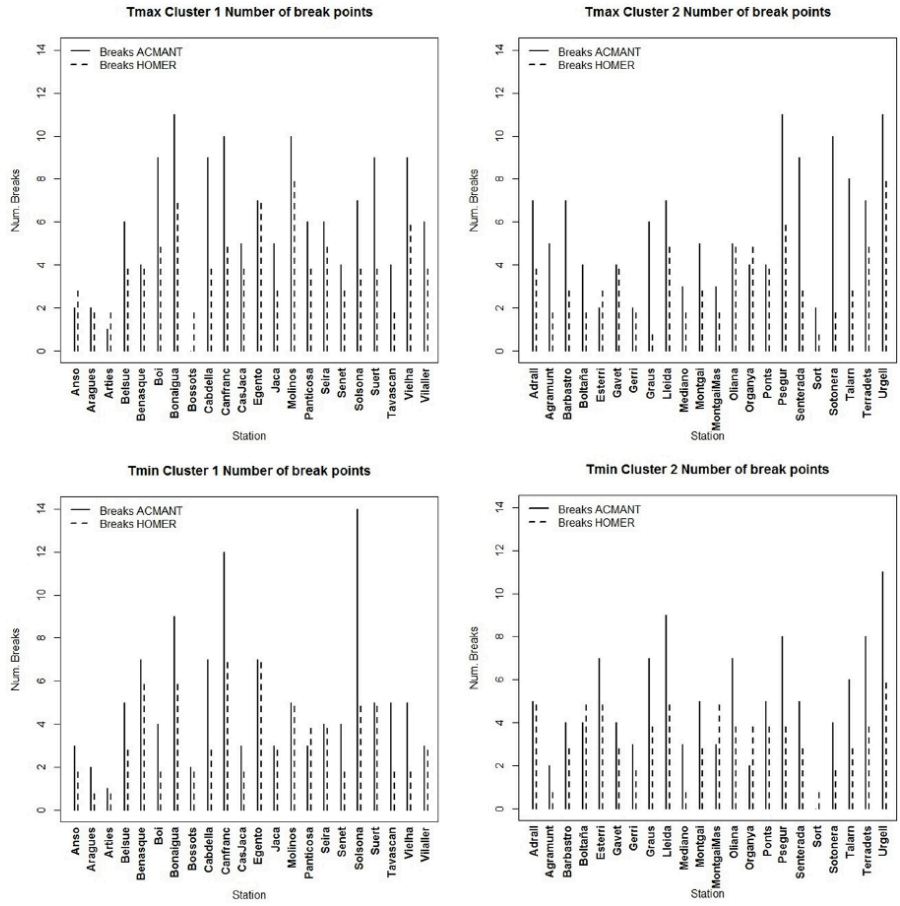

Figure 4. Number of break points detected by ACMANT (continuous line) and HOMER (dashed line) for each station for T_{max} (top panels) and T_{min} (bottom panels) in cluster 1 (left panels) and cluster 2 (right panels).

3.3 Comparison methods

Only periods with data in the QC dataset are considered to compare the output of the two homogenization methods. The period of examination was determined by ACMANT, because ACMANT needs at least 4 spatially comparable series for each section of the homogenization period and this minimum condition is stricter than that of HOMER.

The number of breaks detected by HOMER and ACMANT, spatial connections of homogenized data, as well as trend slopes of homogenized series were analysed. Spatial connections were examined using Spearman Correlation Coefficients (SCC) calculated between all pairs of monthly series for QC data, data homogenized by HOMER and data homogenized by ACMANT in each cluster. The trend analysis was calculated for the period 1961–1990 in all those stations with more than 80 % of the monthly data available during this period. 12 series met with this condition in each cluster. This analysis was performed by linear regression on the annual series including years in which all monthly values were available. Significance of trends was evaluated using the Student's t test ($p < 0.05$) (Wilks, 2011).

4 Results

4.1 Break point analysis

HOMER detected at least 1 break in all series, while ACMANT did not detect any break in two of the 88. However, the maximum number of breaks detected with ACMANT (14) was much higher than that with HOMER (8) as shown in Fig. 4. In 90% of the series ACMANT detected more breaks than HOMER. The average difference was 2 more breaks per series using ACMANT, which de-

Table 1. Slope trends in °C decade^{-1} for the period 1961–1990 for each station with more than 80 % of monthly data in this period. Significant trends (evaluated using the Student's t test with a significance level of $p < 0.05$) are shown in bold.

Cluster	Station	QC-T_{max} (°C dec^{-1})	HO-T_{max} (°C dec^{-1})	AC-T_{max} (°C dec^{-1})	QC-T_{min} (°C dec^{-1})	HO-T_{min} (°C dec^{-1})	AC-T_{min} (°C dec^{-1})
1	Arties	−0.20	0.01	0.27	−0.25	−0.22	0.00
1	Belsue	**0.94**	0.21	**0.68**	**0.64**	0.00	0.16
1	Cabdella	−0.17	0.06	**0.52**	0.00	−0.09	0.09
1	Canfranc	**0.82**	0.04	**0.59**	**0.88**	−0.03	0.15
1	Egento	**0.68**	−0.24	0.18	**1.75**	−0.27	0.03
1	Molinos	0.31	0.05	0.30	−0.10	−0.01	0.20
1	Panticosa	−0.16	0.05	**0.57**	−0.41	−0.13	0.15
1	Seira	0.17	−0.27	**0.44**	0.12	**−0.25**	0.00
1	Senet	0.24	0.15	**0.61**	−0.25	0.04	**0.45**
1	Suert	**0.70**	0.19	**0.75**	−0.21	0.06	0.20
1	Vielha	0.17	0.40	**0.63**	**0.26**	**0.25**	**0.26**
1	Vilaller	**1.21**	**0.39**	**0.77**	−0.01	0.06	0.16
2	Adrall	**1.60**	0.18	**0.32**	**1.25**	−0.01	−0.08
2	Boltaña	**1.04**	0.21	0.19	−0.27	0.24	−0.10
2	Gavet	**0.65**	0.23	**0.32**	−0.27	0.08	−0.12
2	Graus	−0.05	−0.05	0.28	0.29	0.12	−0.15
2	Montgai	**−1.06**	0.21	**0.32**	0.20	0.20	−0.01
2	Oliana	**0.59**	0.15	0.28	**1.15**	0.12	−0.11
2	Ponts	**1.32**	0.27	**0.47**	**−0.73**	**0.38**	0.21
2	Psegur	0.31	−0.01	0.21	**−0.83**	−0.21	−0.22
2	Senterada	**1.54**	0.25	**0.33**	−0.13	0.00	−0.06
2	Sotonera	−0.12	0.11	**0.37**	**0.26**	0.16	−0.05
2	Talarn	−0.20	0.12	**0.37**	−0.01	0.00	−0.01
2	Terradets	0.09	0.09	**0.35**	0.07	0.02	−0.09

tected 5.5 break points per series on average (10 break points per century), than with HOMER, which detected 3.6 (7 break points per century).

To evaluate the similarity between the results obtained by these homogenization methods, break points per year for each station were compared, considering that the timing of a break point can differ by up to 1 year between both methods due to the difference in the rest of break points. For T_{max} in cluster 1 (2), ACMANT detected 143 (126) break points of which 59 (51) were also detected by HOMER. For T_{min} in cluster 1 (2), ACMANT detected 113 (117) break points of which 49 (42) were also detected by HOMER.

As HOMER is an interactive method that allows the user to introduce known break points, all dates identified in the metadata were included. However, some were removed during the homogenization procedure because the magnitude of the break was less than 0.05 °C and their presence didn't show an improvement in the correction of the series compared with the QC data. From the 8 (15) metadata-supported breaks stored for cluster 1 (2), ACMANT detected 2 (4) break points for T_{min} and 4 (6) T_{max} (all of them detected also by HOMER), while HOMER detected 7 (12) for T_{min} and 6 (13) for T_{max}.

4.2 SCC comparison

SCC values are useful indicators to visualize the temporal linear relationship between time series before and after homogenization (Freitas et al., 2013), and in indicating the presence of large inhomogeneities when they exist. In general, the variance of the SCC for the series in cluster 1 was greater than that for cluster 2. The minimum correlation value for the first cluster was 0.65 while for the second cluster the minimum was 0.90, as shown in Figs. 5 and 6. One reason for this may be a large error in the Vielha observatory data (cluster 1) that was detected after the homogenization process: from 2004 to 2007 the seasonal cycle of temperature seems to be inverted or lagged by a few months for both T_{max} and T_{min} (Fig. 7), although the origin of this error is unknown. This error was detected and corrected adequately only for T_{max} with ACMANT. With HOMER, we failed to be recognized due to the smoothness of the annual values. This type of oversight could be avoided using the CLIMATOL QC check that is also included in HOMER. In ACMANT homogenization of T_{min} the seasonal cycle error remained untouched, while using HOMER, it was even propagated to earlier sections of the series.

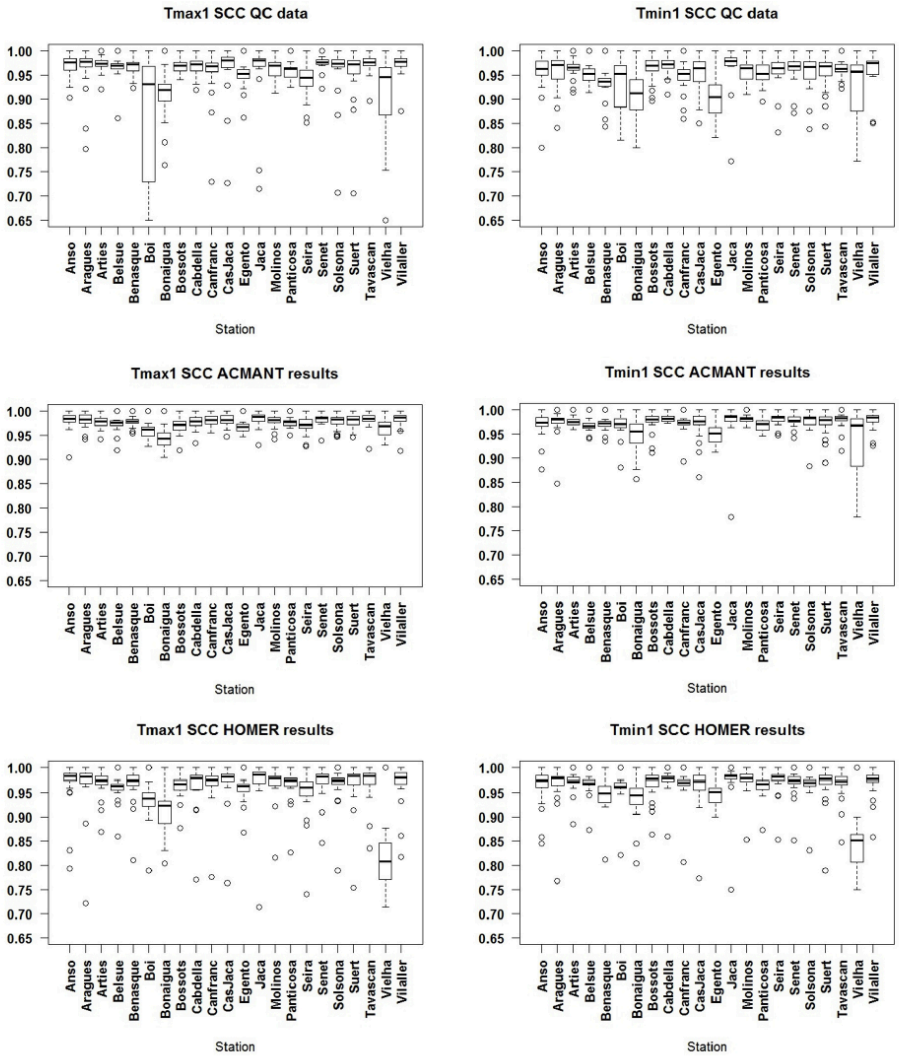

Figure 5. Boxplots of Spearman Correlation Coefficients of QC data (top panels), and ACMANT (middle panels) and HOMER (bottom panels) homogenized data for maximum (left panels) and minimum (right panels) temperature for stations in cluster 1.

4.3 Trend analysis

After homogenization, spatial gradients of trend slopes became smaller, and the number of significant positive trends was reduced as shown in Table 1.

For T_{max}, all 5 significant trends of the 12 series in cluster 1 were positive in the QC data. After homogenization with HOMER, the number of significant and positive trends decreased to 1, while with ACMANT it increased to 9. For cluster 2, 6 of the 12 series had positive and significant trends in the QC data. HOMER didn't return any significant trends for this cluster, while with ACMANT 8 significant positive trends were obtained. None of the homogenization methods returns negative and significant trends for T_{max}. For T_{min} of cluster 1, only 4 positive significant trends occurred in the QC data. HOMER returned 1 positive and 1 negative significant trends, while the ACMANT homogenized series produced 2 positive and zero negative trends. In cluster 2, the QC data presented 3 positive and 2 negative significant trends. After homogenizing, HOMER kept 1 positive but zero negative significant trends, while with ACMANT all trends were not significant.

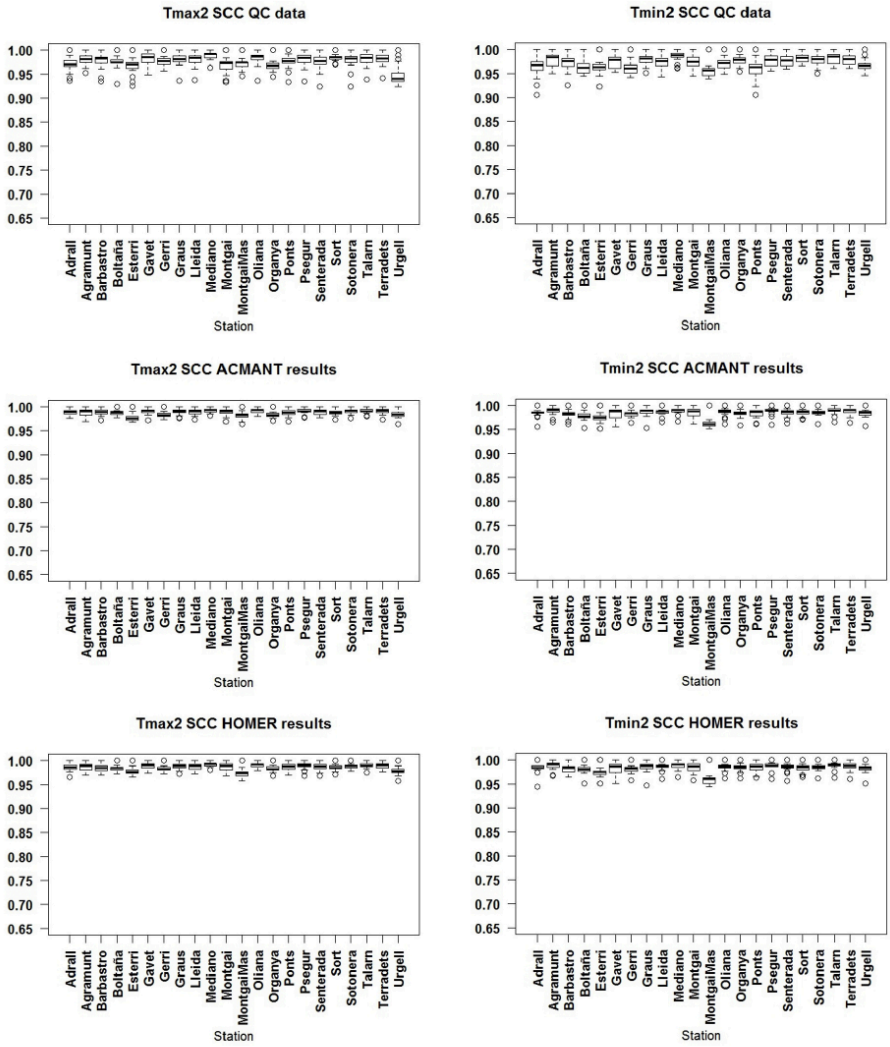

Figure 6. Boxplots of Spearman Correlation Coefficients of QC data (top panels), ACMANT (middle panels) and HOMER (bottom panels) homogenized data for maximum (left panels) and minimum (right panels) temperature for stations in cluster 2.

The relatively large differences between the HOMER homogenization results and ACMANT homogenization results in the mean T_{max} trends and the number of significant positive trends in T_{max} series are unexpected results and their origin requires further analysis.

5 Discussion and conclusions

ACMANT and HOMER are two modern, partly similar, multiple break point homogenization methods, but they have distinct strengths and weaknesses. While automatic methods such as ACMANT are easy to use for large datasets, human intervention and the consideration of metadata is possible only with interactive methods like HOMER.

In this case study of Pyrenees temperatures, ACMANT detected and corrected more breaks than HOMER, which is in agreement with the developed sensitivity of ACMANT to detect short-term biases. Concerning breaks justified by metadata, HOMER detected a larger number than ACMANT, showing the advantage of using interactive homogenization methods. Note however, that one cannot conclude on the accuracy of methods from the number of detected breaks, since

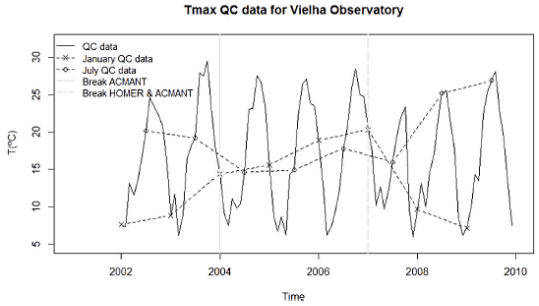

Figure 7. Vielha QC series for T_{max} from 2002 to 2009 continuous line), January data (dashed line and asterisks) and July data (dashed line and circles). Detected breaks of ACMANT (HOMER and ACMANT) are indicated by gray continuous (dashed) vertical lines.

we do not know the number and exact position and size of breaks in the observed dataset. Detailed evaluation of efficiencies requires the use of artificially developed benchmark datasets.

We have identified a serious error in Vielha T_{min} and T_{max} series, which spectacularly affected the SCC values in cluster 1. This error was corrected well with ACMANT for T_{max}, but not for T_{min}, since the control of seasonal changes is included only in the homogenization of T_{max} with ACMANT. Concerning the homogenization with HOMER, the program outputs indicated the error, but the indications were left out of consideration, due to the smoothness of the annual means. This rare error in the data handling of Vielha time series points to the necessity of applying a thorough, multifunctional data quality control, since ideally, homogenization procedures should be applied on datasets that are free from such large errors.

In this case study, average trends for all stations in the period 1961–1990 for T_{max} using HOMER (ACMANT) are 0.12 °C decade^{-1} (0.43 °C decade^{-1}) and, for T_{min}, using HOMER (ACMANT) the average trend slope is 0.03 °C decade^{-1} (0.05 °C decade^{-1}). Comparing these trends with other studies of homogenized Pyrenees temperature data reveals mixed results. A single-station study of annual T_{max} and T_{min} for 1882–1970 (Bücher and Dessens, 1991) described the opposite to what is found here, with a negative trend identified for T_{max} and a positive for T_{min}. Previous homogenization of three stations using HOMER (Esteban et al., 2012) showed significant and positive trends on annual T_{max} for all stations, although no significant trend was identified for annual T_{min} in the period 1935–2008; during the shorter 1950–2008 period however, T_{max} and T_{min} were found to be positive and significant in all of the three stations (Esteban et al., 2012). Finally, a study of annual T_{mean} for the Pyrenees over 1950–2010 showed an increase of 0.2 °C decade^{-1} (Cuadrat et al., 2013). Three factors can explain these differences in the detected trends. First, the different time periods in focus; second, the homogenization methods applied, and third, the differences in the number and geographical distribution of stations.

In conclusion, the high SCC results achieved indicate that the homogenization was generally successful with both HOMER and ACMANT, although the difference in T_{max} trend slopes and particularly the handling of Vielha error points to the need of further methodological analysis.

Acknowledgements. This work was supported by the FP7-SPACE-2013-1 project (Uncertainties in Ensembles of Regional Reanalyses, UERRA) and the MONTCORTES project (CGL2012-33665). We grateful to three anonymous reviewers for comments that helped improve this manuscript.

Edited by: I. Auer
Reviewed by: three anonymous referees

References

Aguilar, E., Auer, I., Brunet, M., Peterson, T. C., and Wieringa, J.: Guidelines on climate metadata and homogenization, WCDMP Report No. 53, WMO-TD 1186, World Meteorological Organization, Geneva, 2003.

Barros, V. R., Field, C. B., Dokken, D. J., Mastrandrea, M. D., Mach, K. J., Bilir, T. E., Chatterjee, M., Ebi, K. L., Estrada, Y. O., Genova, R. C., Girma, B., Kissel, E. S., Levy, A. N., MacCracken, S., Mastrandrea, P. R., and White, L. L. (Eds.): IPCC 2014: Climate Change 2014: Impacts, Adaptation, and Vulnerability. Part B: Regional Aspects, in: Contribution of Working Group II to the Fifth Assessment Report of the Intergovernmental Panel on Climate Change Cambridge University Press, Cambridge, UK and New York, NY, USA, 2014.

Bradley, R. S.: Paleoclimatology: reconstructing climates of the Quaternary, Academic Press, University of Massachusetts, Amherst, USA, 1999.

Brunet, M., Saladié, O., Jones, P., Sigró, J., Aguilar, E., Moberg, A., Lister, D., Whalter, A., and Almarza, C.: A case-study/guidance on the development of long-term daily adjusted temperature datasets, World Meteorological Organization WCDMP Report No. 66, WMO-TD-1425, World Meteorological Organization, Geneva, 2008.

Bücher, A. and Dessens, J.: Secular Trend of Surface Temperature at an Elevated Observatory in the Pyrenees, J. Climate, 4, 859–868, 1991.

Caussinus, H. and Lyazrhi, F.: Choosing a linear model with a random number of change-points and outliers, Ann. Inst. Statist. Math., 49, 761–775, 1997.

Caussinus, H. and Mestre, O.: Detection and correction of artificial shifts in climate series, J. Roy. Stat. Soc. C, 53, 405–425, 2004.

Cuadrat, J. M., Serrano, R., Saz, M.Á., Tejedor, E., Prohom, M., Cunillera, J., Esteban, P., Soubeyroux, J. M., and Deaux, N.: Creación de una base de datos homogeneizada de temperaturas para los Pirineos (1950–2010), Geographicalia, 63–64, 63–74, 2013.

Domonkos, P.: Efficiency evaluation for detecting inhomogeneities by objective homogenisation methods, Theor. Appl. Climatol., 105, 455–467, 2011a.

Domonkos, P.: Adapted Caussinus-Mestre algorithm for networks of temperature series (ACMANT), Int. J. Geosci., 2, 293–309, 2011b.

Domonkos, P.: The ACMANT2 software package, in: Eigth Seminar for Homogenization and Quality Control in Climatological Databases, World Climate Monitoring Program (WCDMP), www.c3.urv.cat/publications/publications.html (last access: 1 March 2015), 2014.

Esteban Vea, P., Prohom Duran, M., and Aguilar E.: Tendencias recientes e índices de cambio climático de la temperatura y la precipitación en Andorra, Pirineos (1935–2008), Pirineos, 167, 87–106, 2012.

Freitas, L., Gonzalez Pereira, M., Caramelo, L., Mendes, M., and Filipe Nunes, L.: Homogeneity of monthly air temperature in Portugal with HOMER and MASH, Idojaras, 117, 69–90, 2013.

Hawkins, D.M.: On the choice of segments in piecewise approximation, J. Inst. Math. Appl., 9, 250–256, 1972.

Kilibarda, M. and Bajat, B.: plotGoogleMaps: the R-based web-mapping tool for thematic spatial data, Geomatica, 66, 37–49, 2012.

López-Moreno, J. I., Goyette, S., and Beniston, M.: Climate change prediction over complex areas: spatial variability of uncertainties and predictions over the Pyrenees from a set of regional climate models, Int. J. Climatol., 28, 1535–1550, 2008.

López-Moreno, J. I., Goyette, S., and Beniston, M.: Impact of climate change on snowpack in the Pyrenees: Horizontal spatial variability and vertical gradients, J. Hydrol., 374, 384–396, 2009.

Mestre, O., Domonkos, P., Picard, F., Auer, I., Robin, S., Lebarbier, E., Böhm, R., Aguilar, E., Guijarro, J., Vertachnik, G., Klancar, M., Dubuisson, B., and Stepanek, P.: HOMER: a homogenization software – methods and applications, Idojaras, 117, 47–67, 2013.

Picard, F., Lebarbier, E., Hoebeke, M., Rigaill, G., Thiam, B., and Robin, S.: Joint segmentation, calling, and normalization of multiple CGH profiles, Biostatistics, 12, 413–428, 2011.

Venema, V. K. C., Mestre, O., Aguilar, E., Auer, I., Guijarro, J. A., Domonkos, P., Vertacnik, G., Szentimrey, T., Stepanek, P., Zahradnicek, P., Viarre, J., Müller-Westermeier, G., Lakatos, M., Williams, C. N., Menne, M. J., Fratianni, S., Cheval, S., Klancar, M., Brunetti, M., Gruber, C., Prohom, M., Lisko, T., Esteban, P., and Brandsma, T.: Benchmarking homogenization algorithms for monthly data, Clim. Past, 8, 89–115, 2012, http://www.clim-past.net/8/89/2012/.

Wilks, D. S.: Statistical methods in the atmospheric sciences, Academic Press, Cornell University, Ithaca, New Yourk, USA, 2011.

Willett, K., Williams, C., Jolliffe, I. T., Lund, R., Alexander, L. V., Brönnimann, S., Vincent, L. A., Easterbrook, S., Venema, V. K. C., Berry, D., Warren, R. E., Lopardo, G., Auchmann, R., Aguilar, E., Menne, M. J., Gallagher, C., Hausfather, Z., Thorarinsdottir, T., and Thorne, P. W.: A framework for benchmarking of homogenisation algorithm performance on the global scale, Geosci. Instrum. Method. Data Syst., 3, 187–200, doi:10.5194/gi-3-187-2014, 2014.

Chapter 3 – Regional anomaly series

Pérez-Zanón, N., Sigró, J., Ashcroft, L., 2016. Temperature and precipitation regional climate series over the central Pyrenees during 1910-2013. Int. J. Climatol. 1–16. doi:10.1002/joc.4823

INTERNATIONAL JOURNAL OF CLIMATOLOGY
Int. J. Climatol. (2016)
Published online in Wiley Online Library
(wileyonlinelibrary.com) DOI: 10.1002/joc.4823

RMetS
Royal Meteorological Society

Temperature and precipitation regional climate series over the central Pyrenees during 1910–2013

Núria Pérez-Zanón, Javier Sigró* and Linden Ashcroft

Center for Climate Change (C3), Campus Terres de l'Ebre, Universitat Rovira i Virgili, Tortosa, Spain

ABSTRACT: Quality controlled homogenized regional anomaly series of temperature and precipitation are obtained for the central Pyrenees for the period 1910–2013. A 0.1 °C decade^{-1} positive trend is found for minimum and maximum annual temperature exceeding the significance level of 0.05 for the whole studied period. A significant warming is found in all seasons except boreal spring in minimum temperature and winter in maximum temperature. The annual regional precipitation anomaly series shows a high inter-annual variability and a slightly negative non-significant trend of −0.6% decade^{-1}. Non-significant negative trends of precipitation are found in all seasons for the whole period examined. Considering the recent period 1970–2013, values of temperature trends are generally higher than those obtained for the whole period. For this latest period, all maximum temperature trends are significant while only the minimum temperature trend in winter is non-significant. Spring is the season that presents the greatest warming, with 0.9 °C decade^{-1} for maximum temperature and 0.4 °C decade^{-1} for minimum temperature. Evaluating the same period for precipitation anomalies, trends in the annual, winter and summer series remain negative, while spring and autumn trends are positive although non-significant. This series represents the longest homogenized climate data set available for the central Pyrenees region, including the newly recovered period 1910–1949, offering new possibilities for climate analysis and paleoclimate proxy calibration.

KEY WORDS mountain climate; climate change; quality control; homogenization; trend analysis; Pyrenees

Received 5 February 2016; Revised 6 May 2016; Accepted 7 June 2016

1. Introduction

The Pyrenees range is located in Western Europe and forms a natural boundary between Spain and France (Ariño *et al.*, 2012) with Atlantic and Mediterranean climatic influences (Beguería *et al.*, 2003).

Owing to its biological richness and water resources, the Pyrenees are a valuable ecosystem that is important for local and regional development of tourism (Marín-Yaseli and Martínez, 2003), energy production, agriculture (Beguería *et al.*, 2003; López-Moreno *et al.*, 2008) and biodiversity (Regato, 2015).

Studying the climate in mountainous regions such as the Pyrenees differs from other environments because they are remote, making it difficult to record data using standard observational methods. Additionally, alpine regions experience large climate variability over short distances, due to local conditions (Barry, 1992). For example, a recent study of the number of precipitation (PPT) and snow winter days for the period 1981–2010 in the western and central Pyrenees shows a relationship between these variables and the weather types in the mountain range (Buisan *et al.*, 2015). These results highlight the importance of long-term observations for reliable climate analysis.

Climate change does not affect all regions equally: the warming rate can be different and even opposite between different areas (Brunet *et al.*, 2007), with mountain ranges being particularly vulnerable to climate change (Beniston, 2003).

Future climate scenarios show a mean decrease in PPT and increase in temperature for the next century in the Spanish Pyrenees region (López-Moreno *et al.*, 2008), accompanied by a sharp reduction in the thickness and duration of snowpack (López-Moreno *et al.*, 2009). The seasonal projected PPT analysis indicates an intensification of extremes: an upward trend of drought periods and a rise in the number of days with intense PPT events (López-Moreno and Beniston, 2008). The number and intensity of warm and very warm days and nights (daily maximum and minimum temperature exceed the percentiles 90th and 99th, respectively) during winter is also projected to increase during the next decades, more in the Pyrenees than the surroundings areas (López-Moreno *et al.*, 2014). Similar results found (an increase in temperature and a reduction in the number of frost days) were also obtained in the north western Mediterranean Basin, again highlighting importance of observational databases in these vulnerable and topographically complex areas (Barrera-Escoda *et al.*, 2014).

For other purposes, such as paleoclimatic studies, a thermopluviometric knowledge is necessary to calibrate natural records (proxies) against instrumental climate data

* Correspondence to: J. Sigró, Center for Climate Change (C3), Campus Terres de l'Ebre, Universitat Rovira i Virgili, Avda. Remolins, 13-15, 43500 Tortosa, Spain. E-mail: javier.sigro@urv.cat

(Romero-Viana *et al.*, 2008; Abrantes *et al.*, 2009; Peña *et al.*, 2015b), and the results of the calibration can be affected by the quality of the instrumental data (Brönnimann, 2015). Previous reconstructions in the Pyrenees used high-quality instrumental data that were not completely representative of the study area. See for example: Dorado Liñán *et al.* (2012), in which only six observatories were used, two of them far from the Pyrenees; Büntgen *et al.* (2008), in which instrumental series from a single close observatory were used, only reconstructing local climate; or in Esper *et al.* (2015), in which the observational gridded data set CRU3.1 was used, computing the average temperature over the study area, against the recommendation of the CRU3.1 authors not to use this data set for trend analysis without comparing with other sources due to the non-homogenized conditions of the individual series (Harris *et al.*, 2014).

In addition to the above, it is recommended by Global Climate Observing System Climate Monitoring Principles (Aguilar *et al.*, 2003) that quality control (QC) and homogenization procedures have to be applied to any instrumental data being used to examine long-term climate variability and change.

In the Pyrenees, some studies of QC and homogeneity of temperature have been undertaken for different spatial and temporal scales using diverse analytical approaches. One high-altitude series was checked for homogeneity using a bivariate test by Bücher and Dessens (1991), Esteban *et al.* (2012) and Cuadrat *et al.* (2013) used HOMER (HOMogenization software in R, Mestre *et al.*, 2013), the same multiple break point homogenization method used in this work, however they only analysed data from three observatories in Andorra and the whole Pyrenees region during the shorter period 1950–2010, respectively. On the other hand, PPT trends have been studied in a quality controlled and homogenized data set for the north eastern Iberian Peninsula, showing the highest values of PPT intensity in the Pyrenees with decreasing trends for the period 1955–2006 (López-Moreno *et al.*, 2010), but without any autocorrelation testing or significant level considered. This work deals with the complete analysis: PPT and temperature for all series in the central Pyrenees and including the newly recovered period 1910–1949.

In this study, a high-quality and long-term (1910–2013) regional anomaly series for PPT and maximum (T_{max}) and minimum temperature (T_{min}) is developed for the central Pyrenees. QC and homogenization procedures have been applied to obtain reliable regional anomaly series. Daily QC has been implemented using Extra QC routing from RClimdex Software (user guide and software available in http://www.c3.urv.cat/data.html) while HOMER, a state-of-the-art homogenization method developed during the Action COST-ES0601 (HOME), has been applied, having been previously tested on temperature data in the study area (Pérez-Zanón *et al.*, 2015). Following homogenization, the regional anomaly series have been calculated applying the Osborn correction (Osborn *et al.*, 1997) that avoids the bias introduced due to the varying sample data.

In Section 2, the data are presented, before being subjected to a detailed QC procedure and homogenization in Section 3. The quality of the homogenized regional series is tested in Section 3, comparing this series to individual observatory series as well as independent homogenized data sets for the Pyrenees region. Using regional anomalies of T_{max}, T_{min} and PPT, climate variability and change in the central Pyrenees is examined in Section 4, focusing on the whole 1910–2013 period as well as the recent 1970–2013 period. Final conclusions are drawn in Section 5.

2. Data

Daily PPT, T_{max} and T_{min} records have been provided by the Spanish National Meteorology Agency (AEMET) and the Catalonia Meteorological Service (SMC). These records came from 155 observatories having either manual or automatic observations (155 series of PPT and 126 series of T_{max} and T_{min}). The data series available from these observatories are of various lengths and cover the period 1910–2013. At the beginning of the study period, these series are not as complete as would be desired. For this reason and to support the homogenization procedure, four series were added from the high-quality Spanish Daily Adjusted Temperature Series (SDATSv2, Brunet *et al.*, 2006) quality controlled databank from observatories located in Pamplona, Huesca, Barcelona and Zaragoza. The spatial distribution of observatories is shown in Figure 1 while the covering period and percentage of available data are shown in Table S1 for the 155 series in the Pyrenees. The annual amount of available daily data for PPT is higher than for both T_{max} and T_{min} for the whole study period, due to the historical interest in PPT measurement by the hydroelectric power stations in the Pyrenees. Figure 2 shows the amount of available daily data for each variable annually. The impact of the Spanish Civil War (1936–1939) is visible by the decrease in available data during that period.

3. Building a homogenized central Pyrenees data set, 1910–2013

3.1. Quality control

From the recording process until the final analysis of climate time series, some errors may be introduced in the data due to changes in the observation place (relocation), measuring instrument or sheltering structure (which allows good air flow across the thermometers but prevents heating from direct sunlight), time of observation, observer, land use and cover, urbanization or because of manipulating (such as unit conversions), formatting, transmitting and archiving data methods. For this reason, QC procedures are applied to detect and identify these errors (Aguilar *et al.*, 2003). ExtraQC routines from RClimdex software, developed through the International Expert Team on Climate Change Detection and Indices (http://www.c3.urv.cat/data/soft/rclimdex_extraqc.zip) have been used.

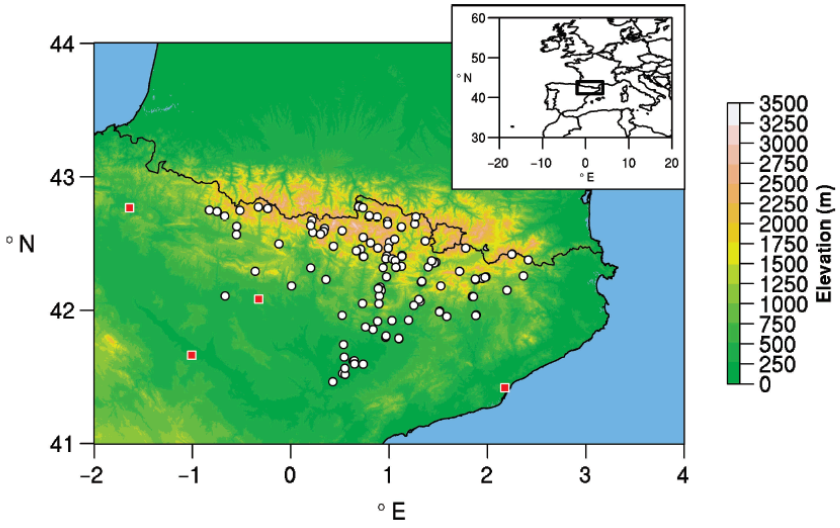

Figure 1. Map of Europe showing the area of study (box) on the top-right corner and observatories spatial distribution around Pyrenees. Squares correspond to the four observatories from SDATSv2 (Brunet *et al.*, 2006) database used for homogenization support.

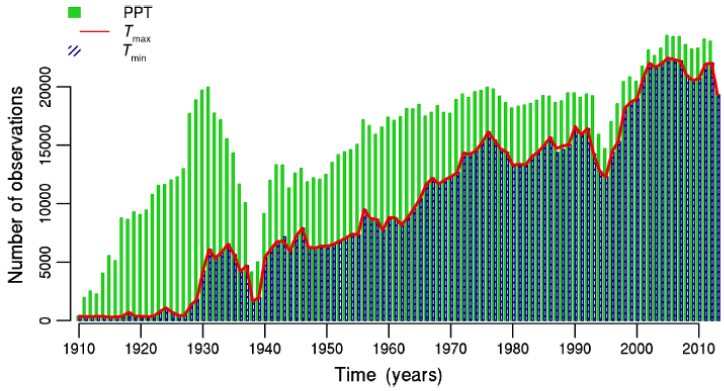

Figure 2. PPT (solid bars), T_{max} (line) and T_{min} (striped bars) daily available data for each year during the period 1910–2013 for the 155 observatories.

Before running the Extra QC routines, the files containing time series should be formatted as the software requires. This step illustrates the need of QC, since some incorrect dates were detected: six dates were corrected and 12 lines were removed because of date repetition.

Taking into account the recommendations from Aguilar *et al.* (2003), gross errors, tolerance, internal consistency and temporal coherency have been checked and summarized in the following statistics for cases that were considered suspect, and evaluated for temporal and spatial coherency, after being flagged by the software:

- Outliers: Values exceeding a threshold defined for lower (upper) bound as the percentile 25 (75) less (plus) three times the interquartile.
- Duplicated dates: includes all dates, which appear more than once in a data file.
- Too large: reported PPT daily values exceeding 200 mm and temperature daily values exceeding 50 °C.
- Jumps: those records where the temperature difference with the previous day is ≥20 °C.
- T_{maxmin}: includes all those cases where maximum temperature is lower than minimum temperature.

Another check was applied to evaluate long continuous periods of null precipitation (called Zero PPT) that are likely due to observation or instrument error.

For the three variables (Table 1), a total amount of 3 744 719 values were checked, from which 17 286 values (0.5%) were flagged as errors after applying the previous criteria and their revision. In total, 99.5% of the flagged suspect data were rejected by replacing the original value to missing data and 0.5% (91) corrected following visual inspection. Most of the rejected data (96.2%) were consecutive zero values of PPT recorded at six observatories: almost a year (334 days) in Barbastro and a total amount of 9281 days for Pobla de Segur.

Table 1. Number of flagged values considered suspicious of being wrong after visual inspection for each daily QC test and variable and summary for those values corrected or rejected (modified to missing data).

Number of suspicious values detected by QC procedure and visual checking										
	Number of corrected values by variable			Number of rejected values by variable			Total number of modifications			
QC test	PPT	T_{max}	T_{min}	PPT	T_{max}	T_{min}	PPT	T_{max}	T_{min}	All
Outliers	9	19	15	8	161	161	17	180	176	373
Duplicated dates	–	–	–	–	–	–	–	–	–	5
Too large	1	0	0	0	0	0	1	0	0	1
Jumps	–	0	1	–	8	1	–	8	2	10
T_{maxmin}	–	10	26	–	128	107	–	138	133	271
Zero PPT	10	–	–	16 616	–	–	16 626	–	–	16 626

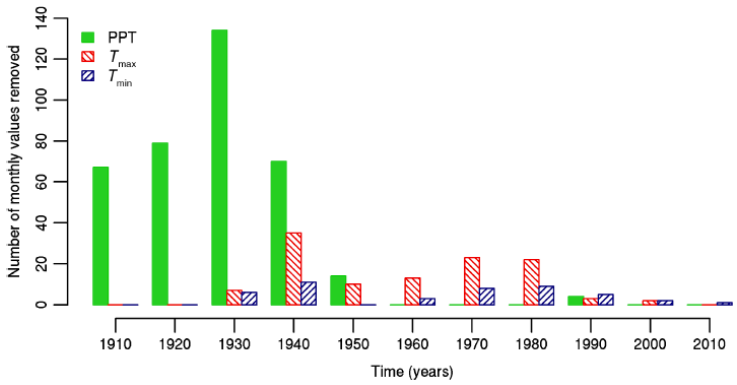

Figure 3. Histogram of number of monthly values removed per decade for PPT, T_{max} and T_{min} as a result of the monthly QC procedure.

Apart from these errors, the most useful indicator to detect suspect values was the Outlier filter. For temperature, 271 incoherent values ($T_{max} < T_{min}$) were found.

3.2. Development of composite series

After applying the daily QC, the distances between observatories were evaluated in order to develop long-term series. A total of 63 PPT time series and 37 T_{max} and T_{min} time series were merged into composite groups, with a maximum of six observatories per group (Table S2). The date of the combination was recorded to be considered in homogenization analysis (Section 3.3). If two merged series had available overlapped data, the most complete was selected. After revising the geographical features, the maximum distance accepted in combinations was 29 km, however the mean distance between the rest of observatories is 2 km. The maximum difference in altitude was 167 m.

Monthly averages of T_{max} and T_{min} were then calculated with the missing data tolerance of no more than seven non-consecutive or five consecutive missing daily values for a month (Pérez-Zanón *et al.*, 2015). Applying the same criteria to PPT, 138 values of the monthly amount (0.27 % of the total monthly values) were calculated even though those months included missing values (Figure S1).

Time series must satisfy minimum requirements in terms of length and completeness to run the homogenization software HOMER. For that reason, series with <270 monthly values were dismissed, except for Bossots observatory which had 254 monthly values for T_{min} and T_{max} in 22 years. After combining data and considering the minimum length requirements, 48 T_{min} and T_{max} series were included in the final data set prepared for homogenization while 60 PPT series were available (Table S3).

Owing to the interactive nature of HOMER, the homogenization procedure was applied over monthly T_{min} and T_{max} in two separate groups of observatories: those which have >1 year of data before 1940 and a period longer than 8 years of consecutive data (21 series) were considered long series and the remaining series (27) which were considered short series and include only data from 1940. The 60 monthly PPT series were all examined at the same time.

Monthly QC was then applied to the previously described group of series to detect additional outliers, using the Fast QC routine included in HOMER, by visual comparison of the monthly and annual differences series within each group. Then, some incoherent monthly values were removed by comparing to neighbouring observatories. For example, for the PPT recorded in Agramunt observatory, no complete year of data is available for the period 1928–1934, only 47 monthly values. This makes it impossible to calculate the annual mean or to apply break detection correctly. Figure 3 shows the histogram of the number of monthly values removed by decade, which

Table 2. Number of outliers identified by the monthly QC procedure in the PPT, T_{max} and T_{min} series.

	PPT	T_{max}	T_{min}
Total number of series	60	48	48
Number of series with outliers detected	8	24	18
Number of outliers detected	368	115	45

shows a bias at the beginning of the study period due to the incompleteness and the quality of the series for PPT. For temperature, the maximum number of data removed occurs in the 1940s, when most of the series began. Table 2 summarizes the number of detected monthly outliers by variable.

3.3. Homogenization

Most long-term meteorological observations are affected by non-climatic factors such as local environment or instrumental changes (Peterson *et al.*, 1998; Brunet *et al.*, 2006). One of these factors can be observatory relocation, which is affecting our combined data set. To correct the series for these kinds of errors, it is necessary to check the homogeneity of the series with statistical tools and/or neighbourhood comparison and, if required, correct the series. The applied homogenization method is a modern one, developed during the HOME Cost Action (Venema *et al.*, 2012), called HOMER (Mestre *et al.*, 2013). HOMER was selected because it includes the best segments and features of some other state-of-the-art methods such as PRODIGE (Caussinus and Mestre, 2004), ACMANT (Domonkos, 2011) and Joint Detection (Picard *et al.*, 2011) and was tested in a homogenization case of study of temperature in the study area (Pérez-Zanón *et al.*, 2015).

HOMER is an interactive method which allows the user to introduce metadata such as how, where and by whom data was recorded (Brunet *et al.*, 2002; Aguilar *et al.*, 2003), and uses the expertise of the climatologist to evaluate the influence of a statistically detected break point. The features of ACMANT detection included in HOMER also allows the detection of the month of a break point in case metadata are not available. However, ACMANT detection and the 'month assess' procedure are only available for temperature data after the first correction, due to the need for a reference series (previously homogenized series) to be computed. The dates of combination of series, recorded during composite series development (Section 3.2) are unfortunately the only metadata available in this study for temperature data. However, for PPT homogenization, the metadata information available in Saladié (2003) was considered, although, it was not introduced in HOMER to avoid overestimating the number of break points detected.

The key steps of applying HOMER to achieve homogenized monthly series are summarized in Figure 4. This procedure is repeated as many times as it is necessary to detect inhomogeneities, taking into account that in the first steps the breaks detected may have a higher amplitude than those detected in next steps, to check them

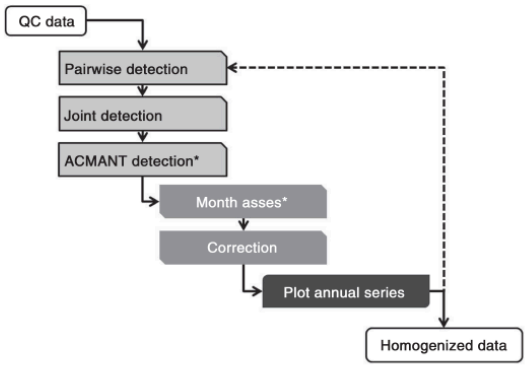

Figure 4. A schematic outlining the application process for HOMER. Those steps indicated with * are only available for temperature homogenization after the first correction.

against metadata and accept or discard those breaks which could be highlighted by the detection methods in previous executions. The homogenization procedure is considered completed when the annual plots of pairwise detection (automatic generated by the software after each correction) do not highlight the same break point more than five times in the inspected series, and the visual comparison between the annual QC time series and the homogenized output does not show any suspicious signal of inhomogeneity.

A total of 407 inhomogeneities were detected (1.2 for PPT and 3.3 for T_{max} and T_{min} per observatory on average). Table 3 summarizes the total number of break points, including those supported by metadata and the maximum number of break points in one series by variable. The maximum number of break points is 13 for the three variables in one series. For temperature data, most of the series had to be corrected: for T_{min} all series had at least one break point detected, and for T_{max} only two series had no breaks points detected. A total of 26 PPT series have been considered homogeneous as no break points were detected.

The lowest break point amplitude in absolute value with supporting metadata was 0.07 °C for T_{min} and 0.11 for PPT (log-transformed PPT data). Ten break points with supporting metadata were simultaneously detected in T_{min} and T_{max}.

Figure 5 shows the annual number of break points detected and the fraction of break points per series, taking into account the number of series with at least the 80% (10 months) of the data available for that year. The maximum number of break points detected were in 1931 with six break points for PPT, 1971 for T_{max} with 12 break

Table 3. Number of break points detected for each variable by the HOMER homogenization procedure.

	PPT	T_{max}	T_{min}
Not supported by metadata	64	167	143
Supported by metadata	9	11	13
Maximum number of break points for a series	6	8	7
Total number of break points	73	178	156

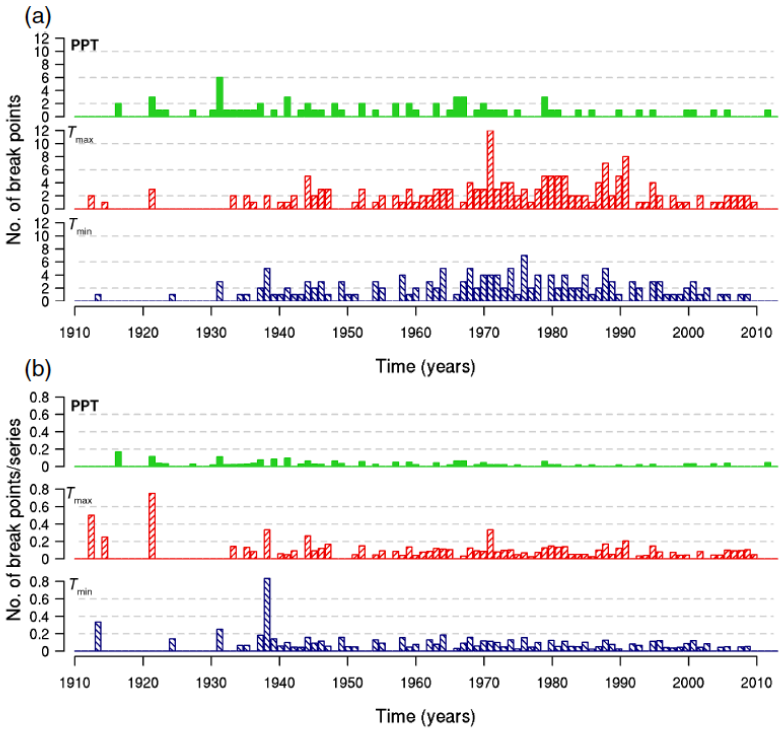

Figure 5. Annual total number of breakpoints detected (a) and a fraction of the annual number of break points detected compared to the number of series available (with 80% of the data available for a year) (b) for PPT (top), T_{max} (middle) and T_{min} (bottom).

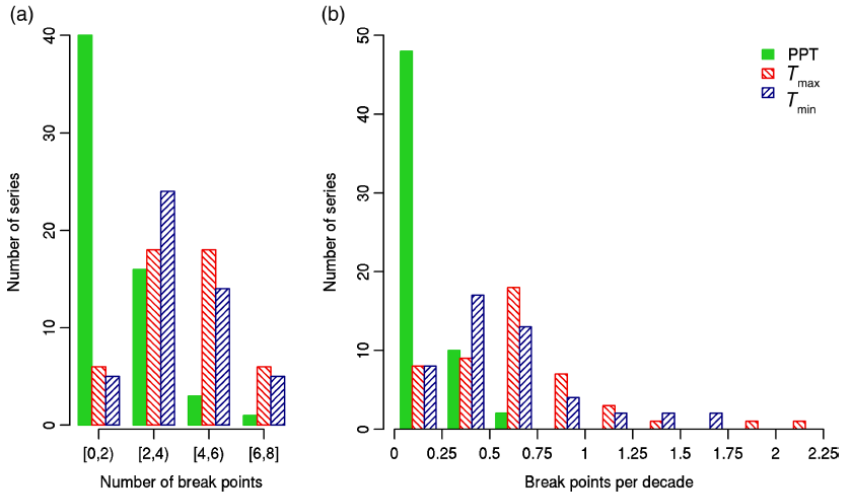

Figure 6. Distribution of series by the number of break points detected (a) and by the break points detected per decade (b) using HOMER for PPT, T_{max} and T_{min}.

points and 1976 with seven break points for T_{min}. In the case of PPT, this maximum number of breaks detected may coincide with the decrease in the number of available observatories during the 1930s. However, in the case of temperature, a change in the signal is detected in the 1970s. For the density of the number of break points per series available, the maximum values are recorded at the beginning of the study period: 1916 for PPT, 1921 for T_{max} and 1938 for T_{min}. These results are due to the low number of data available, and in the case of T_{min}, it coincides with the Spanish Civil War (1936–1939).

Figure 6 shows the distribution of the number of series according to the number of break points detected (Figure 6(a)) and the number of break points detected by

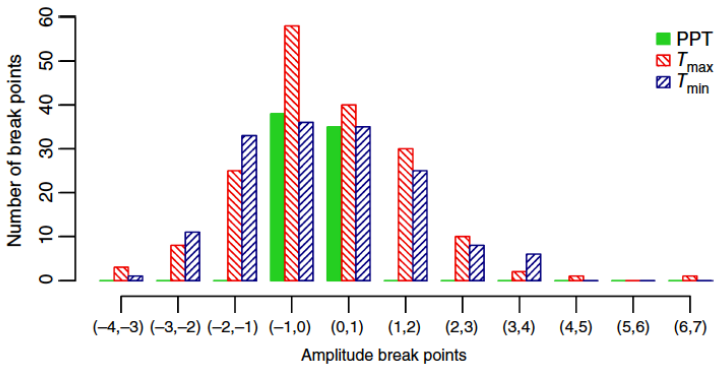

Figure 7. Frequency distribution of the amplitude of the break points detected for PPT (no units), T_{max} and T_{min} (°C units for temperature).

decade (Figure 6(b)). For PPT, between zero and one break point were detected in two-thirds of the series (40 series). The number of break points in a series then decreases rapidly, with six break points the maximum for one series. For temperature, most of the series were corrected using between two and three break points, and a maximum of eight (seven) break points were necessary for one (two) series for T_{max} (T_{min}). The number of break points by decade indicates that our data set is a good station network (as only six T_{max} and T_{min} series have more than one break per decade) considering the previously mentioned difficulties associated with obtained observed series in mountainous areas, and the fact that one break point for mean temperature series in the European western region is expected between every 15 and 20 years (Venema *et al.*, 2012).

Another important factor in assessing the impact of homogenization is the amplitude of the break points detected. Figure 7 shows the frequency distribution of the break points amplitude by variables. Most of the break points are not too large (<|2|), which could be considered a good signal of the network quality data. These results are also similar to the break point amplitude showed by Brunet *et al.* (2006) for SDATSv2 and Trewin (2013) for a daily homogenized temperature data set in Australia.

In Figure 8, the annual anomaly series before (QC) and after (HO) the homogenization procedure are presented, with solid lines showing the mean value for all series, respectively. The impact of homogenization is shown, especially for T_{min} for which the reduction in the annual variability is higher, similar to the results of Brunet *et al.* (2006).

3.4. Regional anomaly climate series

To obtain a representative signal of long-term PPT and temperature evolution for the period 1910–2013 in the central Pyrenees, regional time series are calculated to show the mean and extreme state of Pyrenees climate (following Brunet *et al.*, 2006; Saladié *et al.*, 2008).

Regional anomaly series for PPT, T_{max} and T_{min} have been obtained for annual and seasonal time periods; winter (December to February), spring (March to May), summer (June to August) and autumn (September to November). For each series considered the mean (total) temperature (PPT) was determined for each resolution and the mean value for the base period (1961–1990) was calculated as $\overline{T}$ ($\overline{\text{PPT}}$). Then the anomaly series can be calculated as

$$\Delta T_{obs}(t) = T_{obs}(t) - \overline{T_{obs}} \tag{1}$$

for temperature, and as

$$\Delta \text{PPT}_{obs}(t) = \frac{\text{PPT}_{obs}(t) - \overline{\text{PPT}_{obs}}}{\overline{\text{PPT}^{obs}}} \tag{2}$$

for PPT.

To take into account the bias that the varying sample size may introduce on timeseries formed as average of individual timeseries (Osborn *et al.*, 1997), the regional series have then been calculated by the equation

$$Y(t) = X(t)\sqrt{\frac{n'(t)}{n'(n=N)}} \tag{3}$$

being

$$n'(t) = \frac{n(t)}{1 + [n(t) - 1]\overline{r}} \tag{4}$$

where n is the number of records, $\overline{r}$ is the mean correlation between all pairs of time series, N is the maximum sample size, $X(t)$ is the original regional mean time series and $Y(t)$ is the desired time series with a variance independent of sample size.

3.5. Reliability of the homogenized regional series

To assess the quality of the homogenized regional series developed here, the homogenized data set obtained by the Pyrenees Climate Change Observatory (http://www.opcc-ctp.org/en/actions/climate; Cuadrat *et al.*, 2013) for the period 1950–2010 is used to compute the regional anomaly series by the same methodology presented in this work. The coefficient of correlation is computed between both regional anomaly series for each variable. The lowest correlation value was 0.8 for annual PPT and the highest was 0.95 for spring maximum temperature.

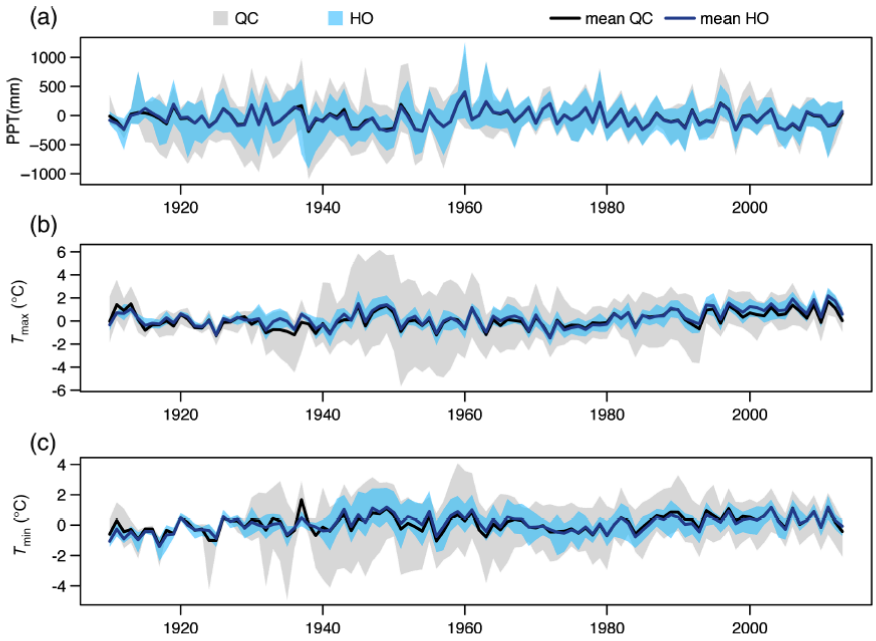

Figure 8. Comparison of individual annual anomaly series (relative to 1961–1990) before (QC) and after (HO) the homogenization procedure for PPT (a), T_{max} (b) and T_{min} (c). The lines represent the mean for the all series before and after the homogenization.

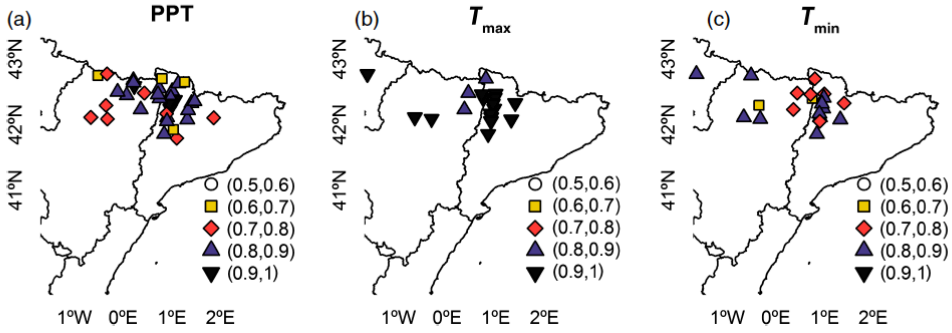

Figure 9. The spatial distribution of correlation coefficients between individual annual series and the regional climate series. All correlations are significant ($p < 0.05$).

This good agreement between both data set for the common period corroborates validity of the presented regional anomaly series. However, it must be noted that small inhomogeneities may remain in our central Pyrenees data set, due to the lack of metadata availability, inherent uncertainties associated with statistical homogenization and the complexity of alpine climates.

The quality of the homogenized regional climate series obtained can also be seen in the good agreement between the regional anomaly series and individual observatory series. The regional anomaly series captures the climate signal of the study area, returning high and significant correlation coefficients between the regional climate series and each individual anomaly series for all variables and temporal resolutions. The annual spatial distribution of correlation coefficients (Figure 9) shows that PPT has the highest variability (minimum value 0.6), while T_{max} correlation coefficients are very similar (minimum value 0.8) and T_{min} correlation coefficients are between 0.6 and 0.8. Owing to a non-constant spatial distribution of the observatories, the highest correlations are found with the highest density of observatories.

The seasonal correlations between the regional series and individual series for PPT (Figure 10) show that winter is the most spatially coherent (correlation values between 0.5 and 0.9), while summer the correlations coefficient are somewhat lower (around 0.7). These differences can be explained by the fact that summer PPT events are generally associated with convective processes which can affect small areas of the Pyrenees, while winter PPT events are more connected with large scale processes that affect the whole Pyrenees region (Llasat and Puigcerver, 1997).

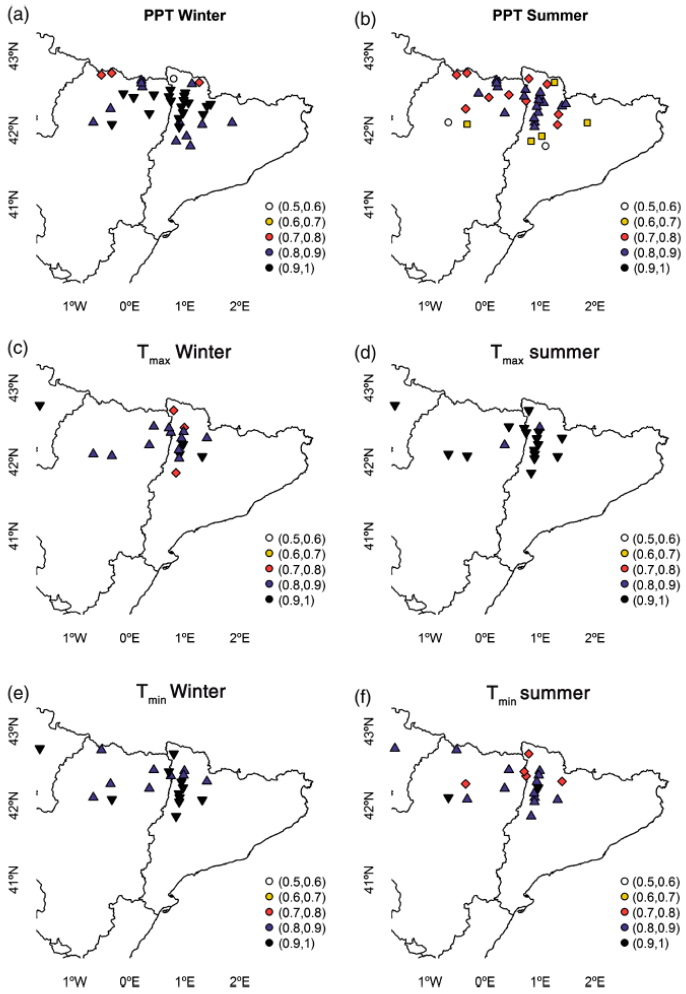

Figure 10. As Figure 9 but for PPT (a and b), T_{max} (c and d) and T_{min} (e and f) for winter (a, c, e) and summer (b, d, f) time series.

On the other hand, the lowest values (0.7) of seasonal T_{max} correlation coefficients are found in winter, while in summer, the minimum correlation coefficient is 0.8 (Figure 10). Seasonal T_{min} correlation coefficients show the opposite behaviour, with summer minimum correlation coefficients around 0.7 and winter slightly higher at 0.8. This difference may be related to the less solar radiation during winter month at this latitude (Barry, 1992) and to the impact of topography, which can have a large impact on minimum temperatures, particularly during clear nights (Trewin, 2005).

4. Central Pyrenees temperature and rainfall, 1910–2013

4.1. Regional trends, 1910–2013

For all regional anomaly series, a trend analysis has been performed using Mann–Kendall test and following the application described by Wang and Swail (2001) in two different periods: for the whole series (1910–2013) and for the recent period (1970–2013). This technique avoids the dependence on autocorrelation for the significance of trends, which can be overestimated by other analysis. The last period has been selected because from 1970 the increase in temperatures across Spain is known to be large (Brunet *et al.*, 2007). Significance of trends was evaluated using the Student's t test ($p < 0.05$) (Wilks, 2011).

The total number of series used is 35 for PPT, 18 for T_{max} and 20 for T_{min} as only the monthly homogenized series which have at least 80% of the values in the base period are used (and dismissing Barcelona observatory which is not representative of the study area).

Figure 11 shows the annual regional anomaly series for PPT, T_{min} and T_{max} and the trends obtained. For the whole series (1910–2013), PPT trend is -0.64% decade^{-1}, T_{max} trend is 0.11 °C decade^{-1} and T_{min} trend is 0.06 °C decade^{-1}, while for the period 1970–2013, PPT trend is -2.70% decade^{-1}, T_{max} trend is 0.57 °C decade^{-1} and T_{min} trend is 0.23 °C decade^{-1}. These trends are

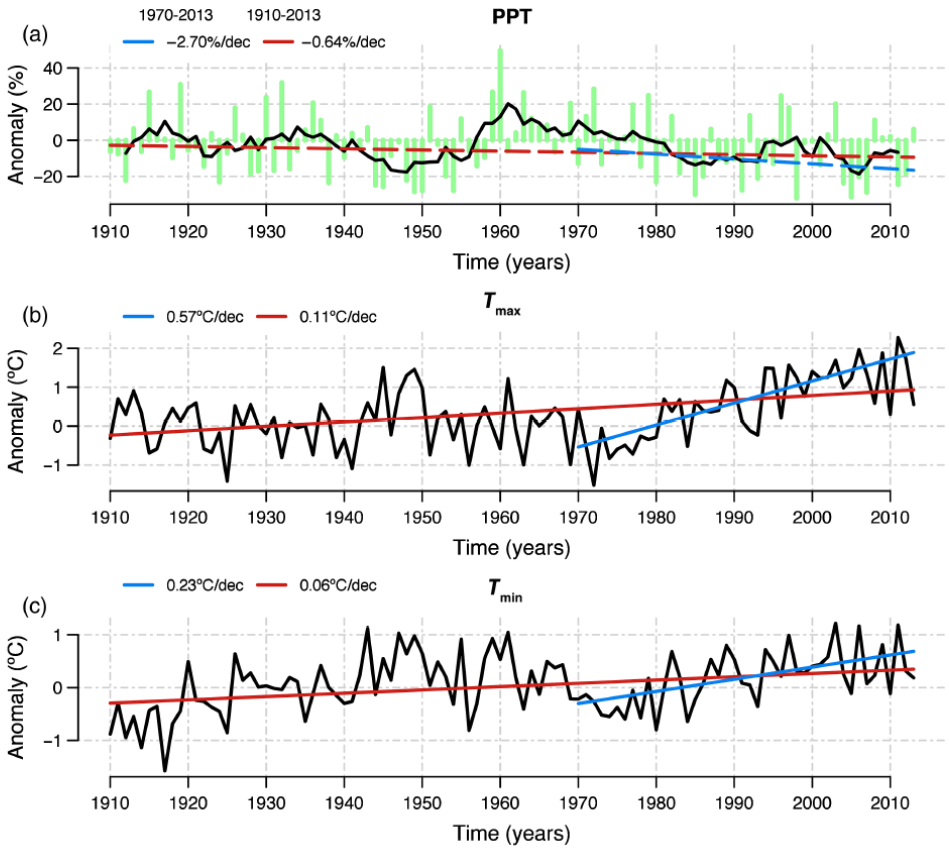

Figure 11. Annual regional anomaly series for PPT (a), T_{max} (b) and T_{min} (c). The trends for the studied periods are plotted in blue (1970–2013) and in red (1910–2013) for each variable and the legend show the value of the slope in each case. Significant trends (continuous lines) and non-significant (dashed lines) are shown in each case. PPT solid line corresponds to a 5-year moving average.

significant in the case of temperature and non-significant for PPT due to its large inter-annual variability.

PPT anomalies series for central Pyrenees are dominated by a high inter-annual variability, however, negative trends are found in all seasons (Figure 12) except for spring during the period 1970–2013. The greatest difference between the seasonal trends is found in winter, when the change in the trends between both periods is $>-7\%$ decade^{-1}. This decrease in winter PPT is in agreement with López-Moreno (2005), who identified a decrease in snowpack depth for the period 1950–1999. On the other hand, an increase in the PPT trend of 2.25% decade^{-1} is found in autumn. These differences may suggest a shift in the rainfall distribution of seasons, however dynamical studies are required to determine the cause of these findings.

T_{max} seasonal anomaly series (Figure 13) shows a clear positive trends, with only winter showing a non-significant trend for the period 1910–2013. The increase in trend values comparing both periods may suggest a higher impact of climate change in the study area for the recent 1970–2013 period. The warmer months of spring and summer display the greatest trends, an interesting result given the potential impact of heat waves and extremes on the regional population and environment (e.g. Peña *et al.*, 2015a). Trends of T_{min} seasonal anomaly series (Figure 14) are not as large as those for T_{max}, with two non-significant periods (spring 1910–2013 and winter 1970–2013). The significant trends for the whole series are 0.12 °C decade^{-1} in winter, 0.07 °C decade^{-1} in summer and 0.09 °C decade^{-1} in autumn, while, for the period 1970–2013, trends are 0.27 °C decade^{-1} in summer, 0.31 °C decade^{-1} in autumn and 0.40 °C decade^{-1} in spring. Table 4 summarizes all the computed trends for both periods taking into account the significance level.

4.2. Central Pyrenees climate variability, 1910–1949

As well as an extended trend analysis, the addition of homogenized climate data for the 1910–1949 period over the central Pyrenees also allows for the examination of inter-annual climate variability in the region during the first half of the 20th century. Considering the threshold of ±10%, dry (wet) years can be defined as those years with anomaly PPT below −10% (10%), while normal years are those years with anomaly PPT between −10 and 10%. For the newly recovered period 1910–1949

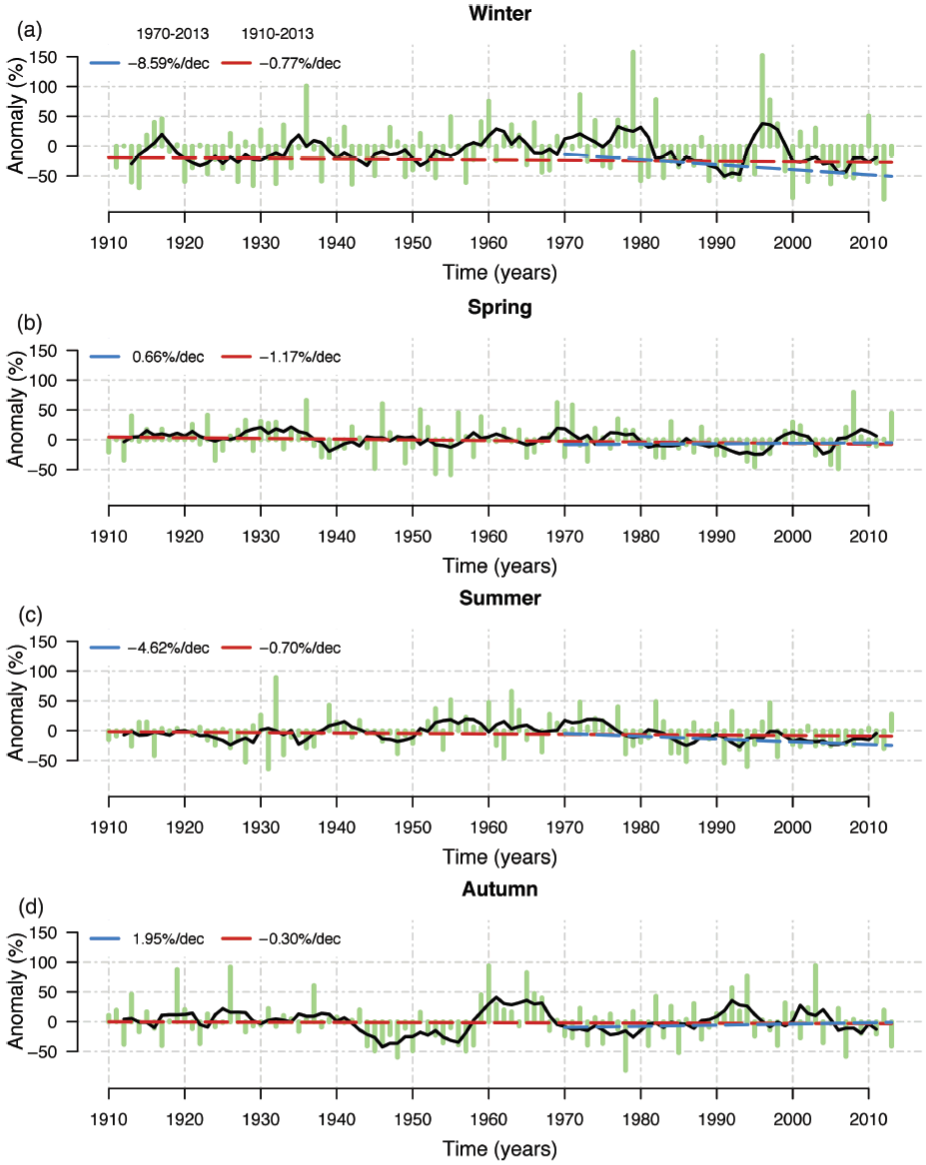

Figure 12. Seasonal regional anomaly series of PPT for the central Pyrenees. The trends for the studied periods 1970–2013 and 1910–2013 are plotted for each variable and the legend show the value of the slope in each case. Significant trends (continuous lines) and non-significant (dashed lines) are shown in each case. Black line corresponds to 5-year moving average.

analysed in this article (Table S4 and Figure 11), 12 (30% of years) dry years and 7 (18%) wet are registered compare to the 26 (41%) dry and 17 (27%) wet years for the next period 1950–2013 for annual regional anomaly series. The number of normal years, 21, does not change between periods but represents 53% of years for the newly recovered period and 33% for the modern period. This result suggests that PPT variability in the central Pyrenees may be becoming more extreme.

Following the filtered anomaly PPT series by a 5-year moving average (Figure 11), 6 years of positive PPT values (1914–1919), largely associated with wet conditions in 1915 and 1919. The 1920s are close to normal as shown in the filtered series shows, presenting 4 dry years and 1 wet but spread out over time. The 4 first years of the 1930s were extremes, alternating wet and dry years, and 2 wet and 1 dry year were observed later (1936–1938) during the Spanish Civil War. A drought emerges towards the end of the 1940s, with 4 dry years registered from 1944 to 1949, and continues to the mid 1950s.

Seasonal series show fewer normal years, especially in winter, for which only 9 years were normal for the

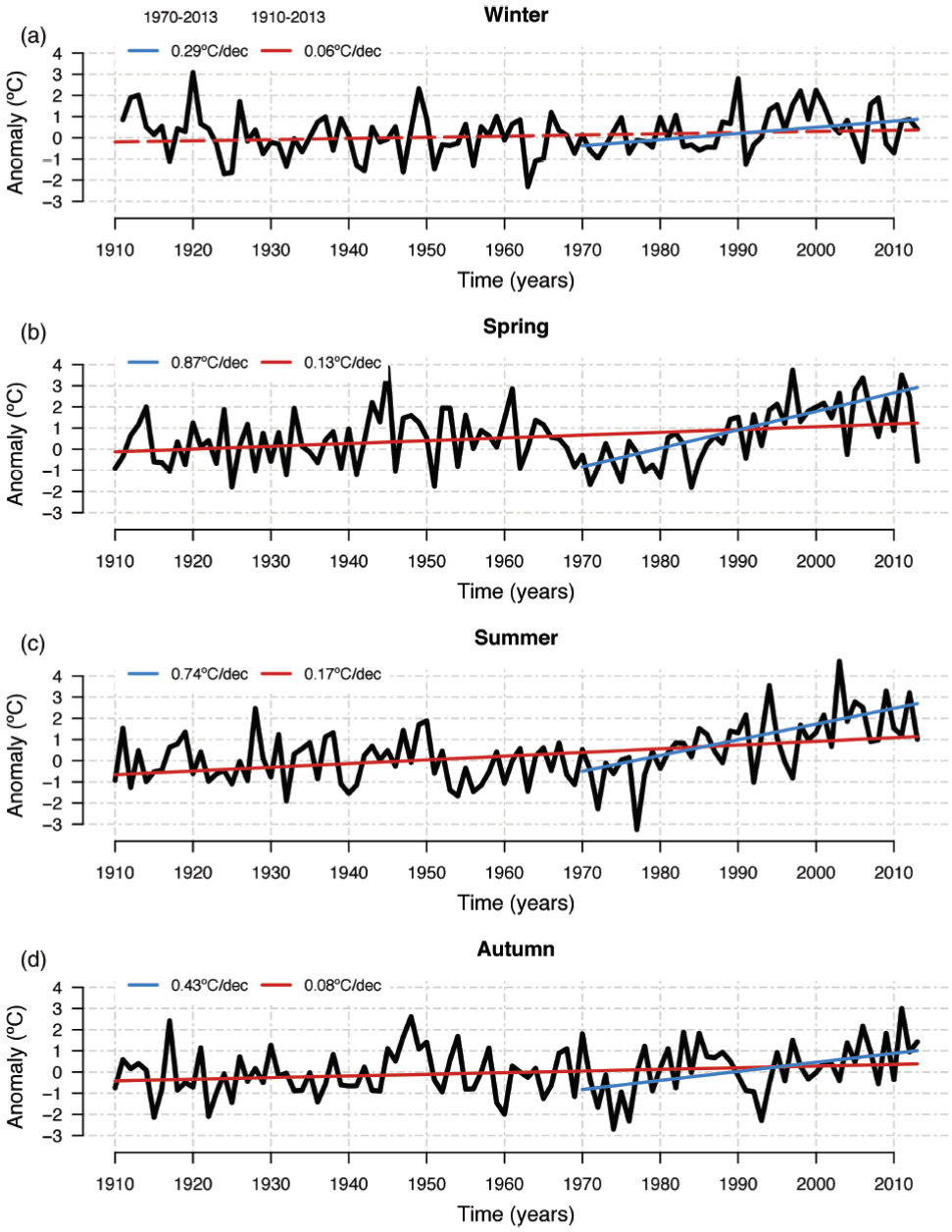

Figure 13. Seasonal regional anomaly series of T_{max} for the central Pyrenees. The trends for the studied periods 1970–2013 and 1910–2013 are plotted for each variable and the legend show the value of the slope in each case. Significant trends (continuous lines) and non-significant (dashed lines) are shown in each case.

newly recovered period 1910–1949 and 3 for the period 1950–2013. Half of the years were dry for winter PPT series in the 1910–1949 period. The longest wet period was recorded for 1915–1917. In the summer PPT series, the longest dry period is observed for 14 years, between 1916 and 1929, during which no wet year was recorded.

For temperature, the threshold for hot and cold years is selected as ±0.5 °C (Table S4). As it would be expected given the temperature trends, the percentage of hot years increases in the modern period (1950–2013) with respect to the newly recovered period (1910–1949) while the percentage of cold years decreases. In particular, T_{max} presents 18 hot years out of the last 20 years of the series (1994–2013). The number of normal years remains close to constant for T_{max} and T_{min} in annual and seasonal resolution.

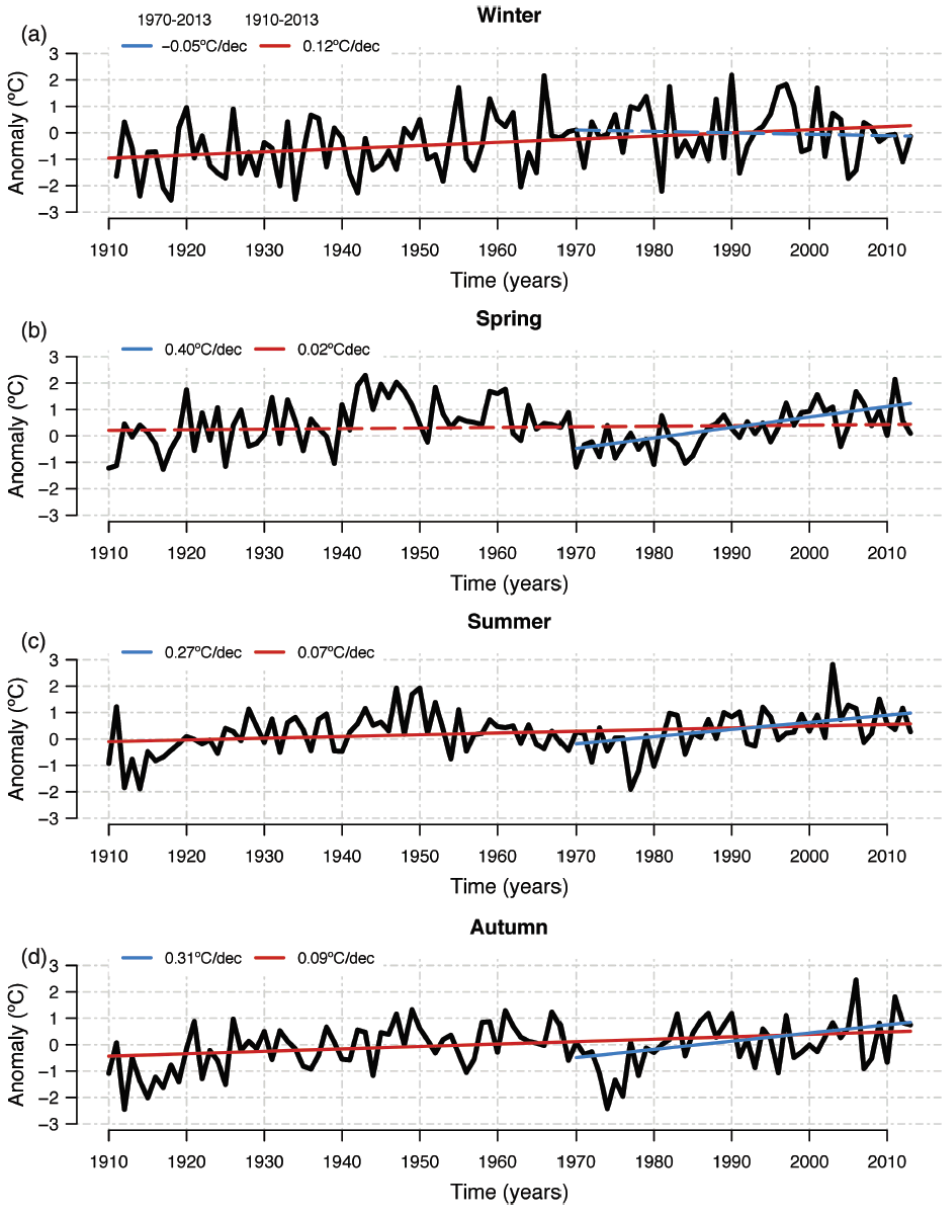

Figure 14. Figure 13, but for T_{min}.

T_{max} annual regional series shows high variability in periods of 4–6 years even individual extremes years until the 1940s decade when a long hot period is shown from 1943 to 1950 when 6 hot years were observed. In winter and summer, the percentage of hot years increase by 14% for the period 1950–2013 with respect to the newly recorded period, while in summer, the percentage of cold years decreased by 12%.

The annual regional anomaly T_{min} series is roughly characterized by three periods: a cold period from 1910 to 1925; a normal period between 1926 (which was hot) and 1942 for which all years were normal except 1935 (which was cold); a hot period from 1943 to 1949 when 4 hot years were observed. The percentage of cold years was reduced to the half in the period 1950–2013, while the percentage of hot years is almost double. In winter, only 3 hot years were observed for the early period, given the longest period of cold and normal years of 13 years between 1937 and 1949. In summer, the 6 cold years observed for the newly period are found until 1917.

4.3. Dependence of trends on altitude

To conduct a preliminary evaluation of the impact of climate change at different altitudes, trends of annual

Table 4. Trend for annual and seasonal regional central Pyrenees series for PPT, T_{max} and T_{min}.

	Trend PPT (% decade^{-1})		Trend T_{max} (°C decade^{-1})		Trend T_{min} (°C decade^{-1})	
	1910–2013	1970–2013	1910–2013	1970–2013	1910–2013	1970–2013
Annual	−0.64	−2.70	**0.11**	**0.57**	**0.06**	**0.23**
Winter	−0.77	−8.59	0.06	**0.29**	**0.12**	−0.05
Spring	−1.17	0.66	**0.13**	**0.87**	0.02	**0.40**
Summer	−0.70	−4.62	**0.17**	**0.74**	**0.07**	**0.27**
Autumn	−0.30	1.95	**0.08**	**0.43**	**0.09**	**0.31**

Significant trends ($p < 0.05$) are shown in bold.

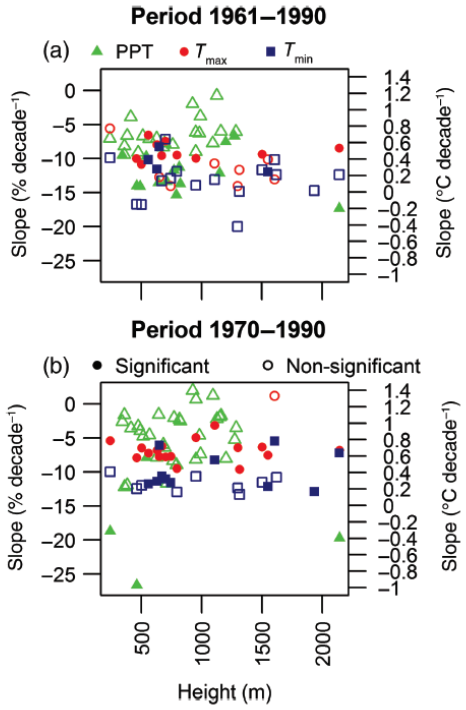

Figure 15. Trends for each anomaly series of individual series for PPT (triangles), T_{max} (circles) and T_{min} (squares) depending on altitude of the observatories. Significant values ($p > 0.05$) are shown as filled symbols while non-significant are empty.

anomalies for the individual series used to compute the regional anomaly series were calculated for 1961–1990 and 1970–2013, using those series with a minimum of 80% of monthly data for 1961–1990. The trends do not show any relation to altitude (Figure 15 and Table S5). PPT trends are negative in the period 1961–1990 for all series, while for the period 1970–2013 three series show positive non-significant trends. T_{max} trends are all positive in both periods, however, there are three negative significant trends for T_{min} during the period 1961–1990. The number of significant trends for PPT decreases in the recent period, while for T_{max}, there is an increase in the number of significant trends. All T_{min} trends are significant for both periods. For PPT, these behaviours are due to the high inter-annual variability, illustrating the important differences in the trends analysis that can occur when different short periods are evaluated. For temperature, the well-known trend increase since the mid 1970s in Europe (IPCC Working Group I, 2001) is clear in the analysis of these individual series as well as the regional series (Section 4).

5. Conclusions

High-quality regional anomaly series of PPT, T_{max} and T_{min} have been obtained for the longest quality controlled and homogenized data set for the central Pyrenees during the period 1910–2013. Owing to the length and quality of the presented regional anomaly series, new possibilities for climate analysis and paleoclimate proxy calibration are now available. The importance of QC and homogenization procedure has been highlighted by the accomplished procedures since several flagged values and inhomogeneities have been detected in the observed series. Improving series and their reliability is demonstrated by the comparison between the quality controlled and the homogenized data, the spatial correlation analysis and the comparison with an independent data set for the regional anomaly series.

Trend analysis has shown a highly significant increase in temperatures and important inter-annual PPT variability, without significant trends, over the central Pyrenees, with some difference between seasonal behaviours and larger temperature trends during the recent period 1970–2013 than the whole period 1910–2013. The trends of annual regional anomaly series are 0.11 °C decade^{-1} for T_{max} and 0.06 °C decade^{-1} for T_{min} for the period 1910–2013, and 0.57 and 0.23 °C decade^{-1} for the period 1970–2013, respectively. No altitude dependence is found for trends in the study area.

The percentage of normal annual PPT years decreases in the period 1950–2013 respect the newly recovered period 1910–1949, increasing dry and wet years. Furthermore, the number of cold years in T_{min} and T_{max} annual regional series decreases comparing both periods while the number of hot years increase. The regional anomaly series will be made available for scientific purposes via the following web site: http://www.c3.urv.cat/data1.html.

Acknowledgements

This work was supported by the MONTCORTES project (CGL2012-33665).

Results obtained from the provided information by the Spanish Meteorological Agency, Agriculture, Food and Environment Ministry. We thank the Shuttle Radar Topography Mission (http://glcf.umd.edu/data/srtm/) for the topographic database, and two anonymous reviewers for their suggestions that helped improve this manuscript.

Supporting Information

The following supporting information is available as part of the online article:
The list of observatories used in this study is provided as a supplementary Table S1 which shows the code of the observatory, the geographical information and the length and completeness of the series. Table S2 shows composite series and Table S3 lists the homogenized series. Table S4 presents the distribution of total and percentage of wet/dry and cold/hot years between the newly 1910–1945 and the latest 1950–2013 periods. Trend values for each observatory are shown in Table S5.

References

Abrantes F, Lopes C, Rodrigues T, Gil I, Witt L, Grimalt J, Harris I. 2009. Proxy calibration to instrumental data set: implications for paleoceanographic reconstructions. *Geochem. Geophys. Geosyst.* **10**(9): 1–15, doi: 10.1029/2009GC002604.

Aguilar E, Auer I, Brunet M, Peterson TC, Wieringa J. 2003. Guidelines on climate metadata and homogenization. World Climate Programme Data and Monitoring WCDMP-No. 53, WMO-TD No. 1186, World Meteorological Organization, WMO, Geneva, Switzerland.

Ariño AH, Otegui J, Villarroya A, De Zabalza AP. 2012. Primary biodiversity data records in the Pyrenees. *Environ. Eng. Manag. J.* **11**(6): 1059–1075.

Barrera-Escoda A, Gonçalves M, Guerreiro D, Cunillera J, Baldasano JM. 2014. Projections of temperature and precipitation extremes in the North Western Mediterranean Basin by dynamical downscaling of climate scenarios at high resolution (1971–2050). *Clim. Change* **122**(4): 567–582, doi: 10.1007/s10584-013-1027-6.

Barry RG. 1992. *Mountain Weather and Climate*. Routledge: London.

Beguería S, López-Moreno JI, Lorente A, Seeger M, García-Ruiz JM. 2003. Assessing the effect of climate oscillations and land-use changes on streamflow in the central Spanish Pyrenees. *AMBIO* **32**(4): 283–286, doi: 10.1579/0044-7447-32.4.283.

Beniston M. 2003. Climatic change in mountain regions: a review of possible impacts. *Clim. Change* **59**(1): 5–31, doi: 10.1023/A:1024458411589.

Brönnimann S. 2015. *Climate Change since 1700*. Springer International Publishing: Cham, Switzerland, doi: 10.1007/978-3-319-19042-6.

Brunet M, Saladié O, Jones P, Sigró J, Aguilar E, Moberg A, Lister D, Walther A, Almarza C. 2002. A case-study/guidance on the development of long-term daily adjusted temperature datasets. WCDMP-66/WMO-TD-1425, World Meteorological Organization, Geneva, Switzerland.

Brunet M, Saladié O, Jones P, Sigró J, Aguilar E, Moberg A, Lister D, Walther A, Lopez D, Almarza C. 2006. The development of a new dataset of Spanish daily adjusted temperature series (SDATS) (1850–2003). *Int. J. Climatol.* **26**(13): 1777–1802, doi: 10.1002/joc.1338.

Brunet M, Jones PD, Sigró J, Saladié O, Aguilar E, Moberg A, Della-Marta PM, Lister D, Walther A, López D. 2007. Temporal and spatial temperature variability and change over Spain during 1850–2005. *J. Geophys. Res.* **112**(D12117): 1–28, doi: 10.1029/2006JD008249.

Bücher A, Dessens J. 1991. Secular trend of surface temperature at an elevated observatory in the Pyrenees. *J. Clim.* **4**: 859–868.

Buisan ST, Saz MA, López-Moreno JI. 2015. Spatial and temporal variability of winter snow and precipitation days in the western and central Spanish Pyrenees. *Int. J. Climatol.* **35**(2): 259–274, doi: 10.1002/joc.3978.

Büntgen U, Frank D, Grudd H, Esper J. 2008. Long-term summer temperature variations in the Pyrenees. *Clim. Dyn.* **31**(6): 615–631, doi: 10.1007/s00382-008-0390-x.

Caussinus H, Mestre O. 2004. Detection and correction of artificial shifts in climate series. *J. R. Stat. Soc. Ser. C Appl. Stat.* **53**(3): 405–425, doi: 10.1111/j.1467-9876.2004.05155.x.

Cuadrat JM, Serrano R, Saz MA, Tejedor E, Prohom M, Cunillera J, Esteban P. 2013. Creación de una base de datos homogenizada de temperaturas para los Pirineos (1950–2010). *Geographicalia* **63–64**: 63–74.

Domonkos P. 2011. Adapted Caussinus-Mestre algorithm for networks of temperature series (ACMANT). *Int. J. Geosci.* **2**(3): 293–309.

Dorado Liñán I, Büntgen U, González-Rouco F, Zorita E, Montávez JP, Gómez-Navarro JJ, Brunet M, Heinrich I, Helle G, Gutiérrez E. 2012. Estimating 750 years of temperature variations and uncertainties in the Pyrenees by tree-ring reconstructions and climate simulations. *Clim. Past* **8**(3): 919–933, doi: 10.5194/cp-8-919-2012.

Esper J, Konter O, Krusic PJ, Saurer M, Holzkämper S, Büntgen U. 2015. Long-term summer temperature variations in the Pyrenees from detrended stable carbon isotopes. *Geochronometria* **42**(1): 53–59, doi: 10.1515/geochr-2015-0006.

Esteban P, Prohom M, Aguilar E. 2012. Tendencias recientes e índices de cambio climático de la temperatura y la precipitación en Andorra, Pirineos (1935–2008). *Pirineos* **167**: 87–106, doi: 10.3989/Pirineos.2012.167005.

Harris I, Jones PD, Osborn TJ, Lister DH. 2014. Updated high-resolution grids of monthly climatic observations – the CRU TS3.10 Dataset. *Int. J. Climatol.* **34**(3): 623–642, doi: 10.1002/joc.3711.

IPCC Working Group I. 2001. Climate change 2001: the scientific basis. *Climate Change 2001: The Scientific Basis* 881. DOI: 10.1256/004316502320517344.

Llasat MC, Puigcerver M. 1997. Total rainfall and convective rainfall in Catalonia, Spain. *Int. J. Climatol.* **17**(15): 1683–1695, doi: 10.1002/(SICI)1097-0088(199712)17:15<1683::AID-JOC220>3.0.CO;2-Q.

López-Moreno JI. 2005. Recent variations of snowpack depth in the central Spanish Pyrenees. *Arct. Antarct. Alp. Res.* **37**(2): 253–260, doi: 10.1657/1523-0430(2005)037[0253:RVOSDI]2.0.CO;2.

López-Moreno JI, Beniston M. 2008. Daily precipitation intensity projected for the 21st century: seasonal changes over the Pyrenees. *Theor. Appl. Climatol.* **95**(3): 375–384, doi: 10.1007/s00704-008-0015-7.

López-Moreno JI, Goyette S, Beniston M. 2008. Climate change prediction over complex areas: spatial variability of uncertainties and prediction over the Pyrenees from a set of regional climate models. *Int. J. Climatol.* **28**(11): 1535–1550, doi: 10.1002/joc1645.

López-Moreno JI, Goyette S, Beniston M. 2009. Impact of climate change on snowpack in the Pyrenees: horizontal spatial variability and vertical gradients. *J. Hydrol.* **374**(3–4): 384–396, doi: 10.1016/j.jhydrol.2009.06.049.

López-Moreno JI, Vicente-Serrano SM, Angulo-Martínez M, Beguería S, Kenawy A. 2010. Trends in daily precipitation on the northeastern Iberian Peninsula, 1955–2006. *Int. J. Climatol.* **30**(7): 1026–1041, doi: 10.1002/joc.1945.

López-Moreno JI, El-Kenawy A, Revuelto J, Azorín-Molina C, Morán-Tejeda E, Lorenzo-Lacruz J, Zabalza J, Vicente-Serrano SM. 2014. Observed trends and future projections for winter warm events in the Ebro Basin, northeast Iberian Peninsula. *Int. J. Climatol.* **34**(1): 49–60, doi: 10.1002/joc.3665.

Marín-Yaseli ML, Martínez TL. 2003. Competing for meadows. *Mt. Res. Dev.* **23**(2): 169–176, doi: 10.1659/0276-4741(2003)023[0169:CFM]2.0.CO;2.

Mestre O, Domonkos P, Picard F, Auer I, Robin S, Lebarbier E, Böhm R, Aguilar E, Guijarro J, Vertachnik G, Klancar M, Dubuisson B, Stepanek P. 2013. HOMER: a homogenization software – methods and applications. *IDŐJÁRÁS* **117**(1): 47–67.

Osborn TJ, Briffa KR, Jones PD. 1997. Adjusting variance for sample-size in tree-ring chronologies and other regional mean timeseries. *Dendrochronologia* **15**: 89–99.

Peña JC, Aran M, Raso JM, Pérez-Zanón N. 2015a. Principal sequence pattern analysis of episodes of excess mortality due to heat in the Barcelona metropolitan area. *Int. J. Biometeorol.* **59**(4): 435–446, doi: 10.1007/s00484-014-0857-x.

Peña JC, Schulte L, Badoux A, Barriendos M, Barrera-Escoda A. 2015b. Influence of solar forcing, climate variability and modes of low-frequency atmospheric variability on summer floods in Switzerland. *Hydrol. Earth Syst. Sci.* **19**(9): 3807–3827, doi: 10.5194/hess-19-3807-2015.

Pérez-Zanón N, Sigró J, Domonkos P, Ashcroft L. 2015. Comparison of HOMER and ACMANT homogenization methods using a central

Pyrenees temperature dataset. *Adv. Sci. Res.* Copernicus GmbH **12**(1): 111–119, doi: 10.5194/asr-12-111-2015.

Peterson TC, Easterling DR, Karl TR, Groisman P, Nicholls N, Plummer N, Torok S, Auer I, Boehm R, Gullet D, Vincent L, Heino R, Tuomenvirta H, Mestre O, Szentimrey T, Salinger J, Førland EJ, Hanssen-Bauer I, Alexandersson H, Jones P, Parker D. 1998. Homogeneity adjustments of *in situ* atmospheric climate data: a review. *Int. J. Climatol.* **18**(13): 1493–1517, doi: 10.1002/(SICI)1097-0088(19981115)18:13<1493::AID-JOC329>3.0.CO;2-T.

Picard F, Lebarbier E, Hoebeke M, Rigaill G, Thiam B, Robin S. 2011. Joint segmentation, calling, and normalization of multiple CGH profiles. *Biostatistics* **12**(3): 413–428, doi: 10.1093/biostatistics/kxq076.

Regato P. 2015. *Southwest Europe: In the Pyrenees Mountains of Spain, France, and Andorra*. *World Wildlife Fund*. http://www.worldwildlife.org/ecoregions/pa0433 (accessed 15 November 2015).

Romero-Viana L, Julià R, Camacho A, Vicente E, Miracle MR. 2008. Climate signal in varve thickness: Lake la Cruz (Spain), a case study. *J. Paleolimnol.* **40**(2): 703–714, doi: 10.1007/s10933-008-9194-6.

Saladié O. 2003. *Variaciones y tendencia secular de la precipitación en el sector nororiental de la Península Ibérica (1850–2000)*. PhD thesis, Universitat de Barcelona, Barcelona, 496 pp.

Saladié Ò, Brunet M, Aguilar E, Sigró J, López D. 2008. Variacions i tendència de la precipitació al sector nord-oriental de la península ibèrica durant el segle XX. *Revista de geografia* **5**: 25–46.

Trewin BC. 2005. A notable frost hollow at Coonabarabran, New South Wales. *Aust. Meteorol. Mag.* **54**(1): 15–21.

Trewin B. 2013. A daily homogenized temperature data set for Australia. *Int. J. Climatol.* **33**(6): 1510–1529, doi: 10.1002/joc.3530.

Venema VKC, Mestre O, Aguilar E, Auer I, Guijarro JA, Domonkos P, Vertacnik G, Szentimrey T, Stepanek P, Zahradnicek P, Viarre J, Müller-Westermeier G, Lakatos M, Williams CN, Menne MJ, Lindau R, Rasol D, Rustemeier E, Kolokythas K, Marinova T, Andresen L, Acquaotta F, Fratianni S, Cheval S, Klancar M, Brunetti M, Gruber C, Prohom Duran M, Lisko T, Esteban P, Brandsma T. 2012. Benchmarking homogenization algorithms for monthly data. *Clim. Past* **8**(1): 89–115, doi: 10.5194/cp-8-89-2012.

Wang XL, Swail VR. 2001. Changes of extreme wave heights in Northern Hemisphere oceans and related atmospheric circulation regimes. *J. Clim.* **14**(10): 2204–2221, doi: 10.1175/1520-0442(2001)014<2204:COEWHI>2.0.CO;2.

Wilks DS. 2011. *Statistical Methods in Atmospheric Science*. Academic Press: Ithaca, NY.

Supplementary material "Temperature and Precipitation regional climate series over the central Pyrenees during 1910–2013"

Núria Pérez-Zanón[a], Javier Sigró[a] and Linden Ashcroft[a]

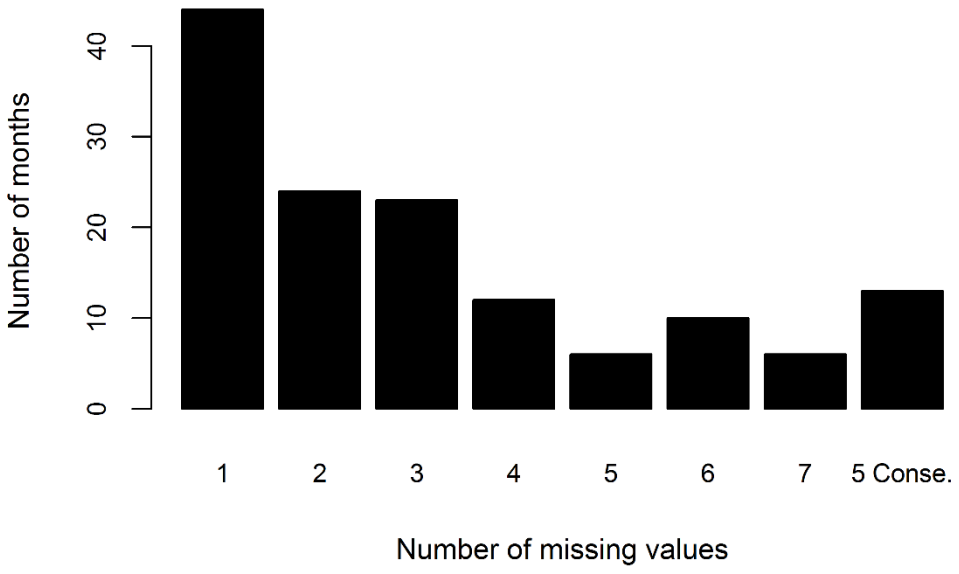

Figure S1.1: Distribution of the number of month with missing values lower or equal than 7 or 5 consecutive days missing values.

Table S.1: Central Pyrenees temperature and precipitation initial network. Code and abbreviated name of station, period and percentage of data for precipitation and temperature and geographical location (elevation and geographical coordinates).

CODE	NAME	PERIOD PPT	% PPT DATA	PERIOD T	% T DATA	Height (m)	Lon (°)	Lat (°)
AR001	Senet	1915-1997	73.2	1929-1997	49.6	1093	0.74	42.55
AR002	Vilaller	1928-1999	77.2	1955-1999	52	925	0.71	42.46
AR008	Boí	1923-1998	62.7	1948-1998	54	1096	0.81	42.51
AR012	Suert	1912-1920	85.7	-	-	845	0.74	42.4
AR013	Suert	1928-1932	93.5	-	-	845	0.74	42.4
AR014	Suert	1945-1998	96.2	1948-1998	80	830	0.74	42.4
AU006	Urgell	1911-1933	78.1	-	-	692	1.46	42.36
AU008	Urgell	1944-1959	100	1944-1959	99.4	703	1.46	42.36
AU009	Urgell	1965-1980	98.6	1968-1980	79.1	686	1.47	42.36
AU010	Urgell	1981-1993	100	1981-1993	100	692	1.46	42.36
AU011	Urgell	1992-2002	47.5	1992-2000	20.5	685	1.47	42.36
AU012	Urgell	2002-2012	71.2	2002-2012	60.5	692	1.46	42.36
AU013	Adrall	1927-2002	87.4	1931-2002	81.4	627	1.4	42.33
AU020	Organyà	1914-1936	75.1	-	-	540	1.33	42.21
AU021	Organyà	1941-1943	74.8	-	-	540	1.33	42.21
AU022	Organyà	1950-1999	100	1972-1999	53.7	549	1.33	42.21
AU023	Oliana	1911-1936	95.7	1931-1935	18.6	475	1.32	42.07
AU024	Oliana	1950-1999	99.3	1950-	98.8	468	1.3	42.08

				1999				
BG001	Lillet	1914-1928	64.9	-	-	848	1.98	42.25
BG002	Lillet	1914-1967	90.6	-	-	880	1.95	42.24
BG003	Lillet	1970-1995	99.6	-	-	880	1.98	42.25
BG016	Berga	1914-1943	86.8	-	-	730	1.84	42.1
BG017	Berga	1956-1988	100	-	-	760	1.84	42.1
BG018	Berga	1989-2008	96.9	1989-2008	93.8	682	1.86	42.1
BG027	Puig-Reig	1917-1972	96.8	-	-	411	1.88	41.97
BG028	Puig-Reig	1972-2012	96.6	-	-	434	1.88	41.96
NO001	Ponts	1915-2006	86.6	1961-2006	45.5	358	1.2	41.93
NO011	Montgai Llorenç	1927-1996	77.3	1934-1996	62.4	240	0.84	41.86
NO013	Montgai	1919-1937	97.7	-	-	280	0.96	41.8
NO014	Montgai	1972-2006	91.8	1972-2006	82.4	293	0.97	41.81
NO027	Avellanes	1915-2007	52	1934-2007	29.5	530	0.76	41.87
PJ003	Estany Gento	1925-1985	98.8	1930-1985	91.3	2142	1	42.51
PJ005	Cabdella	1915-1994	99.5	1930-1992	79.3	1273	0.99	42.47
PJ006	Molinos	1928-1995	96.3	1930-1995	91.4	981	0.98	42.41
PJ007	La Plana	1956-1995	78.5	1956-1995	51.2	888	0.96	42.39
PJ010	Senterada	1925-1992	78.6	1930-1992	66	711	0.94	42.32
PJ015	Psegur	1927-1994	96.5	1934-1992	62.9	525	0.97	42.25
PJ017	Talarn	1915-1996	97	1930-1996	76.7	430	0.91	42.17
PJ019	Tremp	1992-2009	98.1	1992-2007	88.8	467	0.89	42.16

PJ020	Vilamitjana	1916-1937	87.3	-	-	450	0.92	42.15
PJ026	Gavet Conca	1937-1994	96.5	1937-1994	75	382	0.9	42.11
PJ029	Terradets	1936-1996	76	1936-1996	76.1	360	0.9	42.05
PS004	Bonaigua	1922-1968	71.6	1929-1979	67.1	2263	0.98	42.67
PS005	Esterri d'Aneu	1917-1931	99.9	1928-1931	18.3	950	1.12	42.62
PS006	Esterri d'Aneu	1955-2005	85.9	1956-2005	71	952	1.13	42.63
PS014	Tavascan	1920-1994	79.3	1967-1994	36.3	1126	1.26	42.65
PS020	Sort	1911-1917	96.2	-	-	690	1.13	42.41
PS021	Sort	1947-1969	40.1	-	-	685	1.13	42.41
PS022	Sort	1985-2004	100	1985-2004	99.9	679	1.13	42.41
PS024	Mencui	1922-1965	93.1	-	-	1256	1.03	42.38
PS025	Escós	1920-1988	98	1931-1938	7.7	790	1.06	42.37
PS026	Baén	1921-1938	98.5	-	-	1406	1.12	42.33
PS027	Gerri	1914-1938	94.4	-	-	630	1.07	42.32
PS028	Gerri	1984-2012	94.9	1984-2012	81.7	605	1.07	42.32
SE013	Lleida	1914-1926	88.1	1927-1928	4.1	202	0.63	41.62
SE014	Lleida	1915-1994	66.4	1932-1994	47	150	0.65	41.62
SE017	Lleida	1983-1986	87.8	-	-	247	0.54	41.65
SO007	Solsona	1915-1970	87.6	1923-1970	56.1	683	1.51	41.99
SO008	Solsona	1984-2012	86.3	1984-2012	84.1	691	1.51	41.99
UG001	Agramunt	1916-1920	86.1	-	-	338	1.1	41.79
UG002	Agramunt	1928-1934	65.8	-	-	330	1.1	41.79
UG003	Agramunt	1942-1965	78.5	-	-	330	1.1	41.79

UG004	Agramunt	1966-2012	100	1966-2012	91.1	342	1.1	41.79
VA007	Arties	1922-1990	100	1930-1990	42	1160	0.88	42.7
VA009	Vielha	1911-1935	84.5	1915-1934	16.7	965	0.79	42.7
VA010	Vielha	1945-1993	98.6	1945-1993	98.1	951	0.8	42.71
VA013	Bossòst	1922-1923	86.8	-	-	712	0.69	42.79
VA014	Bossòst	1972-1993	98.5	1972-1993	98.5	723	0.69	42.78
9198	Canfranc	1910-2013	98.7	1910-2013	94.4	1160	-0.52	42.75
9201	Cas. Jaca	1914-2013	70	1970-2013	43.2	885	-0.55	42.63
9202	Jaca	1928-2013	43.8	1929-2013	52.6	800	-0.55	42.57
9207	Hecho	1928-2013	63.9	1931-2013	40.4	860	-0.75	42.74
9208	Aragues	1928-2006	53	1970-2006	46.2	980	-0.67	42.71
9212	Anso	1928-2001	59.3	1970-2001	39.6	820	-0.83	42.75
9446	Sallent	1930-2013	75.2	1953-2013	42.6	1285	-0.33	42.77
9451	Panticosa	1911-1993	78	1941-1993	56.3	1660	-0.23	42.76
9454	Biescas	1927-1980	90.3	-	-	875	-0.01	42.63
9489	Sotonera	1911-2013	88.3	1923-2013	74.8	413	-0.67	42.11
9759E	Camporrels	1928-2007	28.4	1992-2007	18.6	628	0.52	41.96
9782	Pineta	1928-2012	93.5	-	-	1150	0.2	42.64
9784	Barrosa	1928-1994	89.6	1979-1994	12.1	1200	0.21	42.68

9789	Gistain	1951-1994	92.5	1966-1994	21.7	1000	0.34	42.61
9789A	Gistain	1928-2013	69.6	-	-	1422	0.33	42.59
9790	Plandescun	1941-1993	98	1986-1993	11.3	1100	0.3	42.57
9794	Bielsa	1928-1989	74.4	1961-1967	8.6	760	0.22	42.58
9817	Fiscal	1928-2013	70.3	-	-	770	-0.12	42.5
9822	Boltaña	1928-2013	77.4	1930-1994	36	643	0.67	42.45
9829	Mediano	1922-2008	81.8	1931-2008	36.2	504	0.2	42.32
9838	Benasque	1912-1977	92.7	1940-1977	52.3	1130	0.52	42.6
9843	Seira	1919-2007	83.9	1929-2007	63.9	815	0.43	42.48
9849	Graus	1928-1990	89.5	1934-1990	86.9	498	0.36	42.23
9850	Graus	1919-1977	66.1	-	-	604	0.01	42.18
9866	Barbastro	1928-2013	52.5	1953-2013	39.7	338	1.25	42.04
9895	Belsue	1918-1994	78.3	1923-1994	57.4	990	-0.36	42.29
CA	Cardener	1996-2012	97.6	1996-2012	97.2	693	1.59	41.95
CB	Llosses	1995-2003	90.4	1995-2003	87.3	700	2.2	42.15
CD	Urgell	1996-2013	97.2	1996-2013	96.5	849	1.43	42.37
CG	Molló	1996-2013	95.9	1996-2013	95.4	1405	2.41	42.38
CI	Sant Pau de Segúries	1996-2013	97.1	1996-2013	96.8	852	2.36	42.26
CJ	Organyà	1996-2013	98.9	1996-2013	97.9	566	1.33	42.22
CN	Guardiola	1996-2005	98.6	1996-	98.2	720	1.88	42.23

				2005				
CO	Torres de Segre	1995-2006	94.3	1995-2006	92	144	0.53	41.53
CP	Sant Romà	1996-2013	99.7	1996-2013	99.3	690	1.04	42.14
CQ	Vilanova	1996-2013	99.1	1996-2013	95.4	594	1.03	42
CR	Quar	1996-2013	97	1996-2013	98	873	1.96	42.08
CT	Suert	1996-2013	98	1996-2013	97.2	823	0.74	42.4
CU	Vielha	1996-2013	96.4	1996-2013	95.4	1002	0.79	42.7
CV	Psegur	1995-2013	97.3	1995-2013	96.2	513	0.96	42.24
DG	Núria	1998-2013	98.1	1998-2013	97.1	1971	2.16	42.4
DP	Das	2001-2013	99.5	2001-2013	98.7	1097	1.87	42.39
UI	Gisclareny	1999-2013	100	1999-2013	99.7	1386	1.76	42.26
UY	Os de Balaguer	1995-2013	100	1995-2013	99.8	576	0.76	41.88
V1	Vallfogona	1990-2013	98.7	1990-2013	97.3	238	0.83	41.78
VE	Aitona	1998-2013	99.3	1998-2013	99.4	97	0.46	41.49
VF	Alcarràs	1998-2013	95.9	1998-2013	97.5	122	0.55	41.56
VH	Gimenells	1996-2013	99.4	1996-2013	99.3	259	0.39	41.66
VI	Lleida	1990-2000	96.6	1990-2000	96.8	190	0.6	41.63
VJ	Lleida	1998-2013	90	1998-2013	97.2	161	0.65	41.6

VK	Raimat	1988-2013	98.9	1988-2013	98.9	286	0.45	41.68
VL	Seròs	1998-2011	93.9	1998-2011	95.5	100	0.41	41.46
VM	Vilanova Segrià	1998-2013	86.5	1998-2013	87.7	222	0.63	41.71
VO	Lladurs	1998-2013	99.8	1998-2013	99.9	785	1.43	42.09
VP	Pinós	1995-2013	99.9	1995-2013	99.9	659	1.54	41.8
VS	Lac Redon	1999-2013	73.6	1999-2013	92.8	2247	0.78	42.64
W5	Oliana	2000-2013	99.9	2000-2013	99.9	490	1.31	42.08
WA	Oliola	2001-2013	100	2001-2013	100	443	1.15	41.88
WB	Albesa	2006-2013	100	2006-2013	100	267	0.67	41.76
WG	Algerri	2000-2013	99.9	2000-2013	99.7	301	0.65	41.8
WI	Maials	2000-2013	99.9	2000-2013	99.9	350	0.48	41.36
WK	Alfarràs	1998-2012	95.9	1998-2012	98	268	0.58	41.82
WM	Queralt	2002-2013	99.5	2002-2013	100	1167	1.83	42.11
WQ	Montsec Ares	2003-2013	97.3	2003-2013	100	1572	0.73	42.05
WV	Guardiola	2005-2013	99.9	2005-2013	100	788	1.87	42.23
WX	Camarasa	2006-2013	99.9	2006-2013	99.9	668	0.88	41.92
X3	Alguaire	2006-2013	100	2006-2013	99.8	370	0.54	41.74
X6	Baldomar	2006-2013	100	2006-2013	100	366	1.03	41.92

X7	Torres de Segre	2007-2013	100	2007-2013	99.9	215	0.55	41.52
XH	Sort	2009-2013	100	2009-2013	99.7	679	1.13	42.41
XM	Els Alamús	2011-2013	100	2011-2013	100	235	0.74	41.59
XN	Seròs-depuradora	2011-2013	99.9	2011-2013	100	89	0.43	41.46
XQ	Tremp	2012-2013	99.8	2012-2013	100	473	0.89	42.16
XT	Solsona	2012-2013	100	2012-2013	100	691	1.51	41.99
XW	Lleida-la Bordeta	2013-2013	100	2013-2013	100	165	0.65	41.6
XY	Alcarràs	2013-2013	99.4	2013-2013	100	122	0.55	41.56
Z1	Bonaigua	2001-2013	74.5	1997-2013	95.4	2266	0.98	42.65
Z2	Boí	2001-2013	80.6	1998-2013	93.7	2535	0.88	42.47
Z3	Malniu	2002-2013	76.4	1999-2013	97.5	2230	1.78	42.47
Z4	Ulldeter	2001-2011	86.4	2000-2011	99.5	2364	2.25	42.42
Z5	Certascan	2003-2013	75	2000-2013	92.2	2400	1.27	42.7
Z6	Sasseuva	2004-2013	77.1	2001-2013	98.7	2228	0.73	42.77
Z7	Espot	2003-2013	85.3	2002-2013	96	2519	1.05	42.53
Z8	el Port del Comte	2004-2013	82.6	2002-2013	99.8	2316	1.52	42.18
Z9	Cadí Nord	2004-2013	89.3	2003-2013	99	2143	1.71	42.29
ZB	Salòria	2004-2013	89.7	2004-	99.3	2451	1.37	42.52

ZC	Ulldeter	2011-2013	100	2013 2011-2013	95.8	2410	2.25	42.42

Table S.2: PPT Composite series obtained by merging individual series. Tmax and Tmin composite series are shown in bold.

Name	**Serie 1**	**Serie 2**	**Serie 3**	**Serie 4**	**Serie 5**	**Serie 6**
Suert	AR012	AR013	**AR014**	**CT**		
Urgell	AU006	**AU008**	**AU009**	**AU010**	**AU011**	**AU012**
Organyà	AU020	AU021	**AU022**	**CJ**		
Oliana	**AU023**	**AU024**	**W5**			
Lillet	BG002	BG003				
Berga	BG016	BG017	BG018			
Puig-Reig	BG027	BG028				
Ponts	**NO001**	**X6**				
Montgai	NO013	NO014				
Avellanes	**NO027**	**UY**				
Psegur	**PJ015**	**CV**				
Talarn	**PJ017**	**PJ019**	**XQ**			
Bonaigua	**PS004**	**Z1**				
Esterri	**PS005**	**PS006**				
Sort	PS020	PS021	**PS022**	**XH**		
Gerri	PS027	PS028				
Lleida	**SE014**	**VJ**	**XW**			
Solsona	**SO007**	**SO008**	**XT**			
Agramunt	UG001	UG002	UG003	UG004		
Vielha	**VA009**	**VA010**				
Bossots	VA013	VA014				
Panticosa	**9451**	**9446**				
Graus	9850	9849				

Table S.3: Selected series to apply HOMER homogenization procedure. All series, except Bossots (in Italics), have been checked for PPT homogeneity. Temperature (Tmax and Tmin) homogenization procedure has been applied in two separately groups: short and long series (See section 3.2). Composite PPT series are indicated with an asterisk (*) and composite temperature (Tmax and Tmin) series with a circumflex accent (^). Support series are provided from SDATSv2 (Brunet et al.*, 2006) and included in all homogenization procedure applied.*

Name	**Group of temperature homognization**	**Name**	**Group of temperature homognization**
Adrall	short	Lillet*	-
Agramunt*	short	Lleida*^	long
Anso	short	Mediano	short
Aragues	short	Mencui	-
Arties	short	Molinos	long
Avellanes*^	short	Montgai	long
Barbastro	short	MontgaiMas*	short
Barrosa	-	Oliana*^	long
Belsue	long	Organya*^	short
Benasque	short	Panticosa*^	short
Berga*	-	Pineta	-
Bielsa	-	Ponts*^	short
Biescas	-	PSegur*^	long
Boi	short	PuigReig*	-
Boltana	short	Seira	short
Bonaigua *^	long	Senet	short
Bossots *	short	Senterada	long
Cabdella	long	Solsona*^	long
Canfranc	long	Sort*^	short
CasJaca	short	Sotonera	long
EGento	long	Suert*^	short
Escos	-	Talarn*^	long
Esterri*^	short	Tavascan	short
Fiscal	-	Terradets	short

GavetConca	short	Urgell*^	short
GerriC*	-	Vielha*^	long
Gistain	-	Vilaller	short
GistainMol	-	Barcelona	support
GrausC*	long	Huesca	support
Hecho	-	Pamplona	support
Jaca	long	Zaragoza	support

Table S.4: Number and percentage (bewteen parenthesis) of the dry/wet/normal for PPT regional anomaly series and cold/hot/normal years for Tmax and Tmin regional.

		PPT			Tmax		Tmin	
		1910–1949	1950–2013		1910–1949	1950–2013	1910–1949	1950–2013
	dry	12 (30)	26 (41)	cold	9 (23)	9 (14)	7 (18)	6 (9)
Annual	wet	7 (18)	17 (27)	hot	10 (25)	25 (39)	5 (13)	14 (22)
	normal	21 (53)	21(33)	normal	21 (53)	30 (47)	28 (70)	44 (69)
	dry	20 (50)	39 (61)	cold	10 (25)	13 (20)	25 (63)	22 (34)
Winter	wet	10 (25)	22 (34)	hot	10 (25)	25 (39)	3 (8)	17 (27)
	normal	9 (23)	3 (5)	normal	20 (50)	26 (41)	11 (28)	25 (39)
	dry	13 (33)	24 (38)	cold	14 (35)	14 (22)	7 (18)	6 (9)
Spring	wet	15 (38)	20 (31)	hot	17 (43)	34 (53)	17 (43)	22 (34)
	normal	12 (30)	20 (31)	normal	9 (23)	16 (25)	16 (40)	36 (56)
	dry	16 (40)	30 (47)	cold	14 (35)	15 (23)	6 (15)	6 (9)
Summer	wet	8 (20)	22 (34)	hot	13 (33)	30 (47)	12 (30)	21 (33)
	normal	16 (40)	12 (19)	normal	13 (33)	19 (30)	22 (55)	37 (58)
	dry	14 (35)	29 (45)	cold	17 (43)	19 (30)	17 (43)	12 (19)
Autumn	wet	13 (33)	26 (41)	hot	10 (25)	23 (36)	6 (15)	21 (33)
	normal	13 (33)	9 (14)	normal	13 (33)	22 (34)	17 (43)	31 (48)

Table S.5: Trend values for each series for the periods 1961–1990 and 1970–2013.

Significant values are shown in bold.

	PPT		Tmin		Tmax	
	1961-1990	1970-2013	1961-1990	1970-2013	1961-1990	1970-2013
Adrall	-7.06	-7.84	0.08	0.35	**0.41**	**0.82**
AgramuntC	**-9.5**	-2.64	-	-	-	-
Barrosa	**-7.54**	-8.01	-	-	-	-
Belsue	-3.8	-7.4	0.21	0.34	-	-
BergaC	-8.34	-5.98	-	-	-	-
Bielsa	-7.96	-8.37	-	-	-	-
Boltaña	**-13.55**	-1.55	-	-	-	-
Cabdella	**-6.7**	-5.25	0.21	**0.64**	**0.53**	**0.67**
Canfranc	-6.04	-1.72	0.02	**0.17**	-	-
Egento	**-17.33**	**-19.7**	-	-	-	-
Escós	**-15.32**	-8.96	-	-	-	-
EsterriC	-9.01	0.66	-	-	-	-
Fiscal	**-11.74**	-2.01	-	-	-	-
GavetConca	-6.64	-11.92	-0.15	0.24	**0.34**	**0.7**
GrausC	**-14.01**	**-26.62**	**0.55**	**0.73**	0.18	**0.59**
Molinos	-6.29	-4.65	0.39	**0.78**	0.16	1.33
Montgai	-7.05	**-18.71**	0.42	0.41	0.77	**0.79**
OlianaC	**-14.11**	-3.96	0.64	**0.32**	**0.62**	**0.59**
OrganyaC	-7.09	-4.57	-	-	-	-
PanticosaC	-6.07	-3.5	-	-	-	-
Pineta	**-12.13**	-1.9	-	-	-	-
PontsC	-9.44	-1.59	-	-	-	-
PSegurC	-6.71	-4.78	0.17	**0.28**	0.07	**0.6**
Seira	**-11.28**	-2.29	-0.42	0.21	0.07	**0.7**
Senet	-7.75	1.25	-	-	-	-
Senterada	**-13.37**	-11.7	0.15	**0.55**	0.35	**0.97**
Sotonera	-3.89	-3.55	0.39	**0.26**	**0.69**	**0.64**
SuertC	**-13.72**	-2.56	0.01	0.13	0.27	**0.44**
TalarnC	-9.11	-3.28	0.14	**0.35**	**0.44**	**0.72**
Tavascan	-0.75	-2.2	-	-	-	-

Terradets	-8.15	-12.19	-0.15	0.2	**0.41**	**0.58**
UrgellC	-7.75	-6.42	-	-	-	-
VielhaC	-6.14	-8.15	**0.24**	**0.23**	0.4	**0.61**
Vilaller	-1.96	1.98	0.27	0.28	**0.46**	**0.71**
Hesca	**-9.7**	**-7.91**	0.25	0.16	**0.45**	**0.45**
Pamplona	-	-	**0.28**	**0.29**	**0.58**	**0.67**

Chapter 4 – Limnological analysis

Vegas-Vilarúbia, T., Corella, P., **Pérez-Zanón, N.**, Buchaca, T., Trapote, M.C., López, P., Sigró, J., Rull, V. Historical shifts in oxygenation regime as recorded in the laminated sediments of lake Montcortès (central Pyrenees): A continental-scale phenomenon? STOTEN [submitted]

HISTORICAL SHIFTS IN OXYGENATION REGIME AS RECORDED IN THE LAMINATED SEDIMENTS OF LAKE MONTCORTÈS (CENTRAL PYRENEES): A CONTINENTAL-SCALE PHENOMENON?

Teresa Vegas-Vilarrúbia[1*](tvegas@ub.edu), Juan Pablo Corella[2], Núria Pérez-Zanón[3], Teresa Buchaca[4], M. Carmen Trapote[1], Pilar López[1], Javier Sigró[3], Valentí Rull[5].

[1] Department of Evolutionary Biology, Ecology and Environmental Sciences, Universitat de Barcelona, Av. Diagonal 643, 08028 Barcelona, Spain.

[2] Institute of Physical Chemistry Rocasolano (CSIC), C/Serrano 119, 28006 Madrid, Spain.

[3]Centre for Climate Change (C3), Universitat Rovira i Virgili, C/ Joanot Martorell 15, Vila-seca, 43500 Tarragona, Spain.

[4] Centre for Advanced Studies of Blanes (CEAB-CSIC), Accés a la Cala St. Francesc 14, 17300 Blanes, Spain.

[5]Laboratory of Paleoecology, Institute of Earth Sciences Jaume Almera (ICTJACSIC), C. Sole i Sabarís s/n, 08028 Barcelona, Spain.

*Corresponding author

KEYWORDS: anoxia, global change, Holocene, hypoxia, micro-XRF core scanning, meromixis, paleolimnology, pigment biomarkers, varves.

ABSTRACT

Recent expansion of anoxia has become a global issue and there is potential for worsening under global warming. At the same time, obtaining proper long-term instrumental oxygen records is difficult, thus reducing the possibility of recording long-term changes in oxygen shifts that can be related with climate or human influence.

Varved lake sediments provide the better time frame to study this phenomenon. We assessed the oxic/anoxic shifts of the varved Lake Montcortès since 1500 AD and tried to determine phases when oxic/anoxic shifts were driven by anthropogenic and when by climatic influences. We combined independent biological and geochemical proxies and work at subdecadal resolution.

Four main scenarios emerged: 1) years with abrupt sediment inputs (A); 2) years with outstanding mixing and oxygenation of the water column associated with diatom growth(B); 3) years with strong stratification, anoxia, intense sulfur bacterial activity and increased biomass production (C); 4) years with stratification and anoxia, but relatively less biomass production (D). In line with current limnologic trends, we found high supra-annual variability in the occurrence of oxygenation events over the last 500 years (subset B). Interestingly, at least 45,3% of the years were mixing years and, like the meromictic ones, mostly occurred arranged in groups of consecutive years, thus alternating years of monomixis with years of meromixis. Most years of D belong to the period 1500-1820 AD, when human activities were the most intense. Most years of A belonged to the climatic unstable period of 1850 -1899AD. Years of B were irregularly distributed but were best represented in the period 1820-1849 AD. Most years of C belonged to the 20th century. More than 90% of the years with climatic instrumental records belonged to B and C.

Severe depopulation by1900 promoted the lake recovery lake, yet anoxia increased again after 1950.Current climate warming seems to be taking control over the oxygenation capacity of the lake, especially since the second half of the 20th century. Our results support recent findings at the global scale.

Introduction

Lake mixing is crucial for oxygenation of the water column and therefore, for lacustrine health. Oxygenation lies on water column stratification, which determines oxygen diffusion to the bottom layers and releases oxygen though respiration. Mixing regimes can shift with climate changes (Hakala, 2004) and human intervention (e.g. Jellison et al., 1998). Recent increase in hypoxia and anoxia around the world has become a global concern and there is potential for worsening undercurrent global warming (Diaz,2001; IPCC, 2014). There are ongoing global projects that address these complex phenomena with diverse approaches (Friedrich el al., 2014), nonetheless there is little emphasis on continental water bodies. A worldwide study conducted on over 300 lakes with laminated sediments found that almost all of these water bodies exhibited changes in oxygenation (the onset of anoxia or reoligotrophication) that were chiefly due to anthropogenic causes (Jenny et al., 2016 a), with urban nutrients as the main primary cause across European lakes (Jenny et al., 2016 b). It is worth noting that oxygen depletion is considered to be one of the main natural causes of species extinction on Earth. In fact, the majority of extinctions appear to have occurred during marine transgressive pulses when anoxic bottom water expanded into epicontinental seas (Barnosky et al., 2011; Hallam and Wignall, 1997, 1999; Pearce et al.,2008).In fact, several contemporary environmental, economic and health issues are related to oxygen deficiency in water bodies, e.g. biodiversity loss from the mortality of benthic organisms, the decline of fisheries (Diaz, 2001) and the release of harmful greenhouse gases (Camargo and Alonso, 2006).

In lacustrine systems, mixing regimes have varied over time. Recent research in typical monomictic Swiss lakes has indicated that the current climate change has already caused a decrease in the frequency of oligomixis (Livingstone 1993) that threatens to generate hypoxia in the deep strata (Livingstone, 1997; Rempfer et al., 2010) and in the redissolution of sedimentary phosphorus (North et al., 2014). In particular, in Lake Zürich, high -quality long -series of temperature and oxygen profiles from the last 50 years show that temperature has increased at all depths. This increase was more pronounced in the epi- and metalimnion than in the hypolimnion; thus, the thermal stability of the lake also increased, causing a prolongation of the stratification period with a corresponding reduction in the homeothermal break. These results are extremely useful for quantifying the effect of current climate change on oxygen concentrations in

deep water (Livingstone, 1997; Jankowski et al, 2006; Rempfer et al, 2009, 2010; North et al, 2014) evidencing that increase in the thermal stratification period tends to favour the onset of hypoxia or anoxia and can eventually lead to meromictic conditions (Adrian et al, 2009; Livingstone, 2003; Peeters et al., 2002; Stefan et al., 1998).

Nonetheless, long -term instrumental data of temperature and oxygen usually do not extend beyond a century, and circumstances where they are available are rather extraordinary, thus reducing the possibility of recording truly long-term changes in present and past hypoxia. Fortunately, oxidisation and reduction (redox) changes, which are often biologically mediated (photosynthesis, respiration, fermentation, etc.) leave imprints in the sedimentary record. The redox conditions in hypolimnion and sediments notably influence the fate of trace metals, the sediments acting as a source or sink, depending on the biogeochemical conditions of the lake and on the redox characteristics of the involved minerals (Davison, 1993; Schaller et al., 1997; Stumm and Morgan, 1996). Therefore, the presence of organic and redox-sensitive inorganic indicators in the sediment has allowed the reconstruction of environmental features related to hypoxia/anoxia further back into the past (see Davies et al. 2015 and literature therein). At best, the concentrations of target minerals can be determined in the stratigraphic record and compared with the oxygen concentrations measured in the water column to evaluate their potential as indicators of deep-water hypoxia (see Friedrich et al., 2014 and literature therein). Nonetheless, the convergence of statistically sound time series of these redox indicators and instrumental oxygen records over the same time period is rather exceptional. Where such concurrent series are not available, extended, high-resolution paleolimnological records offer a valuable tool to assess long-term changes in the mixing regime of lakes, their associated oxic/anoxic shifts and the likely drivers of change. Hence, the relative contribution of both environmental forcings on oxygenation dynamics over the long term remains mainly unknown due to a lack of historical monitoring. Therefore, lakes with varved sediments offer an extraordinary advantage because they allow for high resolution (annual, decadal) paleoenvironmental and paleoclimatic reconstructions with accurate time control (Ojala et al., 2012).

The objective of this study was to assess the evolution of the oxic/anoxic shifts in a temperate lake over the last 500 years, combining independent biological (marker

pigments) and inorganic proxies (trace metals) of hypolimnetic anoxia and environmental conditions. To this purpose we chose Lake Montcortès (Central Pyrenees, Southern Europe) taking advantage of the varved nature of its sediment. Understanding true long-term ecological trends requires the integration of past and present evidence into single and coherent time series at the same resolution, ideally annual to subannual, and lakes with annually-laminated sediments are ideal targets for such purpose (Rull, 2014). In this sense, the Lake Montcortès varved record could provide the necessary paleoecological data to be integrated with modern measures and observations into single past-present, high-resolution continuous records at centennial to millennial timescales, which are needed to resolving long-term ecological processes. We intend to distinguish different phases in the evolution of oxygen shifts over time that can be linked with climatic and/or anthropogenic impacts on the lake's catchment or on the lake itself. Since the relative importance of redox processes depends on the biogeochemical conditions of the lake and on the chemical characteristics of the involved compounds, we supported our research with a present-day monitoring of the lake's oxygenation regime and several associated environmental variables. The results will provide contemporary analogue information that is useful for making insightful inferences when studying the paleolimnological records to infer oxic/anoxic shifts.

2. Environmental settings

Lake Montcortès is situated on the southern flank of the Central Pyrenees, in the Pallars Sobirà region of Catalonia (Spain), at 42° 19′ N, 0° 59′ E and 1027 m altitude (Fig. 1). The lake lies on karst terrain that is primarily characterised by Triassic limestones, marls and evaporites as well as Oligocene-carbonate conglomerates. (Corella et al., 2011b; Rosell, 1994). According to the La Pobla de Segur meteorological station (19 km from Montcortès), the total annual mean precipitation is 668.5 mm, February is the driest month and May is the wettest. The annual mean temperature is 12.8ºC (19.5ºC in July and 2.9ºC in January; meteocat, 2015a). The surrounding vegetation is evergreen with deciduous oak forests (*Quercus rotundifolia* and *Q.pubescens*), conifer forests (*Pinus nigra*), pastures and crops. The littoral belt vegetation is dominated by hygrophyte communities of *Typha domingensis* or *Cladium mariscus*, reed beds of *Phragmites australis*, communities of *Carex riparia*, and rush formations and

grasslands on sporadically flooded soils (Mercadé et al., 2013). The lake surface area is 12.36 ha, with a maximum water depth of ~30 m. There is no permanent inlet and the maximum lake level is controlled by an outlet stream located on the northern shore. Biogenic varves from the Late Holocene are well-preserved in the lake's sedimentary record (Corella et al., 2011b, 2012). These varves are composed of (i) endogenic calcite and (ii) organic detritus; furthermore, detrital layers and turbidites are embedded in the varve succession (Corella et al., 2012).

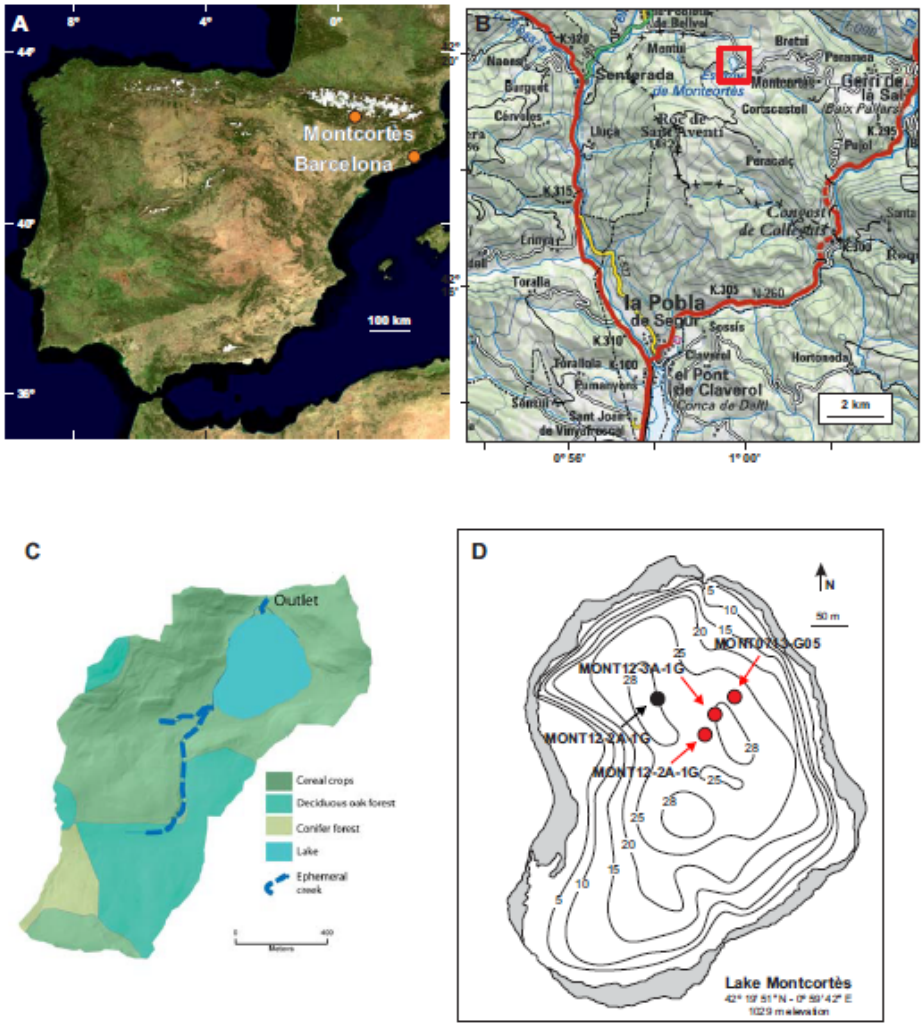

Figure 1: Location (A, B) and land-use map (C) (Corine, EEA, 2000) of L. Montcortès. Bathymetric map (D) showing the position of the studied cores.

3. Materials and Methods.

3.1. Indicators of changes in oxic/anoxic conditions of the lake.

We took advantage of recent developments of high resolution -XRF core scanning techniques as applied to palaeolimnology (Davies et al., 2015) and used several known elements, namely iron (Fe), manganese (Mn), bromine (Br), calcium (Ca), sulfur (S), silica (Si) and titanium (Ti), and derived elemental ratios to survey shifts in the oxic/anoxic conditions of the lake over the last 500 years as reflected in the sediment record. We focused mainly on Fe and Mn using the Fe/Ti, Fe/Mn and Mn/Ti ratios, which are affected by redox changes (Davidson 1993). Since variations in the oxygen content of the water column are mainly driven by photosynthesis and decomposition of organic matter, we also tested bromine (Br) as tracer of organic content in the sediment (e.g. Moreno et al. 2007), the Ca/Ti and Si/Ti ratios as indicators of biologically mediated calcite and silica production respectively, and the S/Ti and S/Fe ratios as indicators of increased organic matter and presence of sulfur compounds such as pyrite (Davies et al., 2015), respectively. Finally, we examined selected marker pigments in the sediments as complementary biomarkers (Leavitt 1993) based on previous knowledge of the lake's microbial life (Camps et al., 1976; Cristina et al., 2000; Serra et al., 2001). We selected isorenieratene, produced by the brown-coloured- photosynthetic green sulfur bacteria (GSB, Chlorobiaceae) as a tracer of euxinia, and okenone, synthesised by purple sulfur bacteria (PSB, Chromatiaceae), as indicators of anoxia. Additionally, beta-carotene is ubiquitous in all algae and a proxy of primary producer's biomass. Finally, oscillaxanthin, which is found in Oscillatoriales, was used as a marker pigment of this order and in general for the presence of cyanobacteria.

3.2. Coring, age model correlations and sampling of the water column

A composite sedimentary sequence from two UWITEC gravity cores (MON12-3A-1G and MON12-2A-1K, 1m length), another one MONT-0713-G05 (1m length) and a long Kullenberg core (MON04-1A-1K, 6,69 m length) were retrieved from the deepest distal lake basin (~30 m water depth) (Fig. 1). The gravity cores MON12-3A-1K and

MON12-2A-1K were stored on the lakeshore to favour consolidation and avoid sediment disturbances during transport to the core repository. The sediment cores were split lengthwise. The age-depth model was based on two independent dating techniques: i) varve counting performed on calcite layers and ii) radiometric dating with ^{210}Pb and ^{14}C. (see Corella et al. 2012, 2014 for further description). Poor varve preservation intervals represent only 1% of the studied sequence and they were interpolated by using the mean varve thickness of the upper and lower centimeters of these intervals. The upper 88 cm of sediment in the MON12-3A-1K core and the upper 94 cm in MONT-0713-G05 core spanned from 1500 AD until present. Sedimentation rates (SR) in core MONT-0713-G05 show fluctuating values according to the lithostratigraphic units defined in Corella et al., (2014). The highest SR were recorded during the period 1902-1844 (SR= 0.8) while lower SR occurred over the periods 1500-1843 (SR 0.1 cm/yr) and 1903 -2012 (SR= 0.12 cm/yr). Stratigraphic correlation among the cores was performed using lithological correlation of distinct event layers through detailed inspection of the thin sections, which were obtained at the Deutsches GeoForschungs Zentrum (Potsdam).

Monthly limnologic field campaigns were carried out between October 2013 and April2016.Water column profiles with a 1 m resolution were obtained for temperature and dissolved oxygen concentrations (O_2) using a multi-parameter water quality sonde Hydrolab DS5 (Hatch Environmental, Colorado, USA). Water samples for dissolved iron (Fe) and manganese (Mn) were collected in the hypolimnion and were filtered through GF/F Whatman filters. Pigments from the water column were captured monthly (October 2013 and September 2015) with a cylindrical sediment trap placed at 20 m depth in the hypolimnion (Bloesch and Burns, 1980). Immediately after sampling, the collected material was filtered through Whatman GF/F filters and frozen.

3.3. Laboratory analyses

Dissolved Fe and Mn concentrations were determined by Inductively Coupled Plasma Atomic Emission Spectroscopy with a Perkin Elmer Optima 8300 spectrometer under

standard conditions, at the Scientific and Technological Centre of the University of Barcelona.

A 0.2 mm resolution X-ray fluorescence (XRF) analysis was performed on the open core MON12-3A-1K, using a XRF AVAATECH core scanner (2000 A, 10-30 kV and 20-50 s measuring time). This technique provides semi-quantitative information given as counts per second (CPS) to obtain high resolution (subdecadal) time series data for the following elements: Fe, Mn, Ca, Si, S, Ti and Br. Fe, Mn Ca, S and Si data were normalised to Ti because they can be incorporated into the lake from the surroundings in the form of unaltered mineral grains, oxides, colloids, or organic complexes. Instead, Ti remains stable once deposited in the lake bottom and is an unambiguous indicator of allochtonous inputs.

Pigments were extracted from the frozen filters in 5-mL of 90% acetone using probe sonication (Sonopuls GM70 Delft, The Netherlands) (50W, 2 min). The extract was centrifuged (4 min at 3000 rpm, 4ºC), filtered through Whatman ANODISC 25(0.1 μm) and analysed with ultra-high-performance liquid chromatography (UHPLC). The UHPLC system (Acquity Waters, Milford, MA, USA) was equipped with an UPLC HSS C18 SB column (dimensions: 2.1 x 100 mm; particle size: 1.8 μm) and with PDA (λ: 300-800 nm). The PDA channel was set at 440 nm for pigment detection and quantification. After a sample injection (7.5 μL), the pigments were eluted with a linear gradient from 100% solvent B (51:36:13 methanol: acetonitrile: MilliQ water, v/v/v 0.3 M ammonium acetate) to 75% B and 25% A (70:30 ethyl acetate: acetonitrile, v/v) for 3 min, followed by 0.45 min of isocratic hold at 75% B and 2 min of linear gradient to 100% of solvent A. The initial conditions (100% B) were linearly recovered in 0.65 min. The flow rate was 0.7 mL min^{-1}. Pigments were identified checking retention times and absorption spectra against a library based on photosynthetic bacterial cultures (Institut d'Ecologia Aquàtica, University of Girona, Catalonia, Spain).

Climate

To investigate what extent climate had an influence on the indicators of anoxia and related variables during the instrumental measurement period, we used the regional anomaly series of precipitation and maximum and minimum temperature for the central

Pyrenees (Pérez-Zanón et al., 2016) covering the period 1910-2013.Climate series were built using quality controlled and homogenised data from observatories placed around the study area and were obtained over annual and seasonal time periods. Theses series represent the longest high-quality climate data set currently available for the Central Pyrenees. We also searched for likely climatic influence on oxic/anoxic shifts for the last 500 years; to this end, we used the northern hemisphere air surface temperature reconstruction (NHTA) of Mann et al. (2009). This high resolution reconstruction has been widely used (e.g. Jungclaus et al., 2010; IPCC, 2014; Hiner et al., 2016; Marlon et al. 2012), since it properly captures the mean regional climatic features of the period of study.

Data analyses

Some critical papers warn that the use of ratios (Y/X, percentages, proportions, etc.) can lead to a wide variety of problems and recommend exploring and making explicit the relationship between numerator and denominator, as well as their joint distribution (e.g. Curran-Everett, 2013; Liermann et al., 2004, and literature therein). In our case, the denominator only plays a role as a common reference, except in the case of S/Fe and Fe/Mn, which were not normalised and where the numerator and denominator exhibited weak or no correlation, respectively. To visualise and compare the patterns of the ratios in the sediment record, we computed Pearson correlation coefficients (r). We relied on the Central Limit Theorem to accept that the ratios and pigments series approach a normal distribution, since the number of data is large (entire XRF measurement series, n=4282; series with annual mean ratios values, n= 505; two to ten years of integrated series for pigment analysis, n=80) (Davis 2002). Moreover, all of the data were $\log_{10}$ transformed prior to applying multivariate analyses, which were performed with the free statistical software PAST, version 3.15 (Hammer et al. 2001). Principal Components Analysis (PCA) was chosen as exploration method after verifying that the underlying gradient length of our data was < 3 standard deviations with Detrended Component Analysis, (Legendre and Legendre 1998). We examined if the resulting groups of scores (A, B, C, D) significantly differed from each other by pairwise comparing the averages

of their elemental ratios by means of the Welch's t-test (Quinn and Keoghs, 2002). Numerical zonation of the stratigraphic sequence was implemented by the constrained hierarchical clustering method CONISS applied on PCA axes, and the number of significant zones was determined by the broken-stick model (Bennet 1996). Both methods were provided by the R package rioja (Juggins, 2009).

4. Results

4.1. Seasonal variations in Fe, Mn, O_2 and bacterial pigments (2013-2016)

The current O_2, Fe and Mn concentrations were measured to explore their seasonal behaviour and relationship with the occurrence of bacterial pigments in (Fig. 2). Oxygen depletion started in the hypolimnion in early spring and an anoxic layer (< 1.5 mg/L) developed during the stratification period reaching different depths, depending on the year. Hypolimnetic oxygen was restored to physical saturation levels by two complete mixing events that occurred in the winter of the years 2014 and 2015, triggering Fe and Mn precipitation in the form of an oxidised compound. Sulfur bacteria thrived in the hypolimnion only when anoxic conditions prevailed and the dissolved Fe and Mn concentrations reached maximum concentrations. The presence of oscillaxanthin was not detected in the water columns. Interestingly, anoxic conditions persisted thorough2016. With the onset of anoxia, the precipitated Mn and Fe oxides started to redissolve.

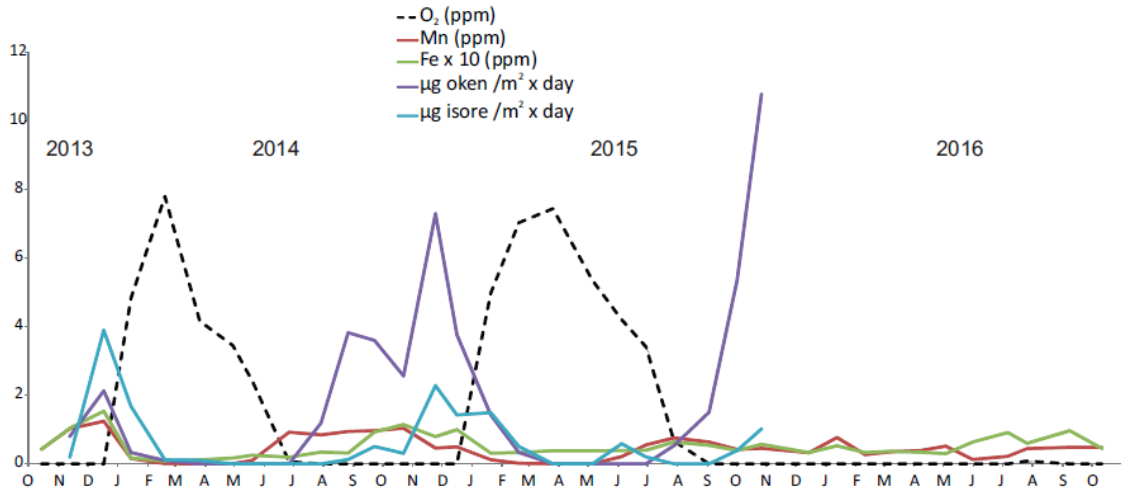

Figure 2: Seasonal variations of mean values of Fe, Mn, $O_2$and bacterial pigments okenone (oken) and isorenieratene (isore) in hypolimnetic waters, between October 2013 and September 2015.

4.2. Elemental ratios in the sediment record

The PCAs helped explore the relationships between elemental ratios, among them and with marker pigments. To characterise the microstructure of the sediment, the first PCA was performed on the ratios derived from the individual XRF measurement units (each 0.2 mm). The eigenvalues of the first two axes obtained with PCA (I) (Fig.3a) were > 1 and the cumulative explained variance was 76.7%, with component C1 explaining twice as much variance (55.4%) as C2 (21.3%). C1 was strongly and positively correlated with Ca/Ti (r = 0.919), Si/Ti (r = 0.901) and S/Ti (r = 0.893) which taken together can be interpreted as indicators of primary production; it also correlated with Mn/Ti (r = 0.888) indicating the enrichment of the sediment with oxidised Mn precipitation. C2

was positively correlated with Fe/Ti (r = 0.802) and Fe/Mn (r = 0,671); both ratios are symptomatic of iron mobilization processes. C2 was also negatively correlated with Br (r = -0.465) suggesting enhanced organic matter supply, and with S/Fe (r = -0.382), which may be related to the formation of iron disulfides under changing redox conditions. The scores represent the positions of the ratio values obtained along the entire sequence and are distributed among the four quadrants of the biplot (A, B, C, D), forming four different subsets of scores that could be analysed and interpreted in terms of the combination of processes related to C1 and C2 (Figure 4b)

The contribution of each subset to every single year during the last 500 years in terms of frequency of types of scores per year was calculated as A= 39.3%, B=24.6%, C=13.5% and D=22%.

A second PCA (II), (Fig.3b) was performed on the annual means of the ratios values, in order to identify variations in the sediment layers across supra-annual time scales in terms of redox reactions, productivity and organic matter. In this analysis, the scores represent individual calendar years (1500 to 2007 AD) instead of single XRF measurements. The eigenvalues of the first three components were > 1 and the cumulative variance explained was 87.0% with C1 accounting for 46.6% of the variance and C2 for 25.5%. Both PCA were similar in terms of the loadings (correlations) on each component (Table A.1, supplementary materials) indicating that the meaning of the results was preserved despite the drastic reduction in the number of analysed cases (88,2%), but the resulting scores were more evenly distributed among the four subsets A, B, C and D (23.5%, 24.3%, 25.3 % and 26.9 %, respectively). We further tested if the four subsets significantly differed from each other by comparing the respective elemental ratios averages. In almost all cases, p-values were low and allowed H_0 (equal means) to be rejected ($\alpha < 0.05$); only in the cases of Fe/Ti for subsets B and D, Mn/Ti for A and D and Ca/Ti for C and D results were inconclusive.

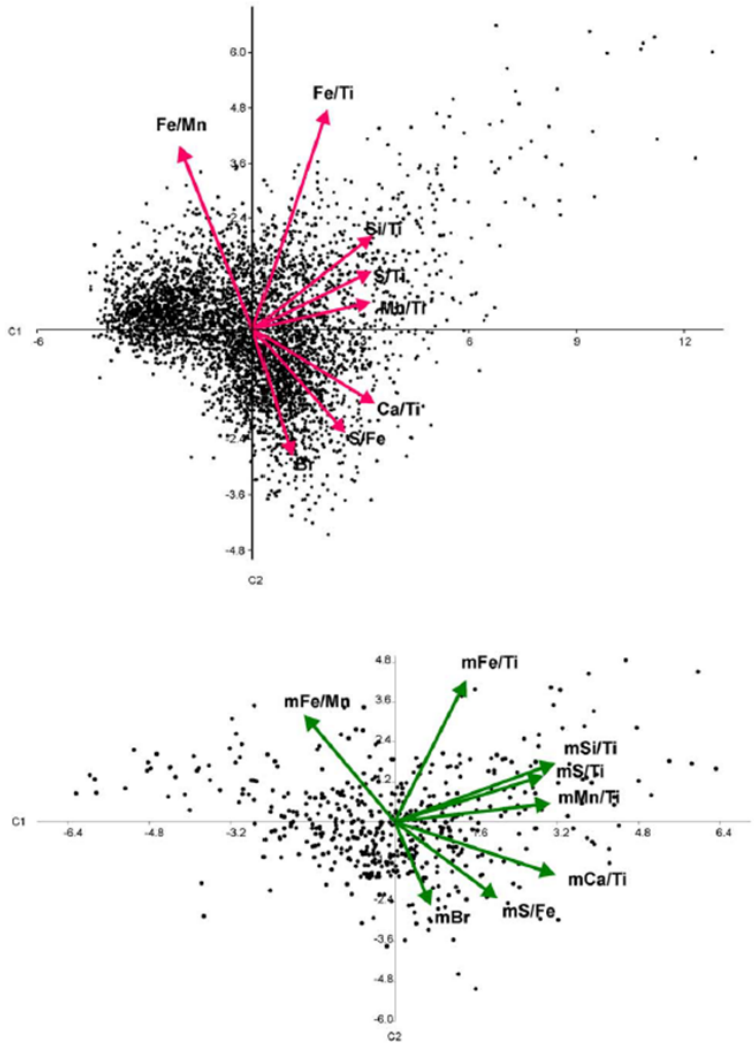

Figure 3: PCA analyses performed on a) all elemental ratios, with dots representing the XRF measurement depths; b) the annual averages of the elemental ratios with dots representing years AD. The arrows indicate the direction and rate of change of the elemental ratios. The biplots are divided in four quadrants from upper left clockwise A, B, C, D.

Finally, one further PCA was carried out to help make inferences from the former two. We combined the marker pigments and the corresponding annual means of the ratios (PCA III, Fig.4a) in order to identify periods where anoxia, euxinia and lake stratification were more intense and the biomass of primary producers was higher. Sediment samples for pigment analysis were taken at the maximum possible resolution

(every 5 mm) but nevertheless, the reduction in cases because of sediment lumping was 81% with respect to PCA II. Therefore, the element ratio values were averaged for the number of years integrated by each sample, which was an average of 6.2± 3.0 years, to make correlations possible. The results were consistent with those of the former two PCA; the eigenvalues of the first three components were > 1 and the cumulative variance explained was 79.0%, with C 1=47.4%. C 2=20.1.7% and C3= 11.2%. The ratios loadings on each component are shown in Table S1. The loading vectors of β-carotene (r =0.844), okenone (r = 0.605), isorenieratene (r=0.616) and oscillataxanthin (r=0.607) were positively correlated with C1, together with Ca/Ti (r=0.940), Mn/Ti(r = 0.815) and Si/Ti (r = 0.723). The pigments were negatively correlated with C2 as opposed to Fe/Ti (r=0.940). S/Ti (r=0.614) and Si/Ti (r=0.640) were the opposite with positive correlations. The fact that the pigments appear in quadrant C and not in D may suggest some variability in characteristics of the anoxic environments., being D probably less productive.

It was possible to single out which years experienced significant mixing events (subset B) and which ones probably remained meromictic or poorly mixed up. Figure 5a shows the microstructure of the sediments deposited within each single year in terms of the relative proportion of types of scores (A, B, C, D) of PC I, thus yielding subannual information. On the other hand, if the scores of PCII (years) are joined in decades or half centuries, it is possible to follow the supra-annual variability in the oxygenation conditions represented by each subset since 1500 AD.

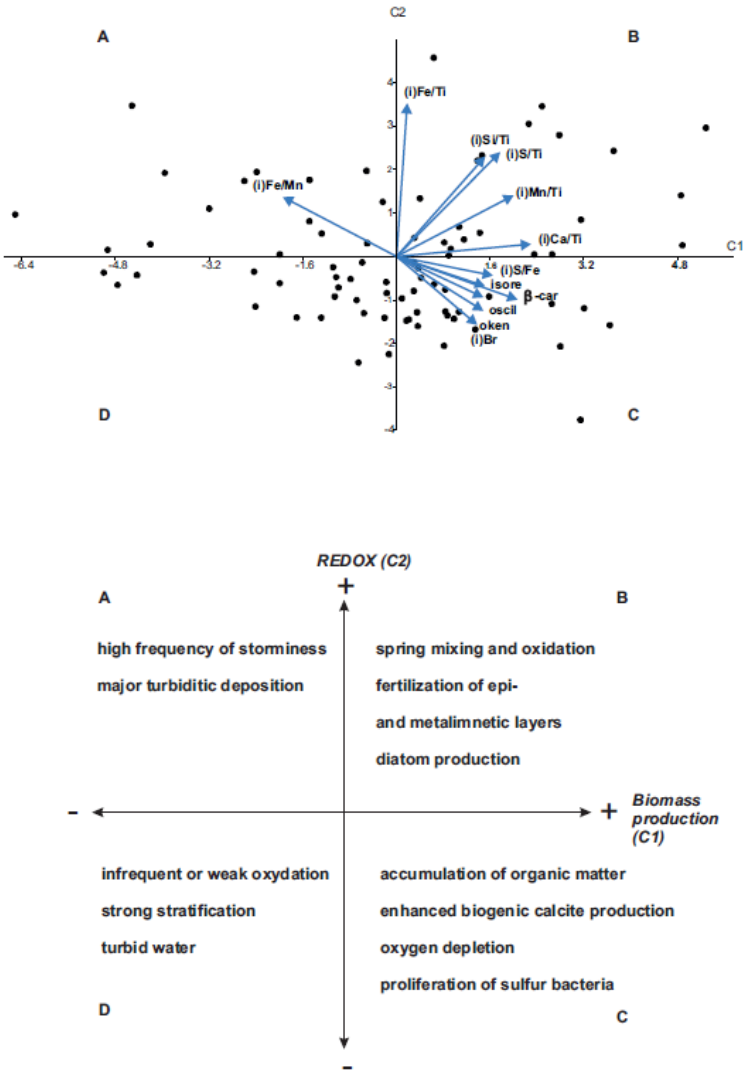

Figure 4: (a) PCA analysis performed on the marker pigment concentrations okenone (oken), isorenieratene (isore), oscillaxanthin (oscil) and β-carotene (β-car) in the sediment samples and the integrated (i) annual means of the elemental ratios. The arrows indicate the direction and rate of change of the elemental ratios. (b): Graphic synthesis of the inferences derived from PCA analyses. The biplots are divided in four quadrants from upper left clockwise A, B, C, D.

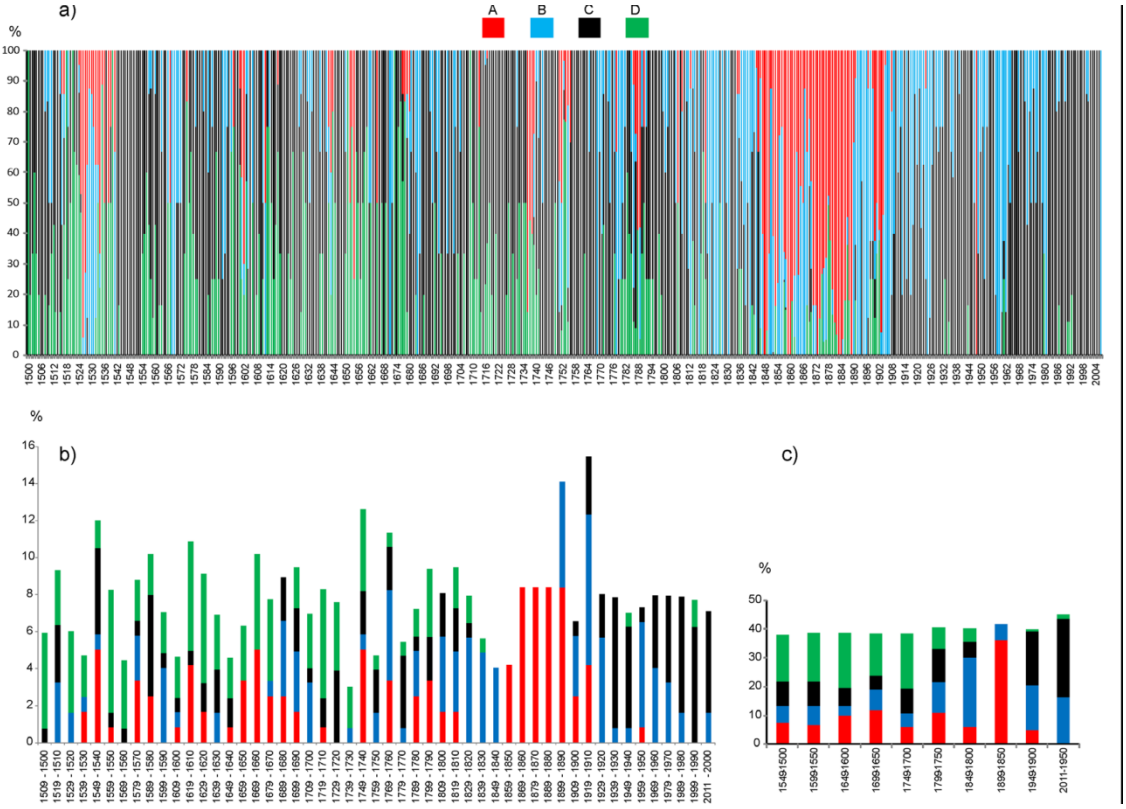

Figure 5: Annual (a), decadal (b) and centennial (c) evolution of the conditions represented by the subsets A, B, C and D, since AD 1500. 4a) the bars represent the relative contribution of the four subsets (PCI) on an annual base; 4b and 4c) the bars show the percentage of years of each subset (PC II) that fall within a particular decade or half century, respectively.

Finally, with the aim of summarising and analysing the temporal oxygenation trend of Lake Montcortès since 1500 AD to present in a more quantitative and objective fashion, we splitted the stratigraphical sequence into smaller but significant zones (time periods) by using C1 and C2 of PCII as inputs. Figure 6 shows the obtained cluster and the four statistically significant periods (SP) that emerged after applying the broken -stick model, namely 1500-1820, 1821-1847, 1848-1904 and 1905-2007 AD.

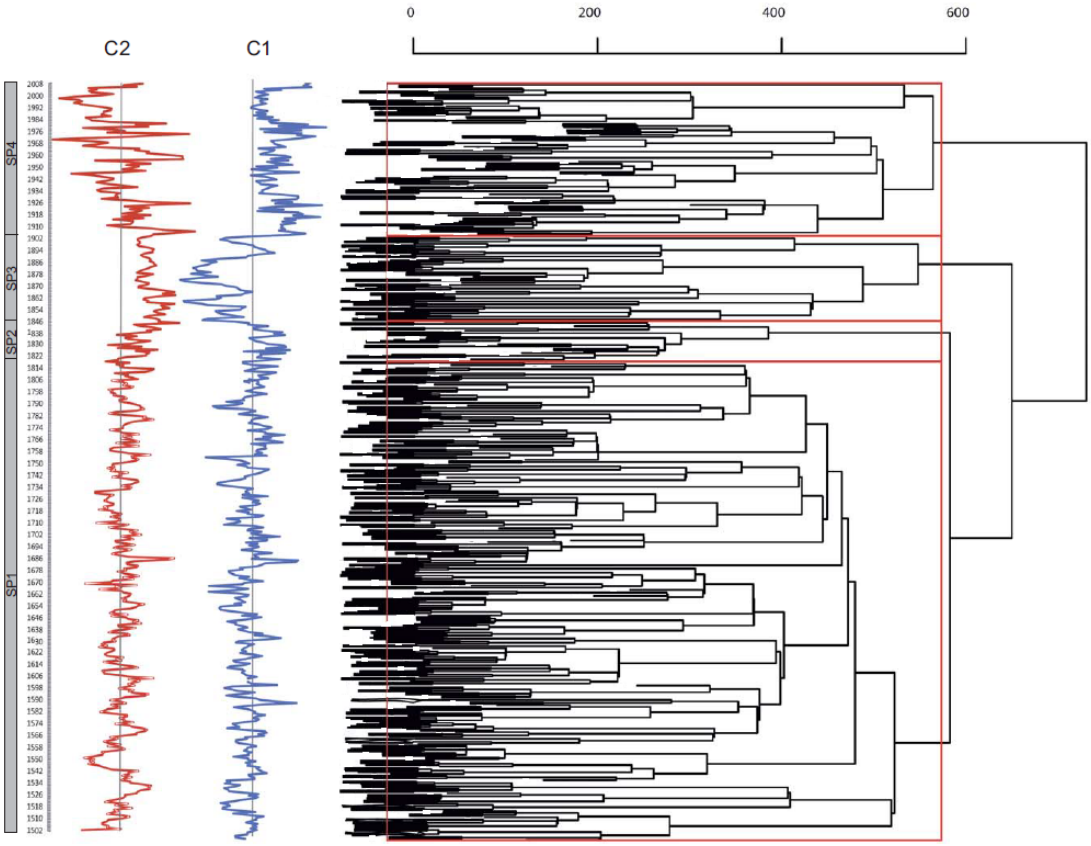

Figure 6: Results of numerical zonation of the lake Moncortès stratigraphic record performed with CONISS and Broken Stick model on the principal components (C) of PCA II. The dendrogram splits the last 500 years in four statistically significant and distinct period (SP).

4.3. Relationship between indicators of oxygen shifts and climate variability

4.3.1. *Relationships with climate variability since 1500 AD*

Global temperatures have varied over the past 500 years. With the aim to assess any trend of the lake's oxic/anoxic conditions associated with shifts in atmospheric temperature, we screened the Northern Hemisphere Temperature Anomaly (NHTA) series of Mann et al. (2009) for correlations with C1, C2, the elemental ratios and Br

(Fig. A.1), over the four SPs identified ($\alpha \leq 0.05$ (Table 1). Main significant correlations appeared during the 20th century and 1821-1847 SP, with negative and positive coefficients, respectively.

Table 1: Summary of correlations with NHTA for each significant period (n.s.: not significant)

	1500-1820	**1821-1847**	**1848-1904**	**1905-2007**
C1	n.s.	n.s.	n.s.	-0,455
C2	n.s.	n.s.	n.s.	-0,437
Fe/Ti	n.s.	n.s.	n.s.	-0,39583
Fe/Mn	n.s.	n.s.	n.s.	n.s.
S/Fe	n.s.	n.s.	n.s.	n.s.
S/Ti	n.s.	n.s.	n.s.	-0,507
Mn/Ti	n.s.	0,540	n.s.	-0,399
Ca/Ti	n.s.	0,503	n.s.	n.s.
Si/Ti	n.s.	0,446	n.s.	-0,455
Br	n.s.	0,475	n.s.	0,589

4.3.2. Relationships with instrumental climatic data

To investigate to what extent the oxic/anoxic shifts in Lake Montcortès could be associated with present climatic variability; we first looked for any relationships between the available instrumental record of climatic variables and the Fe/Ti; Fe/Mn and Mn/Ti ratios. The results obtained for the Fe/Ti ratio were much clearer than those for the Mn/Ti and Fe/Mn ratios, probably because Fe and Ti were entirely uncorrelated since 1900 and hence better reflected the redox transformations of Fe within the lake, i.e. concurrent precipitation with oxygen input into the hypolimnion. Hence, we selected

the cases (years) in which the Fe/Ti ratio exceeded the 95th percentile of the sample values as representative of those years in which mixing very likely occurred and obtained the following: 1925, 1957–1959, 1974 and 1981. We arbitrarily included the year 1979 in this set, as we know for sure that it was a mixing year (Modamio et al., 1988). At the other end, we selected the years not reaching the 5th percentile, because they can provide confidence for non-mixing years: 1945, 1970, 1976 (mixing year also according to Camps et al., 1976), 1995 and 1998 (Fig. 7a). To sum up the information contained in the climatic regional anomaly series and to compare it with these results, each year of the regional anomaly was classified by thresholds of -10% of the precipitation anomaly and -0.45ºC of the minimum temperature anomaly; these thresholds were very close to those used in the area (Meteocat, 2015b). On the other hand, the temperature minima follow a lower trend than the temperature maxima, thus avoiding overestimation of extreme cold events at the beginning of the series. Using these criteria we obtained four different climatic combinations: dry and cold (ppt < = -10% and Tmin <= -0.45ºC), dry and warmer (ppt <= -10% and Tmin > -0.45ºC), wetter and cold (ppt > -10% and Tmin <= -0.45ºC) and wetter and warmer (ppt > -10% and Tmin > -0.45ºC) years (Fig.7b). Except for the 1957-1959 period, the preceding year, previous to the mixing events, turned out to be a cold and dry year, suggesting that the occurrence of a cold and dry year could be a likely precursor or considered external forcing of a mixing year. The 1957–1959 period of extreme Fe/Ti values did not exhibit a clear relationship with climate variables, indicating that other types of environmental conditions could also trigger a mixing event (e.g., strong winds), or that Fe enrichment of the sediment might be due to other processes. On the other hand, the lower ends of the Fe/Ti values, denoting persistent anoxia, were preceded by a period of warmer years (up to 13 years), but other factors could be involved.

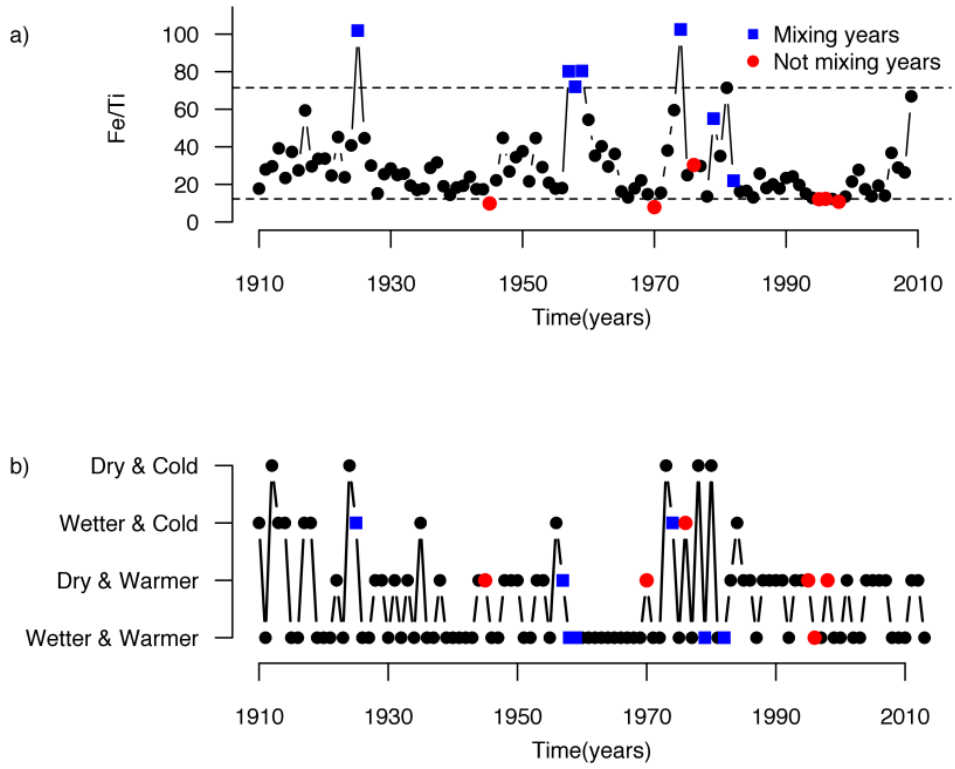

Figure 7: a) Annual evolution of the Fe/Ti ratio during the period 1910–2009. The dashed lines show the 5 and 95 percentile of the sample values. b)Evolution of the year classification by the thresholds applied over the annual regional anomaly series of minimum temperature and precipitation. The blue squares (red circles) indicate the considered mixing (not mixing) years.

This outcome raised the question about the existence of particular climatic patterns (i.e. maximum and minimum temperature and seasonal precipitation anomalies) that characterize the years belonging to each of the four subsets defined by PCA II, at least for the period of instrumental measurements. The result that emerged from this inquiry are represented in Figure 8a; more than 90% of the targeted years belonged to subsets B (35 years) and C (58 years), and the years of subset C were roughly warmer and drier than those of subset B, which was typically due to warm and dry winters. When analysing the temporal succession of these years and its relationship with the corresponding oxic/anoxic conditions (Fig. 8), we were able to outline five fairly conspicuous sequences: 1910–1927 with dominant B years; 1928–1946with more

frequent C years; 1947–1964 with prevailing B years again; 1965–1981with years of subsets B and C occurring in short alternating groups; and finally, 1982–2007 with a clear dominance of subset C years. Between 1965–1981, the regional anomaly series indicated low dispersion around the null anomaly, resulting in alternating short periods of subsets B and C, which could be understood as the natural variability of the lake.

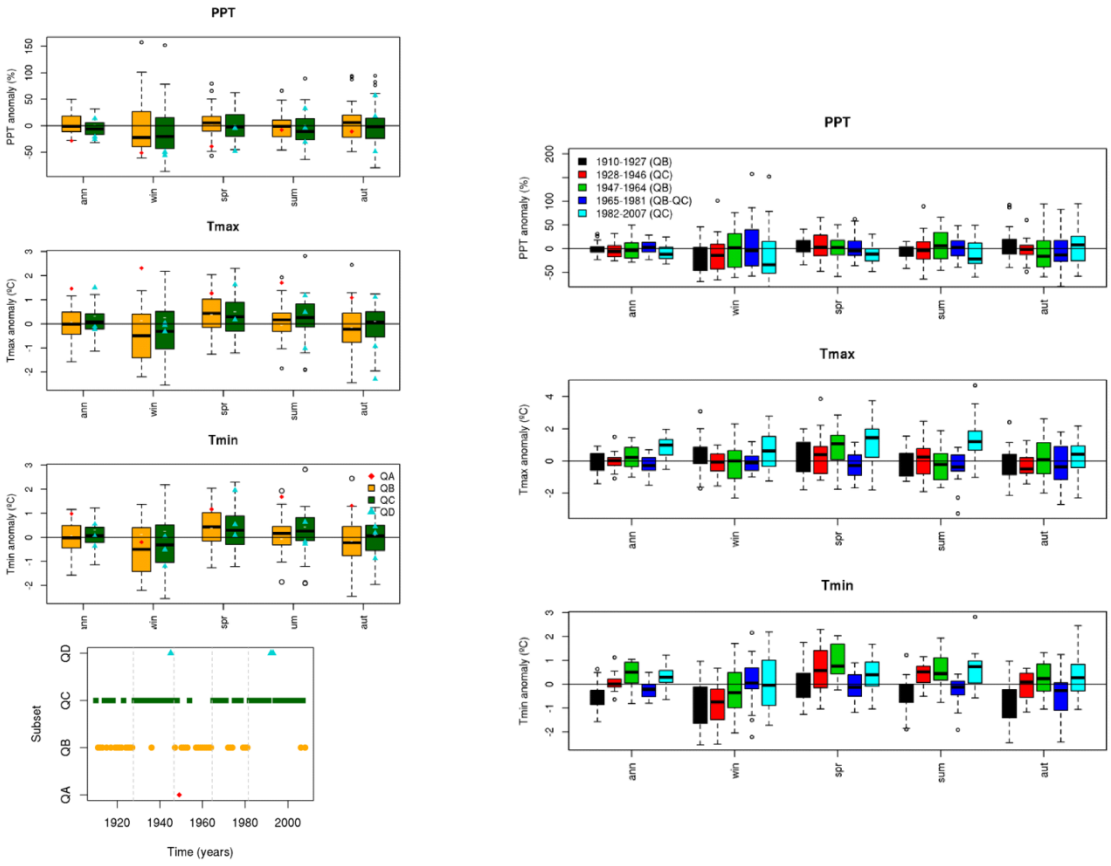

Figure 8: a) Boxplots of annual and seasonal precipitation (top) and minimum (middle) and maximum (bottom) temperature for the subsets B (yellow) and C (green),and dots for values of the respective variables subset A (red diamonds) and B (blue triangles). Course of the subsets over the period 1910–2008. b) Boxplots of annual and seasonal precipitation (top) and minimum (middle) and maximum (bottom) temperature for all the identified periods.

5.Discussion

5.1. Biogeochemical processes at various temporal scales and their oxic/anoxic imprints.

The limnological cycle (2013 to 2016) indicated that the contemporaneous precipitation/redissolution dynamics of Fe and Mn in the water column performed as expected. Fe and Mn become increasingly soluble in reducing lake conditions (Davidson, 1993), with Mn more readily reduced than Fe under anaerobic conditions (Boyle, 2001). Hence, an increase in the Fe/Mn in sediments has been interpreted as indicative of the onset of reducing conditions, followed by Fe/Mn decline as anoxia becomes permanent (Cohen, 2003, see review in Davies et al. 2015). Based on these same properties, increases in Fe/Ti and Mn/Ti ratios have been interpreted as enhanced oxic conditions, highlighting the importance of redox processes relative to catchment supplies. In this regard, the C2s of all three PCA exhibit a gradient in the redox behaviour of Fe. On the one hand, increases (positive C2 side) in Fe/Ti and Fe/Mn reveal the precipitation of iron oxides under oxic conditions and the onset of anoxia, respectively. On the other hand (negative C2 side) their decrease indicates progress towards anoxia accompanied by strong stratification status. Mn/Ti grows towards the positive side of C1 in all three PCA and implies increasing oxygenation of the water column. With this information and looking at the biplot, it becomes evident that quadrat B mainly represents the occurrence of relevant oxygenation events (high Mn/Ti and Fe/Ti values) whereas quadrants A, C and D (Fe/Mn) would inform different degrees of oxygen depletion of the hypolimnion. Si/Ti and S/Ti vectors also raise in quadrant B. Si/Ti has often been used to assess past biogenic and diatom productivity (see review in Davies et al., 2015), In our case, this ratio can be related to diatom spring growth. Interestingly, in Lake Montcortès planktonic diatoms are well represented in the stratigraphic record of the last centuries embedded in the calcite layers, showing an overwhelming prevalence of *C. cyclopuncta* followed by *C.radiosa* (syn. *compta*) (Scussolini et al. 2011).Currently, the same *Cyclotella* taxa produce conspicuous spring growth following silica peaks that move up to the surface during winter turnover (Trapote et al. 2015a), and these outbreaks produce marked oxygen peaks in the water column.

Although sulfur has several sources and forms, S/Ti might be considered here as an indicator of organic matter production because it has been associated with settling organic matter (seston) mainly in oligotrophic lakes, (Mitchell et al., 1990). Authigenic S input into the sediment is probably bound to labile sulfur bearing molecules derived from dead planktonic cells, especially during spring. Another source could be associated with the delayed deposition of dead purple sulfur bacteria that died during oxygenation events, some genera accumulate sulfur globules stored intracellularly (Madigan and Jung, 2009). Finally, a further source of S that is consistent with oxic environments could be the flux of sulfate to the sediments from the reoxidation of dissolved sulfide during mixing events. In summary, we conclude that the years with scores located in quadrant B represent years with relatively outstanding mixing and oxidation of the water column, and therefore, with enhanced fertilisation of the epi- and metalimnion due to nutrient injection from the hypolimnion, once stratification is defeated, resulting in increased diatom biomass. Currently, these processes take place in winter and early spring (Trapote et al, submitted) and probably did so during the last 500 years as well.

In all three PCAs the Ca/Ti vector was best and positively correlated with C1, together with S/Fe, Br and with β-carotene, isorenieratene , okenone and oscillaxanthine. The Ca/Ti ratio was widely accepted as an indicator of endogenic calcite production (see review in Davies et al., 2015). In our case, the increased Ca/Ti and its correlation with β-carotene were indicators of enhanced biogenic calcite production, which very likely accounts for the formation of calcite varve sublayers. The lake's sedimentary record contains finely laminated varves with mm-thick sublaminae of calcite and importantly, the average thickness of calcite sublayers has nearly doubled since the 19thcentury (Corella et al. 2011b, 2012). Parallel studies using sediment traps in Lake Montcortès (Trapote et al 2015b, Trapote et al. submitted) are trying to correlate evidence of the timing, intensity and factors that drive calcite saturation and precipitation. Results indicate that currently, calcium carbonate precipitation is indeed biologically induced, and it mainly occurs in the metalimnion during summer-autumn, when the water column is warmest and is intensely stratified.

Because the Br content has been proposed as a potential proxy for the relatively large changes in organic content in lacustrine sediments (Gilfedder et al., 2011; Phedorin et

al., 2000, 2008) we inquired if this relationship would hold in Lake Montcortès sediment. We looked for statistical correlations (r) with existing datasets of organic content related variables, i.e., total organic carbon (TOC), C/N, total sulfur (TS), and also with total inorganic carbon (TIC) and the incoherent/coherent scattering ratio (inc/coh) (Davies et al., 2015), whose data were available from a twin core (MONT04-1A) at a lower resolution (Corella et al., 2011b) .Indeed Br was significantly ($p< 0.05$) and positively correlated with C/N ($r =0.674$) and with the inc/coh ratios ($r = 0.460$),TS ($r = 0.400$), TIC ($r=0.360$) and TOC ($r = 0.323$); the correlation of Br with the Ca/Ti ratio was rather low ($r = 0.217$, $p< 0.05$). Hence, our results suggest that Br is roughly associated with allochtonous organic matter input and with its storage in the sediment of Lake Montcortès. Consequently, the concurrent positive correlation of Ca/Ti, Br and S/Fe in all three PCA suggests first the accumulation of organic matter due to enhanced detritus sedimentation and second, the slowing of its mineralisation caused by intense oxygen depletion of the hypolimnion (note their negative correlation with Fe/Mn). In the absence of oxygen, oxidation is taken over by the most favourable electron acceptors, i.e.,NO_3^-, MnO_2, FeO(OH), SO_4^{-2} and CO_2, via sequential redox reactions(Holmer and Storkholm, 2001). In fact, Lake Montcortès harbours abundant populations of sulfur bacteria since 1500 AD (Fig. A.3), and the good correlation of these pigments with S/Fe and Br in the third PCA also supports our inferences. Furthermore, the diversity and cycle of current anoxygenic phototrophic sulfur bacteria in Lake Montcortès is known (Cristina et al., 2000). In a much-reduced environment, sulfate can be converted to H_2S by sulfur-reducing bacteria, and the rate of this process is governed by both the availability of organic matter and by sulfate (Bates et al., 1995).The presence of sulfur bacteria also demonstrates hypoxic/anoxic conditions. Isorenieratene is a carotenoid uniquely biosynthesised by the brown-coloured strains of the photosynthetic green sulfur bacteria (PGB, Chlorobiaceae). These bacteria are strict anaerobes that live under an extremely low intensity of light and require sulfide. Their presence indicates a euxinic water column that extends into the photic zone (e.g., Repeta, 1993, Sinninghe Damste et al 1993). Furthermore, purple sulfur bacteria (PSB, Chromatiaceae) are the only producers of the carotenoid okenone, a biomarker also targeted for photic zone euxinia(Van Gemmerden and Mas, 1995). Both green and purple sulfur bacteria are commonly found in the monimolimnion of meromictic lakes (Meyer et al., 2011. Where neither sulfate nor Fe or organic matters are in short supply, iron sulfide minerals can form in both the water column and the sediment (Suits and

Wilkin, 1998; Cohen et al., 2003), and are mostly biologically mediated. As a matter of fact, we trapped framboidal pyrite granules in the water column (unpublished results), and former X-ray diffraction analyses further confirmed the presence of pyrite in the sediments of Lake Montcortès (Corella et al., 2011b).Therefore, S/Fe is highly variable and affected by a wide array of microbiologically mediated reactions and can be interpreted here as an indicator of intense sulfur bacterial activity in accordance with increased lake productivity, stratification and hypolimnetic anoxia, which in summary are the main characteristics of the years scored in quadrat C according to their sedimentary imprint. Oscillaxanthin also appears in quadrant C. In Lake Montcortès, Oscillatoriales were present throughout almost the entire study period, rose abruptly by 1987, and then unexpectedly disappeared by 1992 (Fig. A.3). The fact that oscillaxanthin correlates well with sulfur bacteria in PCA III indicates that Oscillatoriales also prospered well under strong stratified and anoxic conditions. Oscillatoriales thrive well in stratified lakes due to their ability to stabilise their vertical position (e.g.,*Planktohrix rubescens, P.agardhii)* and some migrate upwards and downwards along stratified and illuminated water layers in response to environmental condition (Lavoie et al., 2007 and literature therein; Mur et al., 1999; Reynolds, 1984).Camps et al. (1976) and Modamio et al. (1988) reported massive blooms of the filamentous *P. rubescens* in the metalimnion of Lake Montcortès during the seventies but today they are absent.This species has been known to develop stable summer populations and acclimate to low radiation (Zotina et al., 2003), , becoming persistent in turbid, eutrophic watersheds and thereby outcompeting planktonic algae in light limited environments (Mur et al., 1978, 1999). Many cyanobacteria can out-compete other phytoplankton organisms under conditions of phosphorus or nitrogen limitation owing to their high affinity for these nutrients (Mur et al., 1999). Furthermore, their presence or absence may depend on the forms of available nitrogen that reach a lake derived from human activities..In Lake Montcortès, the nutrient supply may have significantly shifted quantitatively and qualitatively over time (see section 5.2).

In quadrant A, the only growing ratio is Fe/Mn, whereas the ratios that grew in quadrant C decreased in A. However, making inferences is not straightforward. The conditions represented by A occur most frequently between 1850 to 1899, where the sedimentary record shows an abrupt increase of turbidites interbedded within the varve sequence.

Turbidites are sediments that were transported and distributed by density flows. In lakes, their origin can be seismically-induced or generated by severe storms (Osleger et al., 2009). Most likely, in our case the input and deposition of external clastic material altered the values of the ratios downcore, first with abrupt additions of allochtonous entries of mineral oxides, quartz feldspars, calcite and sulfur from the catchment, and secondly because of the dilution effect of the deposition of large quantities of fresh sediment.

5.2. Trends in oxic/anoxic shifts in Lake Montcortès during the last 500 years

The study of the limnological cycle of Montcortès performed in this work and in former studies (Trapote et al., submitted; Camps et al. 1976; Modamio et al. 1988; Cristina et al. 2000) and sedimentology (Corella et al, 2011b; 2012) showed that Lake Montcortès reached seasonal anoxia and even euxinia every year that sometimes persisted year round (meromixis), or instead got interrupted by thorough winter mixing and oxygenation of the water column (monomixis). This evidence suggests that turnover events are rather short and occur with irregular frequency. Moroever they occur when biological activity is dampened, thereby preventing bioturbation of the sediment layers deposited under anoxic conditions, even under mixing conditions. Proof of this is the varved record of the last 500 years that has only been interrupted by turbidites and clastic inputs (Corella et al., 2014).

In line with these findings, figure 5 highlights the high supra-annual variability at which significant oxygenation events seem to have taken place over the last 500 years (subset B). Interestingly, 45,3% of the years appear as mixing years and, like the meromictic ones, mostly occurred arranged in groups of years that enclose consecutive years of monomixis, followed by groups of consecutive years of meromixis (up to one decade in both cases). This highlights the importance of turnover variability of the water column in an environment of annually recurrent spring-summer anoxia. Furthermore, ,a relatively good match exists between the temporal distribution pattern of these groups (Fig 5) with the SP obtained (Fig 6). Subset A (storminess, turbidites) was more frequent between 1850-1900 and matches the SP 1848- 1903. Subset D (relatively less primary production, stratification, anoxia) depicted the 18th century backwards,

matching SP 1500 to 1820. Subset B (oxygenation, fertilization, diatom growth) was quite variable but was best represented between 1820-1849 matching the1821-1847 SP. Subset C (oxygen depletion, higher production, stratification, sulphur bacteria) was very important during the 20th century.

5.3. Humans or climate, which drove, which drives?

Meteorological forcing determines the strength of thermal stability in lakes and in doing so it leaves a notable imprint in the dissolved oxygen's temporal and spatial distribution. On the other hand, enhanced nutrient and organic matter input into lakes promotes eutrophic conditions that trigger hypolimnetic anoxia. In our case, confronting the temporal evolution of Lake Montocortès' biogeochemical conditions (A,B,C,D) with available climatic and anthropogenic information related to the lake's environment may help assess whether the observed oxic /anoxic shifts were driven by climate or by human influence, or both (Fig.9).To this end, this section was split into the four main periods obtained by CONISS and Broken-stick model.

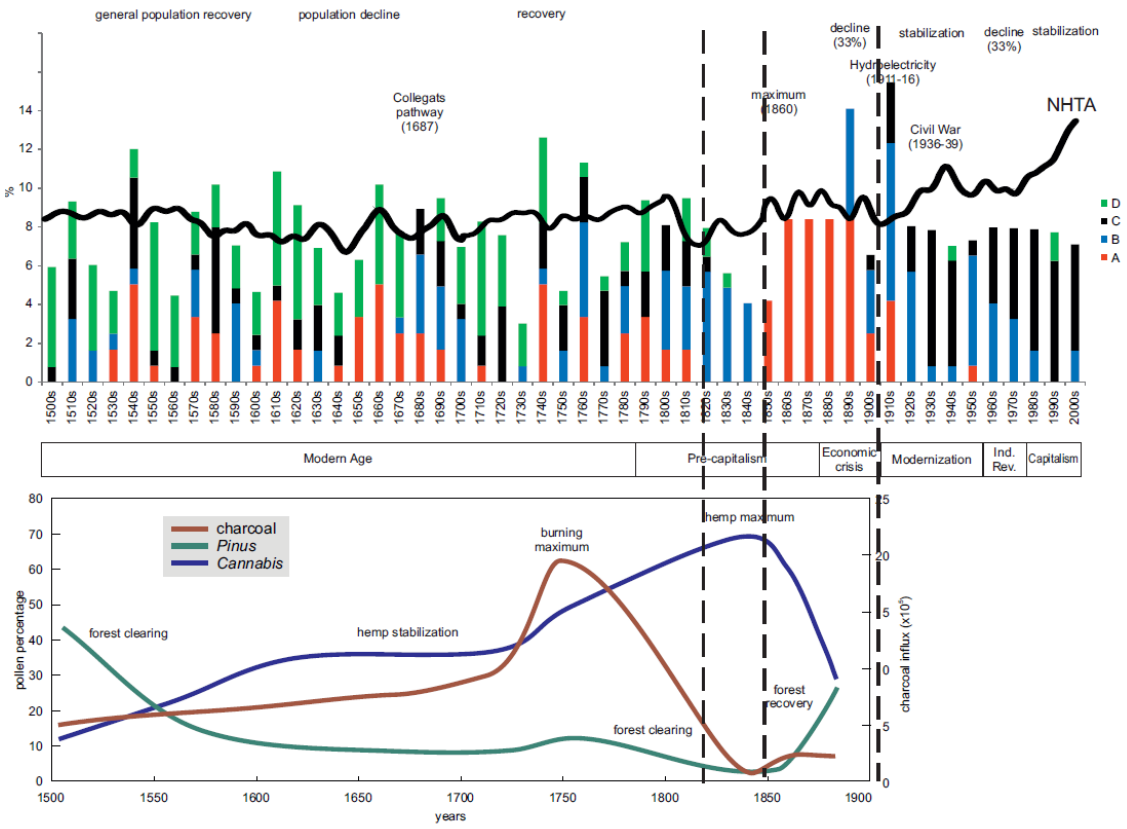

Figure 9: Demographic trends of the Pallars region (top) (Bringué, 2005; Farràs, 2005) and human activities around the lake (bottom) (Rull & Vegas-Vilarrúbia, 2015) potentially affecting the L. Montcortès oxic/anoxic shifts since 1500 AD. The dashed lines separate four statistically significant periods (zones) at 1821 AD, 1848AD and 1905.

1500-18200 AD (86.5-cm)

After 1520 AD, detrital input (A) to the lake began to occur. Until around 1750 AD, the lake was intensely stratified and rather turbid (Fig. 8), with Chromatiaceae and Oscillatoriales as the dominant bacteria (Fig. A.3). Historically, this period belongs to the Modern Age (1500-1789) and is climatically framed in the cold LIA and includes the Maunder minimum (1645-1720 AD, the chilliest point of the Little Ice Age (LIA) (Sánchez-López et al., 2016 and literature therein). On the Iberian Peninsula the hydric availability fluctuated on the Pyrenees with rainfalls showing stationary conditions between 1537 and 1805 AD (Cacho et al., 2010; Morellón et al., 2012; Corella et al., 2016) . This period represents the recovery of the population of the Pallars region which

had been devastated by wars and black pest epidemics during the medieval crisis. The town of Montcortès was home to 50-80 inhabitants (Iglésies, 1969, 1981, 1991) (Fig. A.4), who were the main users of the lake. By 1500 a clear trend towards agriculture and livestock diversification began and pastures and husbandry underwent significant expansion to the detriment of conifer forest. Large eels were cultivated within the lake and leeches abounded (Maluquer i Sostres, 1992). Forest renting and clearing became a habitual practice as well as forest burning, the latter peaking around 1750 (Rull and Vegas Vilarrúbia, 2015). Moreover, the persistent and increasing presence of *Cannabis* (hemp) (Fig.9), strongly suggests that hemp growth was practiced in the neighbourhood (La Pobla, La Pobleta, Gerri de La Sal) and probably, hemp retting was conducted within the lake (Rull and Vegas-Vilarrúbia, 2014), as was the case in the nearby Estanya lakes (Riera et al., 2004). Water hemp retting has been blamed for nutrient enrichment, enhanced turbidity, oxygen depletion and significant changes in community composition of the plankton (Anderson, 1995; Bonneville, 1994; Cheng et al., 2007; Clarke and Merlin, 2013 and literature therein; Vander Werf and Turunen, 2008;). It is clear that all these activities must have profoundly altered the surrounding landscape with inevitable consequences to the lake catchment and the lake itself, leaving a clear imprint in the sediments. In fact, and in agreement with the relevance of Oscillatoriales in the lake, palynological evidence suggests that Lake Montcortès became relatively enriched in N and P during this time lapse as inferred from the replacement of *Cladium* by *Typha* in littoral plant communities, which is typical in situations with sustained increases in nutrient supply to lakes (Scussolini et al., 2011; Rull et al., 2011).

Clastic input stimulated by soil erosion was particularly high between 1508-1547 and 1592-1656 AD (Corella et al., 2016). Furthermore, carbon particles may partly support the assumption of increased water turbidity affecting light transmission and absorption, thus modifying the aquatic habitat and affecting primary production. In effect, the mean Ti values were the highest of the entire study period and indicate detrital input from the catchment. Additionally, fire was used for deforestation and burned surfaces were dedicated to agriculture and livestock. Evidence exists that after forest fires, the export of sediments, nutrients and dissolved organic matter from river catchments increases, with ash and fine sediment preferentially eroded. Once transferred to watersheds, these materials increase the turbidity (Langhans et al., 2016; Smith et al., 2011; Vila-Escalé et

al., 2007). Thus, by extension, it follows that small lakes such as Montcortès could be affected by forest burning in a similar manner.

1821-1847 AD (cm)

During the following years until 1848 (Contemporary period, 1789-present), the lake conditions changed under a scenario of enhanced climate variability that is fairly concurrent with the transition between the LIA and the posterior warming. Fluctuations in hydric availability on the Iberian Peninsula (IP) became stronger, especially towards 1845, and high flood events occurred in the NE of the IP (Barriendos and Rodrigo, 2006; Cacho et al., 2010; Llasat et al., 2005). These climatic phenomena could have favoured the frequency and intensity of mixing in the water column. In fact, in the middle of this period dominated by intense human activity, Mn/Ti, Ca/Ti, Si/Ti and Br seemed to capture a climatic signal. These ratios exhibited significant positive correlations with the mean temperature, suggesting that winter oxygenation of the water column increased stimulating diatom growth. of the water column gradually became the main process leaving an imprint in the sediment (B) and stratification seemed to recede (Fig.9). Simultaneously, the number of inhabitants almost tripled in Montcortès town (Fig. A.4) (Sabartés i Guixés, 1993). Forest burning markedly decreased and the presence of Pinus was minimal. Hemp cultivation and retting continued to increase regionally until its apogee around 1839 (Rull and Vegas-Vilarrúbia, 2015).

1848-1904 AD (cm)

The subsequent five decades witnessed major turbiditic deposition episodes (A) (Fig. 9), which were probably associated with a higher frequency of storminess (Corella et al., 2014). This sedimentary event obscured the interpretation of the sedimentary record for this period in terms of internal lake processes. During this period, commercial activities depleted and the subsistence economy went into crisis, forcing part of the population to emigrate, and the populations of the Pallars and Montcortès diminished by 30% and 40%, respectively (Fig.A.4) (Sabartés i Guixés, 1993). It is reasonable to assume that the anthropogenic pressure on the lake diminished (Fig. 9), allowing certain natural recovery.

1905-2007 (-0.2 cm)

The first two decades of the 20th century showed a notable decrease in external clastic inputs into Lake Montcortès and the reappearance of intense oxygenation events (B) (Fig. 9).This occurred in the context of a manifest, but variable recovery of temperatures after the LIA (Fig. 9).It is not straightforward that meteorological forcing alone was the main cause of the increased oxygen content of the water column during these decades. It is very likely that the notable reduction of anthropogenic activities in the lake catchment lessened the inputs of sediment, nutrients and organic matter into the lake and consequently, the biological oxygen demand decreased and transparency improved. From 1920 until the present, the lake evolved towards a novel situation led by different algae groups and bacteria (C).The frequency of strong oxygenation events diminished gradually and the presence of sulfur bacteria was higher than ever before, especially since the sixties', suggesting more intensive stratification and longer periods of anoxia. Interestingly, related to the instrumental climate record, periods of years with strong oxygenation events alternated with periods of more stable stratification (C) apparently responding to climate forcing, i.e., years of C showed warmer and drier winters. In fact, regional climate experienced highly significant increases in the maximum (T_{max}) and the minimum (T_{min}) temperatures and their increasing rates, especially after 1970 AD, and a decrease in the number of cold years (T_{max} and T_{min}) after 1950 AD. The inter-annual variability in precipitation also rose markedly (Pérez-Zanón et al., 2016). Socially, the modernisation process was interrupted in 1936 AD by the Spanish civil war and the subsequent post-war period until 1950 AD, when a slight economic revitalisation occurred. However, during the Industrial revolution a new, dramatic crisis came about (1960-1980) and the population severely declined as a consequence of mechanisation of field labour and emigration to large industrialised cities. Intensive livestock practices and the tourism industry developed, though with low intensity in the Lake Montcortès catchment. In fact, the number of inhabitants in Montcortès town decreased from 125 in 1900 AD to 26 in 2015AD (Fig.A.4), being this the lowest number recorded during the last 500 years (Sabartés i Guixés, 1993).

5.4. Lake Montcortès in the context of the global spread of hypoxia in lakes

In sum, we suggest that Lake Montcortès experienced prolonged hypolimnetic anoxia during the entire study period. However, , multiple oxygenation events occurred throughout this time lapse, indicating that the volume of the anoxic waters varied depending on the duration and intensity of the oxygenation events, and from the oxygen demand generated by the anthropogenic impacts. From 1900 AD onwards, the human population drastically decreased at a local and regional scale, following a reverse trend from the one shown by the populations of other lakes affected by recent hypoxia (Jenny et al., 2016a,b). Such abrupt land abandonment may be interpreted as a sort of "involuntary" rehabilitation of Lake Montcortès from former land practices. In the second half of the 20th century the lake anoxia exhibited an unparalleled expansion despite ongoing depopulation and in the framework of accelerating rates of global warming (Brunet, 2007; Sánchez-López et al., 2016 and literature therein). These facts clearly suggest that climate forcing could start playing an increasingly prominent role in controlling the lake's ecosystem and environment.

Overall, our results are partly consistent with recent regional and global analyses about the spread of lacustrine hypoxia, especially during recent decades (Jenny et al., 2016a,b). Hence, it notably differs in the origin of anoxia and timing of its onset. In Lake Montcortès, persistent anoxia started early, in the Mid-Holocene (3800 cal yr BP, -1850 AD), and its onset was attributed to a climate-driven lake level rise (Corella et al., 2011b), rather than to human pressure. In fact, Neolithic inhabitants could not have impacted the lake enough to prompt an anoxia outbreak, since they lived in mountain caves and avoided the open plain (Pérez- Almoguera et al., 2011). The time when anthropogenic influences overrode climatic influences onto oxic/anoxic shifts must have been before 1500 AD, considering that evidence exists of fire impact, hemp cultivation, pastures and herbaceous crops since 800 AD (Rull et al., 2011). This suggests that at the beginning of the 16th century, the hypolimnion of Lake Montcortès already suffered from a significant oxygen deficit of double origin.

Contrastingly, Jenny et al. (2016 a,b) informed that in a set of 365 lakes from six continents, lake hypoxia started relatively later, after 1700 AD, due to rising local human pressure, which expanded during the turn of the 20th century and increased rapidly over the last century due to enhanced nutrient input. The lakes of industrialised

countries have not returned to former oxygenated conditions despite restoration efforts. Furthermore, in Europe, the outbreak and expansion of hypoxia after 1850 was bound to urban growth, and neither in this case exhibited signs of sustained recovery of bottom water oxygenation after P input regulations (Jenny et al.,2016b). From their research, these authors conclude that climate shifts did not trigger hypoxia, but that they were responsible for hypoxia fluctuations once the lakes become hypoxic.

From the above evidence it is clear that the oxic/anoxic changes in the hypolimnion of a lake are highly dynamic and the result of manifold climate and anthropogenic factors. However, an important outcome of the aforementioned studies and the present one is that current climate warming seems to be taking control of the oxygenation capacity of lakes at a global scale, regardless of the timing and causes of the onset of hypoxic or anoxic conditions and their ulterior development. Warming of the upper water layers is known to strengthen watercolumn stratification, degas oxygen and increase the volume of hypolimnetic water. Voices of alert warn that the target of 2ºC as a "guard rail" in global temperature increase will be very difficult to achieve, so the likelihood of global temperature raises of 3º and 4ºC within this century is enhanced (New et al., 2011). It follows that a global challenge for societies during the 21thcentury is to maintain lake settings under healthy ecological conditions, whereas the trend seems to be towards climatically induced deterioration. By now, the main drawbacks are the human inability to stop or even control climate change, and the contingency of any prevention, adaptation or restoration actions that might be undertaken. Meanwhile, studying long-term ecological processes seems a good strategy not only to understand the current ecological status of the natural systems under study but also to improve predictions on their future.

The importance of long-term ecological studies for more accurate predictions of the effects of climatic change on future ecosystems is widely recognized, which has led to the establishment of networks of long-term ecological stations around the globe (e.g. https://lternet.edu/). Such networks have already provided useful data for the last decades but ecological trends and processes occurring on higher timescales can only be documented using high-resolution paleoecological records embracing centuries or millennia. Long-term ecological stations situated in the catchments of lakes with varved

sediments, as is the case of Lake Montcortès, would be especially useful in this context (Rull, 2014).

6. Conclusions

We think that our paper offers innovative and novel insights into the issue of the current spreading of hypoxia/anoxia in freshwater bodies. It is also the first time that this problem is addressed, in the Mediterranean region, with a truly long-term perspective and at such a high resolution, thanks to the use of varved lake sediments. One difficulty worldwide to investigate and track the evolution of oxygenation shifts is the lack of long-term oxygen measurements, which usually encompass less than a century and seriously compromise the possibility of recording truly long-term trends. In our paper, we address this problem using a subdecadal resolution and a multiproxy approach that combines independent geochemical and biological proxies, i.e. elemental XRF core scanning measures and biomarkers (pigments). We succeed in distinguishing different phases in the evolution of oxygen shifts over time that can be potentially linked to climatic and/or anthropogenic drivers acting on the lake itself or in its catchment. It is important to stress that we have been able to clearly distinguish pre- and post-industrial oxygenation trends, thus providing a direct connection between oxygen shifts and the ongoing climate change. However, a more refined distinction between the effects of humans and climate is needed and is being addressed in ongoing studies. We believe that our methodological approach is fine-tuned enough and useful to overcome the lack of instrumental data in regions devoid of them, thus facilitating the attainment of a regional scope able to resolve the eventual global trends and synchronicity of the oxygenation shifts in continental water bodies.

7. Acknowledgements

Elisabet Safont, Núria Cañellas, Joan Gomà, Sandra Garcès, Arantzazu Lara and Eric Puche helped in performing the fieldwork. Important demographic and paleoclimate information was provided by Jesús Sánchez (Arxiu Comarcal de Sort) and Myriam Khodri, (IRD/CNRS Université P. et M. Curie), respectively. We acknowledge the

Council of Baix Pallars, the cultural association Lo Vent de Port and the Busseing Pallars Company for their direct involvement in the project and their continuous support. Funding was granted by the Spanish Ministry of Economy and Competitivity (MINECO) (projects MONT-500, ref. CGL2012-33665; GLOBALKARST, ref. CGL2009-08145),the Institute of Catalan Studies (PIRIMOD and POLMONT), and the Catalan University and Research Management Agency (AGAUR)(project 2014 SGR 1207).Training research grants were awarded to M. Carmen Trapote and Núria Pérez-Zanón and funded by MINECO (BES-2013-065846) and the University Rovira i Virgili (Martí Franquès program, 2104PMF-PIPF-22), respectively. Fieldwork permits were provided by the Territorial Service of the department of Agriculture, Livestock, Fishing and Natural Environment of Catalonia.

8. Literature

Adrian, R., O'Reilly, C.M., Zagarese, H., Baines, S.B., Hessen, D.O., Keller, W., Livingstone, D.M., Sommaruga, R., Straile, D., Van Donk, E., Weyhenmeyer, G.A., Winder, M., 2009. Lakes as sentinels of climate change. Limnol. Oceanogr. 54, 2283–2297.

Anderson, N., 1995. Naturally eutrophic lakes: reality, myth or myopia? Trends Ecol. Evol. 10, 137–138. doi:10.1016/S0169-5347(00)89019-9

Bard, E., Frank, M., 2006. Climate change and solar variability: What's new under the sun? Earth Planet. Sci. Lett. 248, 1–14. doi:10.1016/j.epsl.2006.06.016

Bard, E., Raisbeck, G., Yiou, F., Jouzel, J., 2000. Solar irradiance during the last 1200 years based on cosmogenic nuclides. Tellus B 52, 985–992. doi:10.1034/j.1600-0889.2000.d01-7.x

Barnosky, A.D., Matzke, N., Tomiya, S., Wogan, G.O.U., Swartz, B., Quental, T.B., Marshall, C., McGuire, J.L., Lindsey, E.L., Maguire, K.C., Mersey, B., Ferrer, E.A., 2011. Has the Earth's sixth mass extinction already arrived? Nature 471, 51–57. doi:10.1038/nature09678

Barriendos, M., Rodrigo, F.S., 2006. Study of historical flood events on Spanish rivers using documentary data. Hydrol. Sci. J. 51, 765–783. doi:10.1623/hysj.51.5.765

Bates, A.L., Spiker, E.C., Hatcher, P.G., Stout, S.A., Weintraub, V.C., 1995. Sulfur geochemistry of organic-rich sediments from Mud Lake, Florida, U.S.A. Chem. Geol. 121, 245–262. doi:10.1016/0009-2541(94)00122-O

Bennet, K.D. 1996. Experimental Design and Data Analysis for Biologists. New Phytol. 132, 155-170.

Bergman, B., Gallon, J.R., Rai, A.N., Stal, L.J., 1997. N2 Fixation by non-heterocystous cyanobacteria. FEMS Microbiol. Rev. 19, 139–185.

Bloesch, J., Burns, N.M., 1980. A critical review of sedimentation trap technique. Schweizerische Zeitschrift für Hydrol. 42, 15–55. doi:10.1007/BF02502505

Bonneville, F. de., 1994. The book of fine linen. Flammarion, Paris.

Boyle, J.F., 2002. Inorganic geochemical methods in Palaeolimnology, in: Last, W.M., Smol, J.P. (Eds.), Tracking Environmental Change Using Lake Sediments. Volume 2: Physical and Geochemical 724 Methods. Kluwer Academic Publishers, Dordrecht, pp. 83–141. doi:10.1007/0-306-47670-3_5

Bradshaw, R.H.W., Coxon, P., Greig, J.R.A., Hall, A.R., 1981. New fossil evidence for the past cultivation and processing of hemp (Cannabis Sativa L.) in eastern England. New Phytol. 89, 503–510. doi:10.1111/j.1469-8137.1981.tb02331.x

Bringué, J.M., 2005.L'edat moderna. In: Marugan CM, Rapalino, V. (eds: Història del Pallars. Dels orígens als nostres dies. Pagès Editors, Lleida, pp 121–144

Brunet, M., Jones, P.D., Sigró, J., Saladié, O., Aguilar, E., Moberg, A., Della-Marta, P.M., Lister, D., Walther, A., López, D., 2007. Temporal and spatial temperature variability and change over Spain during 1850-2005. J. Geophys. Res. Atmos. 112, 1–28. doi:10.1029/2006JD008249

Cacho, I., Garcés, B. V., Sampériz, P.G., Merino, M.G., Rouco, F.G., Grimalt, J., Menéndez, M., 2010. Capítulo 11 revisión de las reconstrucciones paleoclimáticas en la Península Ibérica desde el último periodo glacial, in: Pérez, F.F., Boscolo, R. (Eds.),

Clima En España: Pasado, Presente Y Futuro. Ministry of the Environment and Rural and Marine Environs and Ministry of Science and Innovation, Madrid, pp. 9–24.

Camargo, J.A., Alonso, Á., 2006. Ecological and toxicological effects of inorganic nitrogen pollution in aquatic ecosystems: A global assessment. Environ. Int. 32, 831–849. doi:10.1016/j.envint.2006.05.002

Camps, J., Gonzalvo, I., Güell, J., López, P., Tejero, A., Toldrà, X., Vallespinós, F., Vicens, M., 1976. El lago de Montcortès, descripción de un ciclo anual. Oecologia Aquat. 2, 99–110.

Cheng, X., Li, S., Shen, Q., Xue, J., 2007. Response of cultural lake eutrophication to hemp-retting in Quidenham Mere of England in post-medieval. Chinese Geogr. Sci. 17, 69–74. doi:10.1007/s11769-007-0069-y

Clarke, R.C., Merlin, M., 2013. Cannabis: evolution and ethnobotany. University of California Press, Berkeley.

Cohen, A.S., 2003. Paleolimnology: the history and evolution of lake systems. Oxford University Press, New York.

Corella, J.P., Amrani, A. El, Sigró, J., Morellón, M., Rico, E., Valero-Garcés, B.L., 2011a. Recent evolution of Lake Arreo, northern Spain: influences of land use change and climate. J. Paleolimnol. 46, 469–485. doi:10.1007/s10933-010-9492-7

Corella, J.P., Moreno, A., Morellón, M., Rull, V., Giralt, S., Rico, M.T., Pérez-Sanz, A., Valero-Garcés, B.L., 2011b. Climate and human impact on a meromictic lake during the last 6,000 years (Montcortès Lake, Central Pyrenees, Spain). J. Paleolimnol. 46, 351–367. doi:10.1007/s10933-010-9443-3

Corella, J.P., Benito, G., Rodriguez-Lloveras, X., Brauer, A., Valero-Garcés, B.L., 2014. Annually-resolved lake record of extreme hydro-meteorological events since AD 1347 in NE Iberian Peninsula. Quat. Sci. Rev. 93, 77–90. doi:10.1016/j.quascirev.2014.03.020

Corella, J.P., Brauer, A., Mangili, C., Rull, V., Vegas-Vilarrúbia, T., Morellón, M., Valero-Garcés, B.L., 2012. The 1.5-ka varved record of Lake Montcortès (southern Pyrenees, NE Spain). Quat. Res. 78, 323–332. doi:10.1016/j.yqres.2012.06.002

Cristina, X.P., Vila, X., Abella, C.A., Bañeras, L., 2000. Anoxygenic phototrophic sulfur bacteria in Montcortès Lake (Spain): the deepest population of Chromatium sp. Proceedings- Int. Assoc. Theor. Applied Limnol. 27, 854–858.

Curran-Everett, D., 2013. Explorations in statistics: the analysis of ratios and normalized data. Adv. Physiol. Educ. 37, 213–219. doi:10.1152/advan.00053.2013

Davies, S.J., Lamb, H.F., Roberts, S.J., 2015. Micro-XRF core scanning in Palaeolimnology: Recent developments, in: Croudace, I.W., Rothwell, R.G. (Eds.), Micro-XRF Studies of Sediment Cores: Applications of a Non-Destructive Tool for the Environmental Sciences. Springer Netherlands, Dordrecht, pp. 189–226. doi:10.1007/978-94-017-9849-5_7

Davis, J.C., 2002. Statistics and data analysis in Geology, 3rd ed. Wiley, New York.

Davison, W., 1993. Iron and manganese in lakes. Earth-Science Rev. 34, 119–163. doi:10.1016/0012-8252(93)90029-7

Diaz, R.J., 2001. Overview of hypoxia around the world. J. Environ. Qual. 30, 275–281. doi:10.2134/jeq2001.302275x

Farràs, F., 2005. El Pallars contemporani. In: Marugan CM, Rapalino, V. (eds): Història del Pallars. Dels orígens als nostres dies. Pagès Editors, Lleida, pp 121–144

Friedrich, J., Janssen, F., Aleynik, D., Bange, H.W., Boltacheva, N., Çagatay, M.N., Dale, A.W., Etiope, G., Erdem, Z., Geraga, M., Gilli, A., Gomoiu, M.T., Hall, P.O.J., Hansson, D., He, Y., Holtappels, M., Kirf, M.K., Kononets, M., Konovalov, S., Lichtschlag, A., Livingstone, D.M., Marinaro, G., Mazlumyan, S., Naeher, S., North, R.P., Papatheodorou, G., Pfannkuche, O., Prien, R., Rehder, G., Schubert, C.J., Soltwedel, T., Sommer, S., Stahl, H., Stanev, E. V., Teaca, A., Tengberg, A., Waldmann, C., Wehrli, B., Wenzhöfer, F., 2014. Investigating hypoxia in aquatic environments: Diverse approaches to addressing a complex phenomenon. Biogeosciences 11, 1215–1259. doi:10.5194/bg-11-1215-2014

Gilfedder, B.S.S., Petri, M., Wessels, M., Biester, H., 2011. Bromine species fluxes from Lake Constance's catchment, and a preliminary lake mass balance. Geochim. Cosmochim. Acta 75, 3385–3401. doi:10.1016/j.gca.2011.03.021

Hakala, A., 2004. Meromixis as a part of lake evolution; observations and a revised classification of true meromictic lakes in Finland. Boreal Environ. Res. 9, 37–53.

Hallam, A., Wignall, P.B., 1999. Mass extinctions and sea-level changes. Earth-Science Rev. 48, 217–250. doi:10.1016/S0012-8252(99)00055-0

Hallam, A., Wignall, P.B., 1997. Mass extinctions and their aftermath. Oxford University Press, Oxford.

Hammer, Ø., Harper, D.A.T. a. T., Ryan, P.D., 2001. PAST: Paleontological statistics software package for education and data analysis. Palaeontol. Electron 4, 1–9.

Hammer, Ø., Harper, D.A.T. a. T., Ryan, P.D., 2001. PAST: Paleontological statistics software package for education and data analysis [WWW Document]. Palaeontol. Electron. URL http://palaeo-electronica.org/2001_1/past/issue1_01.htm (accessed 4.6.17).

Hiner, C.A., Kirby, M.E., Bonuso, N., Patterson, W.P., Palermo, J., Silveira, E., 2016. Late Holocene hydroclimatic variability linked to Pacific forcing: evidence from Abbott Lake, coastal central California. J. Paleolimnol. 56, 299–313. doi:10.1007/s10933-016-9912-4

Holmer, M., Storkholm, P., 2001. Sulphate reduction and sulphur cycling in lake sediments: a review. Freshw. Biol. 46, 431–451. doi:10.1046/j.1365-2427.2001.00687.x

Hutchinson, G. E. 1967. A treatise on limnology. Volume II. Introduction to lake biology and the limnoplankton. John Wiley & Sons, New York, London, and Sydney.

Iglésies, J., 1969. El cens del comte de Floridablanca. 1787 (part de Catalunya). Fundació Salvador Vives i Casajuana, Barcelona.

Iglésies, J., 1981. El fogatge de 1553. Fundació Salvador Vives i Casajuana, Barcelona.

Iglésies, J., 1991. El fogatge de 1497. Fundació Salvador Vives i Casajuana, Barcelona.

IPCC, 2014. Climate Change 2013: The physical science basis. Contribution of working group I to the fifth assessment report of the Intergovernmental Panel on Climate Change, 1st ed. Cambridge University Press, Cambridge. doi:10.1017/CBO9781107415324

Jankowski, T., Livingstone, D.M., Bührer, H., Forster, R., Niederhauser, P., 2006. Consequences of the 2003 European heat wave for lake temperature profiles, thermal stability, and hypolimnetic oxygen depletion: Implications for a warmer world. Limnol. Oceanogr. 51, 815–819. doi:10.4319/lo.2006.51.2.0815

Jellison, R., Romero, J., Melack, J.M., 1998. The onset of meromixis during restoration of Mono Lake, California: Unintended consequences of reducing water diversions. Limnol. Oceanogr. 43, 706–711. doi:10.4319/lo.1998.43.4.0706

Jenny, J.P., Francus, P., Normandeau, A., Lapointe, F., Perga, M.E., Ojala, A., Schimmelmann, A., Zolitschka, B., 2016a. Global spread of hypoxia in freshwater ecosystems during the last three centuries is caused by rising local human pressure. Glob. Chang. Biol. 22, 1481–1489. doi:10.1111/gcb.13193

Jenny, J.P., Normandeau, A., Francus, P., Taranu, Z.E., Gregory-Eaves, I., Lapointe, F., Jautzy, J., Ojala, A.E.K., Dorioz, J.M., Schimmelmann, A., Zolitschka, B., 2016b. Urban point sources of nutrients were the leading cause for the historical spread of hypoxia across European lakes. Proc. Natl. Acad. Sci. U.S.A. 113, 12655–12660. doi:10.1073/pnas.1605480113.

Jungclaus, J.H., Lorenz, S.J., Timmreck, C., Reick, C.H., Brovkin, V., Six, K., Segschneider, J., Giorgetta, M.A., Crowley, T.J., Pongratz, J., Krivova, N.A., Vieira, L.E., Solanki, S.K., Klocke, D., Botzet, M., Esch, M., Gayler, V., Haak, H., Raddatz, T.J., Roeckner, E., Schnur, R., Widmann, H., Claussen, M., Stevens, B., Marotzke, J., 2010. Climate and carbon-cycle variability over the last millennium. Clim. Past 6, 723–737. doi:10.5194/cp-6-723-2010

Juggins S., 2009. R package rioja available from the Internet. http://www.staff.ncl.ac.uk/staff/stephen.juggins

Langhans, C., Smith, H.G., Chong, D.M.O., Nyman, P., Lane, P.N.J., Sheridan, G.J., 2016. A model for assessing water quality risk in catchments prone to wildfire. J. Hydrol. 534, 407–426. doi:10.1016/j.jhydrol.2015.12.048

Lavoie, I., Laurion, I., Warren, A., Vincent, W., 2007. Les fleurs d'eau de cyanobactéries : Revue de littérature., INRS rapport 916. INRS, Centre Eau, Terre et Environnement, Quebec.

Leavitt, P.R., 1993. A review of factors that regulate carotenoid and chlorophyll deposition and fossil pigment abundance. J. Paleolimnol. 9, 109–127.

Legendre, P., L. Legendre. 1998. Numerical Ecology. Elsevier Science BV, Amsterdam, The Netherlands

Liermann, M., Steel, A., Rosing, M., Guttorp, P., 2004. Random denominators and the analysis of ratio data. Environ. Ecol. Stat. 11, 55–71. doi:10.1023/B:EEST.0000011364.71236.f8

Livingstone, D.M., 2003. Impact of secular Climate Change on the thermal structure of a large temperate central European Lake. Clim. Change 57, 205–225. doi:10.1023/A:1022119503144

Livingstone, D.M., 1993. Temporal structure in the deep-water temperature of four Swiss lakes: A short-term climatic change indicator? Verh. Int. Verein. Limnol. 25, 75–81.

Livingstone, D.M., 1997. An example of the simultaneous occurrence of climate-driven "sawtooth" deep-water warming/cooling episodes in several Swiss lakes. Verh. Int. Verein. Limnol. 26, 822–828.

Llasat, M.C., Barriendos, M., Barrera, A., Rigo, T., 2005. Floods in Catalonia (NE Spain) since the 14th century. Climatological and meteorological aspects from historical documentary sources and old instrumental records. J. Hydrol. 313, 32–47. doi:10.1016/j.jhydrol.2005.02.004

Madigan, M.T., Jung, D.O., 2009. An overview of purple bacteria: Systematics, physiology, and habitats, in: Hunter, C.N., Daldal, F., Thurnauer, M.C., Beatty, J.T. (Eds.), The Purple Phototrophic Bacteria. Advances in Photosynthesis and Respiration. Springer Netherlands, Dordrecht, pp. 2–16. doi:10.1007/978-1-4020-8815-5_1

Madoz, P., 1985. Diccionario geográfico-estadístico-histórico de España y sus provincias de ultramar. Madrid 1845-1850, Editat pel. ed. Editorial Curial, Barcelona.

Mann, M.E., Zhang, Z., Rutherford, S., Bradley, R.S., Hughes, M.K., Shindell, D., Ammann, C., Faluvegi, G., Ni, F., 2009. Global signatures and dynamical origins of the Little Ice Age and Medieval Climate Anomaly. Science 326, 1256–1260. doi:10.1126/science.1177303

Marlon, J.R., Bartlein, P.J., Gavin, D.G., Long, C.J., Anderson, R.S., Briles, C.E., Brown, K.J., Colombaroli, D., Hallett, D.J., Power, M.J., Scharf, E.A., Walsh, M.K., 2012. Long-term perspective on wildfires in the western USA. Proc. Natl. Acad. Sci. U. S. A. 109, E535–E543. doi:10.1073/pnas.1112839109

Mercadé, A., Vigo, J., Rull, V., Vegas-Villarrúbia, T., Garcés, S., Lara, A., Cañellas-Boltà, N., 2013. Vegetation and landscape around Lake Montcortès (Catalan pre-Pyrenees) as a tool for palaeoecological studies of lake sediments. Collect. Bot. 32, 87–101. doi:10.3989/collectbot.2013.v32.008

Meteocat, 2015a. Climatologia. El Pallars Jussà. 1961-1990 [WWW Document]. URL http://static-m.meteo.cat/wordpressweb/wp-content/uploads/2014/11/13083422/PallarsJussa.pdf (accessed 1.9.17).

Meteocat, 2015b. Butlletí climàtic de l'any 2014 [WWW Document]. URL http://static-m.meteo.cat/wordpressweb/wp-content/uploads/2015/06/08120043/Butlleti-anual-2014.pdf (accessed 1.11.17).

Meyer, K.M., Macalady, J.L., Fulton, J.M., Kump, L.R., Schaperdoth, I., Freeman, K.H., 2011. Carotenoid biomarkers as an imperfect reflection of the anoxygenic phototrophic community in meromictic Fayetteville Green Lake. Geobiology 9, 321–329. doi:10.1111/j.1472-4669.2011.00285.x

Mitchell, M., Owen, J., Schindler, S., 1990. Factors affecting sulfur incorporation into lake sediments: Paleoecological implications. J. Paleolimnol. 4, 1–22. doi:10.1007/BF00208295

Modamio, X., Pérez, V., Samarra, F., 1988. Limnología del lago de Montcortés (ciclo 1978-79) (Pallars Jussà, Lleida). Oecologia Aquat. 9, 9–17.

Morellón, M., Pérez-Sanz, A., Corella, J.P., Büntgen, U., Catalán, J., González-Sampériz, P., González-Trueba, J.J., López-Sáez, J.A., Moreno, A., Pla-Rabes, S., Saz-Sánchez, M.Á., Scussolini, P., Serrano, E., Steinhilber, F., Stefanova, V., Vegas-Vilarrúbia, T., Valero-Garcés, B., 2012. A multi-proxy perspective on millennium-long climate variability in the southern Pyrenees. Clim. Past 8, 683–700. doi:10.5194/cp-8-683-2012

Moreno, A., Giralt, S., Valero-Garcés, B., Sáez, A., Bao, R., Prego, R., Pueyo, J.J., González-Sampériz, P., Taberner, C., 2007. A 14kyr record of the tropical Andes: The Lago Chungará sequence (18°S, northern Chilean Altiplano). Quat. Int. 161, 4–21. doi:10.1016/j.quaint.2006.10.020

Mur, L.R., Skulberg, O.M., Utkilen, H., 1999. Chapter 2. Cyanobacteria in the environment, in: Chorus, I., Bartram, J. (Eds.), Toxic Cyanobacteria in Water: A Guide to Their Public Health Consequences, Monitoring and Management. E & FN Spon, London and New York, pp. 143–153. doi:10.1016/j.ecoleng.2012.12.089

Mur, L.R., Gons, H.J., Van Liere, L., 1978. Competition of the green alga Scenedesmus and the blue-green alga Oscillatoria in light limited environments. FEMS Microbiol. Lett. 1, 335–338.

New, M., Liverman, D., Schroder, H., Anderson, K., 2011. Four degrees and beyond: the potential for a global temperature increase of four degrees and its implications. Philos. Trans. R. Soc. London A Math. Phys. Eng. Sci. 369, 6–19. doi:10.1098/rsta.2010.0303

North, R.P., North, R.L., Livingstone, D.M., Köster, O., Kipfer, R., 2014. Long-term changes in hypoxia and soluble reactive phosphorus in the hypolimnion of a large

temperate lake: Consequences of a climate regime shift. Glob. Chang. Biol. 20, 811–823. doi:10.1111/gcb.12371

Ojala, A.E.K., Francus, P., Zolitschka, B., Besonen, M., Lamoureux, S.F., 2012. Characteristics of sedimentary varve chronologies – A review. Quat. Sci. Rev. 43, 45–60. doi:10.1016/j.quascirev.2012.04.006

Osleger, D.A., Heyvaert, A.C., Stoner, J.S., Verosub, K.L., 2009. Lacustrine turbidites as indicators of Holocene storminess and climate: Lake Tahoe, California and Nevada. J. Paleolimnol. 42, 103–122. doi:10.1007/s10933-008-9265-8

Quinn G.P., Keough M.J. 2002. Experimental Design and Data Analysis for Biologists. Cambridge University Press. New York. 537 pp.

Pearce, C.R., Cohen, A.S., Coe, A.L., Burton, K.W., 2008. Molybdenum isotope evidence for global ocean anoxia coupled with perturbations to the carbon cycle during the Early Jurassic. Geology 36, 231–234. doi:10.1130/G24446A.1

Peeters, F., Livingstone, D.M., Goudsmit, G.H., Kipfer, R., Forster, R., 2002. Modeling 50 years of historical temperature profiles in a large central European lake. Limnol. Oceanogr. 47, 186–197. doi:10.4319/lo.2002.47.1.0186

Pérez-Almoguera, A., Rafel, N., Arilla, M., Carreras, T., 2011. La ocupación prehistórica y romana de la cavidad M35 del Baix Pallars (Pallars Sobirà, Lleida). Rev. d'Arqueologia Ponent 21, 103–118.

Pérez-Zanón, N., Sigró, J., Ashcroft, L., 2016. Temperature and precipitation regional climate series over the central Pyrenees during 1910-2013. Int. J. Climatol. 1–16. doi:10.1002/joc.4823

Phedorin M.A., Goldberg E.L., Grachev M.A., Levina O.L.,Khlystov O.M., Dolbnya I.P, 2000. The comparison of biogenic silica, Br and Nd distributionsin the sediments of Lake Baikal as proxies of changing paleoclimates of the last 480 kyr. Nucl. Instrum. Meth. A, 448, 400-406.

Phedorin, M.A., Fedotov, A.P., Vorobieva, S.S., Ziborova, G.A., 2008. Signature of long supercycles in the Pleistocene history of Asian limnic systems. J. Paleolimnol. 40, 445–452. doi:10.1007/s10933-007-9172-4

Rempfer, J., Livingstone, D.M., Blodau, C., Forster, R., Niederhauser, P., Kipfer, R., 2010. The effect of the exceptionally mild European winter of 2006–2007 on temperature and oxygen profiles in lakes in Switzerland: A foretaste of the future? Limnol. Oceanogr. 55, 2170–2180. doi:10.4319/lo.2010.55.5.2170

Repeta, D.J., 1993. A high resolution historical record of Holocene anoxygenic primary production in the Black Sea. Geochim. Cosmochim. Acta 57, 4337–4342. doi:10.1016/0016-7037(93)90334-S

Reynolds, C.S., 1984. The ecology of freshwater phytoplankton, Biological Reviews. Cambridge University Press, Cambridge, UK. doi:10.1111/j.1469-185X.1965.tb00803.x

Riera, S., Wansard, G., Julià, R., 2004. 2000-Year environmental history of a karstic lake in the Mediterranean Pre-Pyrenees: The Estanya lakes (Spain). Catena 55, 293–324.

Rosell, J., 1994. Geological Map of Spain and Report. Scale 1: 50,000, Tremp Sheet (252). Instituto Tecnológico Geográfico de España (IGME), Madrid.

Rull, V. 2014. Time continuum and true long term ecology: from theory to practice. Frontiers in Ecology and Evolution 2, 75, doi 10.3389/fevo.2014.00075

Rull, V., González-Sampériz, P., Corella, J.P., Morellón, M., Giralt, S., 2011. Vegetation changes in the southern Pyrenean flank during the last millennium in relation to climate and human activities: the Montcortès lacustrine record. J. Paleolimnol. 46, 387–404. doi:10.1007/s10933-010-9444-2

Rull, V., Vegas-Vilarrúbia, T., 2015. Crops and weeds from the Estany de Montcortés catchment, central Pyrenees, during the last millennium: A comparison of palynological and historical records. Veg. Hist. Archaeobot. 24, 699–710. doi:10.1007/s00334-015-0525-z

Rull, V., Vegas-Vilarrubia, T., 2014. Preliminary report on a mid-19th century Cannabis pollen peak in NE Spain: Historical context and potential chronological significance. The Holocene 24, 1378–1383. doi:10.1177/0959683614540964

Sabartés i Guixés, J.M., 1993. L'èxode Pallarès. Crisi demogràfica i davallada poblacional als Pallars i a l'Alta Ribagorça (1857-1991), Col·lecció Estudis, núm. 3. ed. Garsineu, Tremp.

Sánchez-López, G., Hernández, A., Pla-Rabes, S., Trigo, R.M.M., Toro, M., Granados, I., Sáez, A., Masqué, P., Pueyo, J.J.J., Rubio-Inglés, M.J.J., Giralt, S., 2016. Climate reconstruction for the last two millennia in central Iberia: The role of East Atlantic (EA), North Atlantic Oscillation (NAO) and their interplay over the Iberian Peninsula. Quat. Sci. Rev. 149, 135–150. doi:10.1016/j.quascirev.2016.07.021

Schaller, T., Christoph Moor, H., Wehrli, B., 1997. Sedimentary profiles of Fe, Mn, V, Cr, As and Mo as indicators of benthic redox conditions in Baldeggersee. Aquat. Sci. 59, 345–361. doi:10.1007/BF02522363

Scussolini, P., Vegas-Vilarrúbia, T., Rull, V., Corella, J.P., Valero-Garcés, B., Gomà, J., 2011. Middle and late Holocene climate change and human impact inferred from diatoms, algae and aquatic macrophyte pollen in sediments from Lake Montcortès (NE Iberian Peninsula). J. Paleolimnol. 46, 369–385. doi:10.1007/s10933-011-9524-y

Serra, T., Colomer, J., Cristina, X.P., Vila, X., Arellano, J.B., Casamitjana, X., 2001. Evaluation of laser in situ scattering instrument for measuring concentration of phytoplankton, purple sulfur bacteria, and suspended inorganic sediments in lakes. J. Environ. Eng. 127, 1023–1030. doi:10.1061/(ASCE)0733-9372(2001)127:11(1023)

Sinninghe Damsté, J.S., Wakeham, S.G., Kohnen, M.E.L., Hayes, J.M., de Leeuw, J.W., 1993. A 6,000–year sedimentary molecular record of chemocline excursions in the Black Sea. Nature 362, 827–829. doi:10.1038/362827a0

Smith, H.G., Sheridan, G.J., Lane, P.N.J., Nyman, P., Haydon, S., 2011. Wildfire effects on water quality in forest catchments: A review with implications for water supply. J. Hydrol. 396, 170–192. doi:10.1016/j.jhydrol.2010.10.043

Stefan, H.G., Fang, X., Hondzo, M., 1998. Simulated Climate Change effects on year-round water temperatures in temperate zone lakes. Clim. Change 40, 547–576. doi:10.1023/A:1005371600527

Stumm, W., Morgan, J.J., 1996. Aquatic chemistry: Chemical equilibria and rates in natural waters, 3rd ed. Wiley, New York.

Suits, N.S., Wilkin, R.T., 1998. Pyrite formation in the water column and sediments of a meromictic lake. Geology 26, 1099–1102.

Trapote M.C., López P., Gomà J., Safont E., Cañellas-Boltà N., Buchaca T., Pérez-Zanón N., Sigró J, Rull V., Vegas-Vilarrúbia T. 2015a. Limnological cycle of meromictic lake (Montcortès, Pyrenees) and its relationships to sediment varve formation, in: Proceedings of the American Association of Limnology and Oceanography, Granada, Spain, 23-27 February.

Trapote, M.C., López, P., Puche, E., Safont, E., Cañellas-Boltà, N., Buchaca, T., Pérez-Zanón, N., Sigró, J., Rull, V., Vegas-Vilarrúbia, T., 2015b. Modern limnology and varve formation processes in Lake Montcortès (southern Pyrenees, Spain), in: Proceedings of the American Geophysical Union. Fall Meeting, San Francisco, 14-18 December.

Trapote, M.C., Vegas-Vilarrúbia, T., López, P., Puche, E., Buchaca, T., Cañellas, N., Safont, E., Gomà, J., Corella, P., Rull, V. Annual limnological cycle, sedimentation patterns and varve formation in Lake Montcortès (central Pyrenees). J. Limnol. [submitted]

Van Gemerden, H., Mas, J., 1995. Ecology of Phototrophic Sulfur Bacteria, in: Robert, E., Blankenship, M.T., Madigan, C.E.B. (Eds.), Anoxygenic Photosynthetic Bacteria. Springer, Dordrecht, The Netherlands, pp. 49–85. doi:10.1007/0-306-47954-0_4

van der Werf, H.M.G., Turunen, L., 2008. The environmental impacts of the production of hemp and flax textile yarn. Ind. Crops Prod. 27, 1–10. doi:10.1016/j.indcrop.2007.05.003

Vila-Escalé, M., Vegas-Vilarrúbia, T., Prat, N., 2007. Release of polycyclic aromatic compounds into a Mediterranean creek (Catalonia, NE Spain) after a forest fire. Water Res. 41, 2171–2179. doi:10.1016/j.watres.2006.07.029

Zotina, T., Koster, O., Juttner, F., 2003. Photoheterotrophy and light-dependent uptake of organic and organic nitrogenous compounds by Planktothrix rubescens under low irradiance. Freshw. Biol. 48, 1859–1872. doi:10.1046/j.1365-2427.2003.01134.x

Appendix

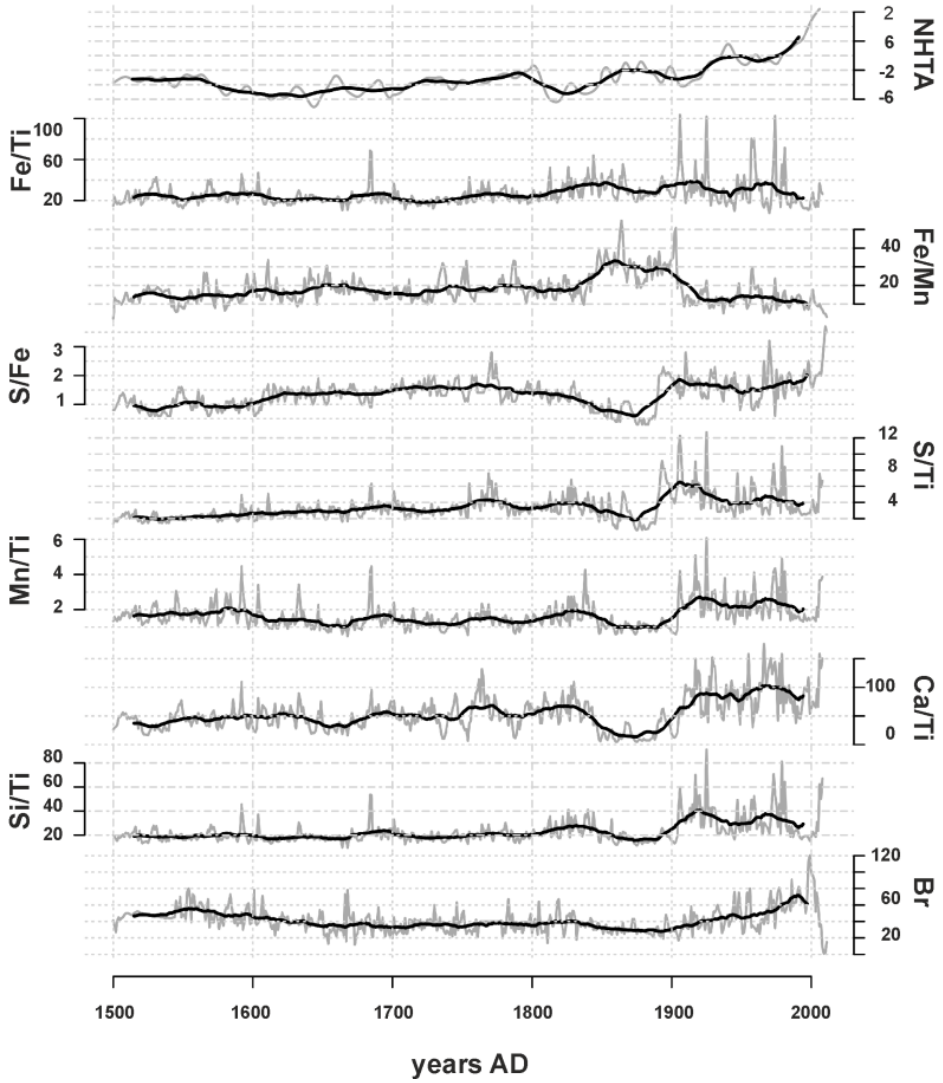

Figure A.1: Temporal variations of the elemental ratios and the mean temperature since 1500 AD.

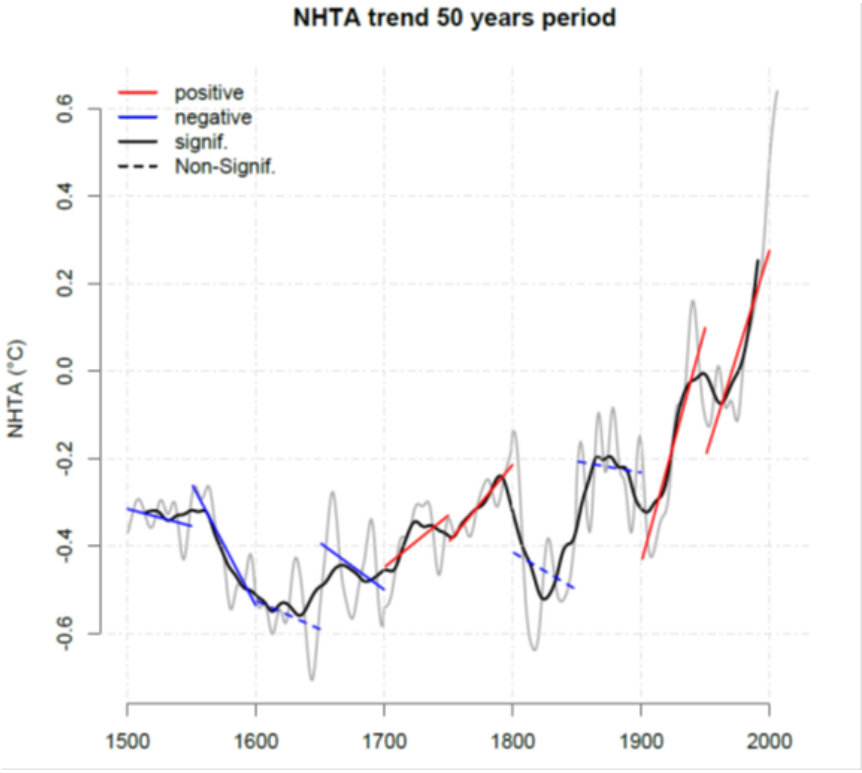

Figure A.2: Evolution (grey line) and 50 years period trend of NHAT. Black line corresponds to 30 years NHTA filter. Positive (Negative) trend values are shown in red (blue) while continuous (dashed) line correspond to significant (non-significant) values.

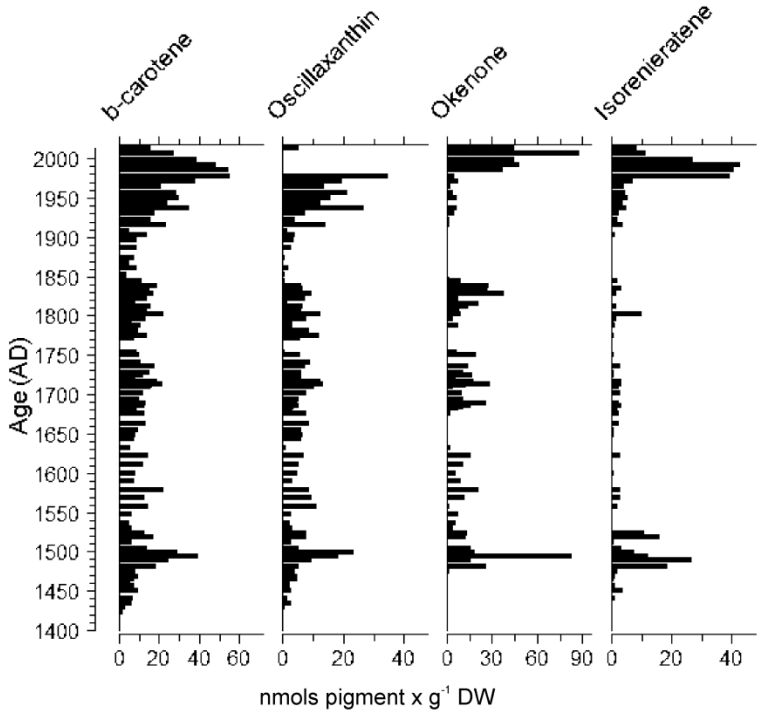

Figure A.3: Temporal variations of pigment biomarkers since 1500 AD.

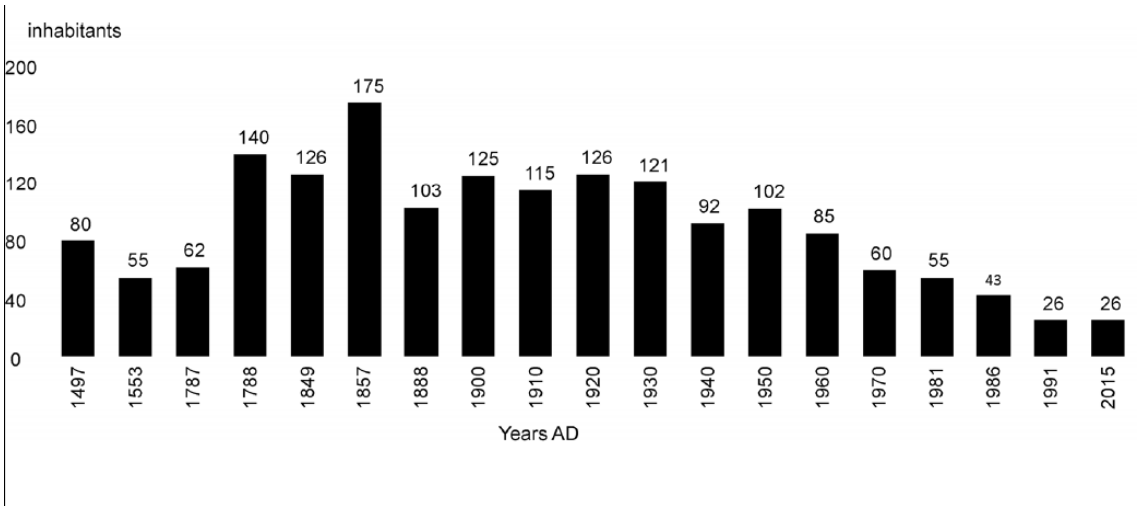

Figure A.4: Demographic behaviour of the Montcortès town since 1500 AD, based on the information compiled by Jesús Sánchez (Iglésies, 1969, 1981, 1991; Sabartés i Guixés, 1993).

Table A.1: Principal component loadings (significant correlations, $p \leq 0.005$).

	PCA (I)		PCA (II)			PCA (III)		
	C 1	C 2	C1	C2	C3	C 1	C 2	C 3
mFe/Ti	0.555	0.802	0.392	0.875	-0.190	0.075	0.939	0.245
mFe/Mn	-0.552	0.671	-0.4949	0.663	0.304	-0,792	0.366	-0,097
mS/Fe	0.699	-0.3821	0.566	-0.476	0.651	0.673	-0,117	-0,650
mS/Ti	0.893	0.211	0.819	0.282	0.427	0.618	0.6136	-0,418
mMn/Ti	0.888	0.09727	0.857	0.112	-0.4073	0.815	0.3745	0.296
mCa/Ti	0.919	-0.2745	0.884	-0.329	0.0829	0.940	0.0769	-0,097
mSi/Ti	0.901	0.342	0.884	0.364	-0.1276	0.723	0.6401	0.170
mBr	0.296	-0.4652	0.200	-0.522	-0.5231	0.563	-0,417	0.430
oken						0.605	-0,333	0.338
isore						0.616	-0,180	0.282
chl a						0.607	-0,250	-0,409
β-car						0.844	-0,264	-0,052
oscil								

Chapter 5 — Weather regimes and tree-rings

Pérez-Zanón, N., Khodri, M., Sigró, J., Gutiérrez, E., 2017: Role of North Atlantic weather regimes in the central Pyrenees climate from instrumental and tree-ring data. [in preparation]

ROLE OF NORTH ATLANTIC WEATHER REGIMES IN THE CENTRAL PYRENEES CLIMATE FROM INSTRUMENTAL AND TREE-RING DATA

Pérez-Zanón, Núria[1], Khodri, Myriam[2]; Sigró, Javier[1]; Gutiérrez, Emilia[3]

[1] Center for Climate Change (C3), Campus Terres de l'Ebre, Universitat Rovira i Virgili, Tortosa, Spain

[2] Laboratoire d'Océanographie et du Climat: Expérimentations et approches numériques, Sorbonne Universités, UPMC Université Paris 06, IPSL, UMR CNRS/IRD/MNHN, F-75005 Paris, France.

[3] Department of Ecology, Fac. BiologyUniversity of BarcelonaBarcelonaSpain

Abstract

One of the advantages provided by the study of a mountain range, as the Pyrenees, is its great biodiversity which provides for natural climate records to allow scientist to reconstruct the past climate. The characterization of regional climate response on a synoptic scale, of the recognized importance for their impact on society, is the first step to later obtain the climate signal contained in natural records. Many studies show the use of natural records covering big areas for the reconstruction of climatic indices such as the NAO or ocean indices like the AMO. However, few studies address synoptic scale climate information containing each natural records prior to the extension of rebuilding larger scale. In this study, the response to the synoptic scale climate the Central Pyrenees in summer in the period 1910-2013 is presented, in order to be a catalogue for future works in climate reconstruction of the area. The case study of tree-rings width response from Central Pyrenees to climate at synoptic scale is addressed. The results show that observed climate in the Pyrenees is leaded by synoptic scale configuration and tree-rings captures the climate variability and change, specially during the instrumental period.

KEY WORDS: Weather Regimes; Pyrenees; Tree-rings; SNAO; Climate;

1. Introduction

Paleoclimate research is being more focus on regional climatic responses to global or hemispherical changes, as regional climate affects societies and forms the basis for efficient adaptation measurements. Proxy-reconstructed paleoclimate records and climate-model comparisons allow to evaluate climate transitions through the analysis of forcing and feedback mechanisms in past climate changes. However, the amplitudes of variation in the hydrological cycle and temperature changes at different time and space scales reconstructed for the last millenniums differ between from one to another research work (Lionello, 2012).

The Pyrenees is a mountainous range in eastern Europe, in the transition between Eurosiberian and Mediterranean ecoclimate regions (Dorado Liñán *et al.*, 2012) and with Atlantic and Mediterranean climatic influences (Beguería *et al.*, 2003; López-Moreno *et al.*, 2008; López-Moreno and Beniston, 2008). This area is of high interest due to its natural richness in biodiversity (López-Moreno *et al.*, 2008; Regato, 2015) and human development by water resources, energy production, tourism (Marín-Yaseli and Martínez, 2003) and agriculture (Beguería *et al.*, 2003; López-Moreno *et al.*, 2008). Some of the features of the Pyrenees makes them one of the most vulnerable areas to climate change (Dorado Liñán *et al.*, 2012): Pyereens is in middle latitudes (Büntgen *et al.*, 2008) in the Mediterranean area (Giorgi, 2006) and is a mountainous area (Beniston, 2003; Melis *et al.*, 2014). Furthermore, due to its biodiversity, Pyrenees are a source of paleoclimate archives such as glaciers (Cuadrat and Martín Vide, 2007), lake sediments (Moreno *et al.*, 2012) and tree-rings (Tardif *et al.*, 2003).

In the Pyrenees, climatic studies have frequently been conducted by scientists from different disciplines, such as biologists, hydrologists or glaciologists, rather than by meteorologists, as it occurs generally in mountain areas. So, climate information is dispersed in the scientific literature and usually focused in a local issue (Barry, 2008). So before reconstructing regional climate using paleoclimate archives, a deep knowledge of the regional climate itself is necessary.

For its part, general atmospheric circulation in the North Atlantic-European sector is characterized by the high-latitude Aleutian and Iceland low-pressure centers dominating

in the North Atlantic during winter, while it moves northward in summer and the anticyclonic Azores high pressure system predominates covering most of the North Atlantic (Hurrell *et al.*, 2003). The annual variability of these pressure centers is captured by the North Atlantic Oscillation (NAO; Walker, 1924) especially in winter, when months are meteorologically more actives (Folland *et al.*, 2009). However, some extreme events, like drought, heat waves and floods, occur in summer (Folland *et al.*, 2009) even hail extreme events (van der Linden *et al.*, 2015). The NAO is frequently defined by the first empirical orthogonal function (EOF) of the seasonal mean sea level pressure in the north Atlantic sector. The winter NAO is stronger and larger spatial extent than the summer NAO (Folland *et al.*, 2009), given some difference in temperature and precipitation spatial patterns: in the positive NAO phase, Northern Europe temperature and precipitation are higher than the normal in winter, while in summer the area of high temperature is reduced to the northwestern of Europe and the precipitation anomaly over this area is negative; in the same phase of the NAO, colder temperatures than the normal are observed in the Northern Africa and drier conditions in the Mediterranean in winter, in contradistinction to summer when temperature and precipitation greater than the normal occurs in the Mediterranean. (http://www.metoffice.gov.uk/research/climate/seasonal-to-decadal/gpc-outlooks/ens-mean/nao-description).

Tree rings have been widely used to reconstruct past climate in North Atlantic and European sectors (such as Cook et al., 1998; Folland et al., 2009; Gray et al., 2004; Wassenburg et al., 2013) due to their capability to preserve large-scale anomalies in the general atmospheric circulation (Briffa *et al.*, 2004; Fritts *et al.*, 1971). Some spices of trees growth in summer season, even temperature reconstructions of May to September in Pyrenees have already published (Büntgen *et al.*, 2008; Dorado Liñán *et al.*, 2012), so a link between summer climate and tree-ring growth is expected. However, tree-rings from mid to low-latitudes are less sensitive to temperature than those from high-latitudes showing less intensity and small spatial correlation when comparing with Sea Surface Temperature (SST) observations (Büntgen *et al.*, 2008).

Because NAO doesn't correlate with temperatures over western Mediterranean, tree-rings from the Pyrenees are not included in big datasets of proxy data to reconstruct NAO (such as in Ortega *et al.*, 2015), while they are included to reconstruct north hemisphere temperature (Stoffel *et al.*, 2015).

As shown above, we face the following inconsistency: while natural registers are considered to be able of capturing large-scale climate, proxies from the Pyrenees are not included in large scale patterns reconstruction. Then, we try to address the following questions: are proxies from Pyrenees able to capture large-scale climate signal? Which climate signal are they capturing and, therefore, which climate information is included when the proxy from Pyrenees are used? Pyrenees proxies should be studied separately from large dataset before other purposes.

Here we present summer (from June to August) synoptic configurations in the North Atlantic-European sector, which lead the regional climate in the central Pyrenees, as a benchmark to be used in future works. Their relation with weather regimes are analysed, as well as the capability of tree-ring width (TRW) as climate proxy records is evaluated.

2. Data

2.1 The Central Pyrenees Regional Climate

A recent study presents the longest anomaly regional series of precipitation (PPT) and maximum (Tmax) and minimum temperature (Tmin) which characterized the observed climate in the central Pyrenees for the period 1910–2013 (Pérez-Zanón *et al.*, 2017). These series were built from the daily quality controlled observed data from 155 manual and automatic weather stations covering the study area. After the monthly homogenization, to remove non-climatic variations from the series, the regional anomaly series of each variable was obtained by averaging the most completed individual series. In the present work, summer (June to August) anomalies were computed using the mean of all series length (Figure 1). In order to take into account the varying sample size on time, the Osborn correction was applied to avoid a bias introduced by a simple average.

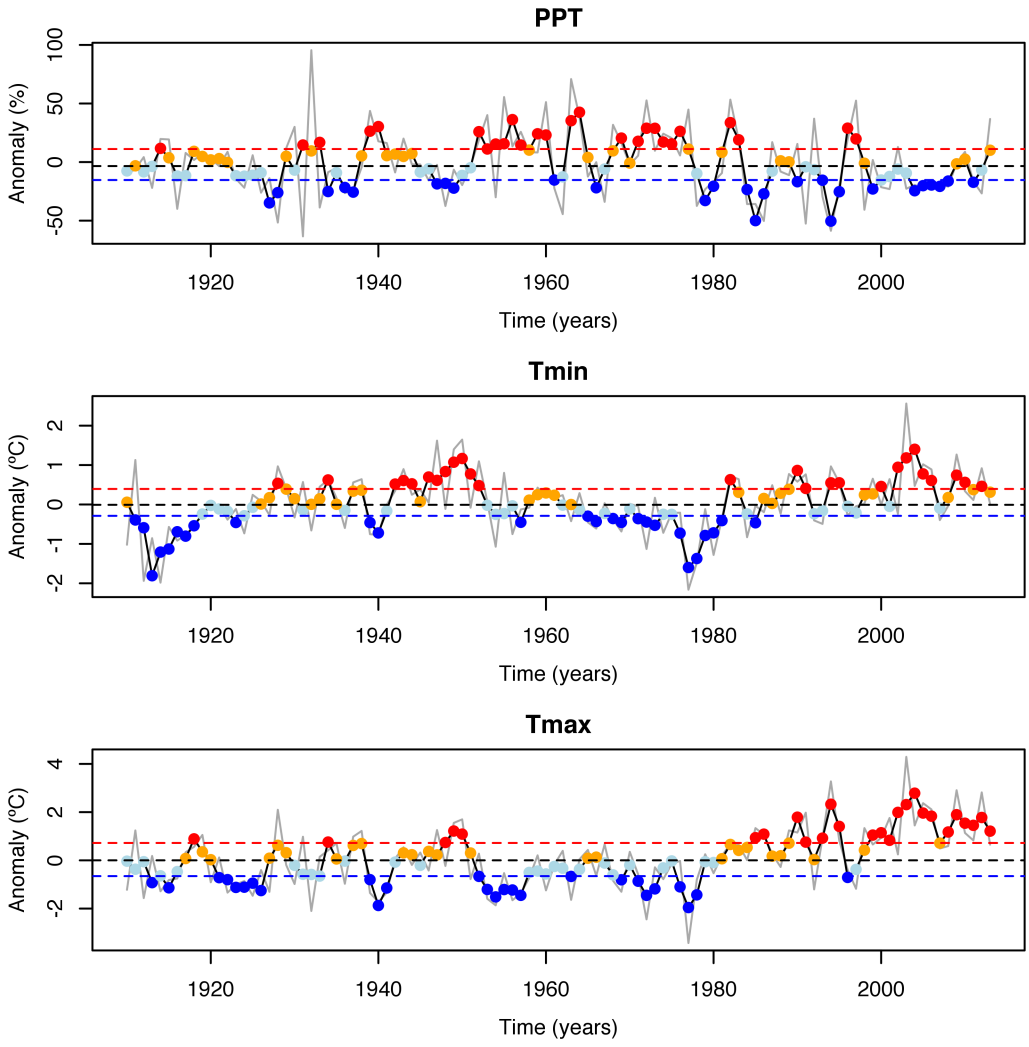

Figure 1: Summer regional anomaly series for PPT (top), Tmin (middle) and Tmax (bottom). Grey (black) line corresponds to the non-filtered (5 years filter, see section 3.2) series. Dashed lines corresponds to the first (Q1, blue), the second (Q2, black) and the third quartile (Q3, red) of the 5 years filtered series. Values less or equal (greater) than Q1 (Q3) are shown as blue (red) dots. Interquartile values are shown in light blue (orange) when they are greater than Q1 (Q2) and less or equal than Q2 (Q3).

2.2 Global Observed Datasets

An ensemble of monthly global observational and reanalysis grids have been selected to analyse the synoptic state of the atmosphere the North Atlantic-European sector (20º–70ºN; 70ºW–40ºE): observed precipitation dataset from the Global Precipitation Climatology Center (GPCC; Schneider *et al.*, 2014), Extended Reconstructed Sea

Surface Temperature v4 (ERSST; Huang *et al.*, 2016), Hadley Sea Level Pressure anomalies (Hadley SLP; Allan *et al.*, 2006), and Precipitation rate (Prate), 2m air temperature (Air), Mean Sea Level Pressure (SLP) and zonal and Meridional winds and Relative Humidity from 20th Century Reanalysis project V2 (20CRP; Compo *et al.*, 2011). Furthermore, daily SLP from 20CRP have been used.

2.3 Tree-rings Chronologies

A dataset of 31 chronologies of TRW of Pinus uncinata id available covering the Pyrenees mountain range, with higher density of observations over the central Pyrenees (Figure 2). The chronologies are built with 1130 cores from 580 trees by absolute dating. The residual chronologies, obtained by applying Friedman function, present a Expressed Population Signal (Wigley *et al.*, 1984) greater than 0.85 confirming the reliability of the common signal for each chronology. They are placed between 1750 and 2451 m height (see Table S1 for details).

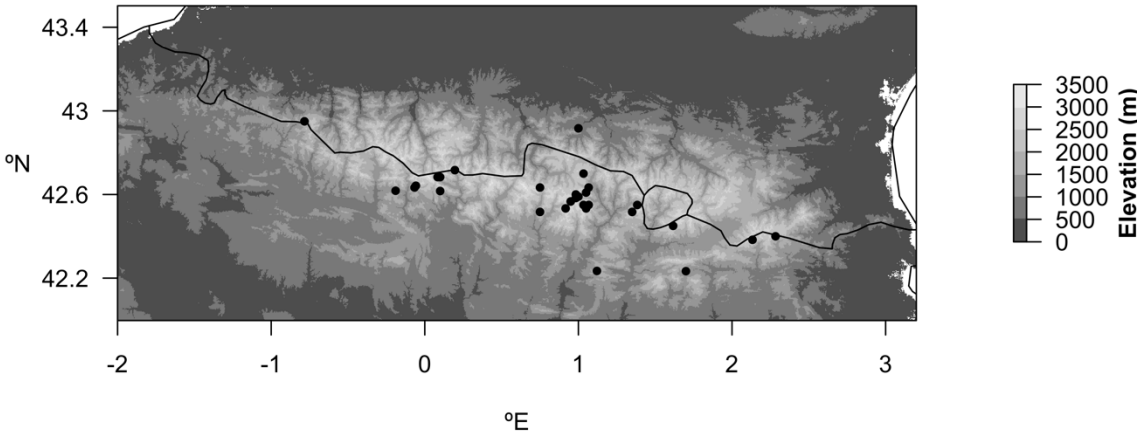

Figure 2: Spatial distribution of the 31 TRW chronologies over Central Pyrenees.

3. Methodology

3.1. North Atlantic – European Sector Weather Regimes

K-means cluster analysis, based on Hartigan and Wong (1979) algorithm, has been applied to summer daily SLP anomalies during the period 1910–2012 to define North Atlantic – European sector weather regimes (WR). Following Cassou et al. (2005), the optimal number of clusters considered is k = 4. Equivalent configurations are found (Figure 3): Blocking (27.3 % of occurrence), Atlantic Low (Atl.Low; 23.1 % of occurrence), Atlantic Ridge (Atl.Ridge; 24.5 % of occurrence) and negative phase of Summer NAO (SNAO-; 25.0 % of occurrence); however, due to differences in the methodology, the percentage of occurrence is a bit different.

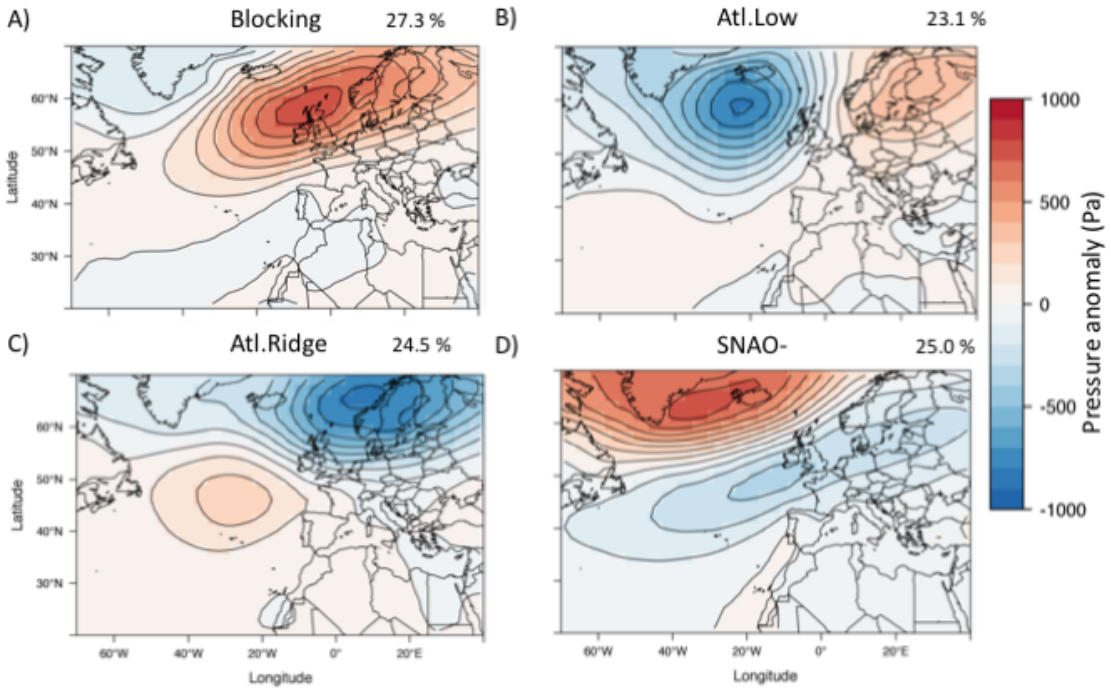

Figure 3: Summer SLP weather regimes computed over the North Atlantic–European sector from 1910 to 2012. Panel A – B correspond to Blocking, Atl.Low, Atl.Ridge and SNAO-, respectively. Contour interval is 100 Pa. Percentage of occurrence for each WR is showed on the top-right of each plot.

It is interesting to highlight that the first and fourth cluster can be interpreted as the positive and negative phases of the SNAO being not symmetrical. Compering with WR

from Cassou *et al.* (2005; see Figure 1 (a-d)), which were computed over 500 hPa geopotential height anomalies, we have found slight differences due to the baroclinicity of the atmosphere. The high pressure center in the Blocking WR is located on the north of the British Islands while, at 500 hPa, it moves towards the east, closes to Scandinavian Peninsula. The Atl.Low is similar in intensity and location of the low pressure center, however, the high pressure center moves from northeastern Europe to center Europe when altitude increase. Comparing Atl.Ridge, the high pressure center in surface is less intense than at 500 hPa. Finally, the SNAO- low pressure center is located at the west of the British Islands in surface while, at 500h Pa, it covers the British Islands and North Sea.

As the cluster analysis has classified each day of summer in one of the WR, the time evolution of each WR can be considered as the annual sum of days for each summer and WR (Figure 4). Considering periods of 20 years, at the beginning of the period, SNAO- predominates although the Atl.Ridge occurrence increase until 1923. Between 1930 and 1949, the Blocking was more frequent. The Atl.Ridge dominates the period 1950–1969, although this period is the most variable, shows in all WR with a big maximum of SNAO-. From 1970 to 1989, Bolcking is the most frequent showing strong variability. Since 1990 until the end of the period, SNAO- dominates, showing a positive trend.

3.2.Temporal and Spatial Analysis

The TRW frequency response of climate has hardly been analysed (Esper *et al.*, 2015a, 2015b) Cook et Kairiukstis, 1990) showing that TRW has low-frequency response than Maximum latewood density because of lower biological persistence (Stoffel *et al.*, 2015). For this reason, and to make climatic and TRW signal comparable, a low pass filtering is necessary for climate series. A Savitzky-Golay Smoothing Filter (Sav-gol) has been selected because of its capability to smooth without losing resolution and amplitude (Press, 2007). Pyrenees regional anomaly series have been filtered by applying a quadratic order 5 years Sav-gol (Figure 1).

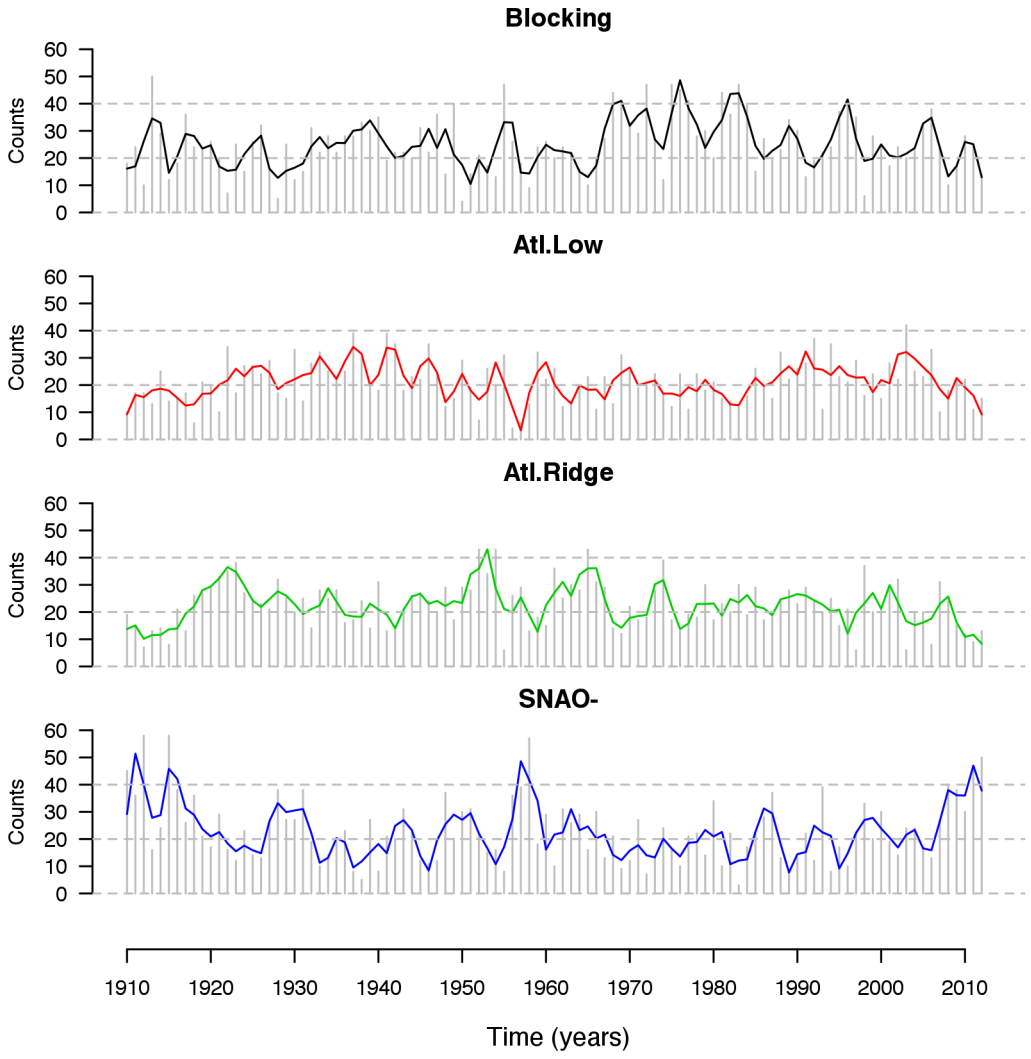

Figure 4: Annual number of summer events of each WR (grey bars) and 5 years Sav-gol filter (continuous line).

The large-scale synoptic configuration of the atmosphere for different observed climate in the Pyrenees have been characterized using composites. First, observed extreme climate and moderate climate variability in the Pyrenees have been defined by applying quartile thresholds in the regional anomaly series of PPT, Tmax and Tmin (Figure 5). We can distinguish between apply the criteria of individual variables or combine two of them. When PPT (Tmax or Tmin) series is considered alone, 3 climatic modes can be defined: Dry (cold), PPT (Tmax or Tmin) values are less than Q1; Moderate, for PPT (Tmax or Tmin) values are greater or equal to Q1 and less than Q3; and wet (warm), for PPT (Tmax or Tmin) values are greater or equal than Q3.

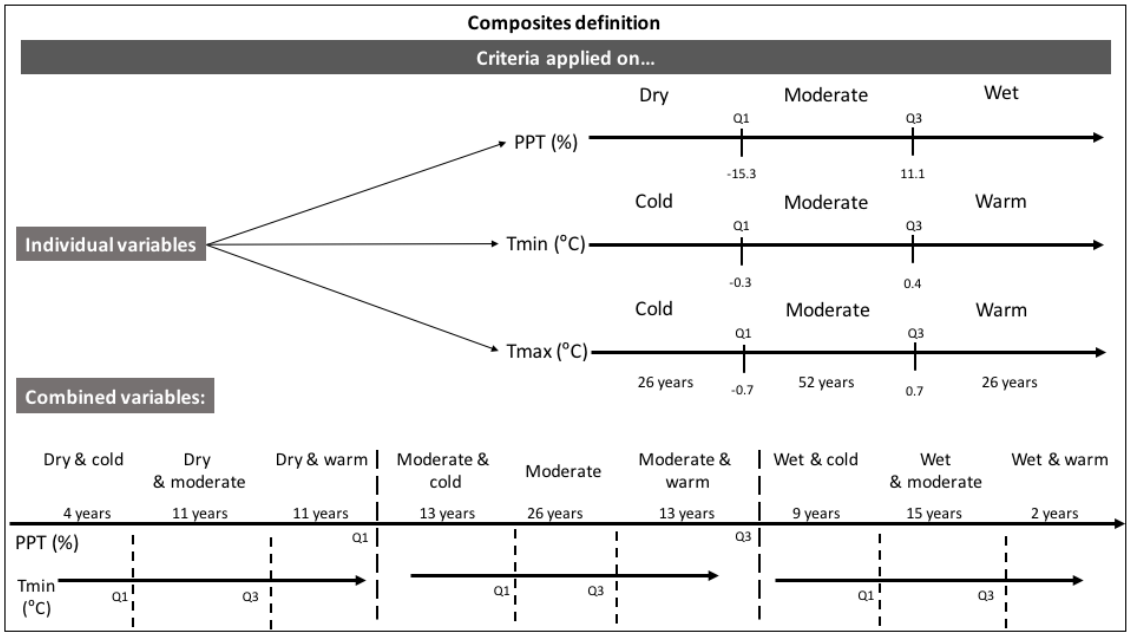

Figure 5: Schematic of the criteria applied to define composites spatial fields of Pyrenees observed climate in individual variables and combined PPT and Tmin criteria. The number of years of each composite is shown.

Furthermore, the combination of PPT and Tmin series has been considered to define climatic modes in the Pyrenees. It should be highlighted that Tmin have been considered instead of Tmax, because Tmax is significantly negatively correlated to PPT. In this case, 9 climatic modes are found: dry and cold ($PPT < Q1_{PPT}$ and $Tmin < Q1_{Tmin}$), dry and moderate ($PPT < Q1_{PPT}$ and $Q1_{Tmin} \leq Tmin < Q3_{Tmin}$), dry and warm ($PPT < Q1_{PPT}$ and $Tmin \geq Q3_{Tmin}$), moderate and cold ($Q1_{PPT} \leq PPT < Q3_{PPT}$ and $Tmin < Q1_{Tmin}$), moderate ($Q1_{PPT} \leq PPT < Q3_{PPT}$ and $Q1_{Tmin} \leq Tmin < Q3_{Tmin}$), moderate and warm ($Q1_{PPT} \leq PPT < Q3_{PPT}$ and $Tmin \geq Q3_{Tmin}$), wet and cold ($PPT \geq Q3_{PPT}$ and $Tmin < Q1_{Tmin}$), wet and moderate ($PPT \geq Q3_{PPT}$ and $Q1_{Tmin} \leq Tmin < Q3_{Tmin}$), wet and warm ($PPT \geq Q3_{PPT}$ and $Tmin \geq Q3_{Tmin}$).

So, composites of Pyrenees observed climatic modes have been obtained by averaging the summer SLP spatial fields (and other spatial fields, not shown) of years belonging to each defined mode (Figure S1 and S2).

Finally, to evaluate the correspondence between temporal series and spatial fields Spearman correlation and significant, using the Student's t test (Wilks, 2011) have been computed.

3.3. Climatic Signal of Tree-rings Chronologies

To improve the reliability of age model in the TRW chronologies dataset, one thousand simulations of each chronology have been running considering a Gaussian error of 1 year for each annual TRW value. In order to extract the common climatic information of all chronologies, a Principal Component Analysis (PCA) in T-mode have been performed over the 31000 simulations over different combinations of trees and periods (Table 1): using all chronologies (31) in different instrumental periods (1910 – 1993 and 1930 – 1993), for all chronologies which cover since 1800 (27) and computing the PCA over all available period (1800 – 1993) or in the instrumental period (1910 – 1993) and considering all chronologies which cover since 1700 (12) and performing the PCA over all available period (1700 – 1993) or in the instrumental period (1910 – 1993); 15 selected is referred to those chronologies which their variance of scores in PC1 and PC2 overcome the third quartile (see Figure S1); as these 15 selected chronologies just cover since 1890, three chronologies have been removed to be able to reconstruct until 1800, so, for these 12 selected chronologies, PCA have been computed over the instrumental period (1910 – 1993) and all available period (1800 – 1993).

However, the variance explained by the first (PC1) and the second (PC2) principal component of all considered cases are not too high, they generally increase when the number of considered chronologies decreases and/or the length of the analysed period increase.

Finally, an equivalent methodology of Pyrenees composites has been applied over PC1 and PC2 of each combination of TRW selection (henceforth called Tree-rings composites). In this case, we will distinguish between high (low) values of PC1 (PC2) instead of wet (dry) or cold (warm) modes.

Table 1: Number of chronologies, starting year of PCA application, reference name for each analysis and percentage of variance of PC1 and PC2.

Number of chronologies	Period of PCA application	Reference name	Variance (%)	
			PC1	PC2
31	1930 – 1993	31 trees 1930	8.38	8.14
31	1910 – 1993	31 trees 1910	8.45	7.04
27	1910 – 1993	27 trees 1910	8.86	7.84
27	1800 – 1993	27 trees 1800	7.86	6.18
12	1910 – 1993	12 trees 1910	10.44	8.76
12	1700 – 1993	12 trees 1700	11.01	7.12
15	1910 – 1993	15 selected 1910	11.67	8.78
12	1910 – 1993	12 selected 1910	13.64	10.43
12	1800 – 1993	12 selected 1800	11.67	9.00

4. Results

4.1 WR and Pyrenees climate

In order to evaluate the temporal relation between the frequency of occurrence of the four WR and the Pyrenees regional series, non-filtered series and different Sav-gol parameters (for 5, 10, 11, 15 and 20 years and quadratic or quartic order) have been applied to the series before correlation analysis (significant level at $\alpha = 0.05$). While SNAO- frequency series doesn't correlate with Pyrenees regional series in any case, Atl.Low frequency evolution shows a significant correlation in most of the cases (Figure 6), being negative with PPT and positive with Tmin and Tmax. Atl.Ridge presents some positive significant correlation with Tmin and Blocking is generally positive correlated to PPT and negative with Tmin while any significant correlation is found with Tmax. The strongest correlations are found for Tmin with Blocking (-0.4) and Atl.Low (0.52).

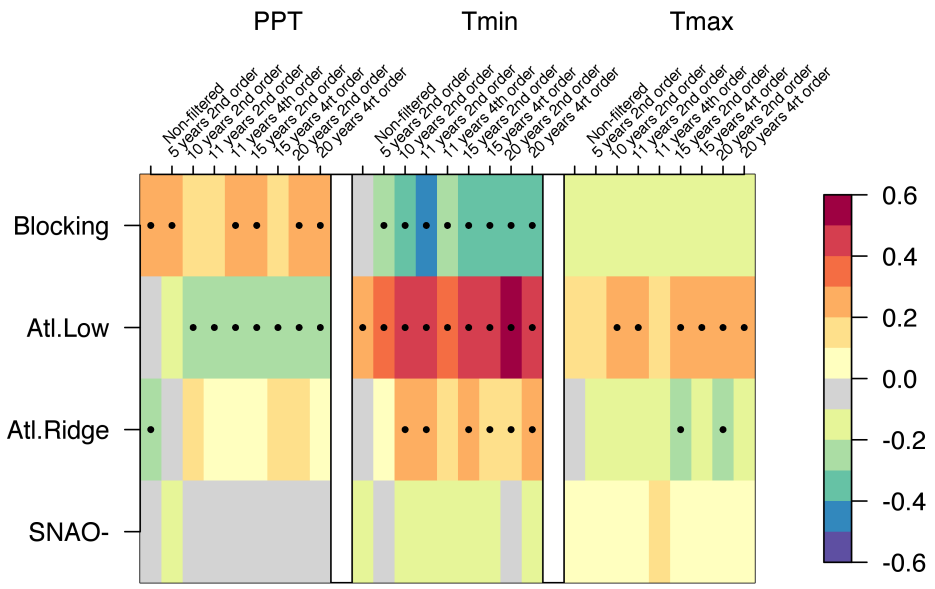

Figure 6: Correlation between WR and PPT, Tmin and Tmax Pyrenees regional series for non-filtered and different Sav-gol parameters. Dots corresponds to significant values at $\alpha = 0.05$.

Spatial Pyrenees composites have been correlated with WR (Figure 7). In general, each composite present one WR dominant (e.g. Tmax moderate year composite versus Blocking), or two with opposite correlation sign (e.g. wet and cold years composite versus Atl.Low and SNAO- WR). PPT composites show the highest correlation magnitude with Bolcking and shows opposite sign with Atl.Ridge for dry years composite and SNAO- for moderate PPT years and warm years composites. The highest correlation in magnitude (-0.81) of Tmin composites occurs with the Atl.Low WR when the cold years are considered. For moderate and warm Tmin years composites, Atl.Ridge returns higher magnitude of correlations than Atl.Low, and opposite sign to SNAO-. Moderate Tmax years composite correlates negatively with Blocking (-0.73). While Atl.Low seems to influence Tmin during all modes considered and a combination of Blocking and Atl.Low lead PPT, Tmax is leaded by different WR.

Figure 7 middle panel shows correlations between WR and composites built applying combining criteria on PPT and Tmin. Comparing dry years composite correlations with WR, an opposite behaviour is found between cold and warm years: correlations with cold (warm) composites are negative (positive) with Blocking and positive (negative) with Atl.Ridge. This fact can support the correlation values of dry and cold composites

even the number of events included are not too large (4 years). Composite of wet years present the highest correlation (0.81) with Blocking when cold years are considered. Finally, moderate precipitation and cold years composite is correlated positively with SNAO- and negatively with Atl.Low.

To acquire a deeper understanding of the atmospheric state during summers of each category in the Pyrenees, the mean percentage of each WR for each composite is shown in Figure 7 bottom panel. The maximum percentage corresponds to the maximum positive correlation in each case, such as wet and cold composite for which Blocking is giving maximum values on both magnitudes. The exception is found for dry and Tmin moderate (maximum percentage of SNAO- and maximum correlation Atl.Ridge) and wet and Tmin composites (maximum percentage Blocking and maximum correlation Atl.Low). On the other hand, the WR with minimum correlation to each composite is generally which presents the minimum percentage of occurrence during those years (6 of 9 cases). This fact can be observed in the same example as before, wet and cold years composite shows minimum correlation with SNAO- which is the WR with minimum percentage of occurrence during these years. For the three other cases, the two minimum values of these magnitudes can be compared, such as for dry and cold years composite, which minimum percentage of occurrence of Atl-Low and Blocking correspond to negative correlations.

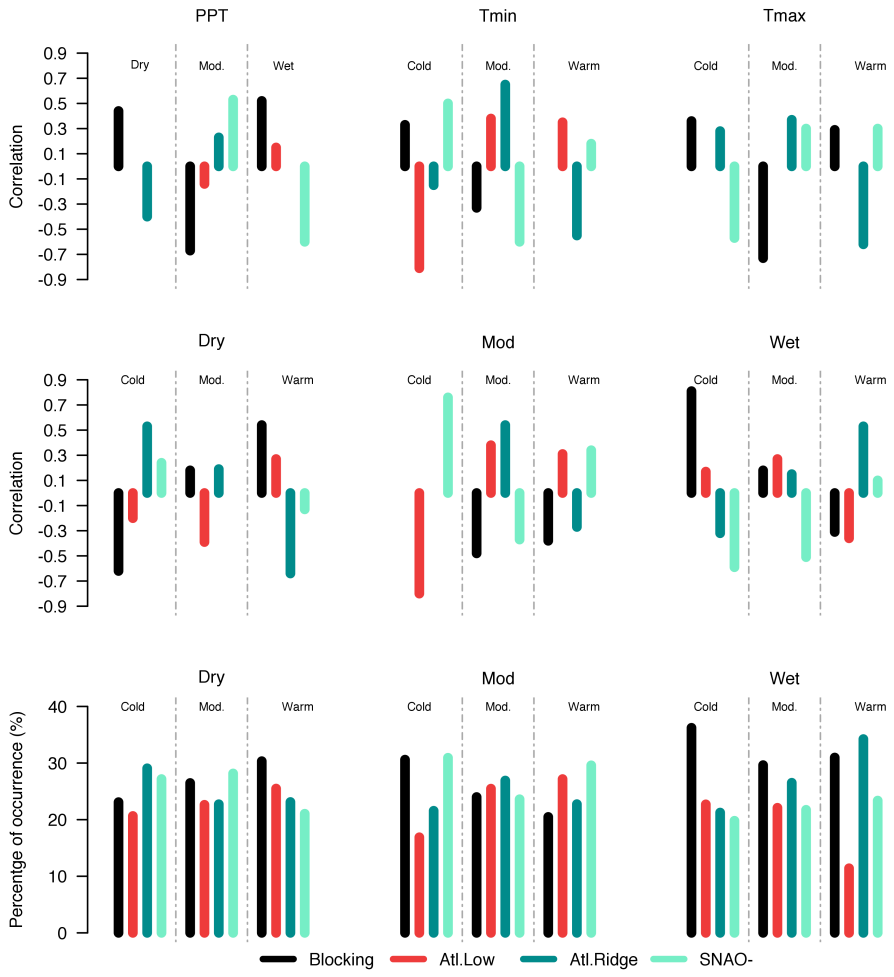

Figure 7: Correlation coefficients between Pyrenees composites and WR and mean percentage of occurrence of WR for years of each composite built by combining criteria on PPT and Tmin. Top panel corresponds to correlation for composites built by criteria applied on individual variables PPT, Tmin and Tmax. Middle panel corresponds to correlations for composites built by combining criteria in PPT and Tmin. Only significant correlation at $\alpha = 0.001$ *are shown.*

4.2 Tree-rings signal and Pyrenees climate

The relation between tree-ring signals captured by the PCA applied in different combination of TRW chronologies and periods and the observed climate in the Pyrenees is analysed by: checking their temporal correlation (between PC1 and PC2 and PPT, Tmin and Tmax) and comparing their spatial composites.

Considering their temporal evolution, correlations between PCs and Tmax are non-significant, except for PC1 when 31 trees in the period 1930 – 1993 are and PC2 when 12 trees in the period 1910 – 1993 are considered (Figure 8). The case which shows the highest number of significant correlations ($\alpha = 0.05$) is 31 trees in the period 1930 – 1993. In this case, PC1 and PC2 correlate positively with PPT and present opposite sign with Tmin. However, the highest correlation (0.45) is found for PPT compared with PC1 for 31 chronologies in the period 1910 – 1993. It is interesting to highlight that the case of 12 selected chronologies in the period 1800 – 1993 returns negative significant correlations for both PCs with PPT.

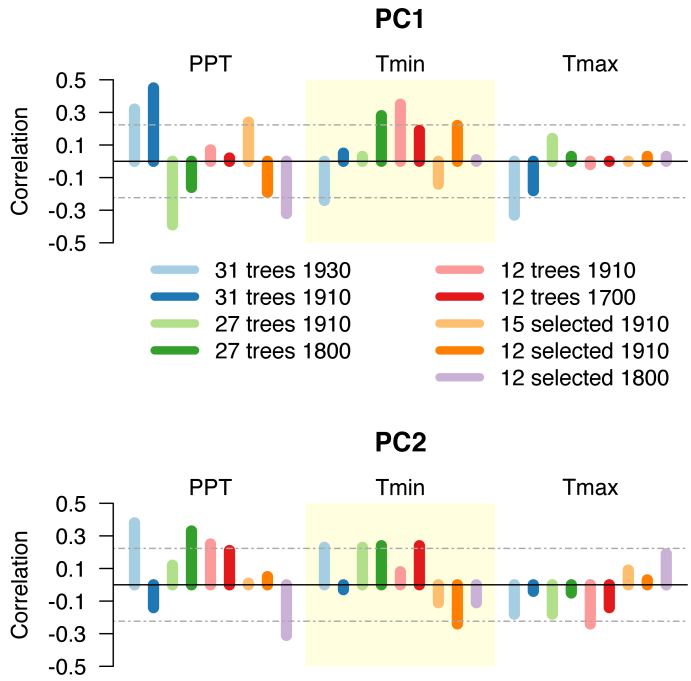

Figure 8: Correlation between Pyrenees regional series of PPT, Tmin and Tmax 5 years quadratic order Sav-gol filtered and PC1 and PC2 for all considered combinations of number of trees and periods to compute PCA in TRW simulations. Horizontal dashed lines indicate the correlation threshold for significance at $\alpha = 0.05$.

Correlations between Pyrenees composites built by applying criteria on individual variables of PPT, Tmin and Tmax and composites of PC1 and PC2 PCA applied on different combinations of TRW chronologies and periods are presented in Figure 9. In general, dry and Tmax warm years composites are negatively correlated with tree-rings

composites, while positive correlations are found for moderate climate and Tmax cold years composites. High PCs values composites correlate strongly in more cases than moderate and low PCs values composites: the highest correlation values (≥ 0.86) is found for moderate Tmin years composite (PC1 of 12 selected trees, PC1 of 12 selected trees and PC2 of 27 trees in the period 1910 – 1993) and the lowest correlation values (≤ -0.75) is found for warm Tmax years composite (PC1 of 31 trees, PC1 of 12 selected trees and PC2 of 27 trees in the period 1910 – 1993).

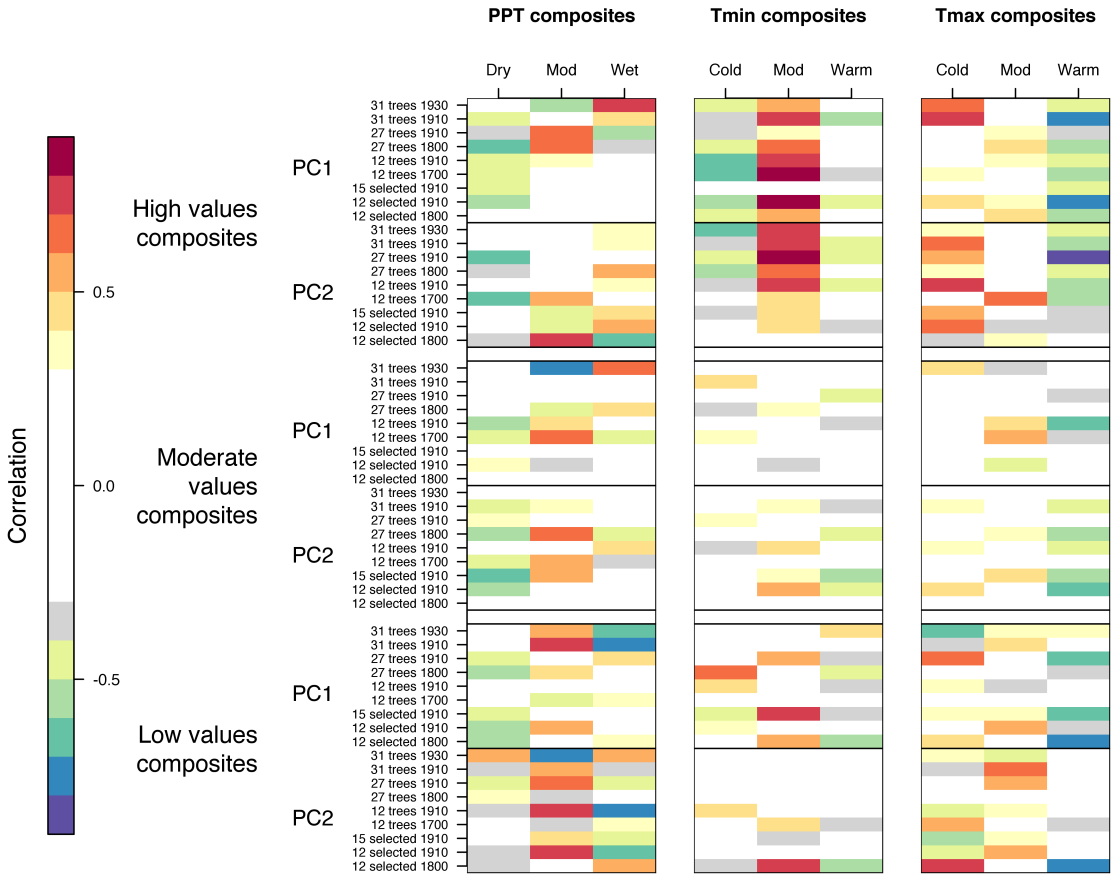

Figure 9: Correlation between composites of PC1 and PC2 of TRW for all considered cases and Pyrenees composites built by applying criteria in individual variables. Coloured values are greater than ± 0.3 (in absolute value) and significant at $\alpha = 0.001$

An equivalent correlation analysis is performed between tree-ring signals composites and Pyrenees composites built by combining criteria on PPT and Tmin (Figure 10). In this case, high values of PCs composites generally correlate negatively with moderate PPT and cold years, and dry and warm years, while positive correlations happen with moderate PPT and Tmin years composites. In the other hand, low values of PCs

composites are negatively correlated to wet and cold and dry and warm years composites. The highest correlations (≥ 0.84) are found between moderate PPT and Tmin years and high PC values composites (PC1 of 27 trees, 12 trees and 12 selected trees) while the lowest (≤ -0.78) between wet and cold years and low PC values (PC1 of 31 trees and PC2 of 12 selected trees in the period 1910 – 1993).

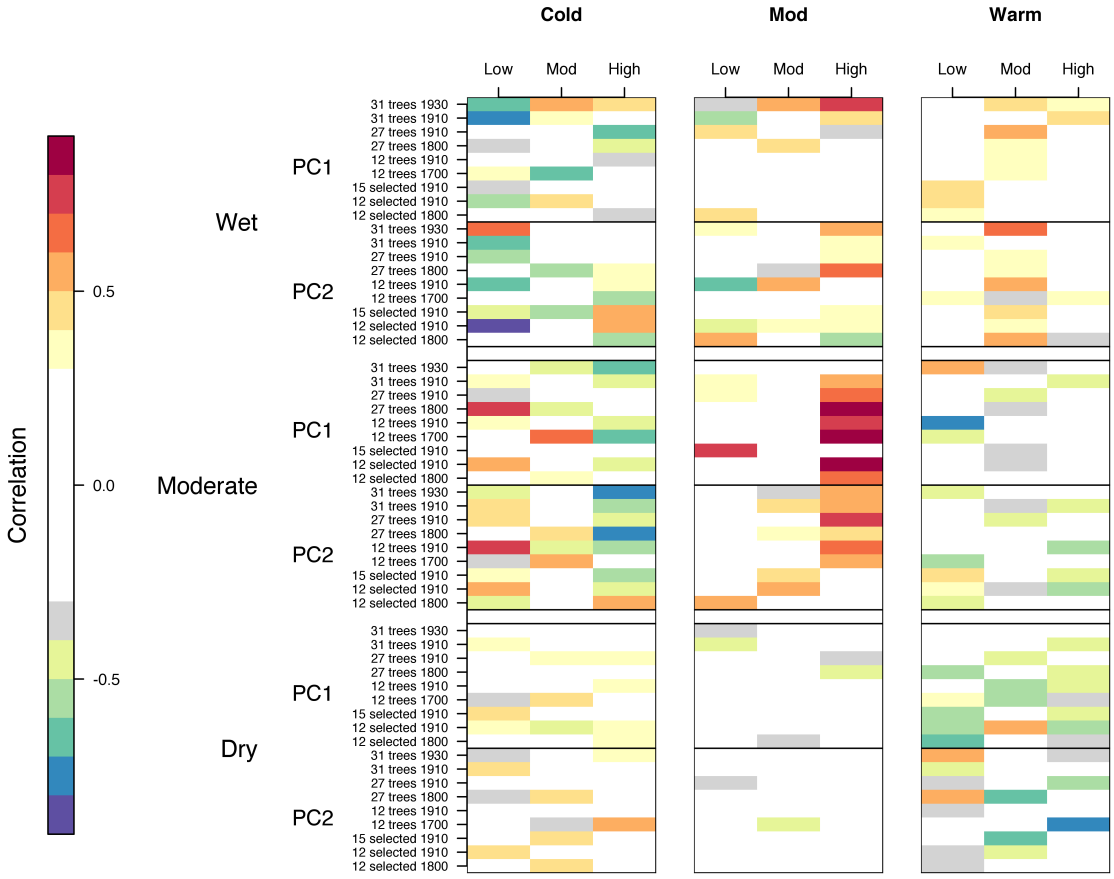

Figure 10: Correlation between composites of PC1 and PC2 of TRW for all considered cases and Pyrenees composites built by combining criteria in PPT (vertical order) and Tmin (horizontal order). Coloured values are greater than ± 0.3 (in absolute value) and significant at $\alpha = 0.001$.

4.3 Tree-rings signal and WR

Spatial correlations between WR and tree-rings signal from PCA over different periods and chronologies have been computed. Generally, high values PCs composites negatively correlate with Blocking and SNAO- and positively with Atl.Ridge and Atl.Low. A different behaviour is found for low values PCs composites which present negative correlation with Blocking and SNAO-. Instead, moderate values composites do not show a clear correlation pattern. The maximum correlation is found between SNAO- and PC2 of 12 selected trees in the period 1910 – 1993. At the other end, correlations lower than -0.74 are obtained between SNAO- and high values of PCs composites (for PC1 of 31 trees in the period 1930 – 1993 and PC2 of 31 and 12 trees, 15 and 12 selected trees in the period 1910 – 1993).

In order to interpret the correlation values, the mean percentage of occurrence of each WR for each PC threshold is computed. In general, a high mean percentage of occurrence returns positive correlation while low mean percentage gives place to negative correlations. However, it also depends on the distribution of the percentage of occurrence, such as low values of PC1 for 31 tree-ring chronologies during the instrumental period 1930 – 1993, which shows an equal distribution of mean percentage returning positive correlation to SNAO- and negative to Blocking while Atl.Low and Atl.Ridge are low correlated.

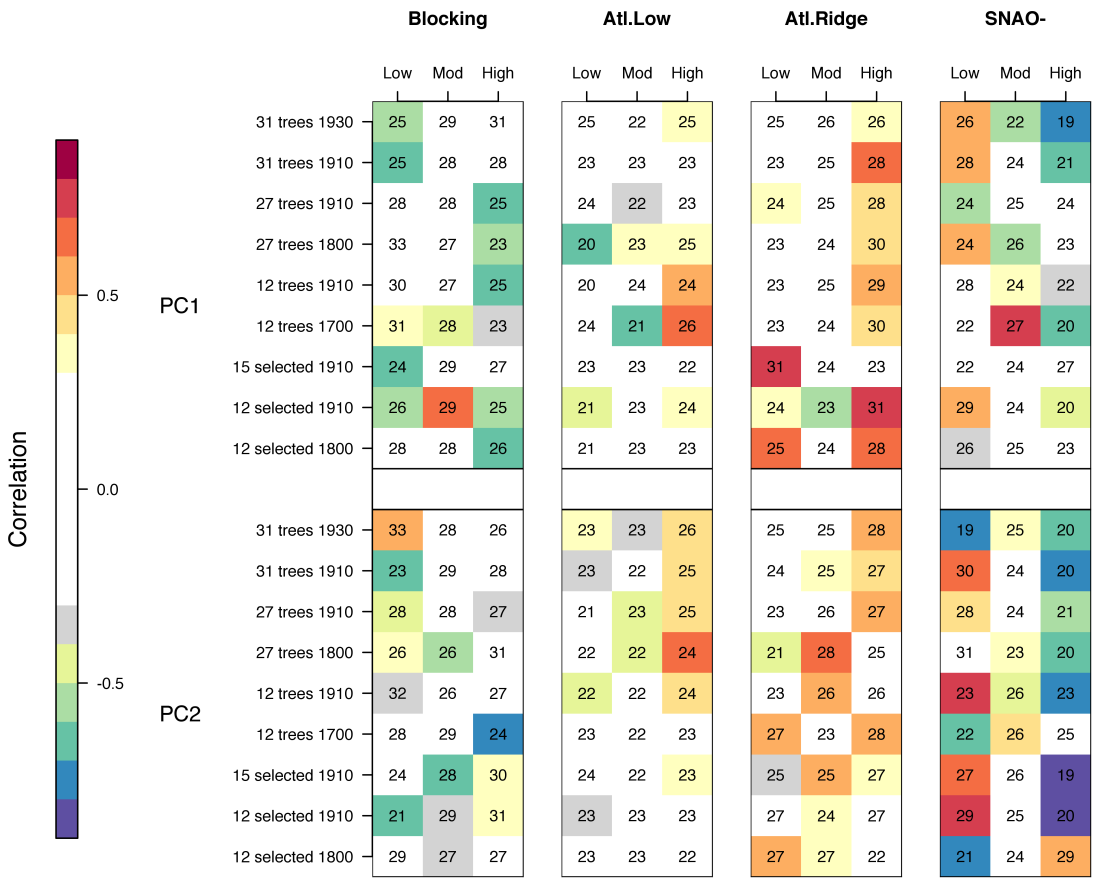

Figure 11: Correlations (colour) between WR and tree-ring signals composites and mean percentage of occurrence (numeric) of each WR. Coloured values are greater than ± 0.3 (in absolute value) and significant at $\alpha = 0.001$

5. Discussion

5.1 Role of WR on Pyrenees observed climate

Complexity of Pyrenees climate is clear through the analysis performed with WR frequency evolution and spatial patterns. Pyrenees latitudinal position, not north enough to make north Atlantic circulation determinant in all climate states, the proximity of the Mediterranean Sea, which works modifying the moisture input and softening temperature expected by the north Atlantic circulation, its east-west extension parallel to the westerly flow, and its orographic complexity are the major factors to this complexity. However, a part of the Pyrenees observed climate is driven by the WR.

Frequency evolution of Blocking is positively correlated with PPT but the correlation values are not too big. On the other hand, composites of PPT are positively correlated with Blocking for dry years composite and negative to SNAO-, the negative (but not symmetrical) face, for wet years composite. So, extreme PPT in the central Pyrenees is driven by SNAO, while moderate PPT is affected by other atmospheric processes of lower scales.

Moreover, Tmin is negatively (positively) correlated to Blocking (Atl.Low) frequency and less strongly (but significantly) negatively to Atl.Ridge. Comparing their time evolution (Figure 12), Tmin shows linkage of different WR over time. The oldest Tmin minimum coincides with a SNAO- minimum and Blocking maximum, the latter Tmin trend follows Atl.Low until 1921, when Tmin follows Atl.Ridge. Between 1934 and 1941 Atl.Low and fluctuations are comparable. Meanwhile, SNAO- variability is opposite to Tmin evolution (1923 – 1941), changing during the next and a half decade. A simultaneous minimum occurs in 1957 in Tmin and Atl.Low, after which a decreasing trend is similar in both signals. From 1973, when a new Tmin occurs, until 1994, Blocking variability strongly coincides with Tmin fluctuations. The maximum of Atl.Low in 2003, and the following years behaviour, is well captured by Tmin.

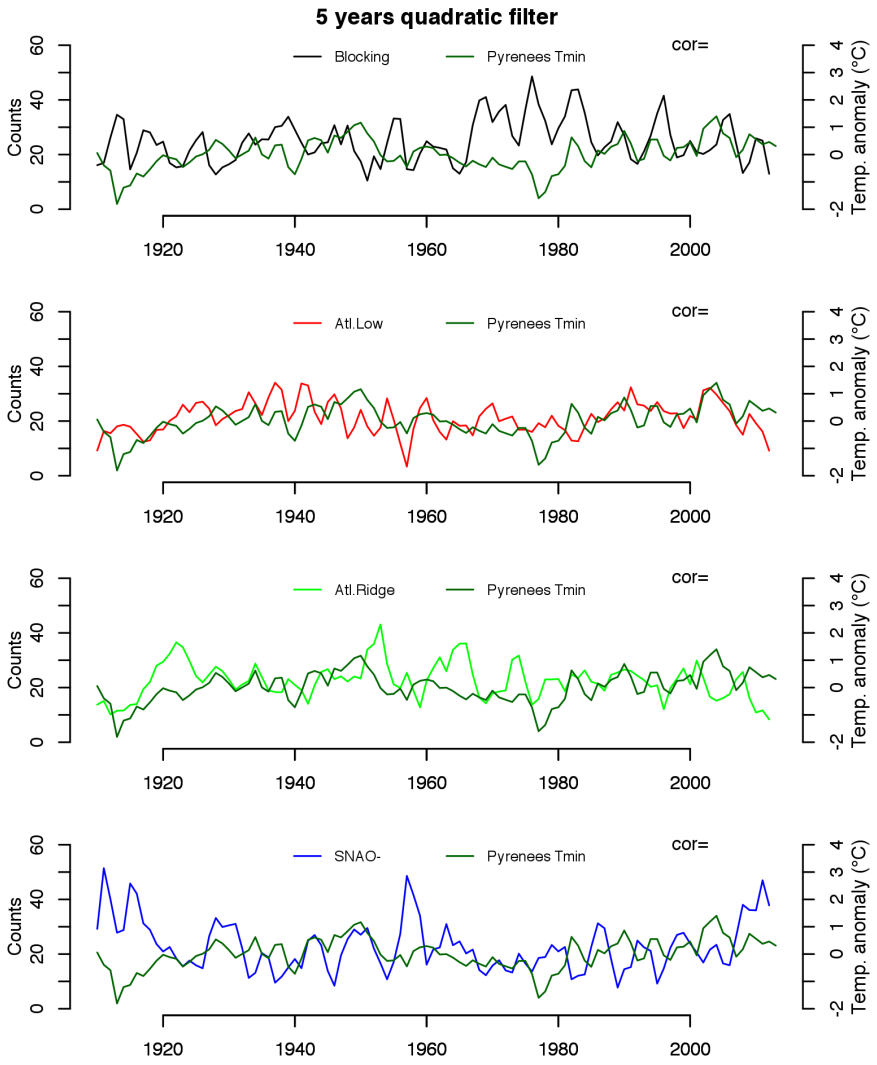

Figure 12: Evolution of Tmin (darkgreen) and each WR 5 years quadratic Sav-gol filtered.

Composites of Tmin show a different face of this behaviour. Cold years composite is negatively correlated to Atl.Low and positive to SNAO-, while warm years composite negatively correlates to Atl.Ridge. Furthermore, moderate Tmin years composite is positively correlated to Atl.Ridge and negatively to SNAO-. Either way, Tmin behaviour is conducted by multiple WR.

Finally, Tmax is not clearly linked to WR, although it is interesting to highlight that Blocking is negatively correlated to moderate Tmax years composites. So, not extreme Tmax years are in negative phase of SNAO, what, given the latitude of the Pyrenees, is in concordance of usual summer temperature.

The combined PPT and Tmin criteria composites allows to obtain a more specific climate catalogue for the central Pyrenees. Persistent Blocking pattern induces wet and cold summers in the Pyrenees, supported by the positive correlation (0.82) between them and the negative correlation (-0.59) between this composite and SNAO- (Figure 13). This reduction in the correlation value is due to the difference of the high pressure center position between Blocking and SNAO- low pressure, being further south in the second case.

Dry and cold composite is characterized by a low pressure centered in northern British Islands and a high pressure in Iceland. The lower extension is shorter than the high pressure in Blocking, however, it is in the same position, which induce a negative correlation between them of -0.62. The positive correlation with Atl.Ridge is more related to the high pressure in the Atlantic ocean, although the position of the two centers of action in Atl.Ridge are displaced respect to those observed in the composite. Nevertheless, Atl.Ridge mean percentage of occurrence is the highest in the years of this composite.

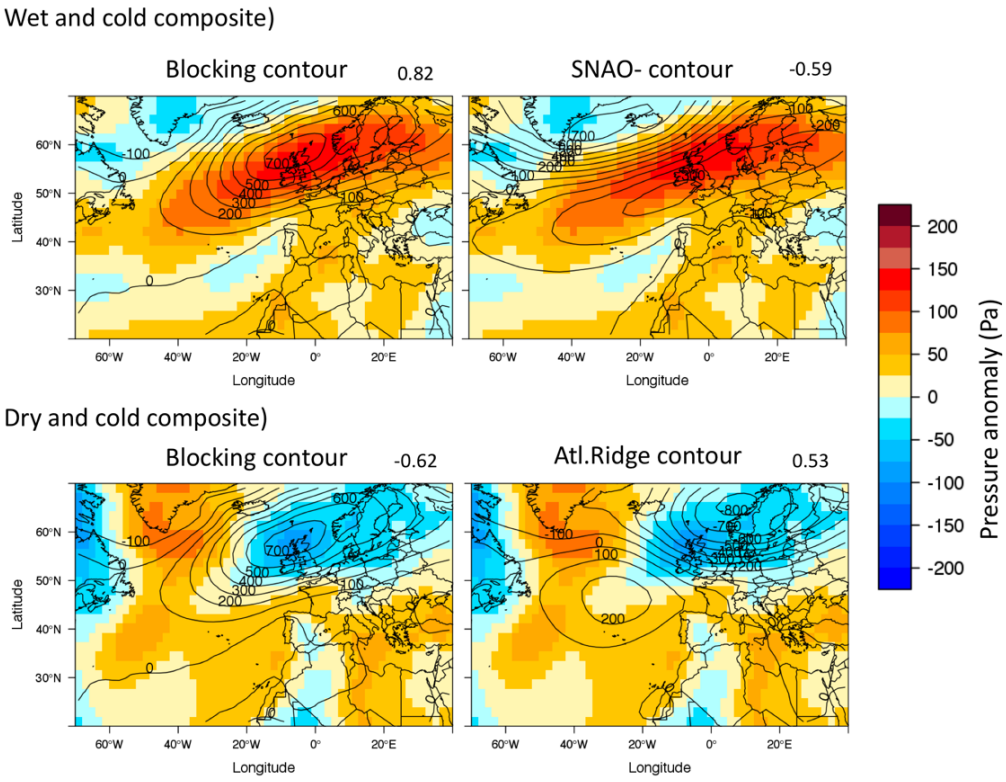

Figure 13: Composite of wet and cold years (top) and dry and cold years (bottom) in colour maps and WR with highest (lowest) correlation values as contour maps. Correlation value is shown in the right-top of each map.

Wet and warm years composite maximum correlation is found for Atl.Ridge (Figure 14), for which the mean percentage of occurrence in these years is also maximized. However, a clear intense dipole arises on this composite such in the Atl.Ridge, the two centers of pressure are displaced: the high pressure is further north in the composite forcing the low pressure center to be further east and giving rise to another high pressure center in east Europe.

For its part, dry and warm composite shows less intense pressure values and correlation sign opposite to dry and cold composite with Blocking and Atl.Ridge. Years of this composite are characterized by a high mean percentage of occurrence of Blocking pattern. The composite shows a high pressure centered over the North Sea, with a smaller extension smaller extension than Blocking high pressure and a low pressure center in the North Atlantic.

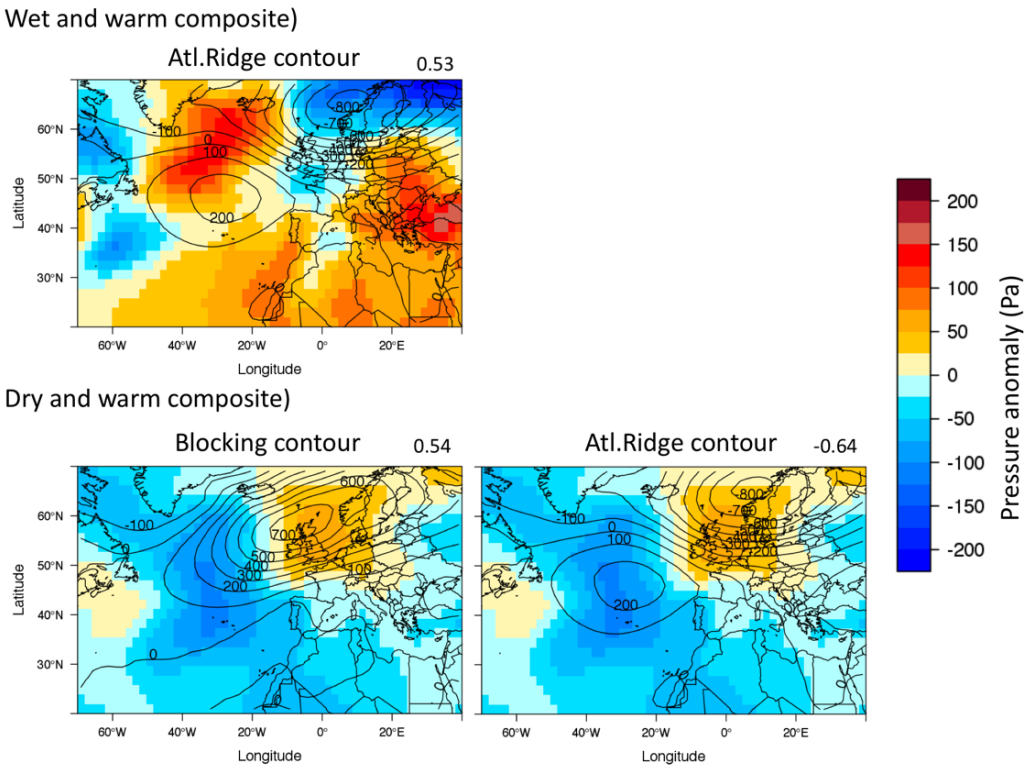

Figure 14: Composites of wet and warm years (top) and dry and warm years (bottom) in colour maps and WR with highest (lowest) correlation values as contour maps. Correlation value is shown in the right-top of each map.

A high intense pressure center in the north Atlantic characterizes the moderate and cold composite, which is in the same position as the low pressure center in the Atl.Low, returning a high negative correlation value. Two low pressure centers, one in the southwestern North Atlantic and another in eastern Europe, give the positive correlation with SNAO-. This composite, in fact, corresponds to an Omega blocking pattern, bringing cold air from the polar region to the Pyrenees.

Finally, the last composite with correlation absolute value higher than 0.51 with one WR is the PPT and Tmin moderate years. In this case, a latitudinal dipole of high pressure in the southwestern North Atlantic and a high pressure extended from Iceland to eastearn Europe releases. The high mean percentage of occurrence of Atl.Low and the low mean percentage of SNAO and Blocking during moderate PPT and Tmin years give rise to this SLP configuration.

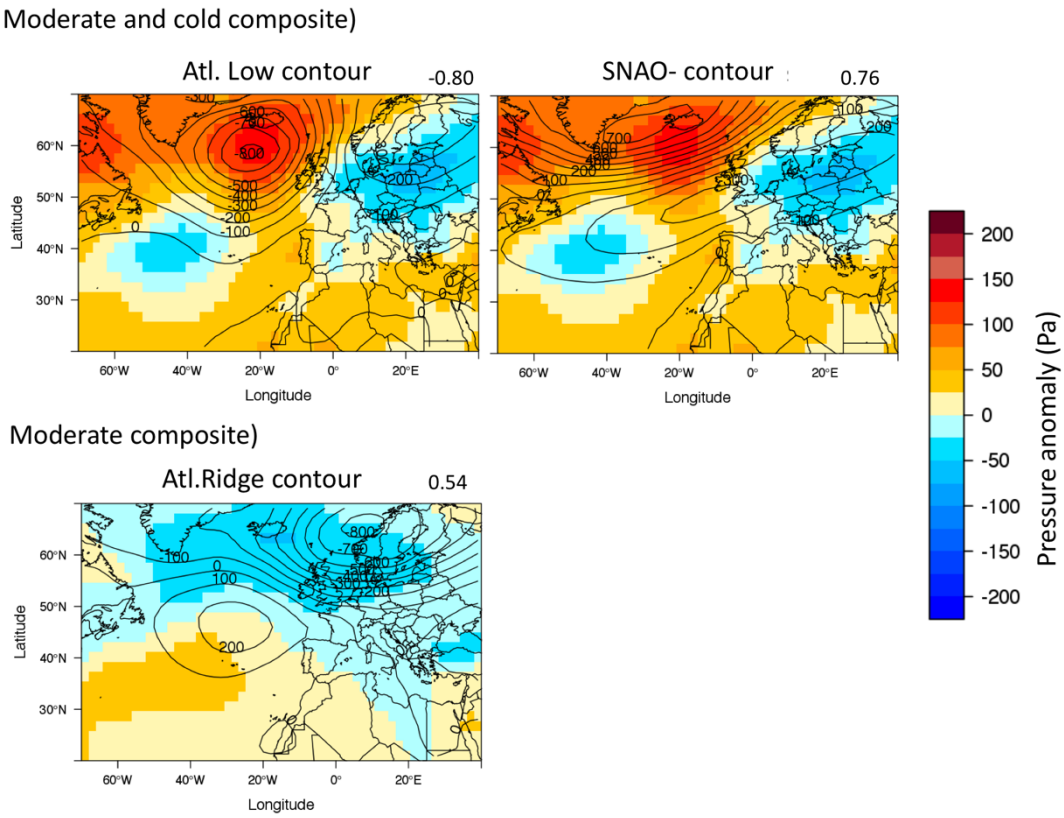

Figure 15: Composites of PPT moderate and cold years (top) and PPT and Tmin moderate years (bottom) in colour maps and WR with highest (lowest) correlation values as contour maps. Correlation value is shown in the right-top of each map.

5.2 Relation between Observed Climate and Tree-ring Signals

The capability of tree-rings signals to capture some states of observed climate in the Pyrenees have been shown in section 4.2. However, only observed climate which is directly influenced by WR can be captured by tree-ring signals. Furthermore, in order to reconstruct past climate, we focus on the longest periods covered by PCA. The highest correlations found for long covering periods are the cases of 12 trees with PCA analysis covering the period 1700 – 1993 and 12 selected trees with PCA analysis covering the period 1800 – 1993.

As we have seen, moderate values of PPT and Tmin composite is correlated with Atl.Ridge and it is captured by high values of PC1 tree-rings signals which are simultaneously correlated to Atl.Ridge. The meaning of the first mode of variability (PC1) could be understood as which captures the normal Pyrenees climate in which one trees grows. The correlation with Atl.Ridge is due to the northern low pressure in Scandinavia, which allow a high pressure in the northwest of Africa, which is not as well captured by this WR (Figure 16). This composite of high PC1 values for 12 selected trees covering the period 1800 – 1993 are also negatively correlated to Blocking pattern, which indicates that during moderate climatic years in the Pyrenees and high PC1 values Blocking pattern is not frequent. In the other hand, low values of this PC1 are also correlated to Atl.Ridge, but not too many cases support this relation, especially when the instrumental period is analysed.

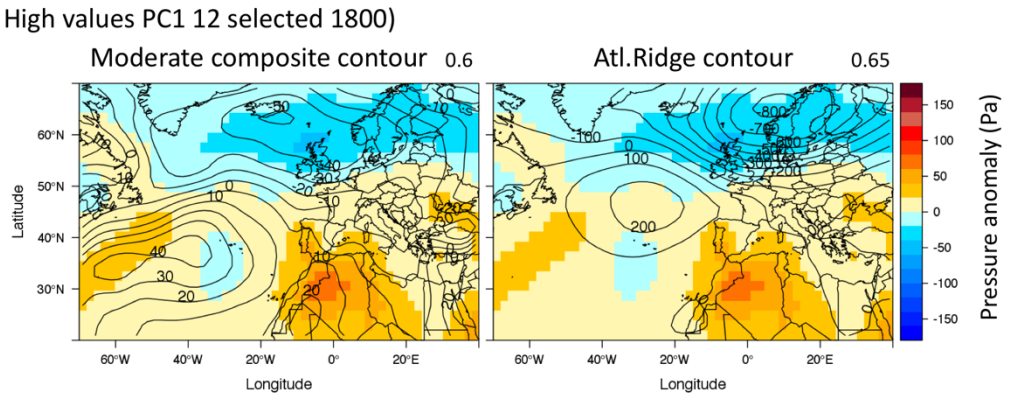

Figure 16: High values PC1 composite from 12 selected trees during the period 1800 – 1993 (colour maps) compared to moderate PPT and Tmin composite (left) and Atl.Ridge (right) contour maps. Correlation values are shown in the top-right of each map.

Moderate PPT and cold years composite is positive correlated to SNAO- as it is shown in the previous section. By its part, moderate values of PC1 for the 12 trees which cover the period 1700 – 1993 are highly correlated to this composite and the same WR (Figure 17). Differences in the position and extension of the low pressure in the north of Europe can be noted, being more extended north to south than the ones in SNAO-. Respect to the moderate PPT and cold composite the emergence of a low pressure in the southwestern region is missed on the composite from PC1 moderate values for this case. This composite is negatively correlated to Atl.Low (Figure 11) as it also occurs with the

moderate PPT and cold composite due to the low percentage of occurrence in those years.

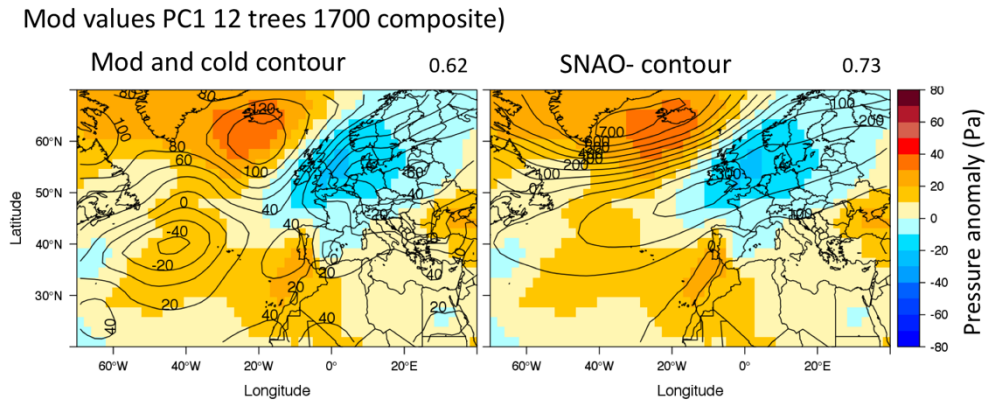

Figure 17: Moderate values PC1 composite from 12 trees during the period 1700 – 1993 (colour maps) compared to moderate PPT and cold composite (left) and SNAO- (right) contour maps. Correlation values are shown in the top-right of each map.

Dry and cold composite correlates to PC2 high values for 12 trees covering the period 1700 – 1993, which, at the same time, correlates to Atl.Ridge (Figure 18). In this case, the low and high pressure captured by PC2 high values are more southern than the ones in Atl.Ridge, allowing low pressure extension through the Mediterranean until north Africa. Also some differences are noted with dry and cold composite, which affects the moisture input in the Pyrenees emerging a moderate wet pattern in high PC2 values composite (Figure 19). Furthermore, this composite of PC2 high values is negatively correlated to dry and warm years composite and Blocking, consistently to Figure 14 for dry and warm composite. This fact can be understood by the capability of TRW signal to capture wet situations in which the growth of trees may be favoured.

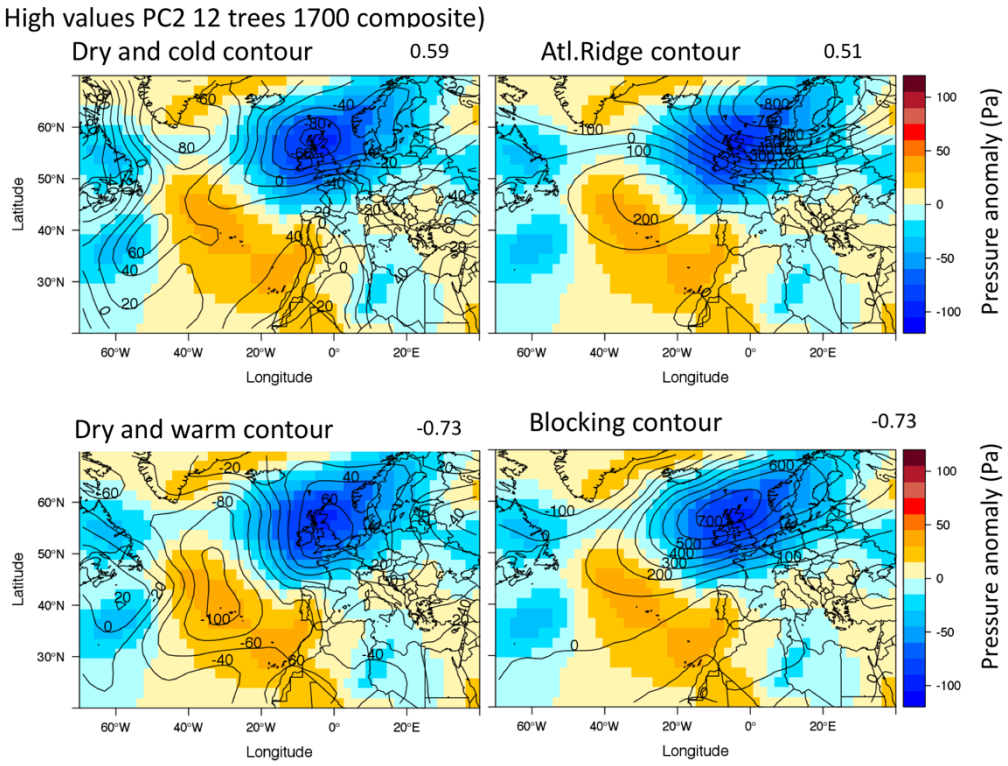

Figure 18: High values PC2 composite from 12 trees during the period 1700 – 1993 (colour maps) compared to dry and cold composite (left) and Atl.Ridge (right) contour maps (top) and to dry and warm composite (left) and Blocking (right) contour maps (bottom). Correlation values are shown in the top-right of each map.

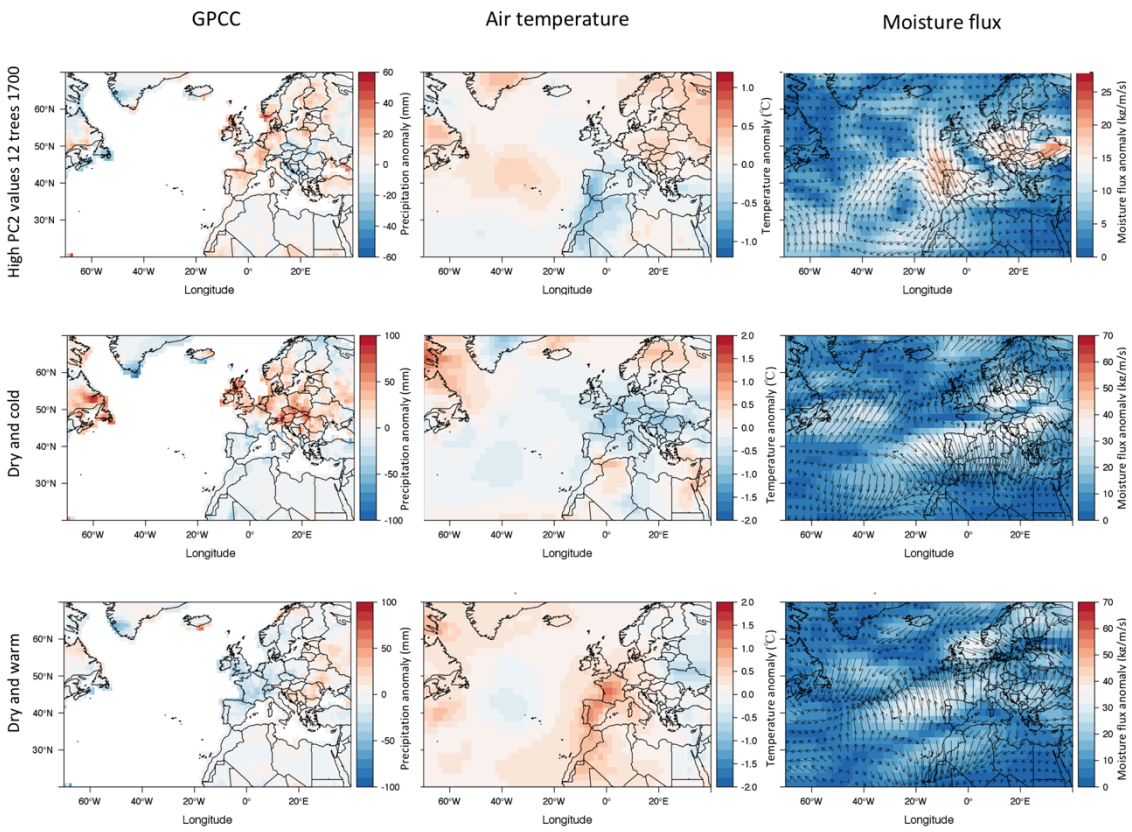

Figure 19: Composites of high values PC2 for GPCC, AIRT and UQ (top) and dry and cold composite for the same variables (middle) and dry and warm composite (bottom).

Wet and moderate Tmin composite has not been discussed in section 5.1 due to its correlation value with WR is not too large, being the maximum found for Atl.Low and negative correlated to SNAO-. However, some PCs of high values show positive correlation with this composite. The highest correlation for long period covered PCA is with PC2 high values for 27 trees covering the period 1800 – 1993 (Figure 20). This shape is opposite to moderate PPT and cold years composite (Figure 15), being its correlation with PC2 high values composite of -0.73. In this case, the Atl.Low is capturing fairly good the position of the low pressure and the high pressure over northern Europe, while the high pressure over Azores islands is missed.

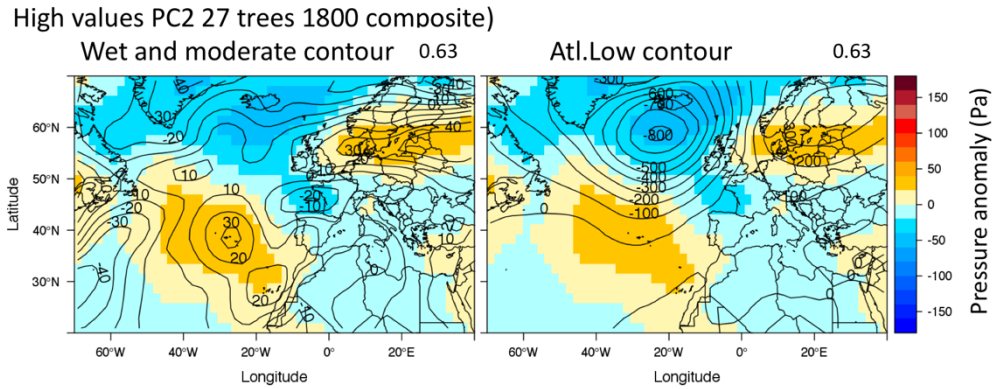

Figure 20: High values PC2 composite from 27 trees during the period 1800 – 1993 (colour maps) compared to wet and moderate Tmin composite (left) and Atl.Low (right) contour maps. Correlation values are shown in the top-right of each map.

6. Conclusions

The regional anomaly series defined in the central Pyrenees have been allowed to obtain the synoptic configurations which emerge on years of extreme and normal climate in the central Pyrenees by using composites.

Different behaviours have been identified: while Atl.Low seems to influence Tmin during all modes considered and a combination of Blocking and Atl.Low lead PPT, Tmax is leaded by different WR. However, the frequency of occurrence of WR seems to be related to the spatial correlation between composites and WR.

The age model error applied on tree-ring chronologies allows to achieve a common signal from tree-rings width in the central Pyrenees by applying a PCA, showing a dependence on the number of considered chronologies compared with the Pyrenees regional series. The differences in the spatial coverage between the regional anomaly series and the chronologies sites can be an explanation of, even being significant, not being high correlation values.

Composites from PC signals have also been correlated with regional anomaly composites obtained by appliying individual or combined criteria in PPT and Tmin giving the chance of interpreting the limitation of tree-rings growth by different

combinations of climatic factors (only due to precipitation or temperature or PPT and Tmin acting simultaneously). Furthermore, a comparison between PC signals and WR have been preformed.

AKWOLEDGEMENTS

The authors would like to thank the NOAA/OAR/ESRL PSD, Boulder, Colorado, USA, for providing 20th Century Reanalysis V2 data, the GPCC Precipitation data and the HadSLP2 data from their Web site http://www.esrl.noaa.gov/psd/.

REFERENCES

Allan R, Ansell T, Allan R, Ansell T. 2006. A New Globally Complete Monthly Historical Gridded Mean Sea Level Pressure Dataset (HadSLP2): 1850–2004. *Journal of Climate* **19**(22): 5816–5842. DOI: 10.1175/JCLI3937.1.

Barry RG. 2008. *Mountain weather and climate*. Routledge: London (UK), 402 pp.

Beguería S, López-Moreno JI, Lorente A, Seeger M, García-Ruiz JM. 2003. Assessing the Effect of Climate Oscillations and Land-use Changes on Streamflow in the Central Spanish Pyrenees. *AMBIO: A Journal of the Human Environment* **32**(4): 283–286. DOI: 10.1579/0044-7447-32.4.283.

Beniston M. 2003. Climatic change in mountain regions: A review of possible impacts. *Climatic Change* **59**(1): 5–31. DOI: 10.1023/A:1024458411589.

Briffa KR, Osborn TJ, Schweingruber FH. 2004. Large-scale temperature inferences from tree rings: a review. *Global and Planetary Change* **40**(1): 11–26. DOI: 10.1016/S0921-8181(03)00095-X.

Büntgen U, Frank D, Grudd H, Esper J. 2008. Long-term summer temperature variations in the Pyrenees. *Climate Dynamics* **31**(6): 615–631. DOI: 10.1007/s00382-008-0390-x.

Cassou C, Terray L, Phillips AS. 2005. Tropical Atlantic Influence on European Heat Waves. *Journal of Climate* **18**(15): 2805–2811. DOI: 10.1175/JCLI3506.1.

Compo GP, Whitaker JS, Sardeshmukh PD, Matsui N, Allan RJ, Yin X, Gleason BE, Vose RS, Rutledge G, Bessemoulin P, Brönnimann S, Brunet M, Crouthamel RI, Grant AN, Groisman PY, Jones PD, Kruk MC, Kruger AC, Marshall GJ, Maugeri M, Mok HY, Nordli Ø, Ross TF, Trigo RM, Wang XL, Woodruff SD, Worley SJ. 2011. The Twentieth Century Reanalysis Project. *Quarterly Journal of the Royal Meteorological Society*. John Wiley & Sons, Ltd. **137**(654): 1–28. DOI: 10.1002/qj.776.

Cook ER, DArrigo RD, Briffa KR. 1998. A reconstruction of the North Atlantic Oscillation using tree-ring chronologies from North Americ and Europe. *The Holocene*. SAGE Publications **8**(1): 9–17. DOI: 10.1191/095968398677793725.

Cuadrat JM, Martín Vide J. 2007. *La climatología española: pasado, presente y futuro*. Prensas Universitarias de Zaragoza, 574 pp.

Dorado Liñán I, Büntgen U, González-Rouco F, Zorita E, Montávez JP, Gómez-Navarro JJ, Brunet M, Heinrich I, Helle G, Gutiérrez E. 2012. Estimating 750 years of temperature variations and uncertainties in the Pyrenees by tree-ring reconstructions and climate simulations. *Climate of the Past* **8**(3): 919–933. DOI: 10.5194/cp-8-919-2012.

Esper J, Schneider L, Smerdon JE, Schöne BR, Büntgen U. 2015. Signals and memory in tree-ring width and density data. *Dendrochronologia* **35**: 62–70. DOI: 10.1016/j.dendro.2015.07.001.

Folland CK, Knight J, Linderholm HW, Fereday D, Ineson S, Hurrell JW. 2009. The Summer North Atlantic Oscillation: Past, Present, and Future. *Journal of Climate* **22**(5): 1082–1103. DOI: 10.1175/2008JCLI2459.1.

Fritts HC, Blasing TJ, Hayden BP, Kutzbach JE, Fritts HC, Blasing TJ, Hayden BP, Kutzbach JE. 1971. Multivariate Techniques for Specifying Tree-Growth and Climate Relationships and for Reconstructing Anomalies in Paleoclimate. *Journal of Applied Meteorology* **10**(5): 845–864. DOI: 10.1175/1520-0450(1971)010<0845:MTFSTG>2.0.CO;2.

Giorgi F. 2006. Climate change hot-spots. *Geophysical Research Letters* **33**(8,L08707): 1–4. DOI: 10.1029/2006GL025734.

Gray ST, Graumlich LJ, Betancourt JL, Pederson GT. 2004. A tree-ring based reconstruction of the Atlantic Multidecadal Oscillation since 1567 A.D. *Geophysical Research Letters* **31**(12): 1–4. DOI: 10.1029/2004GL019932.

Hartigan JA, Wong MA. 1979. Algorithm AS 136: A K-Means Clustering Algorithm. *Applied Statistics* **28**(1): 100–108. DOI: 10.2307/2346830.

Huang B, Thorne PW, Smith TM, Liu W, Lawrimore J, Banzon VF, Zhang H-M, Peterson TC, Menne M, Huang B, Thorne PW, Smith TM, Liu W, Lawrimore J, Banzon VF, Zhang H-M, Peterson TC, Menne M. 2016. Further Exploring and Quantifying Uncertainties for Extended Reconstructed Sea Surface Temperature

(ERSST) Version 4 (v4). *Journal of Climate* **29**(9): 3119–3142. DOI: 10.1175/JCLI-D-15-0430.1.

Hurrell JW, Kushnir Y, Ottersen G, Visbeck M. 2003. An overview of the North Atlantic Oscillation. In: Hurrell JW, Kushnir Y, Ottersen G and Visbeck M (eds) *The North Atlantic Oscillation: Climatic Significance and Environmental Impact*. American Geophysical Union: Washington, D.C., 35. DOI: 10.1029/134GM01.

Lionello P. 2012. *The Climate of the Mediterranean Region: From the past to the future.* Elsevier Science.López-Moreno JI, Beniston M. 2008. Daily precipitation intensity projected for the 21st century: seasonal changes over the Pyrenees. *Theoretical and Applied Climatology* **95**(3): 375–384. DOI: 10.1007/s00704-008-0015-7.

López-Moreno JI, Goyette S, Beniston M. 2008. Climate change prediction over complex areas: spatial variability of uncertainties and prediction over the Pyrenees from a set of regional climate models. *International Journal of Climatology* **28**(11): 1535–1550. DOI: 10.1002/joc1645.

Marín-Yaseli ML, Martínez TL. 2003. Competing for Meadows. *Mountain Research and Development* **23**(2): 169–176. DOI: 10.1659/0276-4741(2003)023[0169:CFM]2.0.CO;2.

Melis MT, Locci F, Dessì F, Frigerio I, Strigaro D, Vuillermoz E. 2014. SHARE Geonetwork, a system for climate and paleoclimate data sharing. In: Ames DP, Quinn NWT and Rizzoli AE (eds) *7th Intl. Congress on Env. Modelling and Software*. San Diego, CA, USA, 8 pp.

Moreno A, Pérez A, Frigola J, Nieto-Moreno V, Rodrigo-Gámiz M, Martrat B, González-Sampériz P, Morellón M, Martín-Puertas C, Corella JP, Belmonte Á, Sancho C, Cacho I, Herrera G, Canals M, Grimalt JO, Jiménez-Espejo F, Martínez-Ruiz F, Vegas-Vilarrúbia T, Valero-Garcés BL. 2012. The Medieval Climate Anomaly in the Iberian Peninsula reconstructed from marine and lake records. *Quaternary Science Reviews* **43**: 16–32.

Ortega P, Lehner F, Swingedouw D, Masson-Delmotte V, Raible CC, Casado M, Yiou P. 2015. A model-tested North Atlantic Oscillation reconstruction for the past

millennium. *Nature*. Nature Publishing Group, a division of Macmillan Publishers Limited. All Rights Reserved. **523**(7558): 71–4. DOI: 10.1038/nature14518.

Pérez-Zanón N, Sigró J, Ashcroft L. 2017. Temperature and precipitation regional climate series over the central Pyrenees during 1910–2013. *International Journal of Climatology* **37**(4): 1922–1937. DOI: 10.1002/joc.4823.

Press WH. 2007. *Numerical recipes: the art of scientific computing*. Cambridge University Press, 1235 pp.

Regato P. 2015. *Southwest Europe: In the Pyrenees Mountains of Spain, France, and Andorra*. *World Wildlife Fund [accessed 11 January 2017]*.

Schneider U, Becker A, Finger P, Meyer-Christoffer A, Ziese M, Rudolf B. 2014. GPCC's new land surface precipitation climatology based on quality-controlled in situ data and its role in quantifying the global water cycle. *Theoretical and Applied Climatology*. Springer Vienna **115**(1–2): 15–40. DOI: 10.1007/s00704-013-0860-x.

Stoffel M, Khodri M, Corona C, Guillet S, Poulain V, Bekki S, Guiot J, Luckman BH, Oppenheimer C, Lebas N, Beniston M, Masson-Delmotte V. 2015. Estimates of volcanic-induced cooling in the Northern Hemisphere over the past 1,500 years. *Nature Geoscience* **8**(10): 784–788. DOI: 10.1038/ngeo2526.

Tardif J, Camarero JJ, Ribas M, Gutiérrez E. 2003. Spatiotemporal variability in tree growth in the Central Pyrenees: Climatic and site influences. *Ecological Monographs* **73**(2): 241–257.

van der Linden P, Dempsey P, Dunn R, Caesar J, Kurnik B, Dankers R, Jol A, Kunz M, van Lanen H, Benestad R, Parry S, Hilden M, Marx A, Mysiak J, Kendon L. 2015. Extreme weather and climate in Europe. ETC/CCA.

Walker GT. 1924. Correlation in seasonal variations of the weather, IX. A further study of world weather. *Memoirs of the India Meteorological Department* **XXIV**(IV): 275–333.

Wassenburg J a., Immenhauser A, Richter DK, Niedermayr A, Riechelmann S, Fietzke J, Scholz D, Jochum KP, Fohlmeister J, Schröder-Ritzrau A, Sabaoui A, Riechelmann DFC, Schneider L, Esper J. 2013. Moroccan speleothem and tree ring records suggest a variable positive state of the North Atlantic Oscillation during the Medieval Warm Period. *Earth and Planetary Science Letters*. Elsevier **375**: 291–302. DOI: 10.1016/j.epsl.2013.05.048.

Wigley TML, Briffa KR, Jones PD, Wigley TML, Briffa KR, Jones PD. 1984. On the Average Value of Correlated Time Series, with Applications in Dendroclimatology and Hydrometeorology. *Journal of Climate and Applied Meteorology* **23**(2): 201–213. DOI: 10.1175/1520-0450(1984)023<0201:OTAVOC>2.0.CO;2.

Wilks DS. 2011. *Statistical methods in atmospheric science*. Academic Press: Ithaca, New York (USA), 613 pp.

Supplementary material "Role of North Atlantic weather regimesn in the central Pyrenees climate from instrumental and tree-ring data"

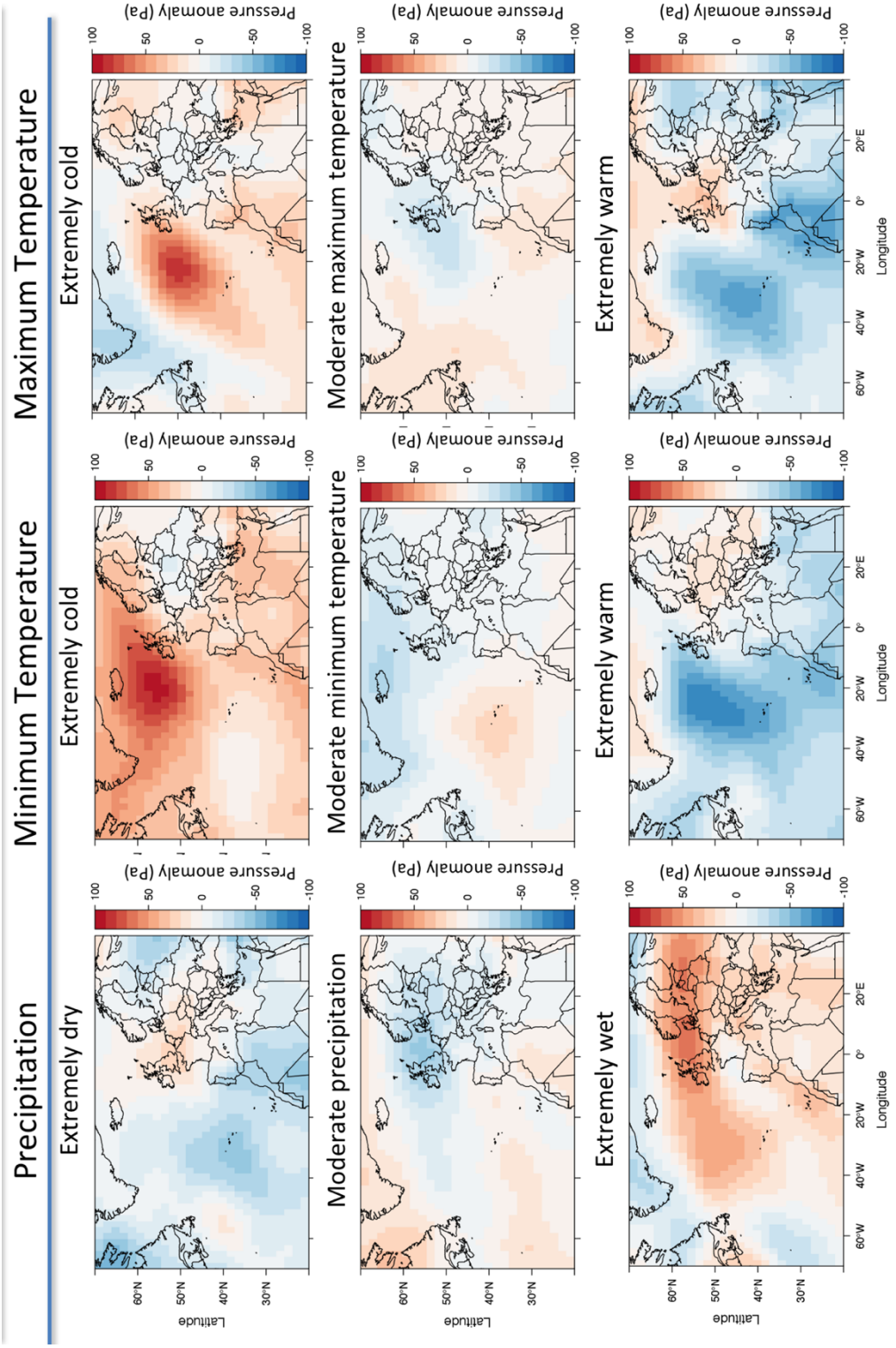

Figure S.1: SLP composites applying criteria over individual variables PPT, Tmin and Tmax.

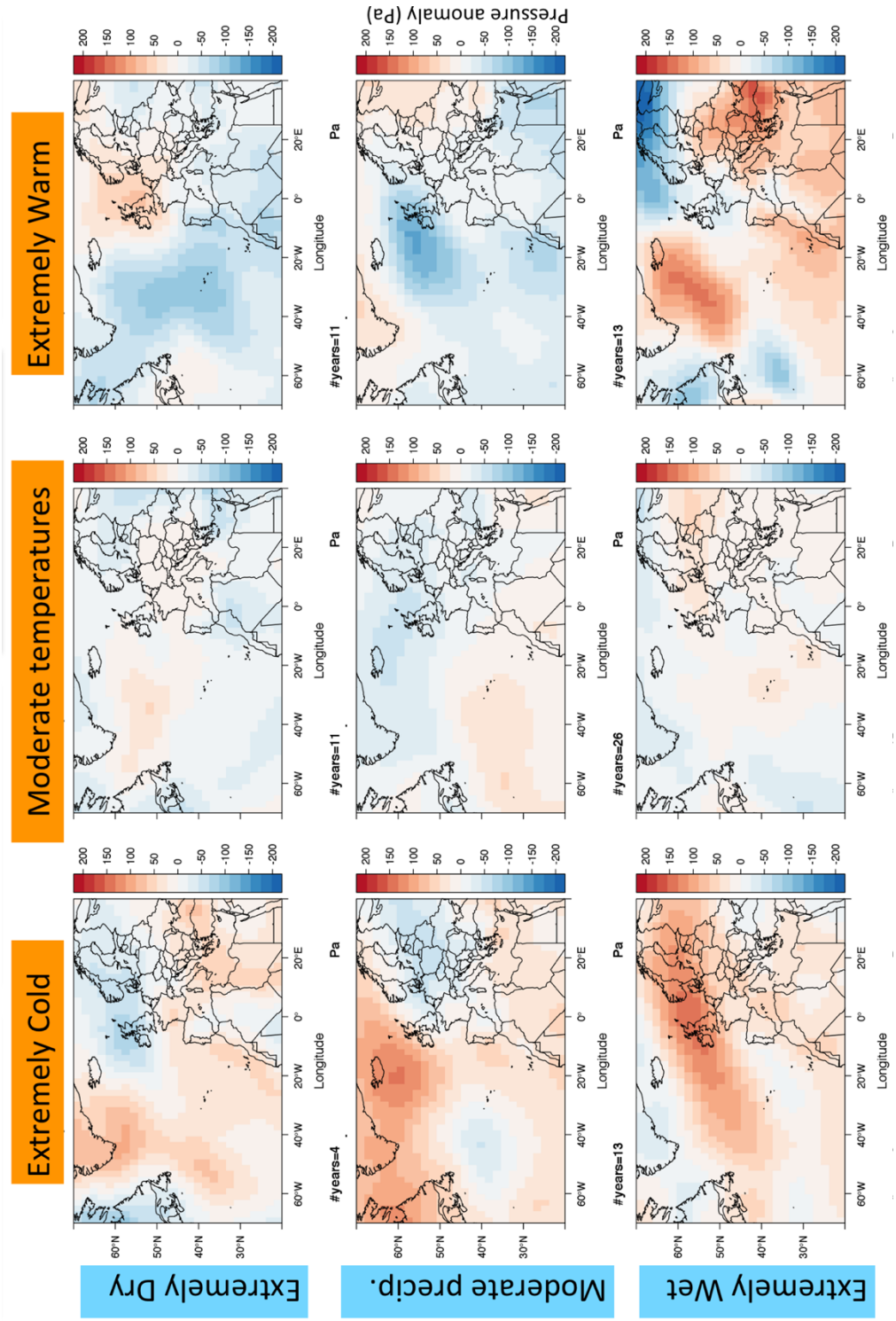

Figure S.2: SLP composites applying criteria over PPT and Tmin.

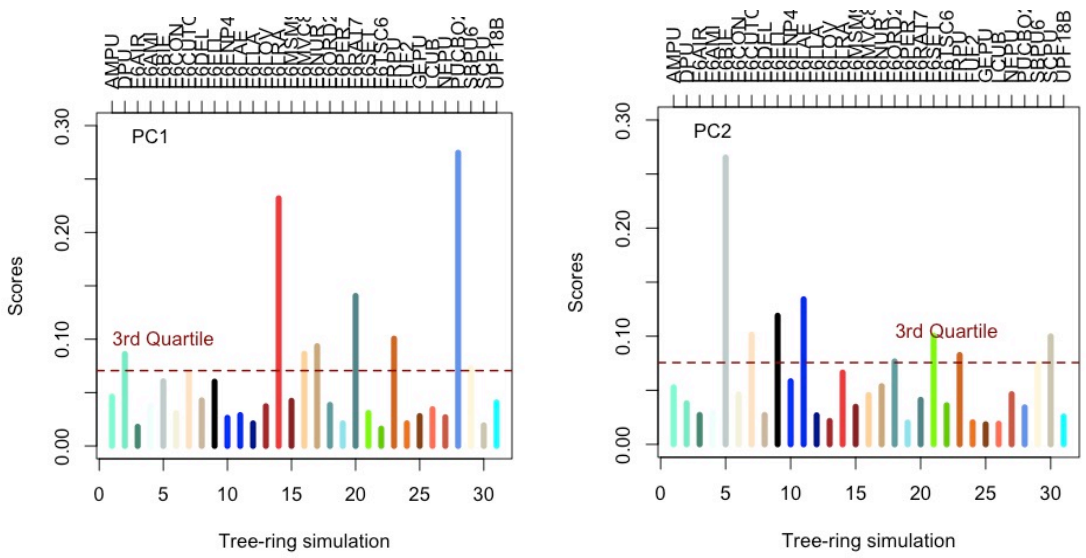

Figure S.3: Variance of scores in PC1 and PC2 overcome the third quartile.

Tables S.1: Description of TRW chronologies analysed: ID, location, number of trees and cores, starting and ending year and source of each chronology.

ID crono	Long	Lat	Height	Nº Trees	Nº Cores	Start Year	Last Year	Source
AMPU	42º 35’	0º 59’ E	2390	12	34	1725	2009	Galván et al, 2015
DPU50e	42º 31’	0º 45’ E	2199	41	86	1760	2006	Batllori & Gutierrez, 2008
E6AIR	42°42' N	1°02'E	2300	14	24	1780	1996	Galván et al, 2015
E6AMI	42º 36' N	0º 59' E	2333	12	25	1770	1995	Gutiérrez et al. 1998, Tardif et al, 2003
E6BIE	42º 43' 00" N	00º 11' 45" E	2100	11	21	1785	1996	Galván et al, 2015

E6CON	42º 38' N	00º 45' E	2106	17	32	1590	1994	Gutiérrez et al. 1998, Tardif et al, 2003
E6CUCT1	42º 37' 05" N	00º 11' 24" W	2150	23	42	1820	1998	Gutiérrez, E. Unpublished data
E6DEL	42º 34' N	0º 57' E	2208	19	42	1585	1995	Gutiérrez et al. 1998, Tardif et al, 2003
E6ELL	42º 33' N	1º 04' E	2076	10	20	1650	1996	Gutiérrez et al. 1998, Tardif et al, 2003
E6ENP4	42º 32' N	1º 03' E	2360	10	19	1785	1996	Gutiérrez et al. 1998, Tardif et al, 2003
E6LAE	42º 41' N	00º 06' E	1990	10	24	1735	1993	Gutiérrez et al. 1998, Tardif et al, 2003
E6LRA	42°57' N	0°46'W	1750	16	31	1755	1999	Gutiérrez et al. 1998, Tardif et al, 2003
E6LLA	42º 32' N	0º 55' E	2250	31	59	1415	1997	Gutiérrez et al. 1998, Tardif et al, 2003
E6LOv	42°34' N	0°57'E	2323	7	10	1721	2011	Galván et al,

E6MSM9	42º 55' N	1º 00' E	2193	8	14	1750	1995	2015 Gutiérrez et al. 1998, Tardif et al, 2003
E6MVC8	42º 38' N	01º 04' E	2017	9	24	1745	1997	Gutiérrez et al. 1998, Tardif et al, 2003
E6NUR	42°23' N	2°08'E	2075	20	37	1790	2001	Gutiérrez, E. Unpublished data
E6ORD2	42º 38' 31" N	00º 03' 29" W	1935	13	24	1685	1998	Camarero et al, 1998
E6PER	42°27' N	1°37'E	2350	20	39	1755	1997	Camarero et al, 1998
E6RAT7	42º 35' 24" N	1º 00' 00" E	2300	10	20	1800	1999	Gutiérrez et al. 1998, Tardif et al, 2003
E6SET	42°24' N	2°17'E	2080	11	19	1845	1999	Gutiérrez, E. Unpublished data
E6TSC6	42º 36' 33" N	1º 03' 00" E	2310	22	34	1765	1995	Gutiérrez et al. 1998, Tardif et al, 2003
FRPU	42º 37’	0º 06’ E	2031	9	26	1490	2009	Camarero et al, 1998
FUF2	42º 33’	1º 23’ E	2352	17	33	1910	2003	Gutiérrez,

								E. Unpublished data
GEPUt	42°36' N	0°59'E	2268	28	64	1505	2009	Galván et al, 2015
LCUBe	42º 31’	1º 21’ E	2363	22	39	1680	2003	Gutiérrez, E. Unpublished data
NEPUt	42º 33’	1º 02’ E	2451	34	57	1525	2009	Galván et al, 2015
PUCBO2	42º14'03.6"N	1°07'14.3"E	1915	16	26	1890	2013	Gutiérrez, E. Unpublished data
SBPU6	42°41' N	0°05'E	2296	36	72	1545	2009	Gutiérrez, E. Unpublished data
SCPU	42°38' N	0°04'W	2247	24	48	1580	2009	Gutiérrez, E. Unpublished data
UPF18B	42°14' N	1°42'E	2100	36	85	1475	2006	Dorado-Liñán et al, 2012

Chapter 6 – Discussion and conclusions

The aim of this chapter is to summarize main findings presented in each chapter and provide a global view of the scientific contribution that they provide, as well as clearly demonstrating how the main aims of this thesis have been achieved. Finally, the new horizon of questions and future work that this study has raised are explored.

6.1. General Discussion

In this section, a summary of the results discussed in each chapter is presented, followed by a global overview of them.

6.1.1. Summary

- Chapter 2 – Comparison of homogenization methods

The comparison of the advanced homogenization methods, ACMANT and HOMER,

applied over the observed temperature data in observatories of the central Pyrenees has enabled the recognition of the available data in the Pyrenees, the difference between the homogenization methods and find errors on the data.

Even though both are, two modern, partly similar, multiple break point homogenization methods, HOMER and ACMANT have distinct strengths and weaknesses, showing different results in some characteristics (Table 1).

Table 1: Advantages of each homogenization method.

		ACMANT	**HOMER**
Number of breaks	More breaks detected	✔	
	More breaks justified by metadata		✔
User dependency	Allow user to introduce metadata		✔
	Easier handling of big datasets	✔	

Furthermore, differences in the trends obtained by applying both methods were found. However, these differences are similar to other research performed in the Pyrenees (Bücher and Dessens, 1991; Cuadrat *et al.*, 2013; Esteban *et al.*, 2012). Three factors can explain the differences that do exist between studies: the different time periods in focus, the homogenization methods applied and the differences in the number and geographical distribution of stations.

The identified Vielha data error is a good example to illustrate the usefulness of simple statistical analysis, such as correlation values, applied before and after homogenization. This error was corrected well with ACMANT for Tmax, but not for Tmin since the control of seasonal changes is included only in the homogenization of Tmax with ACMANT. HOMER outputs indicated the error, but, due to the smoothness of the annual means, it was overlooked. So, the importance of QC to avoid these large errors was manifested and, if HOMER is applied, a thorough revision of their outputs should be performed in the available annual and seasonal time scale outputs.

- Chapter 3 – Regional anomaly series

To obtain high-quality regional anomaly series (Chapter 3), that capture the climate variability and change in the central Pyrenees for the longest available period, HOMER was selected to homogenize the observed data set, because HOMER includes ACMANT detection. Regional anomaly series for PPT, Tmax and Tmin were obtained for annual and seasonal time periods during the period 1910–2013. After applying QC and homogenization procedures, the most completed series were averaged using the Osborn correction that avoids the biases due to the time varying sample size data. Improving series and their reliability is demonstrated by the comparison between the quality controlled and the homogenized data, a spatial correlation analysis and a comparison with an independent data set for the regional anomaly series.

Trend analysis has shown a highly significant increase in temperatures and important inter-annual PPT variability without significant trends over the central Pyrenees. It is interesting to highlight the differences between trends considering the period 1910–2013 or 1970–2013: Tmax and Tmin trends strongly increase during the recent period and PPT trends mostly decrease even if they are not significant (Table 2).

Temperature trends are consistent with the ones obtained in other works developed in the Pyrenees (Esteban *et al.*, 2012) and are similar to trends in the Iberian Peninsula (IP; Brunet *et al.*, 2006). They are also consistent with long term-trends found in different regions of the Alps for the period 1856–1998: ~0.05 ℃/dec in summer, ~0.1 ℃/dec in winter and between ~0.07 and ~0.09 ℃/dec annual mean temperature (Auer *et al.*, 2001). While no altitude dependence has been shown in the central Pyrenees temperature trend, some features of temperature in the Alps are clearly dependent on altitude (Auer *et al.*, 2001). Global scale mean temperature trends have the same magnitude order and present an equivalent increase of trends during the recent period (Jones, 2016).

Table 2: PPT, Tmax and Tmin trends for the two studied periods Significant trends are in bold (Pérez-Zanón *et al.*, 2017).

		Central Pyrenees	
		1910–2013	1970–2013
PPT (%/dec)	Annual	-0.64	-2.70
	Winter	-0.77	-8.59
	Spring	-1.17	-0.66
	Summer	-0.70	-4.62
	Autumn	-0.30	-1.95
Tmax (℃/dec)	Annual	**0.11**	**0.57**
	Winter	0.06	**0.29**
	Spring	**0.13**	**0.87**
	Summer	**0.17**	**0.74**
	Autumn	**0.08**	**0.43**
Tmin (℃/dec)	Annual	**0.06**	**0.23**
	Winter	**0.12**	-0.05
	Spring	0.02	**0.40**
	Summer	**0.07**	**0.27**
	Autumn	**0.09**	**0.31**

Precipitation trends in the central Pyrenees, while not significant (Table 2), showed a tendency to reduction when comparing the entire and the recent period values. These trends are coherent with the analysis of López-Moreno *et al.* (2010), which also showed that some features of precipitation trends can abruptly vary from one observatory to another. Precipitation trends in the IP were analysed by Rodrigo and Trigo (2007), showing a negative trend in the northern IP for daily total amount of precipitation and intensity, while the number of precipitation days didn't show a significant trend.

- Chapter 4 – Limnological analysis

Recent expansion of anoxia in fresh waters, which has become a global issue, has been studied offering innovative and novel insights (Chapter 4). This problem is addressed for the first time in the Mediterranean region using long-term varved lake sediments. A

multiproxy approach and the homogenized regional climate data ensures the reliability of the analysis.

Different phases in the evolution of oxygen shifts over time were detected which can be driven by climate and/or anthropogenic forcings, being able to clearly distinguish pre- and post-industrial oxygenation trends. A direct connection between oxygen shifts and ongoing climate change was found, although, a more refined distinction between the effects of humans and climate is necessary since human effects and climate can overlap in this area.

The regional anomaly series of the central Pyrenees has allowed the investigation of the extent to which the oxic/anoxic shifts in Lake Montcortès could be associated with present climatic variability and change over the last century and to present days. Analysis of the XRF time series of Fe/Ti ratio evolution, which is considered to be an indicator of oxido-reduction variations, yielded interesting results. In this case, a threshold applied to the regional anomaly series was used to define cold and dry years in the Pyrenees, since extreme climate occurrences were supposed to trigger mixing up of the water column and therefore a thorough oxygenation.

This methodology showed that cold and dry years in the Pyrenees could be acting as a precursors or external forcings to the following year's mixing of Montcortès lake water column. However, the 1957–1959 period of three extreme Fe/Ti values did not exhibit a clear relationship with climate variables, indicating that other types of environmental conditions could also trigger a mixing event. High wind speed was suggested as another climatic precursor, but there are insufficient data available in the study area that could support this hypothesis, chiefly, due to the distance between Montcortès lake and meteorological observatories. On the other hand, the lower ends of the Fe/Ti values, denoting persistent anoxia, were preceded by a period of warmer years, but it cannot be ruled out that other factors could be involved.

Summarizing, the classification of subsets obtained from the PCA showed four main (A, B, C and D). Interestingly, at least 45.3% of the years were mixing years and, like the meromictic years, mostly occurred arranged in groups of consecutive years, thus alternating years of monomixis with years of meromixis. However, during the

instrumental period, more than 90% of the targeted years belonged to subsets B and C, and the years of subset C were roughly warmer and drier than those of subset B, which was typically due to warm and dry winters.

The analysis performed between the sediments variables and the NHAT since 1500 showed significant correlations during the 20th century might be affecting some of the mechanisms that control the sedimentation processes linked to oxygen availability, while, previously, regional or local climate and/or human pressure may have played a more determinant role.

- Chapter 5 – Weather regimes and tree-ring data

The manuscript in preparation, shown in chapter 5, deals with the involvement of summer large-scale weather regimes in controlling Pyrenees regional climate and modulating *Pinus Uncinata* tree-rings growth. The presented analyses use composites from the regional anomaly series to define the summer synoptic scale configurations which emerge in years of extreme and normal climate in the central Pyrenees.

These composites, considered individual variables or PPT and Tmin simultaneously, have been compared with the four WR that summarize the summer pressure systems in summer: Blocking, Atl.Low, SNAO- and Atl.Ridge. If individual variables are considered, Tmin is positive correlated with Atl.Low and PPT with Blocking, while a more complex signal is obtained by the spatial comparison between individual and combined PPT and Tmin criteria to define composites.

The age model error applied on TRW chronologies allows to achieved a common signal in the central Pyrenees by applying a PCA. The obtained signals, that are shown to be different depending on the number of chronologies considered, have been compare with the Pyrenees regional series. The differences in the spatial coverage between the regional anomaly series and the chronologies sites can be an explanation of, even presenting significant correlation, the correlation magnitude is not conclusive.

Composites from PC signals have also been correlated with regional anomaly composites giving the chance to interpret the limitation of tree-rings growth by different combinations of climatic factors (only due to precipitation or temperature or PPT and

Tmin acting simultaneously). Furthermore, an evaluation of PC signals to capture, and therefore, to reconstruct WR have been performed.

6.1.2. Global overview

Nowadays, one of the hottest topics in climatology is the low-frequency climate variability and the forcing factors which can be related such as the internal ocean-atmosphere coupling. To study this low-frequency variability, long-term climate data is required. However, long-term climate observations are spatially not as frequently available as it would be desired, especially in mountainous regions, where did not start until the late eighteenth century. So, to be able to improve the scientific knowledge of low-frequency climate variability, it is necessary to obtain long-term climaic series by other procedures. These alternative procedures to direct observation are, typically, the reconstruction of past climate from proxies.

Furthermore, to study the ocean-atmosphere coupling in the Pyrenees latitude, the Atlantic Meridional Overturning Circulation is studied and related to the AMO, which is characterized by the SST (Knudsen *et al.*, 2014; Yamamoto and Palter, 2016). At the same time, AMO is related to NAO (such as Woollings *et al.*, 2014). This means that part of the AMO variability is due to or influencing the atmospheric variability, and, the most frequent mode of variability in the North Atlantic, the NAO, is used to explore this relation. So, not only a long-term series is necessary to explore low frequency climate variability, whether not it should be able to capture large-scale atmospheric variability.

To sum up, the main results of this thesis are a step towards the low-frequency climate knowledge. TRW chronologies are, at least partially, able to capture WR which are the large-scale synoptic atmospheric variability in summer by the applied methodology. The consistency of the obtained signals from TRW chronologies has been checked by relating them to WR and the regional anomaly series. The quantification of their relation, complex to establish, is reliable thanks to the high-quality of the regional anomaly series here presented.

Other studies deal with low-frequency signals and/or the physical mechanisms involved. In the Alps, the links between flood events and solar radiation, volcanic eruptions,

climate variability and North Atlantic dynamics have been explored in the period 1800–2010 (Peña, 2015). Another example is the study of the displacement of the Atlantic intertropical convergence zone (ITCZ) in 2003 warm summer in Europe, suggesting tropical– extratropical Atlantic connection (Cassou *et al.*, 2005). These forcings and mechanisms may influence the central Pyrenees climate despite the variables altered, and the sign and amplitude of their consequence still undetermined.

6.2. Conclusions

In this thesis, the climate of the Pyrenees has been studied using instrumental and proxy data and for different time and spatial scales. The characterization of the observed climate in the central Pyrenees during the instrumental period has been possible thanks to the regional anomaly series obtained and the exploration of the influence of summer weather regimes in the central Pyrenees regional observed climate. On the other hand, the capability of paleoclimate proxies to capture observed climate has been evaluated. Globally, the general aims of the thesis have been achieved and principal conclusions are:

- The application of QC test on climate observations is essential before obtaining a reliable climate result.

- Use HOMER if metadata is available or the user is an expert in homogenization and wants to take the control on the homogenization process.

- Use ACMANT if the dataset to homogenize is big or the user is not an expert in homogenization as it is automatic.

- The thermopluviometric regional anomaly series which characterize the central Pyrenees climate during the period 1910–2013 are determined in annual and seasonal time periods, presenting the newly recovered period 1910–1949.

- The increase of annual Tmax and Tmin in the central Pyrenees is significant in the central Pyrenees and it has been intensified during the recent period, particularly in spring.

- Annual and seasonal PPT in the central Pyrenees show a non-significant decreasing trend, likely due to their high interannual variability.

- No altitude dependency of temperature trends in individual observatories is found.

- The four WR which determine the North Atlantic–European dynamical signature of the summertime atmospheric variability are obtained: Blocking, Atl.Low, Atl.Ridge and SNAO-.

- Compared WR frequency with regional anomaly series from central Pyrenees:

    - Tmin evolution is significant positive correlated to Atl.Low and significant negative correlated to Blocking.

    - PPT evolution is significant negative correlated to Atl.Low and significant negative correlated to Blocking.

- Composites of extreme and normal climate in the central Pyrenees are obtained for individual variables (Tmax, Tmin and PPT) and for a combined PPT and Tmin criteria.

- Cold and dry years in the central Pyrenees could be acting as a precursors or external forcings to the following year's mixing of Montcortès lake water column.

- Periods of warmer years precede lower ends of Fe/Ti values, denoting persistent anoxia of Montcortès lake water column.

- The methodology applied for age model error simulations has enabled a common signal to be obtain for the study area

- The capability of TRW chronologies by applying this methodology to capture regional or large scale climate depends on the number of chronologies considered and their spatial distribution.

This work broadens the knowledge of the climate of the study area and also generates the following resources:

- covering, partially or completely, the period 1910–2013 :

- A dataset of daily quality controlled Tmax, Tmin and PPT data from 155 observatories, either manual or automatic, in the study area.

- A dataset of 60 monthly homogenized PPT series from 60 and 42 monthly homogenized Tmax and Tmin series from the previous observatories.

– A dataset of annual and seasonal regional anomaly series (publically available online http://www.c3.urv.cat/data1.html)

- A catalogue of composites of the North Atlantic – European sector SLP for extreme and mean observed climate in the central Pyrenees.

- A dataset of 31000 age model error simulations of the 31 TRW chronologies being the longest starting in 1415.

6.3. Future work

Next steps could be the reconstruction of the time evolution of one or more WR frequencies taking advantage of the analyses that have already been performed with the tree-ring growth from the central Pyrenees. A similar methodology could be applied to the lake Montcortès sediments, profiting from deep knowledge provided by the analysis from chapter 4 and other Montcortès project publications.

Furthermore, the regional anomaly series open a new horizon of possibilities in the study of climate change and variability in the central Pyrenees:

- analyse the large-scale synoptic pressure systems in winter,

- test climate models in the study area,

- analyse climate projections in the central Pyrenees,

- obtain the homogenized dataset of observatories in the central Pyrenees at daily time scale
- and taking advantage of the daily data, study climatological extreme events in the area,
- explore new possibilities to extend back in time the regional climate knowledge
- and evaluate the possibilities of extend spatially the regional anomaly series.

6.4. References

Auer I, Böhm R, Jurković A, Orlik A, Potzmann R, Schöner W, Ungersböck M, Brunetti M, Nanni T, Maugeri M, Briffa K, Jones P, Efthymiadis D, Mestre O, Moisselin JM, Begert M, Brazdil R, Bochnicek O, Cegnar T, Gaji-Čapka M, Zaninović K, Majstorović Ž, Szalai S, Szentimrey T, Mercalli L. 2005. A new instrumental precipitation dataset for the greater alpine region for the period 1800-2002. *International Journal of Climatology* **25**(2): 139–166. DOI: 10.1002/joc.1135.

Brunet M, Saladié O, Jones P, Sigró J, Aguilar E, Moberg A, Lister D, Walther A, Lopez D, Almarza C. 2006. The Development of a new dataset of Spanish Daily Adjusted Temperature Series (SDATS) (1850-2003). *International Journal of Climatology* **26**(13): 1777–1802. DOI: 10.1002/joc.1338.

Bücher A, Dessens J. 1991. Secular trend of surface temperature at an elevated observatory in the Pyrenees. *Journal of Climate* **4**: 859–868.

Cuadrat JM, Serrano R, Saz MA, Tejedor E, Prohom M, Cunillera J, Esteban P. 2013. Creación de una base de datos homogenizada de temperaturas para los Pirineos (1950-2010). *Geographicalia* **63–64**: 63–74.

Esteban P, Prohom M, Aguilar E. 2012. Tendencias recientes e índices de cambio climático de la temperatura y la precipitación en Andorra, Pirineos (1935-2008). *Pirineos* **167**: 87–106. DOI: 10.3989/Pirineos.2012.167005.

Jones P. 2016. The Reliability of Global and Hemispheric Surface Temperature Records. *Adv. Atmos. Sci* **33**(333): 269–282. DOI: 10.1007/s00376-015-5194-4.

López-Moreno JI, Vicente-Serrano SM, Angulo-Martínez M, Beguería S, Kenawy A. 2010. Trends in daily precipitation on the northeastern Iberian Peninsula, 1955-2006. *International Journal of Climatology* **30**(7): 1026–1041. DOI: 10.1002/joc.1945.

Pérez-Zanón N, Sigró J, Ashcroft L. 2017. Temperature and precipitation regional climate series over the central Pyrenees during 1910–2013. *International Journal of Climatology* **37**(4): 1922–1937. DOI: 10.1002/joc.4823.

Rodrigo FS, Trigo RM. 2007. Trends in daily rainfall in the Iberian Peninsula from 1951 to 2002. *International Journal of Climatology*. John Wiley & Sons, Ltd. **27**(4): 513–529. DOI: 10.1002/joc.1409.

List of abbreviations

AC	Homogenized data after applying ACMANT
ACMANT	Adapted Caussinus-Mestre Algorithm for Networks of Temperature series
AEMET	Spanish National Meteorology Agency
AMO	Atlantic multidecadal Oscillation
Atl.Low	Atlantic Low
Atl.Ridge	Atlantic Ridge
COP21	Twenty-first session of the Conference of the Parties
CPS	Counts Per Second
GCM	Global Climate Models
GSB	Green Sulfur Bacteria
HO	Homogenized data after applying HOMER
HOMER	HOMogenization software in R,
ID	Identification
IP	Iberian Peninsula
IPCC	Intergovernmental Panel on Climate Change
ITCZ	Intertropical Convergence Zone
Lat	Latitue
LIA	Little Ice Age
Long	Longitude
MO	Mediterranean Oscillation
NAO	North Atlantic Oscillation
NHTA	North Hemisphere Temperature Anomaly
NRC	National Research Council
OPCC	Pyrenees Climate Change Observatory
PC	Principal Component
PCA	Principal Component Analysis
PPT	Precipitation
PSB	Purple Sulfur Bacteria

QC	Quality Control
RCM	Regional Climate Models
SCC	Spearman Correlation Coefficients
SDATSv2	Spanish Daily Adjusted Temperature Series
SLP	Sea Level Pressure
SMC	Catalonia Meteorological Service
SNAO	Summer North Atlantic Oscillation
SP	Significant Period
SST	Sea Surface Temperature
TIC	Total Inorganic Carbon
Tmax	Maximum temperature
Tmean	Mean temperature
Tmin	Minimum temperature
TOC	Total Organic Carbon
TRW	Tree Ring Width
TS	Total Sulfur
UERRA	Uncertainties in Ensembles of Regional Reanalyses
UHPLC	Ultra-High Performance Liquid Chromatography
WMO	World Meteorological Organisation
WR	Weather Regime
XRF	X-ray fluorescence

List of tables

List of figures

Chapter 1 – Introduction

Chapter 2 – Comparison of homogenization methods

Chapter 4 – Limnological analysis

Chapter 5 – Weather regimes and tree-rings